THE EFFECTS OF LEPTOMYCIN B ON HPV-INFECTED CELLS

Carol Elizabeth Jolly

A Thesis Submitted for the Degree of PhD
at the
University of St Andrews

2008

The Effects of Leptomycin B on HPV-Infected Cells

By Carol Elizabeth Jolly

A thesis submitted to the University of St Andrews
in partial fulfilment of the requirement of the
degree of Doctor of Philosophy

Bute Medical School

October 2008

Contents

Declaration

I, Carol Elizabeth Jolly, hereby certify that this thesis, which is approximately 58,000 words in length, has been written by me, that it is the record of work carried out by me and that it has not been submitted in any previous application for a higher degree.

I was admitted as a research student in September, 2004 and as a candidate for the degree of Doctor of Philosophy Medicine in October, 2005; the higher study for which this is a record was carried out in the University of St Andrews between 2004 and 2008.

Date_____ _____

I hereby certify that the candidate has fulfilled the conditions of the Resolution and Regulations appropriate for the degree of Doctor of Philosophy Medicine in the University of St Andrews and that the candidate is qualified to submit this thesis in application for that degree.

Date_____ _____

Copyright Declaration

In submitting this thesis to the University of St Andrews we understand that we are giving permission for it to be made available for use in accordance with the regulations of the University Library for the time being in force, subject to any copyright vested in the work not being affected thereby. We also understand that the title and the abstract will be published, and that a copy of the work may be made and supplied to any bona fide library or research worker, that my thesis will be electronically accessible for personal or research use unless exempt by award of an embargo as requested below, and that the library has the right to migrate my thesis into new electronic forms as required to ensure continued access to the thesis. We have obtained any third-party copyright permissions that may be required in order to allow such access and migration, or have requested the appropriate embargo below.
The following is an agreed request by candidate and supervisor regarding the electronic publication of this thesis:

Embargo on both all or part of printed copy and electronic copy for the same fixed period of 5 years on the following ground: publication would preclude future publication;

Date Signature of candidate Signature of supervisor

Acknowledgements

I would like to express my deepest thanks to my supervisor Prof. Simon Herrington. Without his support, guidance, and unrelenting kindness and patience the completion of my research and subsequent thesis would never have been possible.

Many thanks must also go to Dr Sonia Lain for providing endless practical advice and materials.

I would also like to thank the members of the Bute past and present, particularly the members of E-floor who have, over the years, provided a wealth of advice, assistance and support, whilst also proving to be a brilliant group of friends. In particular I would like to thank Dr Lindsey Gray for guidance during my research, Drs Katherine Feeney and Lissa Herron for their patience and help with my thesis and many other things, and Drs Keeley Brookes, Yimin Ren, Fleur Davey and Mrs Tina Briscoe for answering lots of questions and providing great banter and good times.

No research within the Bute could possibly have taken place without the efficiency, assistance and professionalism of the Bute stores team: Iain Grieve, Alex Taylor and Graeme Russell.

Many thanks must also go to the University Dyslexia Adviser, Janice McGregor and the student support team. Janice's practical assistance, support and guidance, in combination with the natural friendliness of the whole team, have made coping with my dyslexia a much more manageable task (even although I still can't spell!!!).

After spending so many years in St Andrews, I would like to thank all those who have made it such a great place to be. In particular, Dawn Rimmer, a great friend through bad times and good.

Finally thanks must also go to my whole family, especially my Mum and Dad for their support, encouragement and love. Their faith in me throughout my academic career has allowed me to pursue the subject I love. P.S. I haven't cured cancer yet!!

List of Abbreviations

Act-casp-3	Activated caspase-3
AEC	3-amino-9-ethylcarbazole
AIF	Apoptosis-inducing factor
AMV	Avian Myeloblastosis Virus
ANT	Adenine nucleotide translocator
APAF1	Apoptotic protease activating factor-1
ATP	Adenosine triphosphate
AU	Arbitrary units
B2M	Beta-2-microglobulin
BAD	Bcl-2-antagonist of cell death
BAK	Bcl-2 homologous antagonist/killer
BAX	Bcl-2 associated X
Bcl-2	B-cell leukaemia/lymphoma 2
BH	Bcl-2 homology
BID	Bcl-2 Interacting Domain
BIM	Bcl-2-interacting mediator of cell death
BOK	Bcl-2-related ovarian killer
BSA	Bovine serum albumen
C/EBPα	CCAAT enhancer-binding protein α
CAD	Caspase-activated deoxyribonuclease
CBP	CREB binding protein
cdk	Cyclin dependent kinase
cDNA	Reverse transcribed mRNA
CFS	Common fragile sites
Ci	Curie
CIAP	Calf intestinal alkaline phosphatase
CIN	Cervical intraepithelial neoplasia
CK18	Cytokeratin 18
CKI	Cyclin-dependent kinase inhibitor
CKI	Cyclin dependent kinase inhibitors
CMV	Cytomegalovirus
COSHH	Control of Substances Hazardous to Health
CRE	*cis* regulatory element
CRIME	CRM1, importin β, etc
CRM1	Chromosome region maintenance 1
CRPV	Cottontail Rabbit papillomavirus
dATP	Deoxyadenosine triphosphate
dCTP	Deoxycytidine triphosphate
dGTP	Deoxyguanosine triphosphate
DIABLO	Direct IAP binding protein with low pI
DISC	Death –inducing signalling complex
DMEM	Dulbecco's modified essential medium
DNA	Deoxyribonucleic acid
DNA	Deoxyribonucleic acid
Dnp53	Dominant negative p53 plasmid pBabe-R248W
dTTP	Deoxythymidine triphosphate
EDTA	Ethylenediaminetetraacetic acid

EGF	Epidermal growth factor
EGFR	Epidermal growth factor receptor
EV	Epidermodysplasia verruciformis
FACS	Fluorescence-Activated Cell Sorting
FADD	Fas-associated death domain protein
Fas-L	Fas ligand
FLIP	FADD-like interleukin-1 β-converting enzyme-like protease
gDNA	Genomic DNA
GDP	Guanidine diphosphate
GFP	Green fluorescent protein
GTP	Guanidine Triphosphate
h	Hours
HBSS	Hanks' balanced salts solution
HCL	Hydrochloric acid
hDLD	Drosophila discs large
HECT	Homologous to the E6-AP carboxyl terminal
HIV	Human immunodeficiency virus
HPV	Human papillomavirus
HRP	Horse radish peroxidase
HSIL	high grade squamous intraepithelial lesion
HSV-1	Herpes simplex virus type 1
hTERT	Human reverse transcriptase
IAP	Inhibitor of apoptosis proteins
ICAD	Caspase-activated deoxyribonuclease inhibitor
IGF	Insulin-like growth factor
IMM	Inner mitochondrial membrane
KGM2	Keratinocyte growth medium 2
LCR	Long control region
LLETZ	Large loop excision of the transformation zone
LMB	Leptomycin B
LSIL	Low grade squamous intraepithelial lesion
MAPK	Mitogen-activated protein kinase
MHC I	Major histocompatibility complex class I
Mo-MuLV	Moloney murine leukaemia virus
mPBST	PBST with milk
Mtc	Mitomycin C
NaCl	Sodium chloride
NaOH	Sodium
NES	Nuclear export signal
NF-κB	nuclear factor kappa B
NLS	Nuclear localisation signal
NNK	Nitrosamine 4-(methylnitrosamino)-1-(3- pyridyl)-1-butanone
nt	Nucleotides
OMM	Outer mitochondrial membrane
ORF	Open reading frame
PAC1	Phosphatase of activated cells 1
Pap	Papanicolaou
PBS	Phosphate buffered saline
PBST	PBS with Tween-20
PBT	1xPBS with BSA

PCNA	Proliferating cell nuclear antigen
PCR	Polymerase Chain Reaction
PDGF	Platelet derived growth factor
PDVF	Polyvinylidene Fluoride
PDZ	*P*SD95/*D*iscs Large/*Z*O-1
PHK	Primary human keratinocyte
PI3K	Phosphatidylinositol 3-kinase
PKB	Protein kinase B
POD	Promyelocytic leukaemia oncogenic domains
pRb	Retinoblastoma protein
PTEN	Phosphatase and tensin homolog
PTPC	Permeability transition pore complex
RAN-GDP	Ran associated GDP
RAN-GTP	Ran associated GTP
ROCK1	Rho kinase 1
RSB	Reducing sample buffer
RT	Reverse transcription
RT-PCR	Reverse transcription PCR
SAPK	Stress-activated protein kinase
SDS	Sodium Dodecyl Sulphate
SDS-PAGE	Sodium Dodecyl Sulphate – Polyacrylamide Gel Electrophoresis
SF2/ASF	Splicing Factor 2/Alternative Splicing Factor
SIL	Squamous intraepithelial lesion
siRNA	Small interfering RNA
SMAC	Second mitochondria-derived activator of caspase
snRNPs	Small nuclear ribonucleoprotein particles
SR	Serine/arginine
SSC	Saline-Sodium Citrate
TBE	Tris buffered EDTA
TBP	TATA-box-binding protein
TBS	Tris buffered saline
TE	Trypsin-EDTA
TGF-β	Transforming growth factor-β
TNF-R	Tumour necrosis factor receptor
TNF-α	Tumour necrosis factor-α
TNS	Trypsin neutralising solution
TopBP1	DNA topoisomerase II-beta-binding protein 1
TRAIL- R1	TNF-related apoptosis-inducing ligand-R1
TSA	Trichostain A
URR	Upstream regulatory region
UVC	Ultraviolet C
v/v	Volume to volume
v/w	Volume to weight
VLP	Virus-like particles
vp	pBabe-puro vector only
wt	Wild type

Abstract

Cervical cancer is a major cause of death in women and is strongly associated with infection by human papillomavirus (HPV). Integration of HPV is thought to form a key step in the formation of cancer, and is thought to involve the upregulation of HPV E6 and E7 due to the loss of E2 transcriptional control. Leptomycin B (LMB), a nuclear export inhibitor, has previously been shown to induce apoptosis in HPV-containing cancer cell lines and HPV 16 E7 or E6/E7 transduced primary keratinocytes, but not in normal cells. This thesis shows that LMB can induce apoptosis and a reduction in the colony survival of derivatives of the W12 cell line that contain HPV 16 in either episomal or integrated form. The HPV genome status, including variations in viral integration type, appears to influence the cumulative and temporal pattern of LMB-induced apoptosis. The effects of LMB were also apparent in cells grown in organotypic raft culture, with differences in behaviour again apparent between cells containing episomal and integrated HPV. As previously noted, treatment with LMB was associated with increased expression of the cell regulators p53 and p21; however, the induction of apoptosis was not dependent upon transcriptionally active p53. It is therefore likely that induction and mediation of LMB-induced apoptosis occurs via alternative, currently unidentified, pathways. These findings suggest that LMB can induce apoptosis in keratinocytes containing HPV 16 in either episomal or integrated form, with genome status and potentially lesion grade likely to influence the response of HPV-associated anogenital lesions to LMB treatment.

Table of Contents

List of Figures

Chapter 4

Chapter 5

Chapter 6

Chapter 7

List of Tables

Page

Chapter 1

Chapter 2

Chapter 1: Introduction

1.1. Human Papillomavirus

Carcinoma of the cervix is a leading cause of cancer-related deaths in women worldwide [1-3], with formation associated with infection by the human papillomavirus (HPV) [4]. Carcinogenesis is known to require the accumulation of numerous cellular alterations involving the increase, decrease or alteration of vital cellular proteins. The presence and integration of high risk HPV appears, in a single step, to provide mechanisms for many of these alterations to occur [5]. Many cervical cancer deaths could be prevented by early detection of cervical intraepithelial neoplasia (CIN), the progenitors of cervical cancer, by the implementation of screening methods such as the UK cervical screening programme. Therefore, the study and treatment of HPV infection is of great importance to the prevention and treatment of cervical neoplasia.

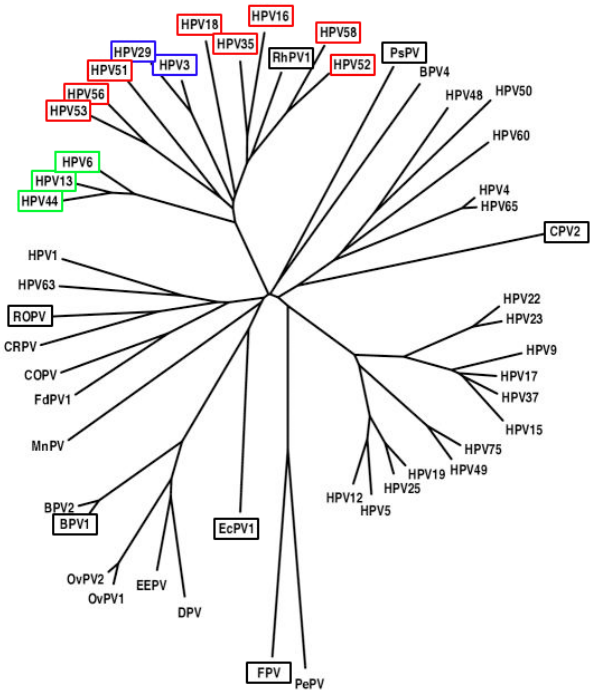

Figure 1.1: A phylogenetic tree displaying some of the papillomavirus family members. The mucosal high (red) and low risk types (blue) are indicated along side cutaneous (blue) and non-human members of the papillomaviruses family (black), as classified by Doorbar (2006) [6]. Based on Tachezy *et al* (2002) [7].

The human papillomaviruses are members of the papillomaviridae taxonomic family (NCBI Taxonomy ID 10581), which contains viruses infecting a number of species such as birds and cattle (figure 1.1). Individual papillomaviruses exhibit strict host species and tissue specificity [8]. Approximately 200 different human papillomavirus types have been identified using DNA sequencing and phylogenetic tree analysis [9]. A HPV type is defined as varying by a minimum of 10% in the E6, E7, and L1 open reading frames (ORF) compared to other known HPV types [10-12]. The human specific papillomaviruses have been identified as one of the most diverse groups of viruses known to cause disease in humans [13]. One specific subset of these viruses infects the human anogenital tract; this group contains approximately 30 different viral types [2] which cluster within a small area of the HPV phylogenetic tree (figure 1.1) [10-12]. The human papillomaviruses can be further categorised into groups or genera that are phylogenetically related, but biologically different. Most HPVs are contained within the alpha and beta genera; the alpha papillomaviruses are associated with mucosal and cutaneous locations and have the potential to cause benign and cancerous lesions (section 1.2), the beta papillomaviruses within the general population are associated with cutaneous latent infections [14].

1.1.1. HPV Structure

HPV is a non-enveloped DNA virus whose genome is contained within a 55nm diameter icosahedral capsid [8] as shown by figure 1.2.

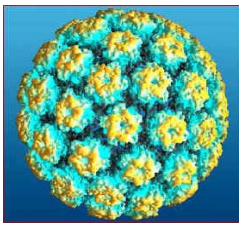

Figure 1.2: Model of HPV illustrating the structure of the viral capsid, highlighting the pentamer of the major capsid protein (yellow). Image generated by Stephen C. Harrison and colleagues, Howard Hughes Medical Institute.

The capsid is formed from pentamers of L1 major capsid protein arranged into 72 capsomeres (60 hexavalent and 12 pentavalent) [8] as illustrated in figure 1.2. The exact location of the minor capsid protein L2 within this structure is unclear, although it appears that it is located beneath the centre of each capsomere [15,16]. However, evidence from cottontail rabbit papillomavirus (CRPV) indicates that a portion is also exposed at the surface of the virion [16]. The viral capsid structure helps to protect the progeny virions from desiccation after release from the epithelial surface [17] and mediates the infectivity of the virion [6].

1.1.2. HPV Life cycle

The human papillomavirus is a strictly epitheliotropic virus, infecting cutaneous or mucosal epithelial locations [18]. The virus enters where the upper epithelium has undergone trauma, allowing viral entry to the actively dividing cells of the basal layer. A small number of basal cells become infected and the virus then spreads to the daughter cells during normal cellular division, hence increasing the number of virally infected cells within the suprabasal layers [6,19]. The cellular receptor utilized by HPV to gain access to host cells is unknown. There is some evidence that the heparin sulphate proteoglycans may be involved in the binding and uptake of the virion [20]. However, a secondary receptor in the form of α_6-integrin cell surface receptors may also play a role [6,21]. After binding to a cell surface receptor the virion is slowly internalised into the cell. The mechanism of this uptake appears to vary between HPV types; in the case of HPV 16 entry occurs via clathrin-mediated endocytosis [6,22]. However, it has been suggested that HPV 31 uses caveolae instead. Related to lipid rafts, the caveolae are formed from collections of glycosphingolipids, cholesterol and various cellular proteins. Unlike clathrin coated vesicles, the caveolae do not fuse with lysosomes and therefore the contents are protected from enzymatic digestion [23-25].

As is commonly seen with other viruses such as SV40 [26], the papillomaviruses do not encode a complete set of replication machinery (such as a DNA polymerase [27]) and therefore must hijack the host cell replication machinery in order to replicate their genome [8]. While the virus remains within the already dividing layers of the basal epithelium minimal viral interference is required for successful maintenance of the viral genome. However, as the host cells ascend towards the surface they exit the cell cycle and begin to differentiate to eventually produce the protective keratinised cells indicative of the upper epithelium; as a consequence, these differentiating cells no longer provide the machinery required for viral DNA replication. Due to the alterations in behaviour of the host cell within the epithelium, the viral life cycle is separated into two distinct phases linked to the differentiation state of the host epithelial cells [8]. In the suprabasal layers the virus must induce the cells to replicate and inhibit their ability to terminally differentiate [28] in order to maintain a replication competent state. As the host epithelial cells migrate toward the surface they provide various cues allowing the virus to co-ordinate its activity with that of the cell, ensuring that the correct cellular machinery is available. The migration of the virus through the epithelium is therefore associated with a spatially regulated expression of the viral genes.

The first phase of the viral life cycle is one of non-productive division, supported by the replication of the undifferentiated cells of the basal epithelium [8], where the necessary host replication machinery is readily available [27]. During this time the virus establishes its episomal genome at a low copy number of approximately 50-100 genomes per cell [18,29]. This non-productive phase is achieved using the DNA replication machinery in a bidirectional theta mode during S-phase [6] to produce one copy of the viral genome per cell cycle [29]. Within the basal layers of the epithelium all the necessary replication machinery is readily available

for both cellular and viral replication, therefore viral interference can be minimised and E6 and E7 can be maintained at very low or non-existent levels [30].

The second 'productive' phase of the viral life cycle is supported by the differentiating cells [8] of the suprabasal epithelium [19]. Here the virus amplifies its DNA to a high copy number using a rolling circle mode of replication [29]. As in non-productive replication the virus hijacks the cellular machinery. However, at this point, reactivation of the replication-dormant cell by the virus is required. This process is aided by the presence of viral proteins particularly E6 and E7, which interact with the host to reactivate the cell and prevent arrest or apoptosis.

As the host cells reach the upper layers of the epithelium, transcription and translation of the complete viral genome is initiated. This includes the late proteins L1 and L2 which are required for encapsulation of the amplified viral DNA sequences. These virions are subsequently released at the epithelial surface [8]. For these later phases of the viral life cycle to occur, the differentiation-dependent promoter p670 (HPV 16) located within the E7 ORF [31] must be up regulated, leading to an increase in the transcription of the genes required for replication of viral DNA [6]. Prior to encapsulation, the L1 protein forms capsomeres within the cytoplasm, and after association with L2, the complex localises to the nuclear promyelocytic leukaemia oncogenic domains (POD, section 2.1) [6,32]. Localisation of viral DNA to this nuclear region for encapsulation is thought to be aided by the presence of the E2 protein which binds to viral DNA [6].

1.1.3. HPV Genome

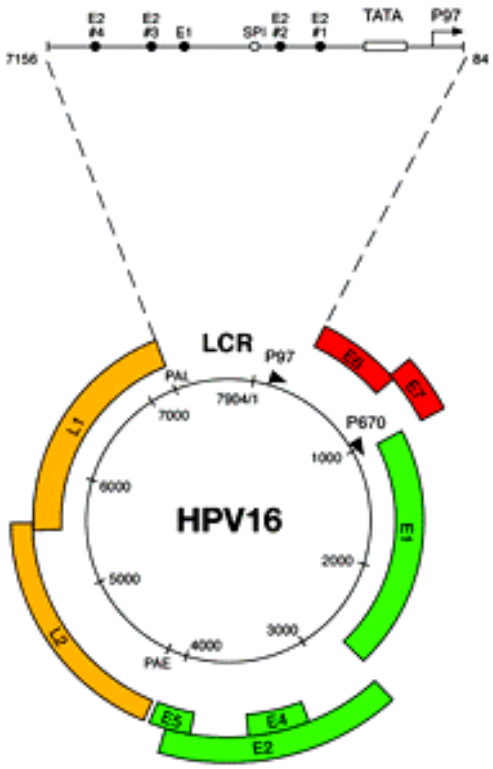

Figure 1.3: Organisation of the HPV 16 genome showing the early genes (green and red) and the late genes (yellow).[6] Reproduced with permission.

HPV encodes a circular genome of approximately 8kb (7.904kb in HPV 16 [33]) with only one strand of the double stranded genome transcribed [9] (figure 1.3). The genome contains the ~ 4kb early and 3kb late ORFs, with the LCR (long control region) located between the early and late ORFs [8,9]. The early genes (E1 to E7) regulate viral gene expression, genomic replication and cellular transformation [8]. The late ORFs L1 and L2 encode the major and minor capsid proteins, required for late viral functions and formation of the complete infectious particle [8].

1.1.4. A Summary of HPV genes

The viral genes perform a wide range of functions designed to aid viral replication. Where the virus establishes a productive infection each viral component plays a defined role, interacting and interfering with a range of viral or host proteins and pathways. To be

successful, the viral proteins must be produced at specific times during the cells migration through the epithelium, and remain under strict viral regulation. In this section a brief overview will be given. Further details of the individual genes are presented in sections 1.1.5-9 and 1.5.

The E1 protein is highly conserved within the papillomaviruses and during a natural infection is expressed at low levels [6]. E1 has important roles in both viral replication and viral genome maintenance [1].

The E2 protein acts as a transcriptional regulator [34] and also aids viral replication by interacting with the E1 protein [35]. In order to replicate, the virus requires the E1 and E2 viral proteins, with the remaining DNA replication machinery provided by the host cell [36]. The E2 protein also has the ability to both activate and repress the expression of the HPV oncogenes forming an important mechanism for controlling viral activity [37] (see section 1.1.5). Inhibition of the HPV 16 p97 viral promoter by E2 allows the virus to reduce the expression of the E6 and E7 [38,39].

The E4 product is encoded by a spliced E1^E4 sequence, and expressed as a fusion protein including the N-terminal region of the E1 protein [40]. The protein is produced late in the early phase of the viral life cycle within the mid and upper suprabasal layers of the epithelium [41]. The exact function of the E4 protein is unknown, although as it is the most abundantly expressed viral protein in HPV-infected epithelia, it is likely to play an important role in the viral life cycle [1]. It has been shown that E4 has the ability to disrupt the keratin network, suggesting a possible role in the later stage of virion production to aid the escape of the virus

at the cell surface [6,42]. However, the presence of E4 is not essential for viral transformation or capsid assembly [43].

E5 is a short 83-amino-acid hydrophobic membrane protein [44] with a role in HPV-associated cellular transformation [45]. The protein is thought to act early in infection, but may also contribute to later phases of the viral life cycle [46]. The E5 protein is known to play a role in the evasion of immune surveillance by preventing the transfer of the host MHC I complex to the cell surface. By compromising the activation of the cytotoxic T-cell based immune response [47]. E5 displays weak oncogenic properties such as the ability to enhance HPV 16-induced immortalisation of human keratinocytes [48], and an association with anchorage-independent growth of human keratinocytes in soft agarose [49]. It has been suggested that E5 may also disrupt endocytic trafficking [50,51] and down regulate gap junction communication in the W12 cell line [52].

The E6 gene encodes one of the two crucial HPV transforming proteins [53] that help to provide a suitable environment within the host cell for the viral life. The E6 protein also plays an important role in carcinogenesis. The major role of E6 is to bind to and cause the degradation of the cellular regulatory protein p53, allowing the virus to circumvent the cell's apoptotic response. This is discussed in further detail in section 4.2.1.

The E7 protein acts as the other major HPV oncogene, targeting the cell cycle regulator protein pRb (retinoblastoma protein) for degradation. The transformation potential of HPV is significantly increased by the presence of the E7 protein [53], which disrupts the relationship between cell differentiation and proliferation in normal keratinocytes, allowing the virus to replicate [2].

L1 encodes the major viral capsid protein which constitutes 80% [54] of the icosahedral capsid [55]. The L1 protein is able to self assemble into virus-like particles (VLPs) even in the absence of the L2 capsid protein or the viral genome [56]. VLPs have been investigated as a possible HPV vaccine source. They are morphologically and immunologically similar to normal virions, and unlike denatured L1 protein VLPs are able to illicit an immunological response [57]. *In vivo* the presence of E2 in combination with L1 is thought to increase the efficiency of encapsulation and infectivity [58,59].

The L2 protein forms the minor protein component of the viral capsid. The exact function of L2 within the capsid is unclear, but it is likely that it plays a role in the infectivity of the HPV virion [8]. It has been suggested that a single L2 unit is located within each capsomere [60], with the C-terminal region of L2 interacting with the central pore of the L1 protein [61]. In addition to its structural function in the viral capsid, L2 also has the ability to bind DNA, and is therefore thought to have other roles during the viral life cycle. Immediately post-infection L2 is thought to be involved in the transfer of uncapsulated viral DNA from the cytoplasm to the nucleus [6,22,62], while later in the viral life cycle the protein is thought to have a role in the selective encapsulation of the viral DNA [63]. Expression of both the L1 and L2 proteins appears to be restricted to the upper epithelium, although mRNA of both genes is present, but untranslated in the lower regions of the epithelium [64,65].

The LCR or upstream regulatory region (URR) is a non-coding region of 850bp located between the early and late ORF, accounting for approximately 12% of the total viral genome [1,66]. This region contains glucocorticoid response elements, *cis* regulatory elements (CREs), the origin of replication [8,67], and also a number of other control regions that aid the regulation

of viral transcription and replication [66]. The tissue tropism of the papillomaviruses is mediated by epithelial specific enhancers located within the LCR [68], which are controlled by the binding of transcription factors, such as nuclear factor 1, in an epithelial cell specific manner [69]. The promoter p97 (HPV 16) is located upstream of the E6 ORF within the URR, and regulates the transcription of both the E6 and E7 genes [37]. p97 possesses a basal activity in primary human keratinocytes that can be modulated by the full-length E2 protein [70-72], acting as a weak activator of p97 and leading to a two-fold increase in activity, or alternatively as a strong repressor of the promoter, causing a hundred-fold decrease in activity, with regulation thought to be concentration dependent [37].

The viral E2, E6, and E7 genes play important roles in the behaviour of the episomal virus and make a substantial contribution to creating the post-integration environment. The roles of these genes are examined below and in section 1.5.

1.1.5. HPV 16 E2

The HPV E2 protein is made up of three functional regions: the N-terminal transactivation domain through which it associates with the E1 protein, the hinge region, and the C-terminal DNA binding domain [6,73-75]. To operate normally E2 requires functional DNA binding and transcriptional activation domains [76].

When acting as a transcriptional regulator in HPV 16, E2 dimerises and associates with four highly conserved palindromic sequences (5'ACCN$_4$CGGT 3'[77]) located within the URR [37]. Once bound E2 recruits E1 to the origin of replication, and acting as a DNA helicase E1 [78] together with E2 instigates a localised distortion of the DNA structure. This enables the binding of additional E1 proteins, which displace E2 and allow the recruitment of the host

replication machinery to the DNA [6]. This machinery includes DNA polymerase α-primase [79,80] which assists in the initiation and elongation of the DNA in preparation for replication [81]. The role of E2 in mediating replication may also involve interaction with the cellular protein DNA topoisomerase II-beta-binding protein 1 (TopBP1), which is thought to have roles in numerous processes such as transcription and replication [82-85]. For transcription and translation to occur E2 must bind the most distal E2 binding sites (sites 3 or 4 in HPV 16), with other cellular factors interacting with the enhancer elements located within the URR [75,86-89]. Low levels of the E2 protein are associated with the initiation of E6 and E7 transcription via activation of the p97 promoter (HPV 16) in combination with p300 and the CCAAT enhancer-binding protein α (C/EBPα) [90]. However, as E2 levels increase, the activity of the p97 promoter is inhibited [6], probably due to the rising levels of E2 protein providing increasing opportunities for interaction with the more proximal binding sites, displacing the cellular transcription factors such as Sp1 and TBP (TATA-box-binding protein) required for the activation of p97 [6,37,75,88].

The E2 protein has been shown to have a role in ensuring the correct segregation of viral genome during host cell division. It acts as an anchor, tethering the viral DNA to the mitotic chromosome [6,16,91-93]. In order to achieve segregation E2 has been proposed to interact with a range of proteins including Brd4 (described in BPV) [94], ChlR1 (described in BPV, HPV 11 and HPV 16) [95,96] and TopBP1 (described in HPV 16) [82].

In the latter stages of the natural infection, as the virus reaches the upper regions the epithelium, it no longer requires cells to be maintained in a replication-competent state; this change in behaviour is thought to be signalled by increasing levels of E2. The rise in levels of the E2 protein within the cell leads to an increased inhibition of the p97 promoter and a

subsequent down regulation of E6 and E7. This causes the loss of the virally-induced replicative environment through a HPV controlled mechanism [6].

1.1.6. HPV 16 E6 and E7

HPV E6 is a small protein of only 150 residues [97] containing two domains, E6 N-terminal (E6N) and E6 C-terminal (E6C). Each of these 75 amino acid regions encodes two zinc binding domains containing two cystine-X-X-cystine (CXXC) motifs [98]. Tandem copies of this carboxyl terminal motif are also found in the HPV E7 protein, suggesting a common evolutionary ancestry for both viral proteins [99].

The E7 gene encodes approximately 100 amino acids forming a small acidic polypeptide that acts as a phosphoprotein. Due to its short half-life of less than 2 hours, the E7 protein is found at low steady state levels within the cell [100]. The amino terminal of the protein contains a casein kinase consensus phosphorylation site [2], while the carboxyl terminal encodes the zinc binding domain shared with E6 [101]. Many interactions of E7 with both nuclear and cytoplasmic proteins occur via the carboxyl region of the protein [2]. Immunofluorescent studies have shown that E7 is mainly nuclear. However, the exact import mechanism is unclear as no obvious nuclear localization sequence has been identified [102]. A number of non-nuclear E7 targets do exist, suggesting that at some point a fraction of E7 may be present in the cytoplasm [100]. Studies have shown that the absence of the E7 gene leads to a failure to amplify the viral DNA and reduced production of the L1 capsid protein [27].

1.1.7. E6/ E7 Gene Transcription

Most eukaryotic organisms produce monocistronic mRNA encoding only a single ORF. However, the presence of multiple ORFs in a single mRNA transcript (polycistronic) is seen

in some viral and cellular mRNA [103]. The human papillomavirus genome is transcribed as bi- or polycistronic sequences that encode multiple viral proteins [104], with the individual genes expressed by alternative splicing of the viral mRNA transcripts. The splicing pattern varies with the phases of the viral life cycle, leading to the changes in protein expression seen during the viral infection [103].

The high risk HPV types have been shown to express both the E6 and E7 genes from a single promoter, while in the low risk HPV types each gene contains its own promoter [105]. The E6/E7 mRNA transcript contain 3 exons and 2 introns [106], with the E6 start codon (AUG) located 5' to the E7 start codon [107]. However, this pattern of E6/E7 transcription is not found within the low risk HPV types where each gene is transcribed from its own promoter [103,108].

HPV 16 has been shown to produce three different E6/E7 transcripts as a consequence of alternative splicing of the pre-mRNA; the full length transcript E6/E7 can be alternatively spliced to form E6*I or E6*II [107,109]. The E6*I transcript is formed by the removal of intron 1 [64] located within the E6 ORF, at nucleotides (nt) 226-409; the E6*II form utilises the same splice donor site at nt 226, but an alternative splice donor site at nt 526 [106,107]. The full length E6/E7 mRNA generates the 16kDa E6 protein with the translation of the E6*I transcript producing a truncated ~8kDa version of the protein that corresponds to the N-terminal region of the full E6 protein [110].

In monocistronic mRNA, the initiation of translation occurs via ribosome scanning; however, in polycistronic mRNA where the common promoter is located upstream of the initial ORF, any subsequent translation of a downstream gene is inhibited by the presence of the first ORF [108]. The E7 ORF, which is located downstream of the E6 ORF, can be translated from the full

E6/E7 and perhaps the E6*I mRNA transcript. Translation of E7 is reported to occur at 25-35% of the E6 level [103], and is thought to be achieved via a leaky scanning mechanism. Leaky scanning occurs where ribosomes bind at the 5' end of the E6/E7 mRNA, but ignore the E6 start codon and continue to scan the transcript until the later E7 start codon is reached; here efficient and accurate translation of E7 can be initiated [103,108]. However, an alternative explanation is provided by Glahder *et al* (2003) [108], who have identified a putative E7 promoter (P542) within the E6 ORF that, although weak, would appear to be able to regulate E7 expression, and therefore provide an alternative mechanism for independent initiation of E7 translation.

The function of the E6*I transcript is unclear; it may simply be used as a template to produce the E7 protein [109]. Alternatively, the translated protein may act to attenuate the levels of the functional E6 protein by reducing the levels of the full length E6/E7, allowing equalisation of E6 and E7 protein expression [103]. It has been reported that the E6*I protein may also interfere with interaction between the full length E6 and cellular E6-AP, preventing the ubiquitin labelling of proteins for proteasomal degradation (section 1.3.1) [111,112]. E6*I would therefore permit the reactivation of a number of cellular proteins important in the stress response, including p53 and the anti-apoptotic proteins BAK [113], BAX [114], and c-Myc [115], allowing the initiation of cell cycle arrest and apoptosis.

1.1.8. The Role of E6 and E7 in Carcinogenesis

HPV E6 and E7 work together in both the normal viral life cycle and also during malignant progression. Although these proteins interact with different cellular targets and undertake distinct roles in the viral lifecycle, the expression of both the E6 and E7 appears necessary for the efficient immortalisation of keratinocytes. E6 has been shown to have a weak effect at the

promotional stage of carcinogenesis associated with the formation of benign tumours, but where benign tumours undergo malignant conversion E6 was found to act strongly [28]. Therefore, although E6 has a reduced effect in the initial production of benign tumours, it does create a more rapid conversion from benign to malignant forms [28]. In contrast to E6, HPV E7 acts primarily at the early stages of carcinogenesis supporting the formation of benign tumours; its contribution to actual malignant conversion is low in comparison to the E6 protein [28].

1.1.9. Integration of the HPV Genome into Host DNA

Premalignant lesions typically contain episomal HPV [116] with the integration of the viral DNA forming a critical early event in oncogenic progression, leading to consequences for both host and virus [117,118]. Integration is an important step in HPV associated neoplasia, although alone it appears to be insufficient to cause malignant progression [119]. Integrated HPV can be present as single copy integration which can occur at more than one location as seen in the cancer cell line SiHa, which contains 2 copies of the viral genome [119]. Alternatively, integration of head-to-tail tandem repeats of the HPV genome can occur within the host genome as shown in the CaSki cell line, which contains 600 copies of the viral genome [119]. Both types of integration pattern are seen in cell lines such as those mentioned, and also *in vivo* [119,120].

Certain oncogenic viruses such as hepatitis B are associated with preferential integration close to host oncogenes or tumour suppressor genes such as hTERT and the platelet derived growth factor (PDGF) receptor [121]. Post-integration alterations in the regulation of these host genes can provide an advantage to the infecting virus [119]. Integration of HPV appears to convey no advantages to the virus itself, with the disruption of viral genes leading to non-productive

infections as later events required for virion production are not supported in the altered post-integration environment [5]. *In vitro*, integration is associated with the development of genomic and phenotypic abnormalities similar to those seen in cervical neoplasia *in vivo* [117].

The site of viral integration within the host genome is not associated with any specific genomic region or cellular motif [5,122], although it has been suggested that in some circumstances genes surrounding the integration site may, if appropriate, contribute to the development of pre-malignant lesions [123]. However, there does appear to be some preference for integration within areas of the host genome known as 'common fragile sites' (CFSs), with high risk HPV types integrating into known CFSs in at least 38% of cases studied [124]. These loci are areas of the normal chromosomal structure prone to breakage in response to stimuli such as tissue culture conditions and chemical agents. These areas are characterised by constrictions, gaps, or breaks within the chromosome structure [125]. The preference for integration within these sites may be purely due to their fragile nature, or their proximity to advantageous host sequences [5]. As foreign DNA vectors show a similar frequency of integration within the CFSs (44%) it appears that these areas are relatively amenable to this type of integration event [5]. It is possible that E6 and E7 induced genetic instability may increase the frequency of CSF breakage and hence increase the opportunity for integration events [5]. A possible predisposition for integration into host genes involved in important cellular mechanisms such as cell division and differentiation has been identified [122]. Frequent transcription of these genes leads to a more open DNA conformation within those regions of the genome, making these areas more accessible to integration [122].

In order to integrate, the viral genome must be linearised by cleavage of the circular episome leading to the disruption of E1 and E2 ORFs [126]. Evidence from cell lines such as W12,

suggests that successful integration does not occur in any other region of the viral genome [119]. This implies that either the E2 gene represents a 'recombinational hot spot', or more likely that cells integrated through E2 disruption have a growth advantage over those where other regions of the viral genome are effected [119]. The mutational inactivation of E1/E2 has been shown to enhance the transforming potential of a number of papillomavirus types [127], leading to an increase in keratinocyte life span [128].

Although the E6 and E7 genes are consistently maintained within the integrated viral genome, the loss of E2 transcriptional control of the p97 promoter leads to a notable increase in their expression, causing a range of effects on both virus and host [42] (section 1.5). Integration can also cause the formation of a viral-cell fusion transcript, where the viral poly-A sequence located at the 3′end of the mRNA is removed [119]. This leads to an increase in the stability of the remaining E6/E7 mRNA due to the absence of the instability elements contained in this region [111,129], leading to further rises in viral oncogene levels [119].

Where numerous separate integration events are present within the host genome, research suggests that selection occurs for cells where only one or at most two actively transcribing copies are present [5,30]. The remaining viral DNA is thought to become transcriptionally silenced via methylation of the viral URR [5,30]. Where integration of concatemers of viral DNA has occurred the viral sequences adjacent to the cellular DNA at the host-viral junction become disrupted in the E2 region. The internal HPV genomes may contain intact copies of the E2 ORF [130]. However, it appears that only the viral sequences located at the host-viral junction containing the disrupted E2 ORF are transcriptionally active [30].

The episomal context in which integration of viral genomes occurs has been suggested to substantially influence its ability to affect both viral and host behaviour [5]. Overexpression of E2 experimentally appears to have little effect on transcription from episomal HPV 16. However, the addition of E2 to cells containing integrated HPV 16 shows that, within this context, E2 mediates a strong reduction in transcription [5,131]. Experimental data provides evidence for mixed populations of episomal and integrated HPV. Peitsaro *et al* (2002) [118] studied 31 lesions with 29 shown to contain mixed populations of episomal and integrated viral DNA. Lesions containing a greater proportion of integrated sequences were shown to undergo more rapid carcinogenic progression [118]. Pett *et al* (2007) [5] have suggested that in a cell containing a mixed population of episomal and integrated HPV the episomally expressed E2 may be able to exert transcriptionally repressive effects over the integrated DNA, hence maintaining control of viral gene expression [132]. This is illustrated by the parental W12 cell line (section 1.6.3.1) in which the loss of remaining E2 expressing episomes occurs prior to the post-integration increases in E6 and E7 expression [133]. It appears that integration alone is insufficient for production of a predominantly integrated population. To achieve this, a separate event involving the loss of any remaining episomes also seems to be required [133].

1.2. Low and High Risk HPV

The human papillomaviruses infect a range of both cutaneous and mucosal locations within the human body. The cutaneous viruses are found in areas such as the surface of the hands and feet and are largely benign [42], while the mucosal types that infect the genital and oral regions have a greater propensity for malignancy.

HPV types can be assigned into two main categories according to whether they pose a low or high risk of carcinogenesis [54]. Viruses within these two categories maintain many similarities,

but crucial differences have led to changes in certain aspects of their behaviour and subsequently their cancer risk. Even within these risk categories there remains considerable variation in behaviour, particularly amongst the high risk viruses where persistence and malignant progression vary considerably [134]. The mucosal low risk genotypes such as HPV 6, 11, 40, and 42 are associated with benign lesions such as anogenital warts (mucosal condylomata acuminata [135]) which affect 1-2% of young adults in many countries [6]. Cutaneous HPV 5 and 8 are classified as high risk and are associated with epidermodysplasia verruciformis (EV) which is especially common in immunocompromised individuals (reviewed in [9]). The high risk mucosal viruses include HPV 16, 18, 31, 33, 35, 45, 56, and 58 [6]. These high risk viral types are not only associated with benign lesion such as warts, but are also implicated in anogenital cancers such as carcinoma of the cervix [54,135-137] and oral cancers such as oropharyngeal carcinoma [138]. Two specific high risk types, HPV 16 and 18 are responsible for more than 90% of cervical and greater than 20% of oral cancers [106].

1.2.1. Low Risk HPV

Low risk HPVs, particularly types 6 and 11, are associated with the formation of benign lesions and are not seen as posing a significant risk of malignant progression. However, these low risk types have been found associated with malignant lesions [139-145], and in the case of HPV 6 no functional differences have been found between the viral genome extracted from benign warts and those associated with malignant lesions [142].

Within the high grade HPV infected lesions a major alteration in the behaviour of the host keratinocytes is seen. In both the normal epithelium and benign lesions the dividing cells are confined to the basal layer, losing this ability to divide as they leave this layer and migrate up

the epithelium. However, within the high risk lesions dividing cells are seen to spread up into the suprabasal layers of the epithelium [30].

The behaviour of low risk viruses may be largely explained by the properties of their E6 and E7 viral proteins. These proteins are potentially oncogenic, but in the low risk viruses E6 and E7 possess a lower binding efficiency than their high risk counterparts for cellular p53 and pRb [146,147] leading to a decrease in their ability to cause damaging cellular disruption. The low and high risk types also show differences in the localization of E6 and E7 within the cell [148]. Both the low risk proteins tend to form punctate patterns within the nucleus, corresponding to the PODs [148]. However, the high risk proteins show differential localization patterns; for example HPV 18 E6 is found in both the nucleus and cytoplasm, including some membrane locations, allowing the virus to interact with membrane-associated host proteins that often have roles in signalling pathways [148]. The HPV 18 E7 protein localises predominantly to the nucleus, forming a diffuse pattern [148]. The distribution of high risk E6 throughout the cell allows interaction with a wider range of host proteins than the nuclear bound low risk types. This is likely to lead to an increased ability to influence the host cell compared with a low risk infection [148].

Most low risk HPV types characteristically do not possess a functional E5 protein, due to the absence of a definable homologous E5 ORF and/or a translation start codon [134]. As E5 is associated with increased transforming ability this absence likely contributes to the benign nature of the low risk infections (section 1.1.4).

Replication in low risk viruses appears to be concentrated in a location close to the PODs [149]. The function of the PODs is unknown, although they may have a general role in

carcinogenesis as they are disrupted in acute myelocytic leukaemia. A range of viral proteins are targeted to these domains, including several regulatory proteins encoded by other DNA viruses [8] such as herpes simplex virus type 1 (HSV-1) [150]. These are targeted to the PODs at an early stage in the viral infection [8] and are thought to be vital to viral replication [151,152]. This localization of low risk HPV may allow them to better utilize the cellular structures and proteins found within the PODs for functions such as viral packaging [148]. This strong association of viral replication with the POD region of the nucleus is not seen in high risk HPV types and may contribute to the attenuated viral replication cycle seen with the high risk viruses in comparison with the low risk types [41].

1.2.2. High Risk HPV

The incidence of HPV infection varies between populations, but is reported to be between 20-40% amongst young women (mean age 25yrs) [6,153], although the life time risk of HPV infection is approximately 80% [154]. HPV infections resolve within 18 months in approximately 80% of cases. This in combination with the adaptation of the immune system, helps to account for the decrease in incidence with increasing age [6,155]. Despite the relatively high prevalence of HPV infections, in 2004 only 2726 cases of cervical cancer were diagnosed within the UK [156]. The high risk HPV types are aetiologically linked to more than 99.7% of all cervical cancers [157], with HPV 16 the most commonly found [158].

Where individuals are unable to clear a high risk HPV infection, cervical intraepithelial neoplasia (CIN) may develop; these lesions then form the precursors to cervical neoplasia. A Costa Rican study found that 19.9% of the HPV 16 positive women were diagnosed with CIN3 or neoplasia either at the beginning of the study or within 5 years [134]. Persistent infection is associated with continuous expression of oncogenic E6 and E7 genes leading to

maintained stimulation of S-phase and cell proliferation, and sustained inhibition of the p53 pathway (sections 1.1.4, 1.1.8-9, 1.13 and 1.5.1). These factors may provide a mechanism by which unresolved mutations are able to accumulate within the cellular genome, potentially contributing to carcinogenic progression. However, evidence also suggests that a more rapid onset mechanism may be present in some cases [6,159].

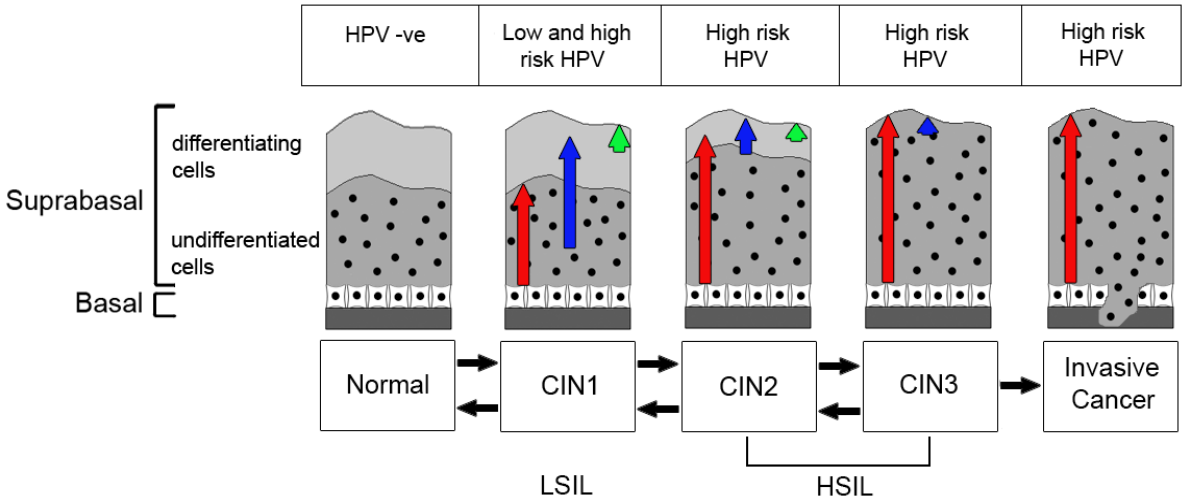

Figure 1.4. The progression of a normal uninfected epithelium to a HPV invasive associated cervical cancer, indicating infection status and histological staging. The expression of the HPV proteins within the undifferentiated and differentiating cells of the suprabasal epithelium are shown; the red arrows indicate the presence of the HPV oncogenes E6 and E7, the blue arrow the remaining early genes and the green arrow the late capsid proteins.

HPV-associated carcinogenesis is a multi-step process where infected cells pass through several stages before forming a carcinogenic lesion [28]. Progression between the different grades is associated with alterations in the behaviour both of the virus and host cell. The lowest grade lesions are described as low grade squamous intraepithelial lesions (LSIL) or CIN grade 1 (CIN1). These can reversibly progress to high grade SIL (HSIL) also defined as CIN2/3. Further irreversible progression to cervical neoplasia may then occur (figure 1.4). Initially viral infection leads to the formation of self limiting warts and precursor lesions [28]. These are characterised by cellular abnormalities which are confined to locations within the epithelium with no invasion of the underlying tissue. These CIN1 lesions are associated with

relatively normal viral gene expression patterns, often maintaining capsid protein production in the upper suprabasal layers, an occurrence less common in the higher grade lesions [6,160]. Persistent infection, in combination with other factors, provides a possible mechanism to enable these lesions to progress to high grades where abnormal cells become apparent throughout the epithelium [28]. The CIN2/3 lesions display a greater alteration in viral gene expression, with increasing oncogenes levels, but a decrease in the remaining early and late viral proteins causes a notable reduction in the productive stages [6]. These high grade lesions may progress further to form an invasive tumour. This often occurs after a prolonged viral infection where the cell is subjected to chronic overexpressed E6 and E7. In most cases anogenital HPV infections are cleared within 1 to 2 years [134] with no lasting rise in cancer risk. However, persistent infection with high risk HPV has been shown to be associated with a considerable increase in the risk of cancer formation [161]. The probability of a CIN2 lesions progressing to CIN3 is estimated to be around 20%, with a subsequent risk of further progression from CIN3 to neoplasia of 40% [6,162]. Research has shown that lesions regress in approximately 70% of CIN1 cases [163], and in 28% of CIN2/3 [164].

In addition to viral persistence, other risk factors are also suggested to play a role in the development of cervical neoplasia. These include the presence of the glucocorticoid and progesterone hormones that influence viral gene expression or changes in methylation and chromatin organisation, altering viral gene expression of episomal and integrated genomes [6]. Smoking has been suggested to increase the risk of HPV-associated anogenital neoplasia by both epidemiological studies [165] and via the identification of significant amounts of tobacco-specific compounds such as nitrosamine 4-(methylnitrosamino)-1-(3- pyridyl)-1-butanone (NNK) in the cervical mucus of smokers [166,167].

The interaction of high risk HPV with the cellular regulators p53 and p21 is vital for the successful replication of the virus, but these interactions have important consequences for the host, particularly in the presence of integrated HPV. The normal function of both p53 and p21 is described below, and the relationship with HPV discussed in sections 1.5.1-2.

1.3. Cellular Regulation by p53 and p21

1.3.1. p53 –'The Guardian of the Genome'

The tumour suppressor gene p53, often termed 'the guardian of the genome' [168], plays a pivotal role in monitoring, regulation and decision making within the cell. p53 is a member of a family of p53-related transcription factors which also includes p63 and p73 [169]; these proteins share the 3 principal functional domains as discussed below, with the central region most highly conserved within the group [169]. In response to a range of cellular stresses, p53 interacts with and co-ordinates numerous cellular components in an attempt to protect the whole organism from the proliferation of cells containing DNA damage or potentially malignant changes [170]. p53 participates in deciding the course of action to be taken in response to the stress stimuli. The cell may try and repair the damage and if successful can allow re-entry into the cell cycle. However, if the stress is too great or repair unsuccessful the only available option may be to apoptose the cell. This important cellular protein is thought to have varying direct or indirect roles in a wide range of processes including cell cycle regulation, genetic stability, blood vessel formation and apoptosis [171]. The absence or mutation of p53 is found in at least 50% of human cancers, illustrating the vital role of p53 within cell cycle control [172,173].

p53 is a 393 amino acid protein which can be divided into 3 distinct structural domains; the amino-terminal domain, the central core region, and the carboxyl terminal domain [174]. The amino terminal region contains the p53 trans-activation domain and also the PXXP motif which has a role in the induction of p53-dependent apoptosis [175]. The central core domain located between residues 102-292 contains the vital DNA binding domain required for transcriptional activity [174]. The carboxyl terminal contains both the nuclear localisation signals and oligomerisation domains. This region is particularly important for the assembly of activated p53 tetramers [174]. Also, sequences near the terminal end of this region are involved in the negative regulation of p53 DNA binding [175].

Inactive p53 is maintained in a latent form [176] with a short half life determined by the rate of proteasomal digestion [138,177]. Proteasomes are found within both the nucleus and cytoplasm, and act as protease enzymes involved in the regulation of protein levels within the cell via degradation [178]. For efficient p53 degradation it appears that the export of the protein from the nucleus to the cytosolic proteasomes is preferable. However, a reduced rate of degradation can be undertaken by the nuclear proteasomes [179]. The labelling of p53 for degradation is undertaken by the nuclear phosphoprotein Mdm2. This prevents the interaction of p53 with transcription machinery and acts as a cellular E3 ubiquitin ligase (figure 1.5) [180,181]. In turn, p53 regulates the expression of Mdm2, creating a negative feedback loop. Ubiquitination acts as a signal allowing the protein degradation machinery to recognise the unwanted labelled protein. The labelling process is undertaken by a multi-enzymatic cascade as summarised in figure 1.5 [182], utilising the group of cellular enzymes E1-4. Initially the ubiquitin peptide is activated by the ubiquitin-activating enzyme E1. It is subsequently transferred to the C-terminal of the target protein [171], either directly by one of the E2 ubiquitin-conjugating enzymes, or indirectly via an E3 ubiquitin-protein ligase such as Mdm2

[182]. Mdm2 is responsible for mono-ubiquitination of p53, but for degradation to occur further ubiquitin molecules must be added by the E4 ubiquitin ligase CBP (CREB binding protein)/p300 [183]. The polyubiquitin chain is recognised by the 26S proteasome which degrades the labelled protein in a ATP-dependent manner [182,184].

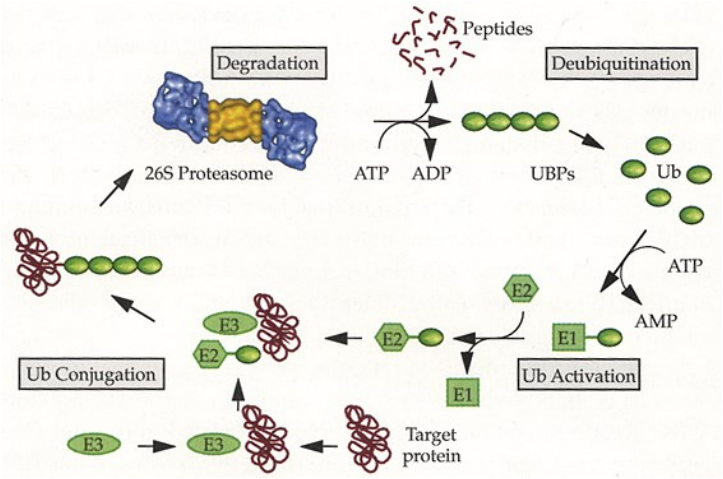

Figure 1.5: The ubiquitin/proteasome pathway for the degradation of proteins within the cell. Taken from Voges *et al* (1999) [185], reprinted, with permission from the Annual Review of Biochemistry, Volume 68 (c) 1999 by Annual Reviews www.annualreviews.org.

p53 is known to shuttle between the nucleus and cytoplasm by ATP-dependent transport in an unstressed cell [186]. It is therefore unsurprising that the protein contains both nuclear localisation (NLS) and nuclear export signals (NES) within its sequence. p53 is known to encode three NLS, which are rich in basic amino acids [186,187]. Also p53 contains two copies of the shorter NES, rich in hydrophobic leucine residues [188,189], with one NES is known to be located within the C-terminal tetramerisation domain of the protein [190]. When the cell is stressed, a bias develops allowing the accumulation of p53 within the nucleus utilising the NLS [176]. When not required, the p53 can be sequestered into the cytoplasm by a number of proteins, including Parc and mot2 that act as cytoplasmic anchors for p53 [176].

p53 can be activated by several different stimuli pathways [171], such as DNA damage in a protein kinase (ATM and Chk2) dependent manner [191], UV radiation, protein kinase inhibitors

in an ATR and casein kinase II dependent manner [192], or via incorrect growth signalling involving p14^{arf} signalling [193,194]. These different activation mechanisms have a common response as p53 becomes transiently stabilised via phosphorylation of residues primarily within the N-terminal region of the protein, causing an inhibition of Mdm2-mediated degradation [138,171]. Stabilisation arises by phosphorylation of serine and threonine residues located mainly within the amino-terminal transactivation domain of p53, but also via acetylation or phosphorylation at the carboxyl terminus [138,171]. The requirement for post activation modification is reflected in the terminal sequences of the protein. The amino terminal contains multiple phosphorylation sites, whilst the carboxyl terminal contains several phosphorylation, acetylation, glycosylation and sumoylation sites [176]. Altering the N-terminal sequences in this manner decreases Mdm2 binding and therefore aids the accumulation of p53 [171]. Modification of the C-terminal is likely to alter the conformation of this region, exposing the centrally located DNA binding motifs normally masked by the C-terminus [171]. Activation of p53 can also occur in response to p14^{arf} signalling which causes a rise in protein levels by reducing degradation via relocation of Mdm2 to a different nuclear region [171].

Activated p53 displays an alteration in its localisation from predominately cytoplasmic to nuclear enabling p53 to undertake transcriptional activity. The nuclear localisation of p53 therefore acts as an important regulatory mechanism [179,195]. Once in the nucleus p53 assembles into tetramers via the interaction of the C-terminal oligomerisation domains. This association masks the NES contained within this region and prevents nuclear export of p53, maintaining potentially transcriptionally active p53 within the nucleus [196,197]. In addition, enhanced nuclear accumulation and transcriptional activity can also be achieved by masking the NES by phosphorylation of the N-terminal at serine 15 [198] and 20 [176,199].

Activation of p53 initiates transcription from as many as 300 different promoter elements, leading to numerous downstream cellular effects [200] (reviewed in ref [201]). p53 therefore has the ability to influence a diverse range of cellular processes including cell cycle regulation, DNA repair, differentiation, development, gene amplification, DNA recombination, chromosome segregation, cell senescence and, where appropriate, apoptosis [170] (section 1.4). The transcriptional activity of p53 is highly regulated via a number of mechanisms, including transcription and translation, protein stability, and post-translational modifications [176].

The context of p53 activation and the environment in which it occurs can influence the outcome of p53 signalling. For example, activation of p53 in the presence of certain cellular proteins such as Myc inhibits transcription of the p21 protein, but allows the transcription of other p53 responsive genes, thus steering the cell towards a more directly apoptotic pathway instead of cell cycle arrest [202].

1.3.2. The p21 Response

An early event in p53 activation is the induction of cell cycle arrest. This can be achieved via the p53-dependent transcription of the cell cycle regulator $p21^{Waf1/CIP1}$, temporarily protecting the cell from p53-dependent apoptosis [203]. p21 is a member of the Cip/Kip family of cyclin-dependent kinase inhibitors (CKIs), with the family also including the proteins $p27^{Kip1}$ and $p57^{Kip1}$ [204]. This evolutionarily conserved protein contains 164 amino acids; the amino terminal region is required for the inhibition of the cyclin/cdk complex, whilst the C-terminal region binds proliferating cell nuclear antigen (PCNA) to inhibit DNA replication [204,205], and also contains a weaker second cyclin binding site [204] and a cyclin dependent kinase binding site [206].

The CKIs act by inhibiting members of the cyclin dependent kinase (cdk) family. These proteins are required for the control of the G_1/S and G_2/M cell cycle checkpoints [207]. Cdks become activated when bound by cyclin proteins; this active complex is then able to phosphorylate numerous cellular proteins including the pRb protein family. pRb binds and prevents functioning of the cell transcription factor E2F [208]. Phosphorylation of pRb causes the release of bound E2F, allowing the transcription of genes whose products are required for subsequent phases of the cell cycle, such as the replication machinery during S-phase [208]. In order to prevent cell cycle progression, p21 binds the cdk-cyclin complex preventing the phosphorylation of pRb, and causing the retention of E2F and the absence of E2F initiated transcription [209,210]. Increased p21 can also cause lower levels of DNA synthesis due the sequestration of cyclin-dependent kinase-2, cyclin E and PCNA (a cofactor of DNA-polymerase δ) into a quaternary complex [27,209]. p21 can interact or compete with many other proteins such as p300 transcriptional activator [211] and GADD45 a p53-responsive stress protein [212]. This enables p21 to influence diverse cellular pathways (reviewed in [204]).

The activity of p21 can be controlled by altering its transcription in either a p53-dependent or independent manner [213], or via post-transcriptional modifications such as mRNA stabilisation in response to ultraviolet C (UVC) [214] and protein stabilisation by kinases p38α and JNK 1 [204,215]. In the presence of viral infection the activation of p21 may represent a response to abnormal DNA synthesis within the suprabasal compartment, experimentally illustrated in organotypic rafts [27]. This p21 response has adverse consequences on the viral life cycle causing a reduction in the amount of possible viral replication by preventing entry into S-phase and mitosis.

The p21 pathway can be activated in a p53-independent manner by several different agents leading to transcriptional activation of the p21 gene [204]. The stimulating agents include phorbol myristoyl acetate (PMA), transforming growth factor-β (TGF-β), calcium, progesterone, E2F, and Trichostain A (TSA, histone deacetylase inhibitor, reviewed [204]). This p53-independent effect can be mediated through activation of the Sp1 protein sub-family of transcription factors, which causes the transcription of a wide range of genes including p21 [204,216].

1.4. Apoptosis

Cells are governed by strict physiological mechanisms that control the rate of proliferation and cell homeostasis. It is therefore vital that all cells have the intrinsic ability to undergo controlled cell death via apoptosis to maintain this homeostasis. Apoptosis is a multi-step, multi-pathway programme, which is tightly controlled by a range of cellular proteins. Faults or abrogation of the apoptotic system can lead to a net gain of abnormal cells which may ultimately lead to cancer.

In normal cells the apoptotic pathways originate in response to a range of stimuli such as DNA damage, hypoxia, or nutrient depletion [111] (figure 1.6). The intracellular component of apoptosis can be initiated via two main routes: the death receptor (extrinsic) or the mitochondrial (intrinsic) pathways, both sharing a common final pathway. Both routes utilize the cysteine aspartyl-specific proteases (caspases) throughout the process. These enzymes act within a cascade leading to the cleavage of specific cellular substrates [217]. Caspase-independent methods of cell death do exist, but their molecular basis is less well understood [218-220]. As the caspase free pathways share only some of the characteristics of apoptosis they are often defined as apoptosis/necrosis–like cell death or paraptosis [217]. The caspase family of

enzymes are part of a process which leads to the dismantling of the normal cellular structures causing biochemical and morphological changes within the cell that are characteristic of apoptosis [217]. Caspases are stored within the cell as inactive procaspases in order to protect the cell, but when required they are activated at the appropriate point in the cascade. Apoptotic signalling can occur through two distinct, but interacting signalling cascades; namely the 'extrinsic' or 'intrinsic' pathways, the route taken being highly dependent on the cell type and the type of upstream signalling received.

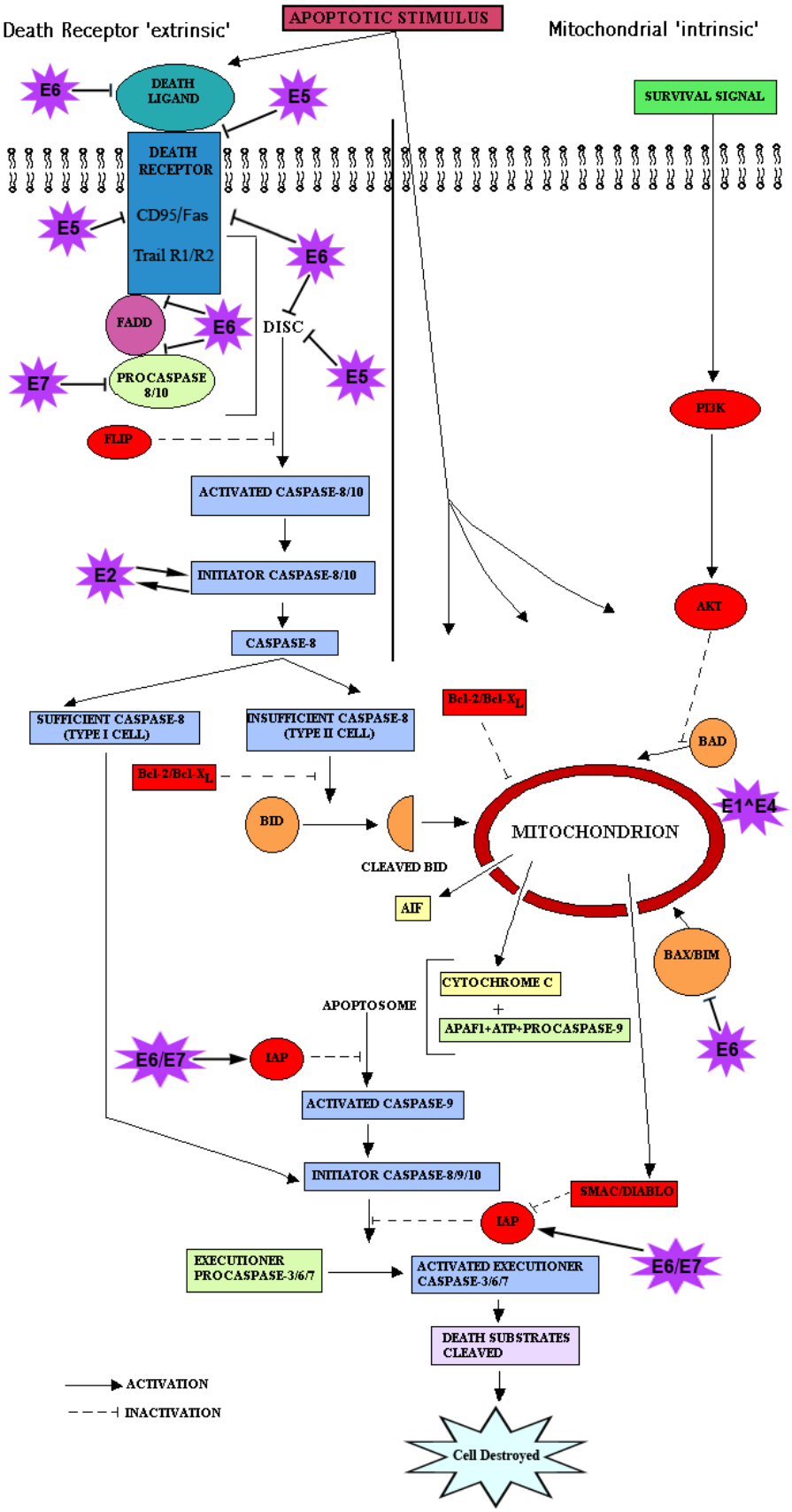

Figure 1.6: An outline of the basic apoptotic initiation pathways controlled by both pro-apoptotic and anti-apoptotic proteins (based on [1]), including the points of interaction by the HPV 16 proteins (see section 1.6.5 for further details).

1.4.1. Death Receptor Apoptotic Pathway

The 'death receptor' or 'extrinsic' apoptotic pathway is mediated by receptors located on the cell surface [217]. The death receptors are members of the tumour necrosis factor receptor (TNF-R) superfamily which contains at least 20 family members with varying functions [221]. The apoptosis related members of the superfamily contain an indicative intracellular 'death domain' of 80 amino acids involved in transmitting the apoptotic signal from the cell surface to the intracellular domain [221]. Pro-apoptotic ligands bind to appropriate cell surface receptors; these include CD95 (Fas/Apo-1 [222]), TNF receptor 1, TRAIL-R1 (TNF-related apoptosis-inducing ligand-R1), and TRAIL-R2, leading to oligomerisation of the receptors' death domain, facilitating interaction with the cytosolic adapter protein FADD (Fas-associated death domain protein, also known as MORT1) [111]. The TNF-R ligands also form a part of the wider TNF family [217], with ligand expression varying between cell types. The Fas ligand (Fas-L) is known to be mainly expressed by T lymphocytes [223] whilst the TNF ligand is expressed primarily by macrophages [221], illustrating the important role of the immune system in the initiation of apoptosis. Other ligands such as TRAIL have been shown to be expressed by many different cell types [221]. The recruitment of pro-caspase- 8 and -10 to the death domain–FADD assemblage creates the death–inducing signalling complex (DISC). Within the DISC, FADD interacts directly with the inactive procaspase enzyme; subsequently the procaspase is cleaved to form the activated 'initiator' caspase. DISC cleavage can be inhibited by FLIPs (FADD-like interleukin-1 β-converting enzyme-like protease, also known as FLICE/ caspase-8 inhibitory proteins), which share homology with procaspase-8, allowing them to competitively inhibit caspase-8 activation [217,224-227].

The quantity of activated caspase-8 produced by the CD95 pathway can vary between cell types. Type I cells including the B lymphoblastoma cell line SKW6.4 and the T cell line H9,

produce sufficient caspase to activate downstream apoptotic mechanisms independently. However, in type II cells such as the T cell lines Jurkat and CEM, the levels of caspase-8 activation are insufficient to independently initiate the full apoptotic cascade. Within these type II cells DISC formation is temporarily delayed and occurs at a lower rate than type I cells. Therefore these cells require the pro-apoptotic signal to be amplified [228]. In type II cells, activated caspase-8 produced at the DISC causes the cleavage of cytosolic BID, a member of the Bcl-2 family. Truncated BID is translocated to the mitochondrion and inserts into the membrane, where it activates BAX and BAK to cause mitochondrial release.

1.4.2. Mitochondrial Apoptotic Pathway

The mitochondrial or intrinsic apoptotic pathway is regulated by members of the Bcl-2 family, whose release is controlled by upstream regulators such as p53. The Bcl-2 family proteins can be either pro-apoptotic or anti-apoptotic [217], a summary of these pro- and anti-apoptotic proteins is shown in Table 1.1.

Anti-apoptotic Proteins	**Pro-apoptotic Proteins**	
Bcl-2	BAX	BLK
Bcl-X	BAK	HRK/DP5
Bcl-$_W$	BOK/MTD	NIP3
Mcl-1	BID	NIX
A1/BFL-1	BAD	NOXA
BOO/DIVA	BIM/BOD	PUMA
NR-13	Bcl-X_S	BMF
Bcl-X_L	BIK/NBK	

Table 1.1: The anti-apoptotic and pro-apoptotic proteins that aid the control of the mitochondrial pathway. [217]

The archetypal family member Bcl-2 (B-cell leukaemia/lymphoma 2) contains a transmembrane and four Bcl-2 homology (BH) domains. These regions can be used to classify the remaining family members [222]. The BH3 domain is common to all family members and is essential for the functioning of the proapoptic proteins [217,229,230]. The anti-apoptotic proteins share BH domains 1, 2, 4 [217]. Many of the Bcl-2 family members are

present within the outer mitochondrial membrane, where they function to stabilize the membrane that protects the cell from the toxic contents held within the mitochondria. The pro-apoptotic proteins can be subdivided into two main groups; the BAX family incorporating BAX (Bcl-2 associated X), BAK (Bcl-2 homologous antagonist/killer) and BOK (Bcl-2-related ovarian killer); and the BH3-only proteins including BID (Bcl-2 Interacting Domain), BAD (Bcl-2-antagonist of cell death), and BIM (Bcl-2-interacting mediator of cell death) [217]. These pro-apoptotic proteins have the ability to shuttle between cellular locations, such as the cytoplasm for BAX, BAD, and BID, or the microtubules for BIM. However, when apoptosis is induced they all translocate to the mitochondria [231].

1.4.3. The Common Mitochondrial Pathway

The release of pro-apoptotic factors from the mitochondria can be initiated by either the death receptor pathway (type II cells), the mitochondrial pathway or via other routes involving phosphatases, kinases or transcription factors (for example p53 and TR3/Nur-77/NGFI-B) [231], as shown in figure 1.6. The exact nature of the interaction between the Bcl-2 family, other mitochondrial proteins and the membranes is still unclear. The insertion of pro-apoptotic signal proteins into the mitochondrial membrane causes permeabilisation of both the outer (OMM) and inner (IMM) mitochondrial membranes [231]. The IMM effect is more transient and restricted to mitochondrial material of less than 1.5kDa, due to the importance of maintaining the electrochemical gradient for its vital role in cellular energy production [231]. One model suggests that the permeabilisation of mitochondrial membranes is controlled by a permeability transition pore complex (PTPC). This multi-protein complex contains an inner membrane component consisting of an adenine nucleotide translocator (ANT), a voltage-dependent anion channel in OMM, and various other proteins [231]. The action of the PTPC may be regulated by an interaction with Bcl-2 [217]. Alternatively, members of the pro-

apoptotic BH3-only family act as death sensors in the cytoplasm or cytoskeleton [217]. In response to an apoptotic signal they interact with the BAX protein sub-family, initiating a conformational change and insertion of the proteins into the mitochondrial membrane. Here they become oligomerised to form protein permeable channels [217]. The conformational change and oligomerisation of BAX and BAK are inhibited by the anti-apoptotic protein Bcl-2 [232]. The initial IMM permeabilisation may also lead to disruption of the osmotic balance of the organelle, causing swelling of the matrix and ultimately lysis of the OMM. The changes seen within the mitochondria in response to the pro-apoptotic signalling may also lead to disruption of ATP production via interruption of the electron transport chain and the creation of reactive oxygen species [233]. These changes within the mitochondria may also further stimulate the cellular stress response, potentially increasing pro-apoptotic signalling.

The increase in mitochondrial membrane permeability allows the release of a range of compounds from their store within the intermembranous space of the organelle [217]. Toxic compounds are normally held in these locations to prevent unauthorised cellular damage. The mitochondrial compounds include apoptogenic factors such as cytochrome c, which is a caspase activator, SMAC (second mitochondria-derived activator of caspase)/DIABLO (direct IAP binding protein with low pI), also a caspase activator, and AIF (apoptosis-inducing factor) a nuclease activator [231,234,235].

Within the cytoplasm, released cytochrome c interacts with cytosolic APAF1 (apoptotic protease activating factor-1) and subsequent binding of pro-caspase-9 then forms the apoptosome [217,236]. The binding of the pro-caspase to this structure allows it to be converted into an active initiator caspase, in an ATP-dependent manner [236].

One possible route for the inhibition of mitochondrion-induced apoptosis is to utilize extra cellular survival signals such as growth factors, cytokines, hormones, and adhesion molecule signals [217]. A lack of survival signals leads to a form of apoptosis known as 'death by neglect' [217]. These signals bind cytosolic PI3K (phosphatidylinositol 3-kinase), which activates AKT, causing deactivation of the BAD protein via phosphorylation [217]. The anti-apoptotic Bcl-2 and Bcl-X_L family members are normally located within the outer mitochondrial membrane and act to protect the cell from mitochondrial faults by preventing abnormal ion movement across the membrane [233].

1.4.4. The Common Final Pathway

As can be seen in figure 1.6 both the death receptor and mitochondrial pathways lead to the activation of a common group of 'initiator' caspases including caspases-8/9/10. In order to allow the continued progression of apoptosis these enzymes cleave and hence activate the inactive forms of caspases-3/6/7 forming the executioner caspases [217]. These executioner caspases are then able to amplify the apoptotic signal by cleaving each other, creating a proteolytic cascade [237] and allowing active controlled cellular breakdown to commence.

Apoptosis can be inhibited at the apoptosome or at the executioner caspase activation stage by the use of the IAP (inhibitor of apoptosis proteins) family of proteins. As illustrated in figure 1.6, these proteins bind caspases and prevent further function [217]. They may also act as an ubiquitin ligase, preventing apoptosis by promoting caspase degradation by the proteasome [217]. In turn, the IAPs can be inhibited by the mitochondrially produced SMAC /DIABLO, which bind IAPs and prevent the inhibition of caspase function [217].

1.4.5. Cellular Consequences of Apoptosis

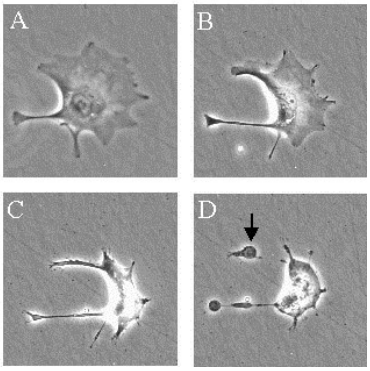

Figure 1.7: The images show time-lapse microscopy of a trophoblast cell undergoing apoptosis (Reproductive and Cardiovascular Disease Research Group, University of London [238]). Image D shows the 'blebbing' effect (marked by arrow) sometimes seen during cellular breakdown.

The activated executioner caspases cleave cellular substrates ('death substrates') leading to the characteristic changes associated with apoptosis [231], as shown in figure 1.7. As part of the apoptotic degradation, inhibition of the endonucleases is removed causing the cleavage of the nuclear lamins that form the lamina of the inner surface of the nuclear envelope [217]. This breakdown of the nuclear lamins forms a prerequisite to the later chromatin condensation and nuclear shrinkage [217]. The DNase CAD (caspase-activated deoxyribonuclease) and its inhibitor (ICAD) form a cytoplasmic complex inactivating the CAD under normal cellular conditions. DNA fragmentation occurs when ICAD is cleaved by the executioner caspaseses releasing CAD to fragment DNA [217]. Cytoskeletal proteins such as actin, plectin, Rho kinase 1 (ROCK1) and gelsolin are broken down, leading to cell fragmentation, blebbing and the formation of apoptotic bodies [217,236], as shown in figure 1.7d. Changes within the plasma membrane allow the exposure of signals such as phosphatidylserine, and alteration of surface sugar molecules. These changes act as signals to nearby phagocytic cells allowing recognition and engulfing of the apoptosed cell [239,240].

1.4.6. Apoptosis and p53

The pro-apoptotic function of p53 forms a vital constituent of tumour suppression [222]. As an important cellular regulator it contributes to both the intrinsic and extrinsic apoptotic pathways in a number of ways. p53 induces the direct or indirect transcriptional up regulation of a range of apoptosis related pro-apoptotic genes. Within the early extrinsic pathway p53 has been shown to transcriptionally upregulate the Fas component of the death receptor allowing increasing downstream apoptotic signalling [241]. However, this p53 function does not seem to be universal [222] and in some cases this induction of Fas is apparently not essential for p53-dependent apoptotic signalling [222,242,243]. The cell can achieve an initial rapid sensitisation to apoptotic signals by enhanced trafficking of the death receptor Fas protein from its stores within the Golgi [244], allowing a bridging response while *de novo* Fas transcription occurs. Another of the death receptor types TRAIL-R2 (KILLER/ DR5) is also upregulated by p53. Signals transduced though this receptor go on to activate a caspase-8-dependent cascade [245] (reviewed by [246]). However, these receptors are only found within limited regions such as spleen, small intestine and thymus [247]. The caspase enzymes perform central roles within the apoptotic network, it is therefore unsurprising that p53 signalling leads to an increase in caspase activation by transcription-dependent (e.g. caspase-1 [248]) and independent mechanisms (e.g. by increasing mitochondrial cytochrome c release, which causes increase caspase-9 activation) [222,249].

Pro-apoptotic proteins within the later extrinsic and also the intrinsic pathway are also upregulated in response to p53 signalling, allowing a more rapid induction of apoptosis. These targets include MAP kinase inhibitor PAC1 (phosphatase of activated cells 1) [250], Bcl-2 family members (PUMA, NOXA, BID, BAX), death receptors 4/5 [170], and apoptosome component APAF-1 [170]. By regulating the transcription of pro-apoptotic BID protein, p53 can

promote the inclusion of the mitochondrial component in the death receptor pathway [222]. A number of either directly or indirectly by p53 inducible genes are involved in the control of mitochondrial membrane integrity, including members of the Bcl-2 family [170] (table 1.1).

The induction of apoptosis by p53 can also be regulated in a transcription/protein synthesis independent manner. It is likely that in normal cells the transcription dependent and independent p53 pathways work together towards the common goal [222]. This is mediated by the localisation of a small fraction of the activated p53 population to the mitochondria [251]. The p53 fragment directly interacts with and inhibits the anti-apoptotic proteins Bcl-XL and Bcl-2, and also causes the oligomerisation of pro-apoptotic BAK. These interactions lead to depolarisation and subsequent permeabilisation of the outer mitochondrial membrane to release cytochrome c and other pro-apoptotic mitochondrial products [170].

The potentially p53-responsive p21 can act as a component of a pro- or anti-apoptotic cascades depending on the cellular requirements [204,252-254]. p21 is known to mediate and interact with the stress-activated protein kinase (SAPK) and p38 mitogen-activated protein kinase families of mitogen-activated protein kinases (MAPKs) [215], both of which have been implicated in apoptotic signalling [255].

In order to reduce the anti-apoptotic influence of p21 on an already apoptotic cell, caspase-3 [256] inactivates the protein by cleaving its C-terminal nuclear localisation signal, and also relocating it from the nucleus to the cytoplasm [192,257]. This cleavage and relocation means that p21 is not only physically distanced from its transcriptional targets within the nucleus [257], but also the absence of the C-terminal domain means it is unable to facilitate the nuclear

localisation of the cyclin/cdk complex, thus preventing any possible attempts to steer the cell from its apoptotic path [258].

1.5. The Influence of the Viral Genes on the Host Cell

In order to successfully replicate within the host cell, HPV must interact with numerous host systems. For replication to occur the virus must be present within a replication competent cell that is expressing the appropriate cellular machinery, for example by interacting with pRb. However, in making these cellular changes the cell's stress systems, such as those requiring p53, are activated, and therefore the virus must deal with these problems.

1.5.1. HPV and the p53 Pathway

The most dramatic effect on the p53 protein is seen in the presence of HPV E6, which induces the rapid ubiquitin-directed proteasomal degradation of p53. The E6 protein does not directly bind p53; degradation is instead achieved by the interaction of E6 with the host protein E6-AP [113]. This HECT domain (homologous to the E6-AP carboxyl terminal) protein acts as a cellular E3 ubiquitin ligase [113], functioning as a member of the proteasomal degradation pathway (section 1.3.1). Although p53 is not a normal substrate for E6-AP, this ubiquitin ligase has been shown to interact with and facilitate the degradation of p53 [259,260]. In the absence of HPV infection it is known to bind the cellular Src kinase family [261] and itself [262], but in the presence of HPV E6 this ubiquitin ligase is co-opted by the virus and induces the ubiquitination and subsequent degradation of p53 [263]. HPV 18 E6 has been shown to cause the redistribution of both GFP-tagged p53 and E6 to the cytoplasm and also an apparent decrease in levels of p53-associated GFP fluorescence in the presence of E6 [179]. Degradation of p53 interrupts a number of cellular pathways in which it normally functions, including those involved in the cellular stress response and genome protection. In this way p53

inactivation may contribute to chromosomal instability such as translocations and aneuploidy, which are seen in the presence of E6 [264].

Unlike E6, the presence of HPV E7 does not alter the normal p53 nuclear localisation or block its nuclear export [138]. The increased levels of p53 seen in E7 expressing cells are not associated with a rise in levels of transcription [138]. Instead raised p53 levels are likely to be a consequence of the enhanced half-life of the protein leading to its stabilisation [138] and also possibly post-transcriptional modifications [265]. This stabilised p53 maintains a wild type conformation and is apparently still able to undergo Mdm2-mediated proteasomal degradation [138]. This interaction of E7 with p53 causes a rise in p53 levels [177]. However, there is some uncertainly as to whether this bound p53 remains transcriptionally active [138,266]. Cells expressing the stabilised p53 grow rapidly, but do not appear to function normally during the apoptotic cascade where levels of the pro-apoptotic p53 targets BAX and TRAIL-R2 do not increase, and therefore the rate of spontaneous apoptosis remains unchanged [138].

1.5.2. HPV and the Cell Cycle

The papillomaviruses must disrupt the normal host control of cell cycle progression in order to replicate in normally replication-incompetent cells, as shown in figure 1.8. The checkpoints which regulate cycle progression are normally controlled by a fine balance of positive and negative regulatory factors, which are vital for normal cellular function [182]. HPV E7 is the primary viral protein responsible for disrupting normal cell cycle regulation; this is achieved by interactions with a range of host proteins overcoming cell-derived inhibition of cell cycle progression. However, without the cooperative efforts of several other viral proteins, particularly E6, the unscheduled proliferation induced by reactivation of the cell cycle would activate cycle arrest and/or apoptosis [267]. Although E7 is the primary viral

protein required to disrupt multiple mitotic checkpoints, the efficiency of this process is increased in the presence of the E6 protein. Therefore the cycle checkpoints retain a greater degree of functionality in cells expressing only E7 [268]. As this cell cycle effect appears to be largely dependent on the interaction of the viral proteins with p53 and pRb [268], the efficiency of this cell cycle control is likely to be reduced in low risk HPV types.

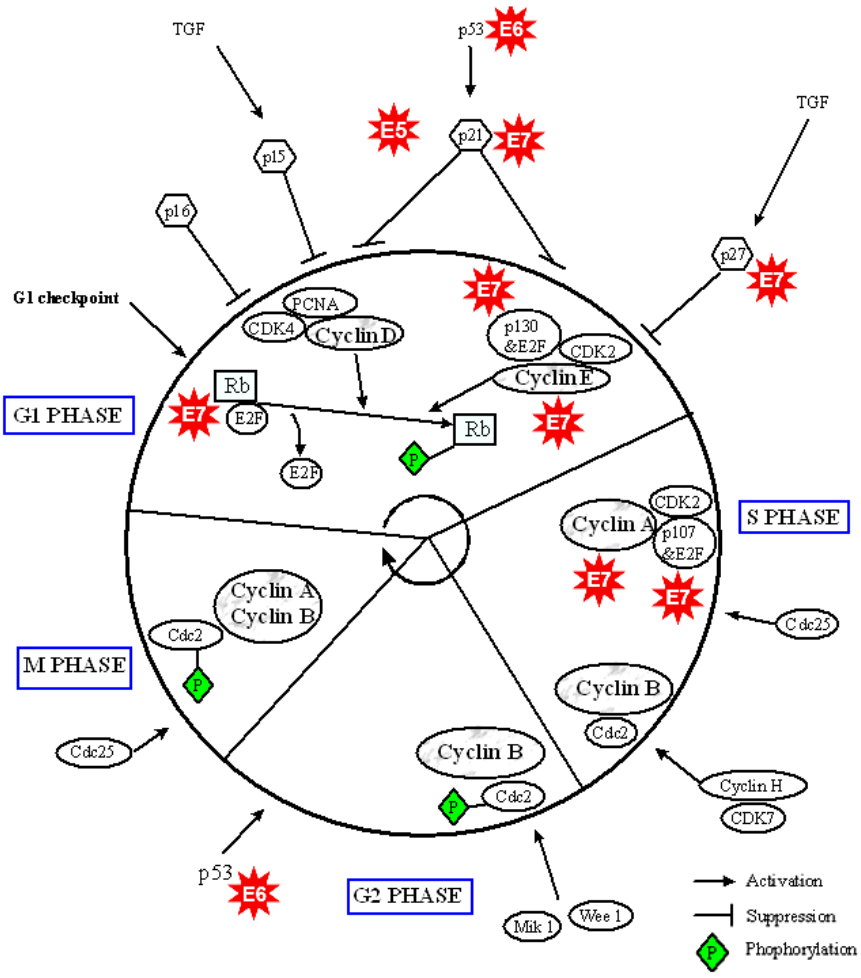

Figure 1.8: The eukaryotic cell cycle is influenced by many cellular factors such as the presence of cyclins and changes in phosphorylation. The cycle has many points at which the high risk HPV genes can influence the host cell cycle. Adapted from Southern and Herrington (2000) [53] with permission from Wiley-Blackwell Publishing.

pRb is a cellular inhibitory protein that associates with a number of proteins including the E2F family of transcription factors. The pRb-E2F complex helps to form the G_1/S checkpoint controlling the initiation DNA synthesis [2]; this is achieved by inhibiting E2F-induced transcription of a number of genes responsible for nucleotide synthesis (e.g. thymidine

kinase), replication (e.g. DNA polymerase α) and cell cycle progression (e.g. cyclin E, cyclin D1, c-myc, b-myb, and cdc2) [6,269]. In order to release E2F, pRb must be phosphorylated by CDK4/6 [1] at specific sites in either the C-terminal region or within the insertion domain of the protein [111,270]. By binding within this region E7 can prevent the interaction of pRb with E2F [271,272] and subsequently enable entry into S-phase. A single E7 protein can bind efficiently to multiple units of pRb and its related proteins p107 and p130, via the interaction of its LXCXE motif with the A/B pocket domain of the pRb family [2,273,274]. Mutations within this region of E7 lead to a reduction in the ability of HPV to transform cells, indicating the importance of pRb inactivation during transformation [275]. Increased degradation of pRb by E7 results in atypically high levels of transcription with a rise in the expression of cyclins A and E [276], either via increased transcription. In addition E7 is able to directly bind and activate the CDK/cyclin complexes independently of pRb [277,278]. E7 can therefore cause an increased level of active CDK2/cyclin A or CDK2/cyclin E complexes within the cell [276,278], helping to control entry into and progression through S-phase, and therefore increased levels enable free movement through S-phase [279]. The degradation of the other pocket proteins p107 and p130 by E7 [280,281] also assists in the HPV driven deregulation of the G_1/S transition [28]. When the inhibition of pRb and its related proteins is combined with E7 induced inactivation of cyclin dependent kinase inhibitors (CKIs) p21 and p27 [282], the break down of the E2F repressor complex results in enhanced progression to DNA synthesis and cell division maintaining the replication competent environment.

Levels of the p53 responsive protein p21, a CKI, are found to be elevated in cells containing wild-type HPV [27], aiding the manipulation of cell cycle checkpoints. Both E6 and E7 are known to interact with p21 and its fellow CKI p27, to manipulate the G_1/S checkpoint to allow progression [283,284]. The interaction of p21 with E7 is thought to occur via the carboxyl

terminal of the E7 protein [283] binding to the C-terminal region of p21 [191]. E7 competes with PCNA, as both processes require interaction via the same C-terminal region this potentially blocks PCNA-dependent inhibition of DNA synthesis and also prevents p21 from inhibiting the cyclin/cdk complex [204,285,286]. Interestingly it has been suggested that, during the productive phase of the viral life cycle, the E7 cell cycle functions may in fact be assisted by the presence of p21 [27]. It has been suggested that p21 may act as a scaffolding factor for the assembly of cyclin-cyclin-dependent kinase complexes facilitating cell cycle progression [27]. HPV E6 generates a relaxation the G_2/M checkpoint probably by interference with the p53 pathway, this allows an increased number of cells to enter mitosis with potential defects, such as multipolar spindles [287,288]. The ability of E7 to overcome the G_2/M checkpoint appears to only be functional when either p21/p27 levels are low, or expression of E7 is sufficiently high. Therefore this E7-mediated effect is more likely to occur in the presence of integrated virus [6,289]. The E5 protein has been shown to play a role in E6/E7 mediated cellular transformation, which is thought to be achieved by the inhibition of p21 [48,290].

HPV E7 has the ability to directly target pRb for proteasome degradation [291]. This may be achieved by the interaction of E7 with the 26S proteasome S4 subunit [2]. However, as S4 binding mutants can still efficiently destabilise pRb, another mechanism may also be available for E7-induced pRb degradation [291].

In contrast to the majority of HPV cell cycle related effects, the viral E2 and E4 proteins have the ability to assist in the reinstatement of the cycle checkpoints. E4 has been shown in certain HPV types including 16 [292] and 18 [6,18,293] to initiate cycle arrest in G_2 by preventing nuclear localisation of cyclin B/CDK1, and therefore counteract E7 induced proliferation [6]. In cells maintaining episomal HPV increased viral E2 transcription leads to activation of p53 and

pRb pathways [294], causing a reactivation of the G_1/S checkpoint, cell senescence and under some circumstances apoptosis [294]. The association of E4 with E2 shown for HPV 16/18 suggests that they may co-operate in the removal of the replicative environment aiding the later phases of a productive infection [6,295].

1.5.3. HPV and Host Genome Replication

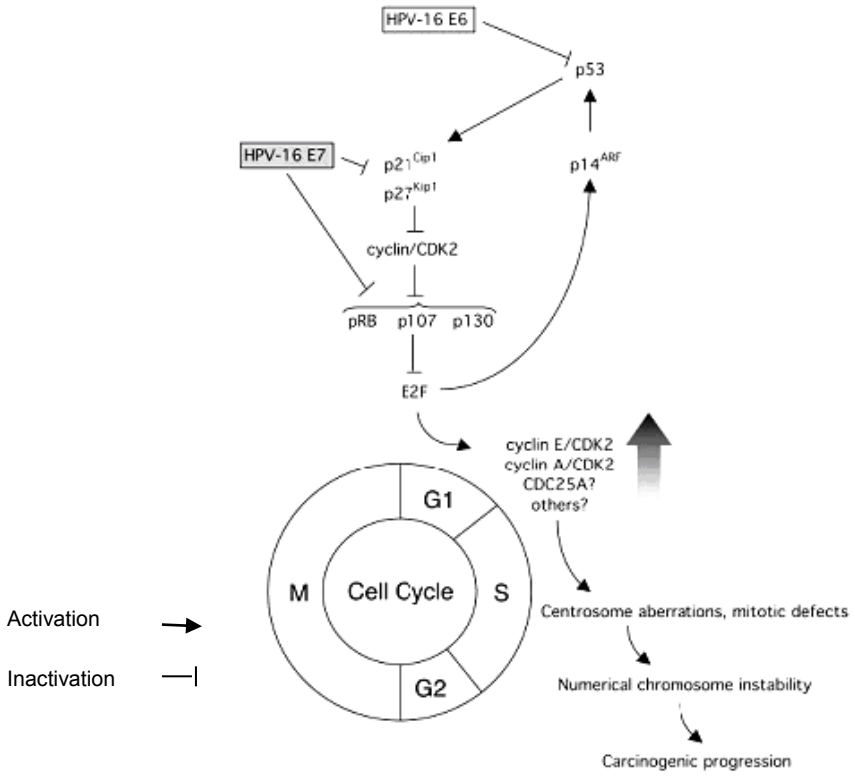

Figure 1.9: The HPV-16 E6 and E7 proteins cause the induction of genetic instability with the consequent probability of carcinogenic progression. This is achieved through the abrogation of the p53 (p21) pathway which leads to increased production of cell cycle regulators, and subsequent disruption. Image taken from Duensing and Munger, 2004 [296] , copyright © 1999-2008 John Wiley & Sons, Inc. Reprinted with permission of Wiley-Liss, Inc. a subsidary of John Wiley & Sons, Inc.

The human papillomavirus must interact with several different parts of the cell cycle regulatory pathway in order to promote an environment suitable for HPV replication and virion production. Several different HPV proteins contribute to this process; the roles of the central HPV oncogenes E6 and E7 are shown in figure 1.9.

HPV E5 is a trans-membrane protein that interacts with the vacuolar ATPase, preventing the influx of protons into acidic vesicles such as endosomes. Consequently, the normal vesicle recycling pathways for signalling molecules such as EGF are disrupted and an environment beneficial for viral replication is maintained (reviewed in [6]).

E7 is known to associate with proteins required for cell proliferation such as histone deacetylases [297], acetyl transferases [297] and the AP-1 transcription complex [298], allowing the virus to drive cellular proliferation [6]. The interaction of E7 with the histone deacetylases and acetyl transferases are thought to involve the C-terminal region of the protein [297].

High risk E6 proteins, but not their low risk counterparts, are known to associate with and cause the degradation of PDZ (*P*SD95/*D*iscs Large/*Z*O-1) domain containing proteins, by E6 binding a short 4 amino acid sequence at the C-terminus of these proteins [299]. The binding of PDZ proteins appears to enable HPV to mediate the reactivation of proliferation in the suprabasal layers [6,300]. PDZ proteins act as 'molecular organising centres', helping to co-ordinate numerous signalling pathways [9]. This group of proteins includes the MAGUK proteins (SAP97/Dlg [301] and MAGI-1, -2 and -3 [302]), MUPP1 and hScribble [303,304], and are known to be involved in cell polarity, cell-cell contact and proliferation. The PDZ proteins are also known to interact with other important cellular pathways, for example MAGI-2 and -3 interact with PTEN (phosphatase and tensin homolog), which forms a component of the protein kinase B (PKB/Akt) signalling pathway [305]. By down regulating PTEN, the PDZ proteins are able to influence the cell contact induced PKB signalling, directly effecting the regulation of growth and polarity. Interacting with other signalling pathways, allows the PDZ proteins to influence cell cycle progression and apoptosis (reviewed in [306]), metastasis (reviewed in [307]), and many other cellular pathways.

Prolonged expression of the high risk HPV types is associated with the accumulation of genetic abnormalities. Genetic instabilities are found in even the earliest abnormal lesions. However, changes such as the gain of chromosome 3q are usually found only in the more invasive tumours [9,308,309]. High risk, but not low risk E7 has the ability to cause rapid disruption of both the centrosomes and centrioles [9,310], with the E6-associated alterations being acquired over a more prolonged time period [218]. Centrosome abnormalities are seen at low levels even in episomal lesions, but increase substantially in number upon integration [310,311]. The centrosomes and centrioles are required for both the production of microtubule organising centres and the mitotic spindle pole bodies, therefore any alteration in their synthesis leads to abnormal numbers of both microtubular structures [2,296]. Because of their importance, any disruption can potentially lead to chromosomal alterations and genomic instabilities such as multinucleation [312] and aneuploidisation, subsequent centrosome related mitotic faults and possible chromosome instability [312], with the consequent increased risk of malignancy.

Telomeres are located at the termini of the eukaryotic chromosome and are important for maintaining chromosome stability during gene replication. Telomeres are maintained by the enzyme telomerase, whose activity is controlled primarily by regulating the expression of the telomerase catalytic component human reverse transcriptase (hTERT) [313]. In most somatic cells telomerase function is lost and hence telomere shortening occurs with every cell division providing a possible mechanism for cell aging [314]. The reactivation of hTERT is a common feature of most malignant cells and the associated renewal of the telomere allows these cells to become immortal [9]. The induction of abnormal replication by the papillomavirus will cause a rapid shortening of the cellular telomere, providing a potential trigger for cell cycle

arrest and apoptosis, and therefore must be counteracted by the virus. The HPV E6 protein has the ability to induce telomerase activity via increased transcription of hTERT [9,314], hence removing restrictions on the lifespan of the infected cells. Further increases in hTERT expression in the presence of both E6 and E7 suggests that E7 may also have a role in this process [314]. To counteract excessive telomerase activity the viral E2 protein has been shown to inhibit the hTERT promoter, providing an additional mechanism for maintaining the control of virally infected cells [313]. Therefore, HPV integration is associated with an increase in telomerase expression due to both a decrease in inhibition of hTERT by E2 loss and an increase in hTERT expression associated with enhanced levels of E6 and E7.

The transforming ability of the virus is further aided by the interaction of HPV E6 with proteins involved in epithelial cell organisation (fibulin-1 [315]), DNA repair (XRCC1 [316]), and cellular differentiation [317]. In the case of cellular differentiation the effect is partially p53-independent, with *in vitro* experiments showing that E6 expressing cells have an increased resistance to calcium induced cell differentiation [317].

1.5.4. HPV and Cellular Structure

Some cellular proteins found associated with E6 are involved in cell-cell interactions and contribute to maintaining cell morphology [28]. Under the control of E6 the atypical functioning of these proteins may contribute to transformation and the abnormal morphology of HPV-infected cells. These cellular proteins include E6 binding protein [318], Paxillin [319], the human homologue of Drosophila discs large (hDlg) a tumour suppressor protein [301], and E6 target protein 1 [320]. E6 also interacts with host proteins involved in cell-cell adhesion, polarity and proliferation control (e.g. hDlg [301]); these interactions aid the transformation of the host cell.

The association of E4 with the keratin intermediate filaments has been suggested to lead to the disruption of the whole keratin network, forming koilocytosis, a cytoplasmic halo effect produced primarily by perinuclear vacuolation [54]. This viral interference with the cell cytoskeleton network may occur to aid the release of mature virions from the tough epithelial cells [42].

1.5.5. The Influence of HPV on Apoptosis

For the virus to survive and successfully replicate it has to interact with, manipulate, and disrupt numerous cellular components and processes. One of the biggest problems faced by the virus is the constant threat of cell-induced apoptosis. Whether or not apoptosis occurs is a fine balance between pro- and anti-apoptotic signals, being mediated directly by the death receptor or mitochondrial pathways and indirectly via signals such as p53 and pRb. In order to control cellular behaviour, HPV must interact with and subdue all of these different components of the wider apoptotic pathway. The abnormal replication induced by E7 in particular leads to a pro-apoptotic response, as shown in E7 containing cells subjected to reduced growth factors [9,321]. In a normal infection the E6 protein forms the central figure in counteracting the cellular response to the virus. In cancer cell lines such as HeLa and SiHa, inhibition of E6 causes apoptosis, illustrating the vital role of this protein in maintaining post-integration cell survival in HPV infected cells [322]. The suppression of the apoptotic response appears to be the primary responsibility of the HPV E6 protein, although other viral proteins also contribute to the response. HPV E7 appears to be able to act in either a pro- or anti-apoptotic manner depending on the predominant signalling environment [323].

1.5.5.1. Anti-apoptotic HPV Behaviour

The recreation of a replication-competent state in the cells of the suprabasal region is detected by the cell and leads to the activation of the protective apoptotic response. To survive, the virus must counteract this apoptotic response not only by interacting with regulatory proteins such as p53 and pRb, but also by manipulating proteins directly involved in the death receptor and mitochondrial apoptotic pathways as shown in figure 1.6.

HPV 16 E5 has been shown to inhibit ligand-mediated apoptosis occurring via the death receptor pathway. However, as the E5 protein is often lost during integration [324], the anti-apoptotic effects of E5 are likely to occur only during the natural viral life cycle [111], and sufficient alternative anti-apoptotic mechanisms are available within the cancer cell lines to prevent apoptosis. When HaCaT cells infected with E5 expression construct are grown in both monolayer [45] and raft culture [325], they display a reduction in FasL or TRAIL mediated apoptotic signalling [325]. This is thought to be achieved by either reducing the expression of the both the CD95-receptor and Fas-receptors or by impairing DISC formation [325].

The HPV E6 protein plays a key role in preventing apoptosis in HPV infected cells by the inactivation of a number of pro-apoptotic proteins via the ubiquitin proteasome pathway [111]. E6 is known to protect cells from apoptosis mediated via TNF-α (Tumour necrosis factor-α) signalling [326]. This effect is not achieved by a decrease in the levels of the TNF-receptor, but by inhibiting the ability of the cytosolic death domain of the receptor to interact with the FADD protein. This can be achieved by the E6 protein binding the C-terminal region of the TNF-death domain [111,323], the death effector domain of the FADD protein [110] or via the accelerated degradation of the FADD protein [110]. By reducing the action of the FADD protein the virus can prevent the activation of pro-caspase-8 and hence inhibit the apoptotic

cascade. Evidence suggests that E6 may also interact with the complete DISC complex, preventing activation of procaspase-8 [110]. Within the mitochondrial pathway the E6 protein is known to associate with the pro-apoptotic proteins BAK and BAX [6] and HPV 18 E6 has been shown to label BAK for proteasomal degradation using the E6-AP ubiquitin pathway [114]. The telomerase enzyme, normally inactive in the majority of adult cells, is reactivated by the E6 protein [327] late in carcinogenesis to allow renewed telomere production; this enables continued DNA replication and removes a possible trigger for cellular senescence and apoptosis [327,328].

E6 and E7 are thought to contribute to the inhibition of apoptosis by upregulation of the c-IAP [329] and also by preventing TNF-α mediated pro-caspase-8 activation probably by an interaction at the level of the DISC complex [323,330,331].

1.5.5.2. The Pro-Apoptotic Functions of HPV

The viral anti-apoptotic functions are important for the success of the HPV life cycle. However, during a normal productive infection the virus also requires virally mediated apoptosis to occur (figure 1.6).

The HPV 16 E1^E4 protein aids apoptosis by binding the mitochondria and inducing detachment of these organelles from the microtubule network, resulting in the formation of a single large mitochondrial cluster adjacent to the nucleus [332]. This clustering is followed by a marked reduction in the mitochondrial membrane potential and the induction of apoptosis via release of mitochondrial pro-apoptotic compounds [332]. E1^E4 has also been shown to bind to and collapse the cytokeratin network [332].

Although the primary roles of E6 and E7 involve the prevention of apoptosis, they also appear to have some pro-apoptotic functions. In TNF-sensitive ovarian cancer cells E6 is able to cause induction of apoptosis associated with the inhibition of NF-κB activation [333], suggesting a role for NF-κB signalling in the anti-apoptotic pathway. Also, E6 induced cell death is associated with the down regulation of p21 [334], directing the cell away from cell cycle arrest and towards apoptosis. As discussed in section 1.1.7 the truncated E6*I protein [111,335] is able to reduce the degradation of p53 and pro-apoptotic proteins such as BAK or BAX [111], and hence increase the presence of these pro-apoptotic stimuli. The HPV E7 protein has been shown to induce apoptosis in the presence or absence of TNF-α [336], this has been suggested to occur via both p53-dependent and independent pathways [336-338]. Possible routes for E7-induced cell death may involve the sensitivity of the cells to TRAIL [339] and FAS [340] induced apoptosis [111].

The E2 protein has been shown to play an important role in the induction of apoptosis in HPV infected cells, with the loss of this function during HPV integration likely to play a role in the development of malignancies. E2 induced apoptosis is thought to occur primarily via the death receptor pathway, leading to the initiation of pro-caspase-8 activation [341]. In the case of HPV 18 E2 this is thought to occur via interaction of the N-terminal region of E2 with members of the death receptor pathway [342]. The pro-apoptotic function of E2 is not thought to require either the DNA binding or transactivation functions of the protein [342,343]. This phenomenon has been seen not only in immortalised cell lines, but also in primary human keratinocytes [342]. In HPV positive and negative cell lines HPV 16 E2 has been shown to induce apoptosis via a p53-dependent pathway [338,344], with the apoptotic response abrogated by the introduction of dominant negative p53 or the absence of additional p53 in p53-null lines [132,345]. However, in HPV 18 and BPV 1 E2-induced cell death appears to occur in a p53-

independent manner, with the presence of dominant negative p53 having little effect on the level of apoptosis [346]. These apparent differences in the p53-dependence of the E2-induced apoptosis may reflect differences in the innate properties of the E2 proteins between the different papillomavirus types. Pro-apoptotic signalling has been shown to be amplified by a truncated form of E2 produced by caspase cleavage [341].

One possible role for HPV induced apoptosis is in aiding the release of viral progeny at the epithelial surface [342]. When keratinocytes terminally differentiate they undergo a form of apoptosis where the dead cells are retained to form the cornified layers of the upper epithelium. This normal epithelial differentiation produces an environment which is inefficient for virion release. Therefore by inducing normal apoptosis of these cells the virus induces a form of cellular destruction that promotes efficient virion release [342]. In particular the presence of E2 and E1^E4 proteins within the upper epithelial layers [347] suggests an important role for these protein in this process. The virus also relies heavily on a healthy cellular environment, so the induction of apoptosis may also be viewed as a measure by which the virus limits the numbers of progeny release and therefore limits detrimental effects upon the host [111].

1.6. p53 Activation in HPV Infected Cells: A Strategy for the Treatment of HPV-Associated Disease

Current management of HPV-associated cervical abnormalities is highly dependent on the early detection of abnormal pre-cancerous or cancerous cells via the cervical smear test [348]. However, the original Papanicolaou (Pap) smear is particularly prone to technical issues such as insufficient cells or the presence of infection, leading to the need for repeat sampling,

therefore, in the UK a phased introduced of liquid based cytology is underway to increased the reliability of the smear test and reducing the requirement for repeat testing [349].

The current treatments offered to those found to have cellular abnormities is highly dependent upon the nature of the changes found. If mild cellular changes are detected by the cervical smear, a colposcopy may be undertaken immediately or after the repeated presence of abnormalities at a 6 month review [349]. However, moderate or severe cellular changes are investigated immediately by colposcopy, at which additional tissue biopsies may also be taken [349].

Where abnormal cells are found they can be removed from isolated parts of the cervix using laser ablation, cold coagulation or cryotherapy. However, where they are found to be more widespread or of a higher grade, more invasive techniques such as LLETZ (large loop excision of the transformation zone), cone biopsy or hysterectomy maybe utilised. If malignant cells are detected the treatment is dependant on the stage of the cancer. At the earliest stages hysterectomy (or cone biopsy in very early lesions) alone may be undertaken, but as the cancer stage increases treatment may involve more invasive surgery, radiotherapy or chemotherapy, either individually or combined [349].

An additional tool to help in the reduction of HPV-associated disease will be provided by the recently introduced bivalent and quadravalent vaccines. Both Cervarix (GlaxoSmithKline, HPV 16/18) and Gardasil (Merck & Co, HPV 6/11/16/18) are based on administration of HPV L1 virus-like particles, leading to the generation of high titres of neutralising antibodies that are reported to efficiently prevent infection [348,350]. It appears that this protective effect may not be type specific, with some evidence of cross-protection against some, but not all,

alternative HPV types [348,350] (e.g. HPV 31 and 45 for Cervarix [351] and HPV 45 for Gardasil [352]). A greater cross-protection may be provide by vaccines based on the L2 capsid protein; however, research suggests that these vaccines illicit a lower level of neutralising antibodies than their L1 counterparts (reviewed by [348]).

Even with the introduction of vaccination programmes in a number of countries, including the UK, HPV-associated neoplasia remains a viable treat to the population. In most counties vaccination is primarily aimed at 12-13 year old girls, with some 'catch up' programmes for 13-18yrs (NHS, UK, accessed 08/10/2008), leaving a the large pool of unvaccinated men and women at risk of HPV infection. In addition to the absence of cross-protection against the whole range of high risk HPVs, these vaccines have been found to be inefficient in women previously infected with HPV 16/18 [353] and have an unknown the duration of protection [350]. Consequently, even those who receive either type of prophylactic vaccination remain at risk from HPV-associated disease and thus continued smear testing is advised (NHS, UK, accessed 08/10/2008).

The early treatment of high risk HPV infection or HPV-associated lesions provides possible novel routes for the prevention of potentially malignant lesions, which may otherwise require the use of more invasive curative or palliative treatments. One possible therapeutic route is to inhibit virus only or virus-host interactions, inhibiting the viral life cycle or enabling a cellular response. This could be achieved in several ways including vaccination, prevention of viral segregation by interference with the E2 protein, or the inhibition of E6 and E7 by complimentary anti-sense transcripts [109].

This aim could also be achieved by inducing apoptosis of infected cells, thus preventing the spread of infection and reducing the potential for malignant progression. As p53 and its downstream proteins form vital components of the apoptotic pathway, they provide several possible treatment routes to reactivate cellular responses. A possible route to prevent the degradation of p53 is to interrupt proteasome activity, preventing the degradation p53 by the proteasome [182]. This effect can be achieved using specific proteasomal inhibitors such the Streptomyces metabolites, lactacystin [354] or via the inhibition of the nuclear phosphoprotein Mdm2. As discussed in section 1.3.1, Mdm2 binds p53 and facilitates ubiquitin-mediated degradation and may provide a possible route for the enhancement of the p53 response [182]. Members of the nutlin family of drugs prevent the interaction between Mdm2 and p53, thus inhibiting the proteasomal degradation of p53 [355-357].

HPV-dependent and independent degradation of p53 is primarily undertaken by proteasomes located within the cytoplasm of the cell (sections 1.3.1 and 1.5.1), with nuclear export performing an important role in the degradation of p53. If nuclear export can be inhibited, p53 will accumulate in the nucleus and potentially facilitate an increase in the transcription of pro-apoptotic genes.

1.6.1. Nuclear Export

The nuclear envelope allows cells to compartmentalise many functions to provide an additional level of regulation by nuclear admission or exclusion. The transfer of mRNA and proteins from the nucleus to the cytoplasm is vital for numerous cellular processes such as translation, cell signalling and apoptosis. The presence of compartments within the cell necessitates mechanisms to facilitate exchange; in the case of nucleo-cytoplasmic transfer the nuclear pore complex is employed. The nuclear pore is an approximately 125MDa complex

found spanning the nuclear envelope [358], maintaining a partially open state to allow the passive diffusion of some small proteins or mRNAs [358]. However, the majority of nuclear pore transport utilises GTP-dependent mechanisms [358], requiring the presence of appropriate transport signal sequences (section 1.3.1).

Nuclear transport via the pore complex is mediated by receptors of the karyopherin family (also known as importins and exportins according to the direction of transport). These molecules act as chaperones, binding the transportable proteins (or mRNA) and facilitating their transport through the nuclear envelope [358]. Individual karyopherins have the ability to bind specific cargo [358] and in the majority of cases are mono-directional [359]. Karyopherin mediated transport is regulated by the small Ran type GTPase, with directionality associated with differently phosphorylated forms of the enzyme [360]. Export from the nucleus is associated with Ran bound to GTP (Ran-GTP), while import requires Ran bound to GDP (Ran-GDP) [360].

Nuclear export employs a range of exportins such as CRM1, CAS1/Cse1 and Exp6 [360,361], each associating with their own cargo. Cargo specificity is regulated primarily by the NES, with the presence of large hydrophobic residues, most commonly leucines, forming a conserved feature of these signals [360]. The actual amino acid sequence of the NES appears to vary considerably between individual exportins, providing a level of specificity to the export system [360]. To facilitate nuclear export the karyopherins first interact with Ran-GTP. They then bind the cargo protein via its NES [362] as illustrated in figure 1.10. In CRM1 the binding of Ran-GTP is thought to take place in the CRIME (CRM1 importin-β etc) domain of the protein [363], with NES interaction thought to occur via the central conserved region of the protein [186]. Once export is complete the complex is dissociated by the conversion of Ran-

GTP into Ran-GDP by the enzymes RanBP1 or Nup358/RanBP2 [360,364,365]. This conversion liberates the exported cargo and Ran-GDP, which is then available for import of material into the nucleus.

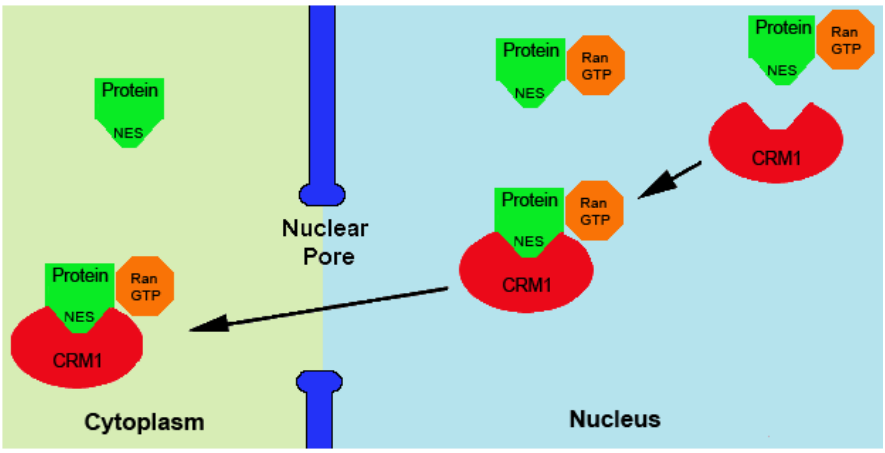

Figure 1.10: A summary of the CRM1 mediated nuclear export via the REV type nuclear pore.

The karyopherin CRM1 (chromosomal region maintenance 1) (36) /exportin 1 has been identified as a NES receptor [366], acting as a universal and conserved mechanism that forms a critical component of the nuclear export mechanisms of numerous different cell types [367,368]. This protein was first described in cold sensitive stains of the yeast *Schizosaccharomyces pombe* (*S. pombe*), where mutations in the CRM1 gene led to deformation of chromosomes [369]. Transcription of CRM1 varies throughout the cell cycle, reaching maximum expression during G_2/M where CRM1 participates in pre-mitotic signalling [370]. However, CRM1 protein levels have been shown to remain constant throughout the cell cycle [370]. CRM1 recognises a leucine-rich NES of the REV type found within a huge range of proteins [371] and also RNA [358]. Numerous different cargos utilise CRM1-mediated transport including important cellular proteins required for cell cycle regulation or transcription such as p53 [360,371]. CRM1 has also been shown to export viral proteins such as the HIV REV protein [372]. The affinity of most REV type NES cargos for the CRM1 protein is lower than in most other exportin-substrate complexes [360]. However, stronger interactions have been shown to be disadvantageous as

they prevent dissociation of the CRM1-Ran-GTP-cargo complex from the nuclear pore [373] and hence prevent the release of the cargo into the cytoplasm.

Treatment with a nuclear export inhibitor could provide a potentially novel treatment for HPV-associated neoplasia. The drug Leptomycin B (LMB) is a known inhibitor of nuclear export and has previously been shown to inhibit nuclear export of p53 [182] and induce apoptosis in a number of HPV positive and negative cell lines [374,375].

1.6.2. Leptomycin B

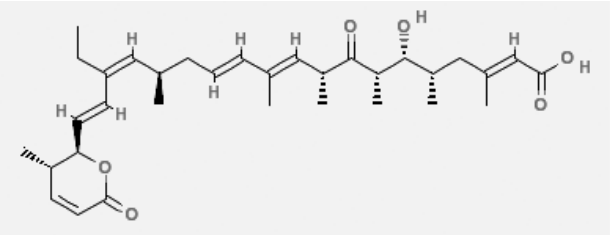

Figure 1.11: Molecular structure of LMB. (CID: 6436291)

LMB, also known as elactocin, CI 940, or PD 114720 is an unsaturated, branched-chained fatty acid formed as secondary metabolite by the fungus-like bacterium S*treptomyces* [371] (figure 1.11). This potent antifungal antibiotic is known to block the eukaryotic cell cycle [134], and is able to inhibit nuclear export of the HIV-1 REV protein, REV-dependent pre-mRNA [134], and a range of other proteins. LMB inhibits nuclear export at low nM concentrations by interacting with CRM1 [134,376], preventing an association between CRM1, Ran-GTP and the cargo protein [182,371,377] (figure 1.12). The actions of LMB appear to be specific to CRM1, with nuclear import appearing to function normally [134].

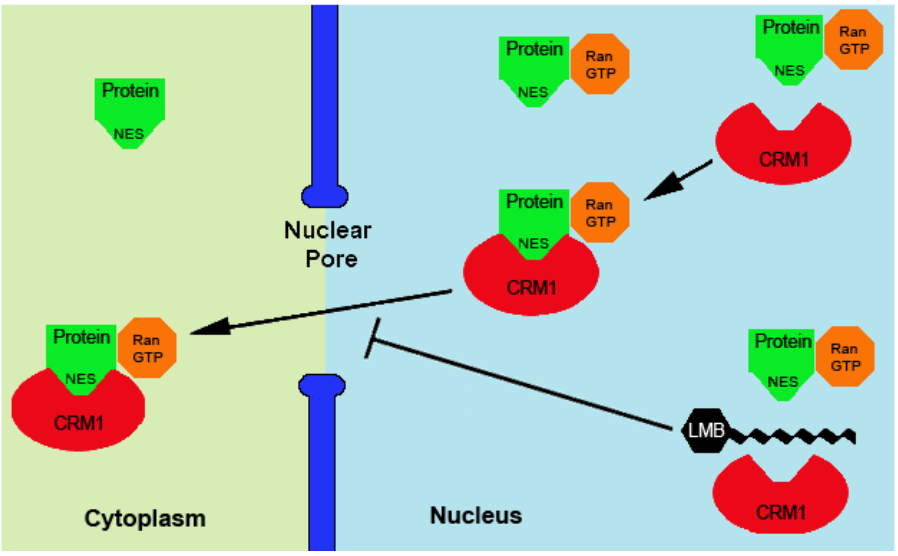

Figure 1.12: A summary of the effect of LMB on CRM1-mediated nuclear export via the REV type nuclear export pore.

LMB binds CRM1 via its α,β unsaturated δ-lactone region, which interacts with the sulphydryl group of the conserved CRM1 cysteine 528 [368]. This interaction is probably achieved by disrupting the hydrogen bonding of cysteine 528 by alkylation [186]. The important role of the conserved cysteine is illustrated in *S. pombe* by the LMB-insensitivity caused by the substitution this critical residue for a serine [186,371]. The interaction of LMB and CRM1 may prevent the formation of an exportable CRM1-Ran-GTP-cargo complex. This may be achieved by LMB preventing conformational changes in exportin that normally occur in response to the binding of an appropriate NES containing protein [186].

Protein	Function	Ref	Protein	Function	Ref
REV	HIV protein	378	Mdm2	p53 inhibitor	190
Actin	Cytoskeletal	379	p27	CDK inhibitor	380
c-Abl	Tyrosine kinase	381	Cdc25	cdc2 phosphatase	382
Cyclin-B1	Cell cycle regulation	383	COX2	prostaglandin synthase	384
p53	Tumour suppressor	385	BRCA1	Tumour suppressor	386
p73	Tumour suppressor	387	BRCA2	Tumour suppressor	388
PKA	Protein Kinase A	372	hTERT	Subunit of telomerase	389
MPF	Megakaryocyte potentiation factor	390	IAP1/2	Caspase inhibitors	391
IκBα	PKA inhibitor	392	XIAP	IAP family member and caspase inhibitor	393
MEK1	mitogen-activated protein kinase kinase 1	367	Survivin	IAP family member and caspase inhibitor	394
MAPK	Mitogen-activated protein (MAP) kinase	395	HPV 16 E2	Viral regulatory protein	396
hGTSE-1	Human G_2 and S phase-expressed-1	397			

Table 1.2: Some of the proteins reported to utilise CRM1-mediated nuclear export and to accumulate in response to LMB.

As shown in table 1.2 LMB influences the localization of a number of proteins which require nucleo-cytoplasmic shuttling [182,376]. The disruption of p53 signalling has been suggested to play an important role in the induction of LMB-induced cell death [182,375]. The addition of LMB to wild type primary human keratinocytes has shown that no apoptosis, genotoxicity or long-term effects on cell growth occur [374]. LMB treatment of primary human keratinocytes (PHKs) transduced with HPV 16 E7 or E6/E7, and HPV 16 infected cancer cell lines CaSki and SiHa leads to an accumulation of p53 in the nucleus and the induction of apoptosis [203,385,398]. Increased levels of apoptosis in response to LMB have also been demonstrated in other non-HPV associated cell lines such as human leukaemia cells (U937) [399], prostatic cancer cell line LNCaP [375] and in cells expressing the abnormal BCR-ABL fusion protein [400]. In these cases, the primary cause of the sensitivity to LMB is not the presence of a viral infection, but carcinogenic transformation or the addition of constructs expressing the products of abnormal gene translocations. The common link between all these cases of

increased sensitivity is the considerable alterations occurring in vital cell regulatory systems which appear to be sufficient to alter the LMB related behaviour of the cells.

Phase I clinical trials have shown that intravenous treatment with LMB caused 'anorexia and malaise' leading to a recommendation for no further trials of intravenous LMB [401]. However, topical application of LMB is thought be a promising approach for the development of a novel anti-cancer treatment [182]. It has been suggested that LMB would be most efficient at treating tumours containing wild type p53 such as that found in high risk HPV infected cells [374] or alternatively cells that contain alterations in cellular systems such as the BCR-Abl cells. However, some of the effects seen in response to LMB may not be primarily due to accumulation of p53; the disrupted shuttling of other CRM1 exportable proteins may provide a considerable contribution to the LMB-induced effects, causing the disruption of a range of cellular processes [182].

Most cell lines established from cervical cancers contain integrated HPV 16/18 sequences (CaSki, SiHa and HeLa) and provide useful models for the behaviour of HPV in a malignant environment. These cells have provided insights into many aspects of the virus including its genome, transcription and life cycle. However, these models do not allow investigation of the earlier pre-malignant events important in the development of both a normal productive infection and cervical cancer. The W12 line and its derivatives provide an alternative model for the study of HPV-associated neoplasia. These cells are immortal and formed from a natural infection, and therefore provide a valuable and unique resource to study the mechanisms associated with HPV infection in non-malignant cells [51,117].

1.6.3 The W12 Keratinocytes a Model of Cervical Neoplasia

1.6.3.1. The Parental W12 Cell Line

The parental W12 cell line was derived by Stanley *et al* (1989) [18] from a low grade SIL histologically diagnosed as a CIN 1 lesion [117]. The tissue was obtained from a 22 year old female patient with a history of vulval condylomata and abnormal cervical smears, showing mild atypia and koilocytosis, with the biopsy taken from the anterior lip of the cervix close to the squamocolumnar junction [18]. The W12 line was established from the tissue biopsy cultured on lethally irradiated Swiss 3T3 feeder cells, the cells formed colonies that displayed typical basal keratinocyte morphology in monolayer culture [18]. However, these cells remain dependent on a feeder layer to maintain this normal keratinocyte behaviour [18]. When cultured it was found that normal keratinocyte behaviour could be encouraged by the addition of cholera toxin to increase plating efficiency and epidermal growth factor to increase colony size. During *in vivo* culture the differentiated parental W12 cells have been shown to be capable of producing HPV virions [402]. At early passage the parental W12 cell line harbours at least 100 copies of the episomal HPV 16 genome and has been shown to express the HPV E7 protein [19,117]. Uncut W12 DNA analysis indicates that the native episomal DNA occurs in primarily the supercoiled or open-circular forms [18,27,117], containing no major deletions, insertions or re-arrangements. When digested with *Bam*HI the genome is cut once, forming an indicative 7.9kb band after Southern blot analysis [133]. Subsequent analysis of the parental population has suggested that it is heterogeneous in nature, with cells containing episomal and/or integrated HPV genomes [119].

As has been observed in the malignant progression of a typical HPV infection *in vivo*, the HPV 16 episomes contained within the parental W12 cells undergo spontaneous integration

into the host DNA during long term culture [133]. This viral integration in the W12 cells is associated with an increased colony forming efficiency and growth rate, along with a subsequent accumulation of cytogenetic abnormalities similar to those seen *in vivo* [117]. When parental W12 cells are maintained in culture in the presence of lethally irradiated Swiss 3T3 feeder cells, the genome status of the cells gradually alters from one of almost entirely episomal HPV (at approximately passage 10), though a mixed population of episomal and integrated viral genomes (at approximately passage 14), to a purely integrated HPV culture at approximately passage 22 [117]. The parental W12 culture by approximately passage 14 is likely to consist of a heterogeneous population, containing a mixture of cells with both episomal and integrated HPV [18,119].

HPV integration in the parental W12 lines has been shown to be associated with increased expression of the HPV E7 and loss of HPV E2 [117]. Integration also leads to a 12.3 fold increase in the expression of insulin-like growth factor (IGF)-II and 4.7 fold increase in the epidermal growth factor receptor (EGFR) [117]. The increase in both of these factors may help to stimulate the growth of the W12 cells following integration, and may reflect changes occurring during *in vivo* carcinogenesis [117].

1.6.3.2. The W12 Derivatives

Derivative	Clone Number	Viral Copy Number	Integration Type
W12 Derivatives			
E_{50}	20850	1000	N/A
E_{63}	20863	1000	N/A
I_{02}	201402	5	1
I_{22}	20822	3	1
I_{31}	20831	60	2
I_{61}	20861	30	2
HPV 16 containing cell lines			
SiHa	N/A	2	1
CaSki	N/A	600	2

Table 1.3: A summary of the major properties of the episomal and integrated W12 derivatives, along side two HPV 16 infected cancer cell lines known to contain the viral genome integrated in a similar manner to the W12 derivatives [119].

The W12 derivatives are made up of two episomal (E_{50} and E_{63}) and four integrated cell lines (I_{02}, I_{22}, I_{31} and I_{61}) which provide a model of early HPV-associated changes. The W12 derivatives were cloned by Jeon *et al* (1995) [119] by the selection of individual colonies from growing cultures of the W12 parental line. A summary of their major properties are shown in table 1.3. All derivatives, with the exception of I_{02} were selected from parental W12 cells at early passages 14 or 15. The I_{02} line was formed from a later passage 17 of the parental line, from which all the derived clones contained the same integration event involving disruption of the E2 ORF [119]. This same integration event was also found in the passage 17 population of parental cells, suggesting that this integration event had become dominant within the late passage parental W12 population [119]. In order to prevent integration of HPV DNA in the episomal derivatives the cells must be maintained in specialised complete F-medium. Under these conditions the viral episomes have been shown to be stably expressed at the same level for at least 100 cell generations [119].

Integrated W12 derivatives can also be classified by the type of integration event that has occurred. Both type 1 and 2 integration have also been noted *in vivo* and are associated with amplification of the viral and nearby host sequences [119]. The cells with type 1 integration contain single copies of the viral genome integrated at each event causing disruption within the E2 ORF; this form of integration is present in the I_{02} and I_{22} W12 derivatives and also the cervical carcinoma-derived cell line SiHa [119]. In the I_{22} cell line, viral genome cleavage has been mapped to nucleotide 3732 and it appears the integration has occurred in a region of the host genome with no homology to known gene coding sequences [119]. The I_{31} and I_{61} derivatives have undergone type 2 integration, also seen in the cervical carcinoma-derived cell line CaSki. This type of integration is associated with the insertion of head-to-tail tandem repeats (concatemers) of full length viral DNA flanked by disrupted viral sequences [119]. Jeon *et al* (1995) [119] suggest integration and disruption of the E2 ORF in the type 2 integrants; although this appears likely the exact location of the disruption could not be confirmed due to the presence of multiple full length viral sequences.

The published E6 levels of the W12 derivatives suggest that, integration is associated with a substantial increase in E6 expression compared with the episomal W12 lines, expression was particularly high in the type 2 integrated I_{61} derivative [403]. The integrated lines, with the exception of I_{02}, also displayed much greater expression of the E7 protein compared with the episomal lines, with E7 shown to strongly contribute to the growth advantage of the integrated cells [119]. Increased E6 and E7 levels may contribute to the selective growth advantage of these cells with integrated derivatives expressing higher levels displaying greater growth advantage over the episomal lines. The higher levels of the E6/E7 proteins is facilitated by the disruption of E2 which is likely to have occurred in both types of integration; however,

other factors may also play a role in the growth advantage of the cells containing integrated sequences including increased mRNA stability [119,129] and the clonal nature of the derivatives.

W12 cells can be induced to differentiate in monolayer by culturing at high density in 1.2mM calcium [65]. Alternatively the cells can be grown in organotypic raft culture to produce a model of a squamous epithelium. Within the suprabasal layers of episomal W12 rafts large dysplastic cells with enlarged nuclei have been observed [27], which show low levels of staining for markers of differentiation such as K10, involurin and filaggrin [27]. The rafted episomal W12 derivatives have also been shown to be capable of producing virus-like particles [404]. Although both the parental W12 line and its episomal or integrated derivatives can be induced to differentiate, they fail to form colonies in soft agar, indicating that even where integration has occurred the cells appear to remain non-tumourigenic [27] and therefore provide a good model for the early stages of cervical cancer.

1.6.4. The Predicted Affect of LMB on HPV 16 Infected Cells

As treatment of normal cells with LMB has been shown to induce a recoverable cell cycle arrest but not apoptosis [374], the HPV infection must mediate the response to LMB in some way. The rise in p53 reported in a number of cell lines is a predicted mechanism for LMB-induced apoptosis.

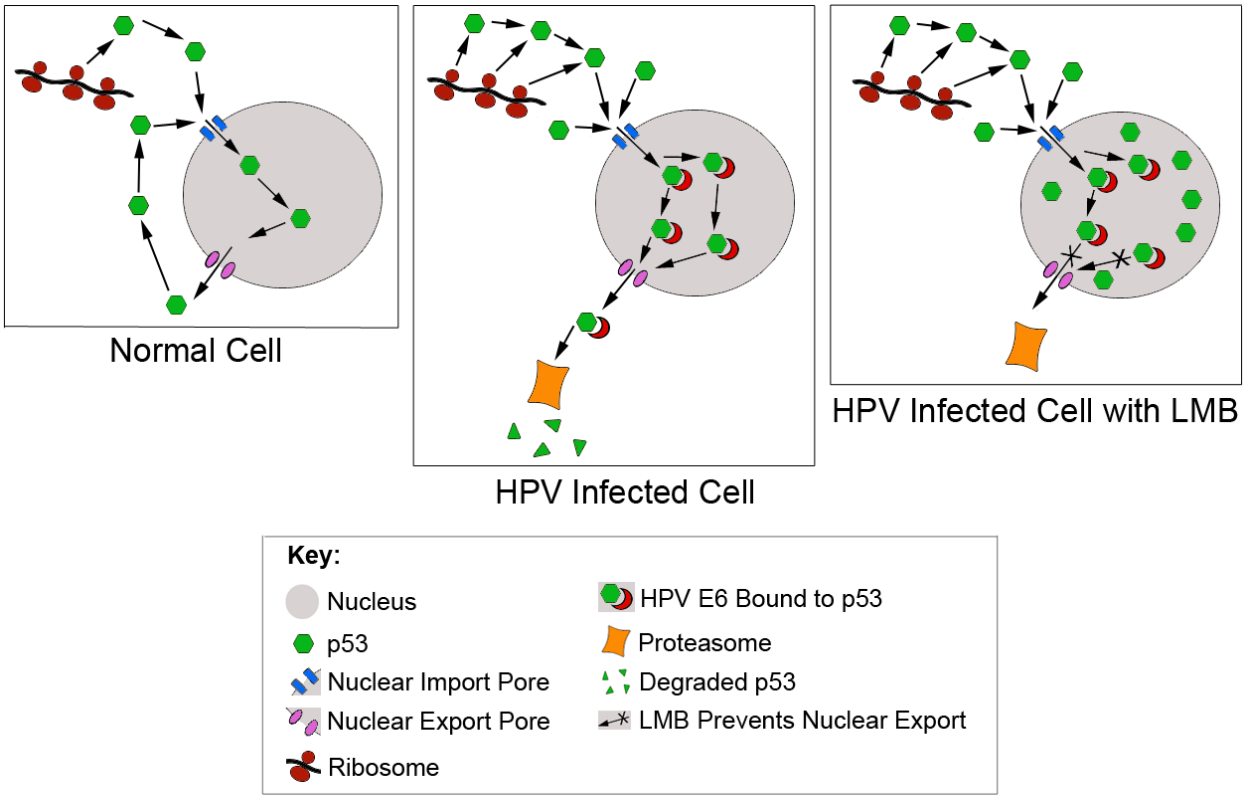

Figure 1.13: The predicted affect of LMB on cells infected with HPV 16. The shuttling of p53 between the nucleus and the cytoplasm is shown in normal uninfected cells and cells infected with HPV 16 in the presence and absence of LMB.

In normal uninfected cells, p53 is one of a number of proteins known to shuttle between the nucleus and the cytoplasm, utilising the CRM1-mediated nuclear export. In the absence of cellular stress p53 levels are low due to a short half life maintained by proteasomal degradation (section 1.3.1). LMB treatment of these cells will lead to the accumulation of p53, but due to the low resting levels this LMB-induced build-up of p53 should be insufficient to initiate apoptosis. Infection with HPV 16 is associated with viral interference in a number of cellular pathways, particularly those involved with cell cycle control primarily via E7 (section 1.5.2) and also the possible induction of chromosomal instability associated with E6 and E7 expression (section 1.5.3). These disruptions initiate a cellular response co-ordinated primarily by p53, which itself is neutralised by HPV proteins including E6 (section 1.5.1) as illustrated in figure 1.13. Treatment of HPV 16 infected cells with LMB should prevent the CRM1-mediated export of p53 from the nucleus by HPV E6. When combined with the

greater background levels of p53, increased levels of apoptosis are likely to be induced (figure 1.13).

Chapter 2: Materials and Methods

Unless otherwise stated all chemicals are from BDH, see appendix A for full details of suppliers.

2.1. Ethics, Health and Safety, and Genetic Modification

Where relevant, research was undertaken with appropriate assessments of the ethical considerations and health and safety (COSHH) regulations, including those specifically concerning the use of genetically modified organisms and radioactive material.

2.2. Cell lines

The cell lines used during these studies are described briefly here, further details on the culture of these cells can be found in section 2.4.

2.2.1. W12 Derivatives

The W12 cervical keratinocyte derivatives were a kind gift from P. Lambert (University of Wisconsin, USA) and are described in further detail in section 1.9.2. The W12 derivatives studied were clones 20850 (E_{50}), 20863 (E_{63}), 201402 (I_{02}), 20822 (I_{22}), 20831 (I_{31}), and 20861 (I_{61}) [119].

2.2.2. J2 3T3

J2 3T3 is an immortal mouse fibroblast cell line used to provide feeder support for culture of W12 derivatives in both monolayer and raft culture. These cells were a kind gift from Fiona Watt (London Research Institute, London, UK).

2.2.3. CaSki

CaSki is an adherent human cervical epithelial cell line obtained from ATCC (CRL-1550). These cells are derived from a metastatic epidermoid carcinoma of the small bowel mesentery of a 40 year old Caucasian female [405]. They contain integrated HPV 16 at approximately 600 copies per cell, although there are some reports suggesting that HPV 18 type sequences may also be present [406].

2.2.4. SiHa

SiHa is an adherent human epithelial cell line derived from a grade II cervical squamous cell carcinoma acquired from ATCC (HTB-35). The cell line was established using post-surgery primary tumour fragments from a 55 year old female Japanese patient [407]. They contain integrated HPV 16 at approximately 1 to 2 copies per cell and have been shown to be hypertriploid [407].

2.2.5. Primary Human Keratinocytes

Normal human epidermal keratinocytes were derived from human neonatal foreskin obtained during surgical operations (PromoCell). For ethics documentation please see appendix D.

2.2.6. PHKs Transduced with HPV 16 E7 or E6/E7

PHKs were retrovirally transduced with either the HPV 16 E7 or E6/E7 using retroviral transduction (transductions undertaken by R. Lyman as described by Gray *et al* (2007) [374]). The HPV 16 E7 and E6/E7 constructs are contained within Moloney murine leukaemia virus (Mo-MuLV) derived retroviral vectors which are stably expressed in packaging cell lines obtained from the ATCC (CRL 2202-7), as described by Halbert *et al* (1991) [408] .

2.2.7. U2OS

The human osteosarcoma cell line U2OS was derived in 1964 from a moderately differentiated sarcoma of the tibia from a 15 year old female (HTB-96). U2OS cells display an epithelioid morphology and express wild type p53 and pRb [409,410].

2.2.8. U2OS Transfected with HPV 16 E2

U2OS cells transfected with neomycin resistant pCMV4-HPV 16 E2 or empty pCMV4 vector were a kind gift of Prof I. Morgan (University of Glasgow, UK) [411]. The clones stably express either HPV 16 E2 (clones HPV-16E2-B3/A4) or empty pCMV4 (clones Vec-1-3/D3).

2.2.9. RetroPack PT67 Retroviral Packaging line

RetroPack PT67 cells are a NIH/3T3 fibroblast based cell line which express the 10A1 viral envelope. These cells contain the viral genes encoding structural proteins *gag*, *pol* and *env* required for viral envelope production, but are deficient in the RNA packaging signal (Ψ^+). The retroviral vector includes the gene of interest but also contains the retroviral packaging signal, transcription and processing components. When the vector is inserted into PT67 cells they produce replication incompetent infectious viral particles at high titres. The separation of the packaging signal from the *gag*, *pol* and *env* genes minimises the chances of replication competent virions being produced via the recombination of the two sets of retroviral genes.

2.3. LMB

The drug Leptomycin B (LMB) was a kind gift from Novartis, in collaboration with Dr. S. Lain (University of Dundee, UK). LMB stock solutions were stored at -80ºC as 10mM, 1mM, or 0.1mM stocks in absolute alcohol. Immediately before use, the LMB was diluted in the appropriate medium to form working solutions of 200nM or 100µM. All alcohol stocks

were maintained on dry ice when removed from -80 ºC to reduce potential evaporation. Treatment doses used during these studies are summarised in Table 2.1: see individual experimental protocols for further details.

Experiment	Section	Concentration of LMB	Length of Treatment	Results Chapters
Morphology	2.5	2nM	40h	3
Raft Culture	2.6	50nM	72h	3/4/5
Immunocytochemistry	2.10	2nM	38h	4
Colony Survival	2.11	2nM/20nM/50nM/100nM	40h	3
Analysis of Protein – standard	2.12	2nM	38h	5
Analysis of Protein - time course	2.12.7.2	2nM	12h/24h/36h /48h	4/5
Analysis of Protein - Dnp53	2.12.7.5	2nM	38h	6
Luciferase Assay	2.19.2	2nM	12-26h	6

Table 2.1: LMB treatment concentrations and times used in the experiments described with the appropriate results chapters.

2.4. Tissue Culture

2.4.1. Normal Cell Culture

All cell lines were maintained in culture as described here unless otherwise stated.

Cells were grown in T75 (80cm^3) tissue culture flasks (NUNC) in a 37°C humidified environment with 5% CO_2. Cultures were maintained in Dulbecco's modified essential medium plus supplements (complete DMEM, appendix B1.1.). Fresh medium at room temperature was provided every ~48h, with all waste media and other liquid cell culture waste treated with 2% Virkon (Fisher Scientific) for approximately 24h prior to disposal.

Cells were passaged when cultures reached approximately 70-80% confluence, as qualitatively assessed by phase contrast microscopy. Flasks were washed briefly in 3ml trypsin-EDTA (TE, 0.05 % (w/v) trypsin and 0.53mM EDTA, Gibco/Invitrogen) and incubated with a further 1ml TE (37°C, 5% CO_2) for 5 min or until detached (not exceeding

10min). Detached cells were resuspended in up to 15ml complete DMEM, and centrifuged at 145*g* for 5min. The supernatant was discarded and the cells resuspended in 3ml complete DMEM, before seeding at desired density.

For specific seeding densities a Coulter counter (Z series, Beckman Coulter) was used. To quantify cell numbers 40µl of the cell suspension was combined with 20ml coulter isoton solution (Beckman Coulter). Counting was achieved using a 350fl aperture with all readings taken in triplicate and the mean used to determine cell number.

2.4.2. W12 Cell Culture

The culture of W12 cells requires the presence of a mitomycin C (mtc, Sigma-Aldrich) treated J2 3T3 feeder layer. Before use the mtc was first diluted in 5mQ water (dH_2O) to form a 200µg/ml stock and stored at 4°C for a maximum of 14 days. Growing J2 3T3 cultures were treated with 1:100 of the 200µg/ml mtc stock (2µg/ml final concentration) and incubated for 3 hours in normal culture conditions. Cells were then passaged as described above and seeded into T75 flasks containing incomplete F-medium at 1-2 x 10^5. The mtc treated feeder cells were left overnight in standard culture conditions before the addition of W12 cells. To passage, the W12 cultures were first incubated for 1min at room temperature in 0.02% (w/v) EDTA and washed briefly with 1x phosphate buffered saline (1xPBS, Oxoid). Cells were then trypsinised as described in section 2.4.1, although due to the highly adherent nature of the W12 cells, cultures were trypsinised for a maximum of 10min with any remaining adherent cells removed by scrapping. After collection by centrifugation the cells were seeded onto the feeder layer at between $5x10^5$ – $1x10^6$. Approximately 24 hours later 1:1000 of 10µg/ml Epidermal Growth factor (EGF, Sigma-Aldrich) was added to the W12 flasks giving a final concentration of 10ng/ml and forming complete F-medium. Fresh complete F-medium was provided approximately every 48h.

2.4.3. PHK+ HPV 16 E7 or E6/7 Cell Culture

Retrovirally transduced PHK cells were produced by R. Lyman, using supernatant derived from pLXSN-E7 or E6/7 containing PA317 packaging cells (ATCC, CRL-2203/5) in a manner described in section 2.8. Transduced PHK cells were grown in standard culture conditions using keratinocyte growth medium 2 (KGM2, PromoCell) until cultures were 60-80% confluent, as qualitatively assessed by phase contrast microscopy. All solutions used to passage the primary cells were sourced from PromoCell and pre-warmed to 37 ºC prior to use. Cells were first rinsed with 5ml Hanks' balanced salts solution (HBSS), followed by incubation in 5ml trypsin-EDTA (0.04% (w/v) trypsin and 0.03% (w/v) EDTA) initially at 37 ºC for 2min, then at room temperature for up to a total of 10min. When approximately 50% of the cells were detached, the flask was gently tapped to loosen remaining attached cells. 5ml of the trypsin neutralising solution (TNS) was added and the collected cells centrifuged at 145*g* for 4min at room temperature. After removal of supernatant, the cells were resuspended in 3ml KGM2 and seeded into flasks at appropriate seeding density, dependant on experimental requirements. Fresh KGM2 was provided to growing cells approximately every 48h.

2.4.4. Cryogenic Storage of Cell Lines

For long term storage, cells were harvested as described as described in section 2.4.3, and centrifuged cells resuspended in 3ml of the appropriate medium containing 10% (v/v) DMSO. Cryotubes (NUNC) with 0.5-1ml of the DMSO-containing cell suspension were then chilled to -80ºC at a rate of 1ºC/minute using an isopropanol-containing 'Mr. Frosty' (Nalgene) and after 24h vials were transferred to liquid nitrogen for long term storage.

The PHKs were frozen for long term storage using a specialised protocol. After harvesting as described in section 2.4.3, the pelleted cells (at approximately 1-5 x 10^5) were resuspended in Cryo-SFM (PromoCell) then transferred to -80ºC and then liquid nitrogen as described above.

2.4.5. Rescue of Cryogenically Stored Cell Lines

All cells with the exception of the PT67 lines were defrosted by rapid thawing in a 37ºC water bath, then transferred into culture flasks containing the appropriate pre-warmed medium. The W12 derivatives were defrosted onto pre-treated feeder cells prepared as described in section 2.4.2. To remove the cryo-preservative, the medium on defrosted cells was changed after 24h of standard culture. The PT67 packaging lines were defrosted at 37ºC, with 1ml of warmed medium then added into the cryotube and the contents transferred into a 15ml falcon tube with a further 5ml of medium. The cells were then centrifuged at 145*g* for 5min, resuspended and transferred into a T75 flask.

2.5. Morphological Effects of LMB

The W12 derivatives were grown as described above in T25 flasks until approximately 70% confluent. The cells were then treated with 2nM LMB for 40h in normal culture conditions. Treated cultures and untreated controls were then visually assessed for the effects of LMB on each cell line, with a photographic record made using a digital camera (Nikon Coolpix 4500) at x200 magnification.

2.6. Organotypic Raft Culture

While at the air-liquid interface raft cultures were particularly vulnerable to infection, therefore special care was taken to double swab all equipment with 70% ethanol and/or autoclave as necessary.

2.6.1. Preparation of Collagen Plugs (Day 1)

As collagen solidifies at room temperature, all equipment in contact with collagen was pre-chilled on ice prior to and during the procedure. To prepare the plugs J2 3T3 fibroblasts were trypsinised and cell number established as previously described (section 2.4.1), $5x10^5$ cells per plug were transferred to a fresh 15ml falcon tube and re-centrifuged. The fibroblasts were resuspended in 1ml 10x DMEM (10.5g 10x DMEM Powder (Gibco/Invitrogen) in 10.5ml dH_2O) and 1ml 10x Recon buffer (1.1g sodium bicarbonate and 2.4g HEPES in 50ml dH_2O, 0.22µm filter sterilised before use). Prior to use the collagen (rat tail, type 1, Upstate/ Millipore) was diluted on ice with 0.02M glacial acetic acid to a final concentration of 4mg/ml allowing 2ml diluted collagen per plug. The resuspended cells were then gently added to the diluted collagen and mixed carefully by inverting to avoid bubbles within the collagen, returning to ice regularly during mixing to prevent premature solidification. 2ml of collagen-cell mix was transferred into the appropriate number of wells of a sterile 6-well plate and rocked to spread evenly. To maintain a sterile environment the 6-well plate was placed into a sterile, humidified, and gassed environment. This was achieved by placing a sheet of autoclaved paper moistened with sterile autoclaved 18MQ water into a 70% ethanol sterilised Tupperware box, which was then manually gassed with 5%CO_2/air and sealed before removal from the culture hood. Collagen plugs were then maintained at 37ºC overnight to allow full solidification of the collagen.

2.6.2. Addition of W12 Cells to Collagen Plug (Day 2-8)

To complete the plug preparation, W12 cells were passaged as described in section 2.4.2 and resuspended in F-medium at approximately 1x 10^6/ml; 2ml of this suspension was then added to each plug which were then returned to the sterile humidified environment for 24h. At this point the EGF was added to the medium of each well as described in section 2.4.2 and the rafts left for a further 3 days before fresh complete F-medium was provided. The W12 cells were left to establish on the surface of the plug for a further 3 days before transfer.

2.6.3 Transfer of Plugs to Raft Mesh (Day 9)

Figure 2.1: The arrangement of the keratinocyte-covered collagen plug at the air liquid interface on a raft mesh platform.

The rafts were raised to the air liquid interface by transfer to a wire mesh platform (figure 2.1). The platform was produced by bending the edges of a 78mm diameter wire mesh disc (40 Meshed 0.01mm diameter wire, Johnson Screens), forming four approximately 5mm high legs (autoclave sterilised).

To transfer, the mesh platform was placed into a 90mm tissue culture Petri dish with approximately 18-20ml of complete F-medium sufficient to reach the base of, but not to cover the mesh. In the 6-well plates, the medium was removed from above the keratinocyte plugs and the raft was then detached from the sides of the well. A pair of sterile spatulas was then used to transfer the plugs from the 6-well plate to the mesh, ensuring that the keratinocytes surface seeded remained uppermost. Rafts were returned to the sterile humidified environment and left for 14 days to form an epithelium-like structure, with fresh complete F-medium provided every 2 days. 24 days after transfer (day 32) rafts were treated with 50nM LMB for 72h, with drug administered into the medium below the rafts. After treatment, rafts

were fixed in 10 % neutral buffered formalin for 24h and transferred to the departmental histology service to be embedded in paraffin wax. 5µm sections of the embedded rafts stained by haematoxylin and eosin were also provided by the histology service in order to assess the raft structure.

2.7. Stable Transfection of Cultured Cells

2.7.1. Dominant Negative p53 Plasmid

The retroviral packaging line PT67 was transfected with the dominant negative p53 construct pBabe-R248W (Dnp53, a kind gift from Dr E. Androphy, University of Massachusetts, USA) [412] or the pBabe construct (ADDgene). The transfection protocol was also undertaken in the absence of DNA (negative control) to allow the assessment of any transfection related cytotoxicity and also as a positive control for the effects of the mammalian antibiotic puromycin on untransfected cells.

2.7.2. Puromycin Dose Response

In order to establish the puromycin dose required to induce death in the PT67 and W12 derivatives, a dose response experiment was undertaken. The PT67 cells and the W12 derivatives E_{50} and I_{22} were seeded in 6-well plates and treated with 0, 2, 4, 6, 8 and 10µg/ml of puromycin with the rate of cell loss monitored for approximately 72h to determine the optimal dose.

2.7.3. Transfection of Packaging Cells

The PT67 cells were seeded at $5x10^4$ in a 6-well plate and grown until 60-80% confluent, with fresh media provided on the day of transfection. For each well the transfection reagent was prepared by diluting 3µl of GeneJammer (Stratagene) in 97µl of incomplete DMEM (in the

absence of fetal calf serum and penicillin-streptomycin-glutamine) with the reagent added directly into the media. The reagent/media solution was then incubated at room temperature for 5min, followed by the addition of 2µg of Dnp53 or pBabe plasmid DNA (section 2.17). The transfection solution was incubated for a further 40min at room temperature, then added dropwise to the appropriate cultures. The cells were then grown under normal conditions for 24-48h until semi-confluent; cells were then passaged into a T75 flask and left for a further 24h under normal culture conditions prior to the commencement of puromycin treatment. Initially cells were treated at 2µg/ml puromycin, but after 9 days viable cells still remained in the control flasks which formed colonies when selection was removed. Therefore cells were passaged at 12 days after the start of selection, and selection continued at the higher concentration of 3µg/ml. At this treatment level the remaining control cells died rapidly and the vector only cells grew well. This treatment proved too toxic for the p53 compromised cells which required re-transfection and selection with 2.5µg/ml puromycin for 6 days. Transfected cells were cryo-preserved (section 2.4.4) and cells retained for DNA extraction to assess the presence of the construct in the stably transduced cells (section 2.15.4).

2.8. Stable Transduction of W12 and PHK Cells

Retroviral transduction of the Dnp53 plasmid or pBabe plasmid was undertaken on the W12 derivatives E_{50}, I_{22} and I_{31} and also the previously transduced PHK lines expressing E7 and E6/E7.

2.8.1. Transduction

Two T75 flasks each of the Dnp53, pBabe and wild type transfected PT67 cells were cultured as previously described until approximately 70-100% confluent. The W12 and PHK cells were passaged into T25 culture flasks: W12 derivatives at $9x10^4$ (on feeder cells as described

previously) and PHK cells at $4.7x10^4$. Cultures were grown until colonies contained approximately 4 cells. At this point the medium on the PT67 cultures was removed and one set given incomplete F-medium (for transduction of the W12 cells), and the other given KGM2 (for transduction of PHK lines). These flasks were then left overnight to accumulate virions within the supernatant.

The following day the colonies within the W12 and PHK flasks were typically at the 8 cell stage and ready to be transduced. The retroviral supernatant containing the virions was removed from the PT67 flasks and passed though a 0.45µm Millex-HA filter (Millipore) to remove any contaminating fibroblasts. Polybrene (hexadimethrine bromide, Sigma-Aldrich) was diluted to 12µg/ml in F-medium or KGM2 and combined 1:1 with the appropriate retroviral supernatant in the W12 or PHK flasks. The cultures were left in contact with the retroviral supernatant for approximately 10h for transduction to occur, after which the retroviral media was removed and cultures were left overnight prior to selection.

2.8.2. Selection of Transduced Cells

Transduced cells were selected using the mammalian antibiotic puromycin. The W12 derivatives were treated at 0.5µg/ml, whilst the PHK lines were treated at 1µg/ml puromycin (M. Lewis, Liverpool).

The J2 3T3 feeder cells were untransduced and therefore susceptible to antibiotic treatment. Therefore, post-transduction W12 cells were grown in conditioned media provided by culturing J2 3T3 in the presence of incomplete F-media for at least 24h then filtering (0.45µm) to eliminate contaminating fibroblasts with storage at 4°C. When required the media was diluted in complete F-medium (~1:3) and the appropriate volume of EGF and puromycin (if required) were added. Cultures were passaged when approximately 70% confluent and maintained under selection until the control flask contained no live cells. To

confirm that selection was complete, puromycin treatment was removed, the flasks rinsed with 1xPBS and fresh media provided: the control flask was then monitored for any colony formation. Where colonies were initially detected, selection was reapplied to all cultures at 0.25µg/ml for 36h followed by 0.3µg/ml for a further 24h.

After selection was removed the Dnp53 and pBabe only transduced cells were cultured as normal, with the W12 cells maintained in conditioned media until cultures were confluent, when cells were cryo-preserved (section 2.4.4).

2.8.3. Stable Transduction of U20S Cells

The transduction with Dnp53 was repeated with the U2OS cell line as described above, but with the following modifications. Cells were passaged into T25 flasks at approximately $2x10^5$ and transduced with DMEM containing transduction solutions. Post-transduction cells were selected for 7 days with 1µg/ml puromycin, rinsed and left for 24h before passaging into fresh T75 flasks and also aliquots taken for cryo-preservation.

2.9. Southern Blot

The Southern blot analysis of DNA was optimised using *Bam*HI purified HPV 16 DNA (pEFHPV-16W12E, GenBank Accession No. AF125673, kind gift of P. Lambert, University of Wisconsin, USA). Sample and plasmid DNA production and purification are described in sections 2.17 and 2.18. W12 plasmid DNA at concentrations of 10ng, 1ng, 100pg, 10pg, and 1pg was used to optimise the protocol and establish sensitivity of the ^{32}P labelled probe. After optimisation the experimental protocol was undertaken using Hirt extracted W12 cellular DNA, with the purified plasmid DNA utilised as both probe and positive control sample.

2.9.1. Hirt Extraction of DNA

Hirt extraction [413] of W12 DNA was undertaken to obtain samples enriched with low molecular weight episomal HPV DNA. The W12 derivatives E_{50}, E_{63}, and I_{22} were grown in T75 flasks as described previously, until approximately 70% confluent. To harvest, flasks were washed twice with 1xPBS, then incubated for 5min in 800µl of Hirt solution (0.6% (w/v) SDS and 10mM EDTA). Flasks were then scraped and the cells collected into a 1.5ml microcentrofuge tube. 200µl of 5M sodium chloride was then added and shaken to mix. The samples were incubated overnight at 4°C to allow the precipitation of genomic DNA and cellular debris. The next day the samples were centrifuged at 9878*g* for 30min at 4°C and the supernatant was transferred to a fresh 1.5ml microcentrofuge tube, discarding the pellet. Phenol/chloroform extraction of the DNA was undertaken by transferring each sample into two fresh tubes each containing 500µl of phenol/chloroform. Samples were vortexed for approximately 2min, then centrifuged for 15min at 9878*g*. The upper phase of the sample was carefully removed and transferred into a fresh microcentrofuge tube containing 100µl of 3M sodium acetate (pH 5.2) and 1ml 100% ethanol. This mix was then incubated at -20°C for approximately 1h to precipitate the DNA. The samples were centrifuged at 9878*g* for 30min, with the supernatant carefully removed and discarded. The DNA pellet was washed with 500µl of 70% ethanol shaking briefly to resuspend the pellet, then centrifuged at 9878*g* for 20min. The majority of the supernatant was removed and the pellet air dried for approximately 10min. Each sample was then resuspended in 50µl of dH_2O and the DNA from the same sample pooled, before storing at -20°C.

2.9.2 DNA Quantification

The Hirt extracted DNA was quantified using the Qubit Fluorometer HS DNA (Invitrogen). Fresh Quant-iT working solution was produced by diluting Quant-iT dsDNA BR reagent

1:200 in dsDNA BR buffer. 10µl of each of the two HS dsDNA standards and 10µl of a 1:10 dilution of the extracted DNA were diluted in 190µl of the Quant-iT working solution, then vortexed for 2-3s, before incubation at room temperature for 2min. The fluorometer HS setting was selected and the machine calibrated using the two standards, the sample readings were then taken and DNA concentrations established using the following equation:-

$$\text{DNA Concentration (ng/µl)} = \text{Qubit value} \times \left(\frac{200}{10}\right)$$
$$= (\text{x dilution factor}) \times 1000$$

2.9.3. *Bam*HI Purification of W12 Plasmid DNA

The W12 plasmid pEFHPV-16W12E is cloned into the pUC18 vector at *Bam*HI restriction sites [19]. Therefore to excise (purify) the W12 DNA from the plasmid backbone *Bam*HI digestion and gel purification were undertaken. 2µg of the W12 plasmid DNA (sections 2.17 and 2.18) was digested with 10 units of *Bam*HI (Promega) in the presence of 0.1mg/ml acetylated bovine serum albumin (Promega) in a 40µl reaction. The digestion was performed for 4h at 37ºC then stored at -20ºC.

Purified W12 plasmid DNA was separated from the plasmid backbone on a 1% agarose gel alongside hyperladder I (75V, ~2h). When sufficiently separated the bands were visualised using a UV lamp (Ultratec) and the insert DNA band excised into a 1.5ml microcentrofuge tube. The purified DNA was then extracted from the gel using QIAquick Gel Extraction kit (Qiagen). The gel slice was weighed and 300µl of buffer QG per 100mg of gel was added and the gel heated at 50°C until the gel had melted (~10min). To this 100µl of isopropanol per 100mg of gel was added and the sample applied to the QIAquick column which was centrifuged for 1min at 9878*g* in a microcentrofuge with the through flow discarded. To remove any remaining traces of agarose a further 500µl of buffer QG was added to the column and then centrifuged at 9878*g* for a further 1min. The column was dried by spinning

at 9878*g* for 1min before the DNA was eluted into a clean 1.5ml microcentrofuge tube by the addition of 50µl autoclaved 18MQ H_2O followed by a 1min spin at 9878*g*. The DNA was then stored at -20°C.

2.9.4. *Bam*HI and *Hin*dIII Digestion

In order to assess the status of the HPV genomes the Hirt extracted DNA underwent digestion with either the single HPV cutter *Bam*HI (Promega), or the non-HPV cutter *Hin*dIII (Promega). For each sample 2.4µg of Hirt extracted DNA was digested with 24 units of *Bam*HI or *Hin*dIII, in the presence of 0.1mg/ml acetylated bovine serum albumin in a 50µl reaction. The solution was mixed and centrifuged briefly before incubating at 37°C for 4h, with the DNA stored at -20°C. Full length W12 purified plasmid DNA was also digested with both *Bam*HI and *Hin*dIII as described above for control purposes.

2.9.5. Gel Electrophoresis

To separate the DNA by base pair size the Hirt extracted DNA (digested or undigested) and plasmid DNA samples were heated at 56°C for 3 min and loaded onto a 1% agarose midi gel (section 2.12). Electrophoresis was then undertaken at 100V for 7.5h with progression assessed under UV light. When electrophoresis was complete the position of the DNA on the gel was photographically recorded, excess gel removed and the upper right hand corner of the gel removed for orientation.

2.9.6. Alkaline Transfer

In preparation for transfer the agarose gel was rinsed twice in dH_2O and the DNA depurinated in 30ml 0.25M HCl with gentle agitation for 30min. The gel was washed twice in dH_2O then

incubated with gentle agitation in 30ml alkaline transfer buffer (0.4M NaOH and 1M NaCl) for 35min, with fresh buffer provided after 15min.

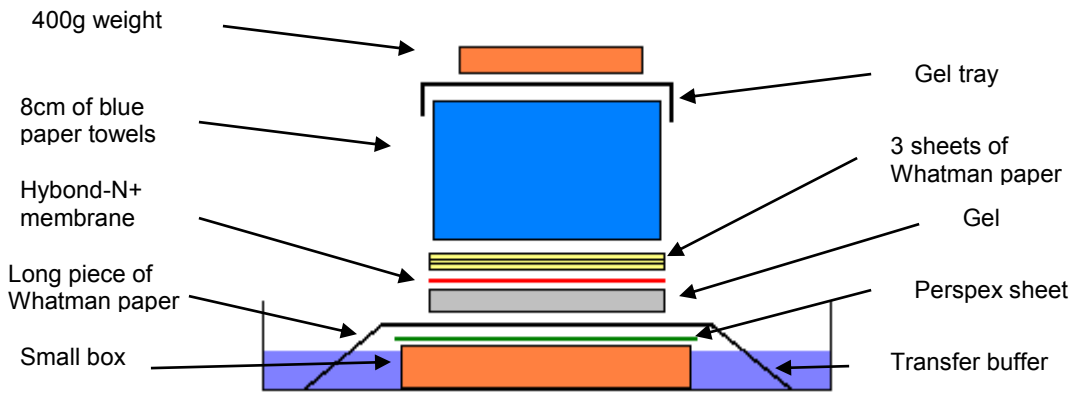

Figure 2.2: The assembly of a Southern blot passive transfer apparatus for the transfer of DNA from agarose gel to hybond-N^+ membrane.

The transfer apparatus was set up as shown in figure 2.2, in a box containing approximately 1L of alkaline transfer buffer. The base section of Whatman paper was gel width, but approximately 5 gel widths long to act as a wick for the passive upwards transfer of buffer. The gel was placed onto the base sheet with the cut corner of the gel to the left, and to prevent aberrant movement of buffer, the area surrounding the gel was sealed with nescofilm. Hybond-N+ membrane (GE Healthcare) was pre-cut (including cut corner for orientation) then placed onto the gel, followed by 3 further sheets of Whatman paper. The surface of the stack was rolled with a Perspex rod to remove any bubbles. Finally 8cm of paper towels and an approximately 400g weight were added and the apparatus left overnight at room temperature for passive transfer of the DNA. After transfer the positions of the lanes were marked on the membrane which was then washed twice in 2x SSC (from 10x stock: 175.3g sodium chloride and 88.2g sodium citrate in 1L dH_2O pH7), air dried and stored at 4°C until ready for hybridisation.

2.9.7. Probe Preparation

The ^{32}P labelled probe was produced by random priming of the *Bam*HI purified W12 plasmid DNA (section 2.9.3) with α[5'-^{32}P] labelled dCTP (500µCi/18.5MBq, PerkinElmer). 25ng of purified W12 plasmid DNA in 30µl dH_2O was mixed with approximately 125ng 10x hexanucleotide mix (Roche) and denatured at 95°C for 2min followed by transfer to ice for 1min. After a brief spin the remaining constituents of the random prime mix were added: 100µM of a 5mM stock dNTP solution (1:1:1 dTTP, dATP and dGTP), 1 in 5 of random priming buffer (appendix B3.1, note 10mM DTT was added at immediately prior to use) and 50µCi [α-^{32}P] dCTP (10mCi/ml stock). The reaction was made up to 50µl with 18MQ dH_2O before the addition of 5 units of DNA polymerase 1 large (Klenow) fragment (Promega). The labelling mix was incubated at room temperature for 60min, with the reaction was stopped by the addition of 10µl stop buffer (appendix B3.2).

2.9.7.1 Probe Purification

Unincorporated nucleotides were removed using the NucAway spin column system (Ambion). The column was hydrated by the addition of 650µl dH2O, vortexed and bubbles removed by flicking. The column was then incubated at room temperature for 15min and stored at 4°C. Immediately prior to use the hydrated column was centrifuged at ~750*g* for 2min to remove excess fluid. The probe was added to the column and centrifuged for 2min at 750*g*. The column was rinsed with 60µl of dH_2O and re-centrifuged with combined fractions of purified probe stored at 4°C.

2.9.8. Southern Blot Hybridisation

The sample-containing membrane was removed from 4°C and rinsed once in 6x SSC. The hybridisation solution was prepared as described in appendix B3.4, with 100.9µl salmon

sperm DNA (Sigma-Aldrich) denatured at 99°C for 10min immediately before addition to 10ml of hybridisation solution, pre-warmed to 68°C. The membrane was blocked in the prepared hybridisation solution at 68°C for 3h in a rolling hybridiser (Hybaid). The ^{32}P labelled probe was denatured at 99°C for 5min and chilled on ice, before addition to 10ml of fresh hybridisation solution prepared as described above. The membrane was then left to hybridise in the presence of the probe overnight at 68°C.

2.9.9. Southern Blot Detection

The membrane was removed from the hybridisation solution and washed twice with shaking at 37°C for 5min in prewarmed 2x SSC with 0.1% (w/v) SDS. The membrane was then wrapped in cling film in preparation for detection. Initial detection was obtained using Instant Imager phosphoImager (Packard) exposed for approximately 3h. After the initial reading the membrane was then transferred to an X-ray cassette with film and left to develop for 1-6 days at -80°C to reduce background disturbance. The film was developed using the standard protocol (section 2.11.5).

2.10. Immunocytochemistry

2.10.1. Immunocytochemistry of Monolayer cells

W12 derivatives were cultured on Lab-Tek chamber slides (Nunc) which provide both a media chamber for cell culture and a rubber gasket (figure 2.3). The gasket acts as a seal during cell culture and can also provide a barrier to retain small amounts of liquid during staining protocols if required.

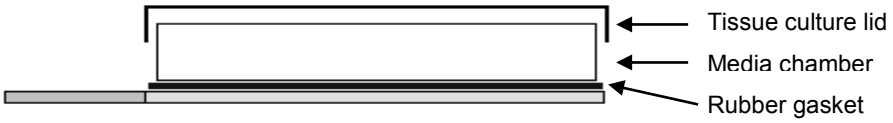

Figure 2.3: The components of a Lab-Tec chamber slide used for monolayer immunocytochemistry.

2.10.1.1. Staining systems

Two different staining systems were utilised for immunocytochemistry; the slides were either stained within a humidified chamber or Shandon sequenza system (Thermo Electron). When using the humidified system the chamber slide rubber gasket was retained to act as a barrier to maintain liquid coverage, with incubations undertaken in an inverted box lined with dampened tissue to provide the required humidified environment.

Alternatively, the chamber slide gasket was removed and the Shandon sequenza system was used. Here slides were loaded into the slide coverplate under 1xPBS and transferred into a slide rack which clamps together the slide and coverplate holding the two surfaces in close proximity. This system utilises gravity flow to draw fluid from the upper chamber of the coverplate into close contact with slide, maintaining an even coverage of the cells until the next solution is added to the upper chamber.

The two staining systems require different fluid volumes in order to maintain a constant coverage of the slide surface: for antibodies the humidified chamber used 250µl of diluted antibody, whereas the Shandon system required only 150µl. For slide washes, for the humidified chamber system two 1xPBS rinses were undertaken manually in separate Coplin jars for 2 minutes each; for the Shandon system two additions of approximately 2ml 1xPBS into the upper chamber were used allowing each to drain under gravity.

2.10.1.2. Preparation and Staining Protocol

The chamber slides were seeded with $1.5x10^2$ mtc treated feeder cells in 2ml of complete F-media as previously described. The following day W12 cells were passaged (section 2.4.2)

and seeded onto the mtc treated feeder layer at 1.5 x 10^2, with EGF added ~24h after passaging (section 2.4.2). Cultures were grown until approximately 60% confluent then treated with 2nM LMB for 38h under normal culture conditions.

After treatment the slides were separated from the media chamber and where required the slide gasket was removed before transferring to 1xPBS. Cells were fixed in ice cold methanol for 30mins at –20 °C, rinsed twice in 1xPBS, and blocked in PBT (1xPBS + 1 % BSA (bovine serum albumin)) for 10mins. When staining for activated caspase-3 (act-casp-3) a peroxidase block was required to reduce innate peroxidase activity associated with higher background staining with this antibody. The block was achieved by incubating slides for 10min at room temperature in 67% methanol, 3% hydrogen peroxide solution. The primary antibodies were incubated for 1h at antibody specific dilutions (for further details see appendix B4.1.1 and B4.2.1). Slides were then rinsed twice in 1xPBS before incubation with the appropriate biotinylated secondary antibody for 30mins diluted in PBT (appendix B4.1.2). Slides then received a further two washes with 1xPBS before incubation with 500µl streptavidin-HRP (1:150, Dako) for 30 mins. Detection was carried out using a 3-amino-9-ethylcarbazole (AEC) staining kit (Sigma-Aldrich-Aldrich) utilising the peroxidase functions of the streptavidin-HRP to catalyse the conversion of the AEC substrate to an insoluble red end product. After a final rinse in dH_2O slides in the Shandon system were removed from the cassettes, and all slides counterstained in haematoxylin (VectorLabs) for approximately 20s. Slides were then rinsed several times in tap water, air dried and coverslips mounted using glycerol buffer (1:1 Glycerol:1xPBS) sealed using clear nail varnish.

To assess apoptosis the positively stained cells were counted systematically from one edge of the slide at x500 magnification. Slides were counted until the proportion of positive cells reached a plateau, as assessed using the running mean method.

2.10.2. Immunocytochemistry of Raft Cultures

Prior to immunocytochemistry, antigen retrieval was performed on 5µm thick sections of paraffin embedded raft cultures. Slides were initially baked for 1hour at 60ºC, before washing twice for 5min in histoclear solution (VWR). Slides were then subjected to two 100% ethanol washes (2min each) and a 2min 100% methanol wash. All washes were undertaken on a gently rocking platform. In preparation for antigen retrieval 1L of 0.01M citric acid (pH6) was preheated for 10min at full power in an 850 W microwave, bringing the citric acid to correct temperature for retrieval. Dewaxed slides were transferred to cold tap water and gently brought to retrieval temperature by the gradual addition of hot water over approx 2-5min. The prepared slides were then transferred to the pressure cooker (Launch Diagnostics) containing the pre-warmed 0.01M citric acid and slides were gently agitated to remove any bubbles present. Slides were then microwaved at pressure on full power for approximately 18min. Slides were transferred from the pressure cooker directly to hot tap water and gently cooled to room temperature by the gradual addition of cold tap water before proceeding. Slides were loaded into the Shandon staining system (using 1x Tris buffered saline (1xTBS) in place of 1xPBS) and any endogenous peroxidase activity was blocked as previously described (section 2.10.1.2). Immunocytochemistry was undertaken on the rafts using the ABC elite Vectorstain mouse or universal staining kits, dependent on the primary. The rafts were blocked in the appropriate 1xTBS diluted serum (1.5% Vectorstain serum) for 20min, before incubation with 150µl primary antibody diluted in blocking solution for 30min (appendix B4.1.1 and B4.2.1). Slides were washed twice with 1xTBS, before incubating for a further 30min with the appropriate biotinylated secondary antibody, diluted 1:200 in blocking solution. The biotinylated secondary antibodies used were a component of the staining kit and not those listed in appendix B4.1.2. After the secondary antibody the rafts were again washed twice with1xTBS and incubated for 30min in the ABC solution (5ml TBS, 2 drops of

reagent A and 2 drops of reagent B prepared 30min before use). Finally two 1xTBS washes were undertaken before detection with the AEC staining kit as described in section 2.10.1.2. Coverslips were mounted using glycerol buffer and sealed with clear nail varnish.

2.11. Colony Survival Assay

The effect of LMB on the colony forming ability of the W12 derivatives, transduced PHKs and HPV infected cancer cell lines CaSki and SiHa was assessed by the colony survival assay. Initially colony forming ability of the E_{63} and I_{22} was tested at different seeding densities to determine the appropriate number of cells to seed after LMB treatment. Cells were seeded in 90mm Petri dishes as described below at approximately 300, 600, 900, 1200 and 1500 cells, and the colony numbers formed were assessed.

For the experimental colony survival assay mtc treated feeder cells were seeded at 5×10^4 in T25 flasks (section 2.4.2) with 6.5×10^5 E_{63} or I_{22}, and the PHK cells expressing E7 were seeded at 4×10^5/T25 flask. Cells were cultured as normal until approximately 50% confluent: at this point the more rapidly growing CaSki and SiHa cell lines were seeded into T25 flasks at 2.5×10^5/flask. Cultures were grown for a further 2 days until approximately 70-80% confluent before treatment with 0nM, 2nM, 20nM, 50nM or 100nM LMB for 40h in standard culture conditions. After treatment the flasks were rinsed twice with 1xPBS and fresh media provided. Post-treatment cultures were then left overnight to recover before passaging. The treated cells were seeded into a 90mm Petri dish at a density of approximately 200 cells, with pre-prepared mtc treated feeder cells provided where required. Cells were then cultured under standard conditions until visible colonies formed in all plates. The media was then removed, the plates rinsed in 1xPBS and cells fixed in ice cold methanol for 30min. Colonies were stained with 5% (v/v) Giemsa (BDH) for 10min and rinsed in dH_2O. The colony number was counted and colony size measured on scanned images (HP psc 1215 scanner) using Scion

Image program, with all measurements in mm^2. Where required microscopic identification of colonies was undertaken using phase contrast microscopy, with the morphologically different J2 3T3 cells disregarded.

2.12. Analysis of Protein Expression

2.12.1. Sample Preparation

2.12.1.1. Cell Harvesting

Cells were grown using an appropriate culture protocol until semi confluent and treated with LMB as indicated in sections 2.4 and 2.12.7. To harvest media was transferred to a 15ml falcon tube to collect any cells in suspension and centrifuged at 145*g* for 5min, the supernatant discarded, and the resultant pellet was stored on ice. Adherent cells were harvested by double scraping, with each followed by collection of cells in 4ml 1xPBS and addition to the appropriate pellet. Flasks were given a final 4ml 1xPBS wash and the collected cells were centrifuged as previously described. The resultant supernatant was discarded, the pellet resuspended in 1ml 1xPBS and transferred to a 1.5ml microcentrofuge. Samples were given a final spin at maximum speed in a microcentrifuge for 5min, the supernatant discarded and pellets snap frozen in liquid nitrogen and stored at -80°C.

2.12.1.2. Cell Lysis

The cell pellets were disrupted by flicking, then lysed by the addition of 50-200µl of Laemmli reducing sample buffer (RSB, see appendix B1.5). To complete the lysis the samples were passed though a 25 gauge needle approximately 10 times, and heated at 95°C for 5min: the resultant lysates were then stored at -20°C.

2.12.1.3. Protein Quantification

Protein levels were quantified using a Qubit Fluorometer (Invitrogen). Quant-iT working solution was prepared by diluting the protein reagent 1:200 in the appropriate buffer, allowing 200µl for each of the 3 protein standards and samples. The protein standards were prepared by diluting 10µl of the appropriate standard in 190µl of the Quant-iT working solution, producing a total assay volume of 200µl: solutions were then vortexed for 2-3s. For each experimental sample a 1:10 dilution of protein lysate was prepared (1µl sample and 9µl dH_2O) and combined with 190µl of the Quant-iT working solution before vortexing for 2-3s. Standards and experimental samples were then incubated for a minimum of 15min at room temperature. The fluorometer was calibrated using the 3 protein standards: the experimental samples were then measured in µg/ml. If protein concentrations were outside the fluorometer's quantifiable range the quantification was repeated using either neat sample or 1:100 dilution as required. Final protein quantities were calculated using the following equation:-

$$\text{Protein Concentration } (\mu g/\mu l) = \text{Qubit value} \times \left(\frac{200}{10}\right)$$
$$= (\text{x dilution factor}) \times 1000$$

2.12.2. Sodium Dodecyl Sulphate – Polyacrylamide Gel Electrophoresis

Sodium Dodecyl Sulphate – Polyacrylamide Gel Electrophoresis (SDS-PAGE) was undertaken using the Hoefer Mighty Small mini electrophoresis system (Hoefer), to separate the proteins according to their molecular weight, prior to Western analysis. Firstly the resolving gel was prepared (see appendix B2.1), with the gel percentage determined by the molecular weight of the target proteins: for details of gel percentages used for these studies please see appendix B4.2.2. The resolving gel was overlaid with a layer of 70% ethanol to level the gel surface and prevent drying, then left to polymerise at room temperature for a minimum of 30min. Once polymerised, the ethanol was removed and the stacking gel

prepared as listed in appendix B2.3. When added to the surface of the resolving gel either a 10 well (standard analysis) or 15 well (time course) 1.5mm comb was inserted into the resolving gel and left to polymerise for at least 15min.

2.12.2.1. Gel Sample Preparation

Gel samples were prepared using 20µg of the experimental protein lysate, made up to the loading volume with appropriate volume of bromophenol blue containing reducing sample buffer (approximately 0.001% (w/v) bromphenol blue). Loading volumes varied according to well number, 20µl for 10 wells and 17µl for 15 wells. Prior to loading, proteins were denatured at 95°C for 5min, and centrifuged briefly. The broad range prestained protein marker (New England Biolabs) was prepared by diluting 4µl of marker in 13µl (15 well) or 16µl (10 well) of loading buffer.

2.12.2.2. Acrylamide Gel Electrophoresis

Gels were loaded into the running rig containing 1x running buffer prepared from 10x stock buffer (100ml in 900ml, see appendix B2.5). Electrophoresis was initially undertaken at 100mV until samples entered the resolving gel (after approximately 15min). The voltage was then increased to 150mV and the gels were left for approximately 1h or until samples had run a sufficient distance to provide suitable separation (as assessed by the progression of the bromophenol blue stain and protein standard).

2.12.3. Transfer of Proteins to PDVF membrane

Hybond-P PDVF membrane (GE Healthcare) was cut to size and orientated by the removal of one corner. To activate the PDVF membrane, it was soaked for 10s in 100% methanol and rinsed for 5min in dH_2O, then equilibrated for at least 10min in 1x transfer buffer. 1L 1x

transfer buffer was prepared by combining 100ml 10x transfer buffer (appendix B2.5) in 50ml 100% methanol and 850ml dH_2O.

After the termination of electrophoresis, gels were removed, the stacking section discarded, and the upper right corner of the gel removed to provide orientation. The resolving gel was transferred to a large container of 1x transfer buffer and soaked briefly. The transfer stack was assembled as shown in figure 2.4, ensuring that the black side of the cassette formed the base of the stack. Whatman blotting paper was cut to size, and along with the transfer sponges was briefly soaked in 1x transfer buffer before use. After the positioning of the upper Whatman paper over the membrane, the surface was rolled to remove any bubbles.

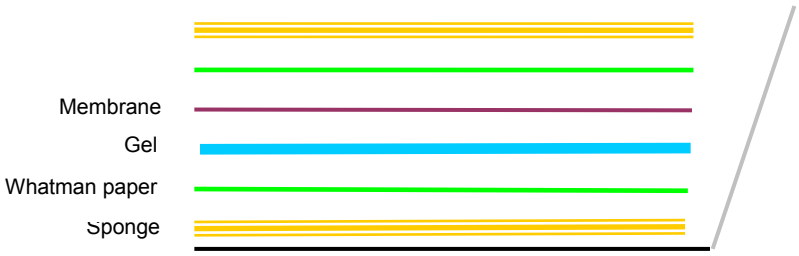

Figure 2.4: The assembly of the stack for the transfer of protein from SDS-PAGE gel to PDVF membrane.

The Hoefer transfer rig was filled with approximately 1L of 1x transfer buffer and the loaded transfer cassette was placed into the rig hinge side up with the black side facing forward. Protein transfer was achieved by applying a constant current of 100mV for 1h: the unit was cooled by passing running tap water through the base of the transfer rig. When the transfer was complete the gel was discarded and the positions of the molecular weight marker bands were marked on the membrane. The appearance of the ladder on the membrane was indicative of a successful transfer: this was confirmed by visualising the transferred protein by soaking the membrane for approximately 2min in Ponceau S solution (0.1% Ponceau S (w/v), 5% acetic acid (v/v)). This was followed by several washes in 1x PBS with 0.1% Tween-20

(PBST). If the protein lanes displayed considerable unequal loading or disruption by bubbles then the membrane was discarded.

2.12.4. Western Blotting

The membrane was blocked for 1h in approximately 20ml PBST containing 5% (w/v) semi-skimmed powdered milk (mPBST) at room temperature. The blot was then incubated overnight at 4°C in 5-10ml of the primary antibody, diluted in fresh blocking solution at an antibody-dependent dilution (appendix B4.2.2). The primary antibody solution was then removed and the membrane washed twice washes in approximately 50ml of PBST for approximately 15min per wash. The membrane was then incubated with 5-10ml of the appropriate HRP-conjugated secondary antibody (Pierce) at 1:10 000 in PBST/mPBST (appendix B4.2.2) for 1h at room temperature. Finally the blot underwent six larger volume 10min washes in PBST to remove excess secondary antibody. All incubations and washes were undertaken with gentle rocking.

2.12.5. Detection

Bands were visualised with Immobilon Western chemiluminescent HRP substrate detection system (Millipore), mixing the luminol and peroxide solutions in a 1:1 ratio. The signal was detected on Fuji film X-ray film (Fisher) exposed for an antibody-dependent period of time (appendix B4.4), then developed by incubating in Kodak GBX developer (Sigma-Aldrich) for 1min, then 1-2min in Kodak Unifix (Sigma-Aldrich) finally rinsing briefly in tap water. Developed films were then scanned using a HP psc 1215 and, where necessary, quantification was achieved using ImageJ software (National Institute of Health (NIH), USA) with all measurements given as integrated density in arbitrary units (AU) normalised against β-Actin.

2.12.6. Stripping and Reprobing of Membranes

Where a membrane required reprobing for an alternative protein of a similar molecular weight, the membrane was stripped. This was achieved using 4 washes in 10% (v/v) glacial acetic acid for 5-10min each, followed by at least 4x10min washes in 10ml PBST. After stripping, the membrane was blocked again before proceeding with the addition of the new primary antibody. In all the western blots shown in this thesis the membrane was stripped before reprobing for β-Actin.

Where the molecular weight of the additional protein was sufficiently different from the initial protein and did not interfere with the detection of the second protein, the membrane was washed twice for 10min in 1xPBS prior to the addition of the new primary antibody, with no repeat blocking required.

2.12.7. Experiment-Specific Protocol Variations

2.12.7.1. Analysis of Cytokeratin 18 Protein Expression

In order to utilise the M30 antibody, the expression and any variation in the levels of cytokeratin 18 (CK18) were assessed using protein lysates from all the W12 derivatives. The expression of CK18 within the PHK cells has been confirmed by Gray *et al* (2006) [374].

2.12.7.2. Time Course Analysis of Protein

In order to analyse the progression of the apoptotic response over time, a 48h time course was performed. All flasks were provided with fresh medium immediately prior to LMB treatment and to obtain baseline protein expression one flask from each cell line was harvested at this point. Further flasks were then treated with 2nM LMB and harvested at 12h, 24h, 36h, and 48h after treatment alongside time matched untreated controls. Cells were harvested and analysed as described in the standard protein assay, with 15 well acrylamide gel

electrophoresis. For the analysis of M30 and act-casp-3 individual membranes were used; however for p53 and p21 the same membrane was utilised unstripped.

This protocol was repeated to analyse the contribution of mtc treated J2 3T3 feeder cells to the LMB-induced effects, with treated E7 transduced PHKs used as a positive control. Mtc treated J2 3T3 cells were seeded at the same concentration used for the W12 cell time course and maintain under W12 culture conditions. J2 fibroblasts and E7-transduced cells were treated with 2nM LMB for 48h and harvested as normal. The expression of act-casp-3, M30 and β-actin in 25µl of J2 lysate (maximum loading volume) and 20µg of E7 lysate were assessed as previously described.

2.12.7.3. Low Confluence Analysis of HPV 16 E2 Protein

To assess expression of the HPV 16 E2 protein in the W12 derivatives, the cells were cultured as normal without LMB treatment. To obtain maximum E2 expression, the W12 derivatives were harvested while highly subconfluent (approximately 50% as qualitatively assessed by phase contrast microscopy). U2OS cells transfected with HPV 16 E2 (clone E2B3) or pCMV4 (clone D3) were utilised as positive and negative controls for E2 expression. Due to the presence of non-specific bands in the predicted E2 region of the membrane on initial gels using the mini electrophoresis system, an 8% SDS-PAGE midi gel (Hoefer SE600) was used to provide maximum separation within this region of the gel. The protein analysis was undertaken as described above, with the following exceptions. Due to the increased size of the midi gel both the resolving and stacking gels were left for 1h (instead of 30min) to polymerise. Samples consisted of 15µg of E2 expressing and vector only U2OS lysates, along with 70µg of the low confluence W12 lysates (made up to 30µl). Samples were loaded alongside 12µl of molecular weight marker, and run at 25mA for approximately 5.5h. To reduce any heat damage to the protein due to prolonged electrophoresis the rig was cooled by the circulation of running tap water and placement of the rig in an ice bath. After

electrophoresis the gel was trimmed. In order to maximise protein transfer the trimmed gel was soaked for approximately 15min in transfer buffer to remove any contaminating SDS (section 2.12.3). Membrane blocking was carried out as described in section 2.12.4 for 1.5h prior to addition of the primary antibody TGV261. The membranes were incubated overnight at 4°C in 12ml of diluted primary antibody to ensure complete coverage of the membrane (appendix B4.4). To maximise detection and to minimise background staining, the secondary antibody was diluted in 3% mPBST. As *in vivo* expression of the E2 protein is very low, maximum sensitivity was achieved during detection using the supersensitive SuperSignal West Femto Maximum Sensitivity Substrate (Pierce) mixing the luminal, peroxide and 1xPBS in a 1:1:5 ratio, and detected initially for 10min followed by a further 1h exposure. To further increase sensitivity and reduce background the x-ray cassette was lined with reflective material.

2.12.7.4. Alkaline Phosphatase Digestion of Protein

To assess the phosphorylation state of the p21 protein in the W12 derivatives, an alkaline phosphatase digestion was undertaken. Digestion was undertaken on 20µg of non-time course protein lysate (prepared as described in section 2.12.1.); the samples were incubated with 1 unit of calf intestinal alkaline phosphatase (CIAP) (Promega) and 1µl of the appropriate buffer for 30min at 37ºC. Digested protein was stored at -20ºC before being analysed as described for the standard protein assay.

2.12.7.5. Analysis of p21 Protein using C-Terminal and Internally Located Antibodies

To assess the expression of the p21 doublet 40µg of time course lysate (12h+LMB, section 2.12.7.2) from W12 derivatives E_{50}, E_{63}, I_{02} and I_{31}, separated in duplicate by SDS-PAGE (section 2.12.2) and transferred to PDVF (section 2.12.3). The membrane was cut and

western analysis was undertaken using either the C-terminal antibody SX118 or internally located antibody EA10 (see appendix B4.4), as described in section 2.12.7.2.

2.12.7.6. LMB Treatment U2OS Cells

Any potential LMB response in the U2OS cell line and any role of HPV 16 E2 in the LMB response was analysed by treatment of U2OS cells transfected with HPV 16 E2 (clone E2B3), pCMV4 vector (clone D3) and non-time course W12 derivatives, with 2nM LMB for 38h (section 2.3). Cultures were harvested and protein analysis undertaken for activated caspase-3 and M30 by western blot, as described in section 2.12.1-6. In this case the membrane blocking which was undertaken overnight at 4°C, with the antibodies incubated at room temperature for 1h.

2.12.7.7. LMB Treatment of Dominant Negative p53 Cells

The contribution of the p53 response to LMB induced apoptosis was assessed by the treatment of wild type (wt) and Dnp53 (and vector only) transduced W12 derivatives E_{50}, I_{22} and I_{31}, and the PHK lines containing E7 and E6/E7. Dnp53, pBabe only and wt cultures were grown in T25 flasks until approximately 60-70% confluent; cells were then treated for 38h with 2nM LMB as described in section 2.3. Cultures were harvested as described previously with lysis undertaken in 15ml falcon tubes followed by transfer to 1.5ml microcentrofuge tubes for storage. As the experiment was undertaken on cells seeded in T25 flasks, quantification was undertaken using the Qubit system with 1µl of neat lysate due to lower cell numbers. Alterations in expression of the apoptotic markers act-casp-3 and M30 were then assessed as described in sections 2.12.4-6, with the exception of M30 where the membrane was blocked overnight at 4°C, with antibody incubation at room temperature for 1h.

2.13. Agarose Gel Electrophoresis

Agarose gel electrophoresis was undertaken to separate DNA templates by base pair size using an agarose gel matrix. The gels were made by combining 1% (w/v) agarose (Bioline) with 1x Tris-Borate-EDTA (TBE, Sigma-Aldrich) from 10x stock solution. The gel mix was heated in an 850w microwave at medium power until the agarose melted to form a clear solution (1-3min); for details see table 2.2.

	Total volume	**10x TBE**	**Water**	**1% Agarose**	**Ethidium Bromide**
Mini gel	50ml	5ml	45ml	0.5g	2.5µl
Midi gel	150ml	15ml	135ml	1.5g	7.5µl

Table 2.2: The quantities of gel components require for the production of 1 or 2% agarose mini and midi gels used in gel electrophoresis.

To detect the presence of DNA, 0.05% ethidium bromide (Sigma-Aldrich) was added and the gel poured into the gel tray with the appropriate comb. Gels were allowed to set for at least 30min before use. Either Agragel mini (Biometra) or HU13 midi (SCIE-PlAS) rigs were used according to the number of samples and amount of band separation required.

Electrophoresis was undertaken in an appropriate volume of 1x TBE sufficient to cover the surface of the gel. To load, 8µl of sample was combined with 2µl of 5x loading buffer; each gel was also loaded with 4µl hyperladder I or II (Bioline). Samples were then subjected to 80- 150V depending on the size of the gel and required resolution, for approximately 1-1.5h or until sufficiently separated. The passage of DNA through the gel was assessed by illumination under UV (302nM) light and photographic records acquired using the Syngene UV Transilluminator system (Syngene).

2.14. Extraction of DNA and RNA from Cultured Cells

Cells were cultured as normal until approximately 70-80% confluent and harvested as previously described (section 2.4). After centrifugation cells were resuspended in 0.5-1ml 1x PBS and transferred into a 1.5ml microcentrofuge tube. The cell suspension was then centrifuged at 9878*g* for 5min and the supernatant discarded. If the DNA/RNA extraction was not to be carried out immediately, the cell pellet was snap frozen in liquid nitrogen and stored at -80°C.

2.14.1. DNA Extraction

DNA was extracted using the Wizard genomic DNA Purification Kit (Promega). To each cell pellet 600µl of nuclei lysis solution was added and mixed until no clumps remained. Contaminating RNA was removed with 3µl of RNase solution incubated at 37°C for 30min. The sample was allowed to equilibrate to room temperature for 5min before 200µl of protein precipitation solution was added and the sample vortexed briefly to mix. The sample was then incubated for 5min on ice and centrifuged at 9878*g* for 4min to pellet the precipitated protein. The DNA containing supernatant was transferred to a fresh 1.5ml microcentrofuge tube containing 600µl of room temperature isopropanol and mixed. The solution was centrifuged for 1min at 9878*g* and the supernatant carefully removed and discarded. The DNA pellet was then washed in 600µl of 70% ethanol, and centrifuged at 9878*g* for 1min. The ethanol wash was discarded and the pellet air dried for approximately 15min, with the DNA resuspended in 100µl of rehydration solution and left to rehydrate overnight at 4°C, with long term storage at -20°C.

2.14.2. RNA Extraction

RNA extraction was undertaken using the RNeasy Minikit (Qiagen). The harvested cells were mixed with 600µl of buffer RLT (including 1:100 of β-mercaptoethanol (Sigma-Aldrich)). The sample was homogenised by passing the lysate 10 times though a 20 gauge needle fitted to a sterile 1ml syringe and 600µl of 70% ethanol then added. Up to 700µl of the sample was then placed onto the RNeasy mini column and centrifuged at 9878*g* for 15s: the through flow was discarded and the process repeated with the remainder of the sample. The column was washed by the addition of 700µl of buffer RW1 followed by a 15s spin. Two further 500µl washes with buffer RPE were performed with each followed by a 2min centrifuge at 9878*g*. To ensure that any remaining wash solution was removed an additional 1min spin was also undertaken. The RNA was eluted into a fresh 1.5ml microcentrifuge tube by the addition of 50µl autoclaved 18MQ water followed by centrifugation for 1 min at 9878*g*; this was repeated with a further 50µl of dH_2O with the resulting RNA stored at -80°C.

2.15. Reverse Transcription

In order to analyse mRNA expression, reverse transcription of extracted RNA was undertaken using reverse transcriptase derived from avian myeloblastosis virus (AMV, Roche). Reverse transcription and PCR reactions were all undertaken in thin walled 0.2ml microcentrifuge tubes (Fisher). All dH_2O and equipment including blocked pipette tips (ART 10 reach, VWR) were subjected to UV light treatment (autocrosslink setting, UV stratalinker 2400, Statagene) to reduce the presence of contaminating DNA, DNase or RNase. DNase digestion, reverse transcription and PCR reactions were all undertaken in a Biometra Tpersonal thermal cycler (Biometra), with the heated lid temperature set at 10°C above the maximum reaction temperature.

2.15.1. DNase Digestion of RNA

To remove contaminating genomic DNA from the extracted RNA a DNase digest was undertaken using RQ1 RNase-free DNase (Promega). The digest was undertaken using 6µg of RNA mixed with 3µl of 10x RQ1 reaction buffer and 6 units of RQ1 DNase in a 30µl reaction. The digestion mix was centrifuged briefly before incubating at 37ºC for 30min; 1µl RQ1 DNase stop solution was then added followed by a 10min incubation at 65°C. The digested RNA was then stored at -80°C.

2.15.2. Reverse Transcription

The reverse transcription reaction was undertaken on the DNase digested RNA both in the presence (RT+) and absence (RT-) of AMV reverse transcriptase to control for the presence of any remaining genomic DNA (gDNA) contamination. To reverse transcribe, 1µg of digested RNA was combined with 1µl of 10x hexanucleotide mix (0.06A_{200}U/ul, Roche) in a reaction volume of 13µl, with two reactions for each cell line to provide RNA for RT+ and RT- reactions. The sample was then denatured at 65ºC for 10min and transferred directly to ice for 1min. Two master mix solutions were then prepared: in the RT- master mix the AMV component was replace with an equivalent volume of dH_2O. The master mix for 8 samples was as follows; 4.5 µl protector RNase inhibitor (20U/reaction, Roche), 36µl AMV buffer (Roche), 18µl of 10mM PCR nucleotide mix (Roche), and where appropriate 4.5µl AMV (10U/reaction).

The reverse transcription mix was prepared by combining the 13µl RNA/hexamer mix with 7µl of the appropriate master mix solution and centrifuging briefly. The reverse transcription was undertaken by heating for 10min at 25ºC, 30min at 55ºC and then immediate transfer to

ice. The AMV enzyme was inactivated by heating at 95ºC for 2min, with the resulting cDNA stored at -20ºC.

2.16. Polymerase Chain Reaction

Polymerase Chain Reaction (PCR) was undertaken using template DNA from either the host, the viral genome (gDNA) or reverse transcribed mRNA (cDNA). Where cDNA was used the PCR reaction was undertaken on both the RT+ and RT- samples, using primers for the gene of interest and the housekeeping gene beta-2-microglobulin (B2M) to detect DNA contamination in either the RT+ or RT- samples. CaSki cell gDNA was also used in the PCR reactions as a positive control for the primer of interest and B2M.

2.16.1 E2 PCR and RT-PCR

Analysis of E2 within the viral genomic DNA was undertaken using 0.5µl of E_{50}, E_{63} and CaSki template, and 1µl I_{02}, I_{22}, I_{31}, I_{61} and SiHa template, while analysis of cDNA was undertaken using 1µl (50ng) of the reverse transcribed cDNA. The template DNA was combined with 12.5µl of PCR ReadyMix containing 3mM magnesium chloride (Sigma-Aldrich-Aldrich), 2µl of forward and reverse primers (Sigma-Aldrich, Table 2.3) in a reaction volume of 25µl.

Target	Direction	Primer	Primer Sequence (5'-3')	Band Size	Ref
E2 Amplimer A	Forward	A1	AGGACGAGGACAAG GAAAA	A1-A2 = 476bp	Graham *et al*, 2000 [414]
	Reverse	A2	ACTTGACCCTCTACC ACAGTTACT		
E2 Amplimer B	Forward	B1	TTGTGAAGAAGCATC AGTAACT	B1-B2 = 478bp B1-C2 = 702bp	Graham *et al*, 2000 [414]
	Reverse	B2	TAAAGTATTAGCATC ACCTT		
E2 Amplimer C	Forward	C1	GTAATAGTAACACTA CACCCATA	C1-C2 = 277bp	Graham *et al*, 2000 [414]
	Reverse	C2	GGATGCAGTATCAA GATTTGTT		
E2 - Additional	Reverse	C3	GGACGTATTAATAG GCAGAC	C1-C3 = 345bp B1-C3 = 770bp	N/A
B2M	Forward	B2M1	ACTGAATTCACCCCC ACTGA	gDNA = 740bp cDNA = 114bp	Zhang *et al*, 2005 [415]
	Reverse	B2M2	CCTCCATGATGCTGC TTACA		

Table 2.3: Primers used for the amplification of the E2 ORF by PCR or RT-PCR including B2M control. B2M sizes are given for genomic (gDNA) and reverse transcribed (cDNA) templates.

Amplification was undertaken using the following program:-

1. Initial denaturation at **94ºC** for **1min**
2. Denature at **94ºC** for **1min**
3. Anneal at primer dependent temperature for **50s** (see table 2.4)
4. Elongate at **72ºC** for **1m 30s** (repeat steps 2-4 34 times)
5. Final incubation at **72ºC** for **10min**
6. Pause at **4ºC**

	Annealing Temp
E2 Amplimer A	58°C
E2 Amplimer B	54°C
E2 Amplimer C	55°C
E2 Additional	58°C
B2M	54 - 58°C

Table 2.4: The annealing temperatures, agarose gel percentages and hyperladders used in the PCR analysis for the E2 amplimers. For details of primers see appendix B5.

The PCR products were analysed by running on a 1% agarose gel with hyperladder II (for further details see agarose gel electrophoresis section 2.12.).

2.16.2. E6/E7 PCR and RT-PCR

Amplification of the E6/E7 ORF products described in Selinka *et al* 1998 [109] was undertaken as described for E2 PCR using 1µl (50ng) of reverse transcribed cDNA.

Target	Direction	Primer Name	Primer Sequence (5'-3')	Band Size	Ref
E6/E7	Forward	S3	ACAGTTATGCAC AGAGCTGC	E6/E7 = 525bp E6*I = 434bp E6*II = 226bp	Selinka *et al*, 1998 [109]
	Reverse	S4	CTCCTCCTCTGA GCTGTCAT		
B2M	Forward	B2M1	ACTGAATTCACC CCCACTGA	gDNA = 740bp cDNA = 114bp	Zhang *et al*, 2005 [415]

Table 2.5: Primers used for the amplification of the E6/E7 ORF by PCR or RT-PCR including the beta-2-microglobulin (B2M) control. Band sizes for B2M are given for viral genomic (gDNA) and reverse transcribed (cDNA) templates.

The PCR was undertaken using the primers in table 2.5, combined with the program below and products analysed on a 1% agarose gel using hyperladder I.

1. Initial denaturation **94ºC** for **3min**
2. Denature at **94ºC** for **1min**
3. Anneal at **55ºC** temperature for **45s**
4. Elongate at **72ºC** for **1min** (repeat steps 2-4 29 times)
5. Final incubation at **72ºC** for **10min**
6. Pause at **4ºC**

2.16.3. E7 RT-PCR

Amplification of the E7 ORF products was undertaken as described for E2 PCR using 1µl of reverse transcribed cDNA derived from PHK transduced with E7 or E6/E7. Primers as

described by Nees *et al* (2000) [416] are shown below (table 2.6), were annealed at 58°C, with products analysed on 1% agarose gels alongside hyperladder II.

Target	Direction	Primer Name	Primer Sequence (5'-3')	Band Size	Reference
E7	Forward	E7-1	ATGACAGCTCAG AGGAGGAG	E7 = 176bp	Nees *et al*, 2000 [416]
	Reverse	E7-2	TCATAGTGTGCCC ATTAACAG		
B2M	Forward	B2M1	ACTGAATTCACCC CCACTGA	gDNA = 740bp cDNA = 114bp	Zhang *et al*, 2005 [415]
	Reverse	B2M2	CCTCCATGATGCT GCTTACA		

Table 2.6: Primers used for the amplification of the E7 ORF by RT-PCR, including the B2M control. Band sizes for B2M are given for viral genomic (gDNA) and reverse transcribed (cDNA) templates.

2.16.4 Dnp53R248W PCR

PCR analysis was undertaken to detect the presence of the Dnp53R248W plasmid using 0.1µg of template from the PT67, W12, PHK, and U2OS cells containing either Dnp53 or vector only. PCR was undertaken using primers shown in table 2.7 and the E2 programme (2.16.1) with an annealing temperature of 68°C. PCR products were analysed on 1% agarose gels alongside hyperladder I.

Target	Direction	Primer Name	Primer Sequence (5'-3')	Band Size	Source
Dnp53R248W	Forward	pLXSN2S	TTCATCTGGACCT GGGTCTTCAGT	467bp	Androphy, USA
	Reverse	P53A	TCAAGCCCTTTGT ACACCCTAAGC		

Table 2.7 Primers used for the amplification of the Dnp53R248W by PCR from transfected cells.

2.17. Transformation and Culture of Bacteria

2.17.1. Preparation of LB-Agar Plates

LB-Agar was prepared by mixing Miller's LB broth base (Luria broth base, Invitrogen) with 1.2% (w/v) Select agar (Invitrogen) and autoclave sterilised. When required the agar was melted in a microwave at medium power until completely dissolved and placed into a water bath to equilibrate to 50°C. Where appropriate, ampicillin was added to plates to a final concentration of 50µg/ ml (stock solution of 50mg/ml). Approximately 30ml of either plain agar (for control plates) or agar with ampicillin were poured into 90mm Petri dishes and left to set for at least 30min.

2.17.2. Bacterial Transformation

Bacterial transformation was undertaken using XL Ultra competent *E.coli* (Stratagene), stored at -80°C. All the plasmids (table 2.8) were resistant to ampicillin, which was used to select successfully transformed bacterial cells. A non-transformed bacterial control was also undertaken to confirm antibiotic selection.

Plasmid	**Use**
pEFHPV-16W12E	W12 plasmid DNA
Dnp53R248W	Dominant negative p53
pBabe-puro	Vector only control for Dnp53
pSynp53	p53 driven firefly luciferase reporter
pRL-CMV	Renilla luciferase

Table 2.8: Plasmids used for bacterial transformation.

To transform, 2µl of beta-mercaptoethanol was added to 50µl aliquots of competent cells and incubated on ice for a total of 10min, stirring every 2min. Approximately 50ng of plasmid DNA was then added and the mixture incubated on ice for 30min. The bacterial cells were then heat-shocked at 42°C for 30 seconds and placed immediately on ice for 2min. To the

heat shocked bacteria 950µl of LB broth (25g/L LB broth mix (Invitrogen) autoclave sterilised) was added and the samples shaken at 37°C, ~250rpm for 1h. The samples were then centrifuged at 500*g* for 3min, approximately 800µl of the supernatant was removed and the pellet resuspended in the remaining ~200µl of the remaining broth.

Freshly transformed or previously transformed cells (from glycerol stocks or bacterial stabs) were plated onto LB-agar plates containing 50µg/ml ampicillin and left to grow overnight at 37°C to allow selection of transformed colonies.

2.17.3. Bulk Growth of Transformed Bacterial Colonies

Bacteria from glycerol stocks or selected agar plate colonies were grown in 3-6ml of LB broth containing 1µl/ml ampicillin in preparation for plasmid extraction. Either a scraping from a glycerol stock or a single colony from a plate was used to inoculate the bacterial culture. The bacteria were then grown overnight (~18h) at 37°C shaking at 220rpm, and the plasmid DNA extracted as described in section 2.17.

2.17.4. Long Term Storage of Transformed Bacteria

Once transformed the bacteria were stored as glycerol stocks at -80°C. Stocks were produced by mixing ~ 600µl of the overnight bacteria culture with 400µl of 50% (v/v) sterile glycerol in a 1.5ml cryotube.

2.18. Extraction of Plasmid DNA

Extraction of plasmid DNA from transformed bacteria was undertaken using the Plasmid Mini Kit (Qiagen). The bacterial culture was transferred into a 1.5ml microcentrofuge tube by spinning 1.5ml aliquots at 8000*g* (5min), with the supernatant removed and discarded. The

bacterial pellets were then resuspended in 300µl of buffer P1 and disrupted. To this solution 300µl of buffer P2 was added and the sample incubated for 5min at room temperature. The protein was precipitated by the addition of 300µl of chilled buffer P3, mixed by inverting and incubated on ice for 5min. Samples were remixed before centrifuging for 10min at 9878*g*. The resultant supernatant was transferred onto a QIAGEN-tip 20 (equilibrated in advance by the addition of 1ml buffer QBT) and left to empty under gravitational flow. The column was washed by 4 separate 1ml additions of buffer QC, and the DNA eluted from the column into a clean 1.5ml microcentrifuge tube by 800µl of buffer QF. The DNA was precipitated with 560µl of room temperature isopropanol and collected by centrifuging at 9878*g* for 30min. The supernatant was discarded, the pellet washed in 1ml 70% ethanol and centrifuged for 30min at 9878*g*. After the ethanol was removed the DNA pellet was air dried for 5min, then resuspended in 50µl of autoclaved 18MQ dH_2O and rehydrated at room temperature overnight before storage at -20°C.

2.19. p53 Reporter Assay of Dnp53R248W

In order to confirm the DNA binding deficiency of dominant negative p53 (Dnp53R248W) a p53 driven luciferase reporter system was used. The pSynp53 plasmid (kind gift from K. Gaston, University of Bristol)[417] contains the p53 promoter upstream of the firefly luciferase gene and hence acts as a reporter of p53 DNA binding by the production of the 61kDa firefly luciferase protein. Dual transfection with *Renilla* luciferase (pRL-CMV, kind gift of J. Parish, University of St Andrews) provided an internal control for transfection efficiency.

2.19.1. Transfection with pSyn-53 and pRL-CMV

For each Dnp53 transduced cell line, Dnp53, vector only, and wild type cells were seeded into 6 wells each of a 6-well plate. Cells were then cultured until approximately 50% confluent

before transfection as described in section 2.7.3 (in the absence of antibiotic selection). For each transduced line cells were either transiently transfected with pSynp53 and pRL-CMV (figure 9) or left untransfected. After 24-48h fresh media was provided. Subsequently half the transfected and untransfected cells were treated with 2nM LMB prior to harvest (table 2.9).

Experiment	pSynp53	pRL-CMV	Transfection time	Treatment Time
Wt U2OS, PHK E7	1µg	50ng	48h	12h
Dnp53 U2OS	1µg	50ng	24h	26h

Table 2.9: Protocol details for the preparation of samples for dual luciferase assay using pSynp53 and pRL-CMV.

2.19.2. Dual-Luciferase Reporter assay for p53 Activity

To harvest, the medium was removed and wells rinsed with 0.5-1ml 1xPBS. To lyse the cells, 500µl of 1x passive lysis buffer (Promega) was added and the plate rocked at room temperature for approximately 15-30min. The lysates were transferred to 1.5ml microcentrifuge tubes and stored at 4ºC. Detection of luciferase activity was undertaken using the Dual-Luciferase reporter assay system (Promega). The luminescence signal was detected using the Flurostar Optima microplate reader (BMG LABTECH), programmed with a 2 second pre-measurement delay and a 10 second per well measurement period. To detect the firefly signal 100µl of Luciferase Assay Reagent II (LARII) was combined with 20µl of cell lysate in a black microtest 96-well plate (Becton and Dickinson), pipetting 3 times and luminescent readings taken. The *Renilla* luciferase was detected by the addition of 100µl of 1x Stop&Glo reagent (1 volume Stop&Glo substrate to 50 volumes Stop&Glo buffer) to the existing samples in the 96-well plate, gently vortexed and measurements repeated.

To assess the activation of pSynp53 the mean of the control (untransfected) wells was calculated and subtracted from each transfected sample for both pSynp53 and pRL-CMV readings giving the adjusted values for each. To correct for variations in transfection efficiency the adjusted pSynp53 value was divided by the adjusted pRL-CMV to give the final reading.

Chapter 3: The Status of HPV 16 in Cells Expressing Episomal and Integrated Viral Genomes

3.1. Introduction

The W12 derivatives provide a useful model of the early stages of HPV 16-associated neoplasia. The presence of the whole HPV 16 genome derived from a low grade lesion means these derivatives act as an alternative to cells expressing only selected viral genes such as the E7 and E6/E7 transduced PHKs, and HPV-associated cancer cell lines such as CaSki and SiHa. Integration of the normally episomal genome with its subsequent effects on viral gene expression is thought to have important consequences for the formation of potentially malignant lesions and may also influence their response to LMB. It is therefore important to confirm the status of the HPV 16 genome within the W12 derivatives. As E2, E6 and E7 all appear to play important roles in the response to integration it is of interest to establish the expression of these viral genes within the cell lines studied.

3.2. Methods

The assessment of HPV integration in the W12 derivatives was undertaken by Southern blot analysis using ^{32}P labelled HPV DNA probe as described in section 2.9. E2 protein expression was detected via SDS-PAGE in combination with Western blot analysis as described in section 2.12, with the status of the E2 and E6/E7 genes assessed using polymerase chain reaction (PCR, section 2.16) on genomic DNA or reverse transcribed cDNA, as described in sections 2.14-2.16.

3.3. Results

3.3.1. Analysis of the Physical State of HPV 16 in the W12 Derivatives

Southern blot analysis of the episomal W12 derivatives E_{50} and E_{63}, in combination with representatives of type 1 (I_{22}) and type 2 integration (I_{31}), was undertaken to confirm the physical status of the HPV genome (figure 3.1). Predominantly episomal viral genomes within the uncut episomal W12 derivatives were indicated by the presence of high levels of both the open circular and supercoiled forms of HPV 16 DNA [418]. The presence of episomes was confirmed by the production of a 7.9kb band after *Bam*HI digestion [131], consistent with linearisation of the viral genomes by cutting at a single site within the HPV genome (nt 6150 in HPV 16 [129]). However, the E_{63} derivative did show the presence of some remnant supercoiled DNA after *Bam*HI treatment. This may represent incomplete digestion or the presence of some integrated HPV sequences within these cells. If this band represents the presence of integrated sequences, this may provide a possible explanation for the presence of higher E7 protein levels in E_{63} (0.12) than in E_{50} (0.017) as reported by Jeon *et al* (1995)[119]. The E_{50} and E_{63} viral genomes appear largely insensitive to digestion with *Hin*dIII. The restriction sites of this enzyme are known to be present within host human DNA but absent from the HPV genome; therefore the episomal derivatives are negative for the host-virus hybrid sequences associated with integration. A slight downwards shift was present within both the episomal derivatives compared with the undigested samples; however, this band alteration was notably less than that present within the *Hin*dIII digested integrated derivatives. This shift within the episomal lines is possibly to be due differences in the salt concentration between the digested and undigested samples, with changes in salt concentrations associated with the buffers required for *Hin*dIII digestion.

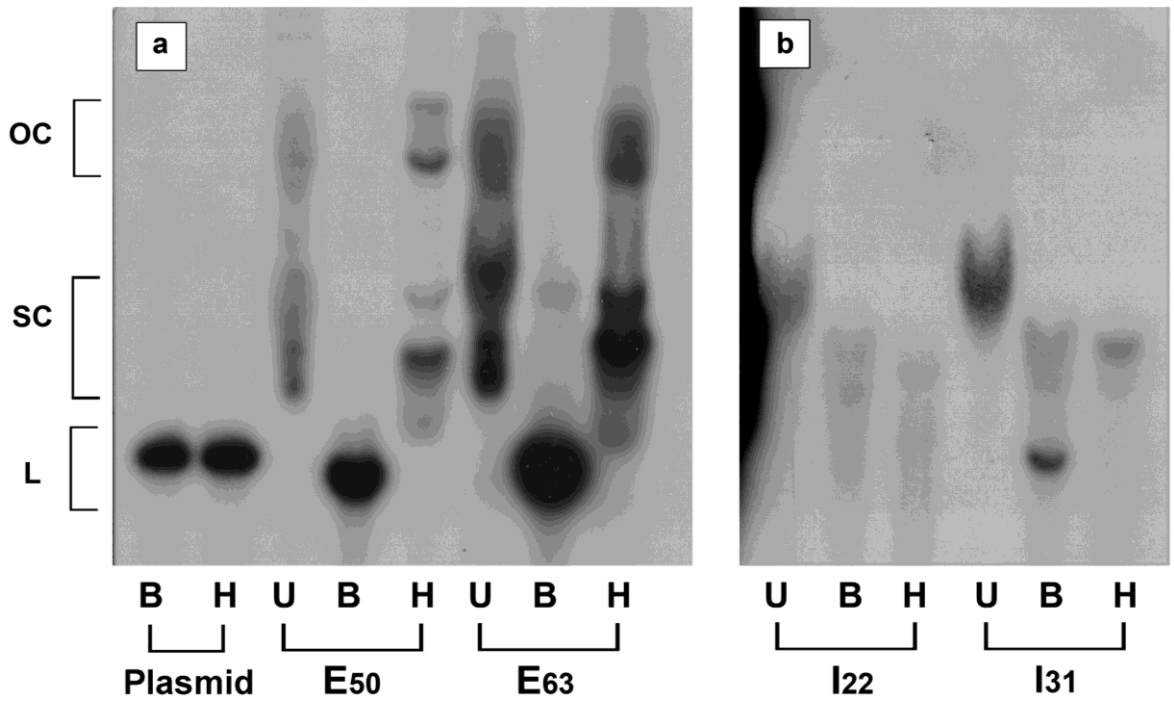

Figure 3.1: Southern blot analysis of the genome status of W12 derivatives. DNA from W12 derivatives E_{50}, E_{63}, I_{22} and I_{31} was Hirt extracted and run as either undigested (U), *Bam*H1 digested (B) or *Hin*dIII digested (H). HPV 16 plasmid DNA (pEFHPV-16W12E) either *Bam*H1 or *Hin*dIII digested were utilised as a control marker (Plasmid). (a) Extracts from the episomal W12 derivatives and plasmid control (3 day exposure), and (b) extracts containing integrated viral genomes (6 day exposure). The positions of open-circular (OC), supercoiled (SC) and linear (L) forms of HPV 16 DNA are indicated on the left of the figure.

Hirt extraction was used to enrich samples for low molecular weight DNA including the episomal viral genomes. As a consequence the integrated HPV genomes present in I_{22} and I_{31} were more difficult to detect during this procedure, therefore longer exposure times were required (6 days instead of 3 days) as shown in figure 3.1b. Neither representative integrated derivative displayed open-coiled HPV DNA in the undigested samples. Full-length HPV sequences were not identified in I_{22} after *Bam*HI digestion, consistent with the presence of the single copy type 1 integration of HPV 16 (section 1.6.3). As previously noted by Jeon *et al* (1995) [119], full-length HPV genomes were present in I_{31} DNA after *Bam*HI digestion, indicating the presence of type 2 integrated HPV containing multiple full length viral genomes (section 1.6.3.2). Digestion with *Hin*dIII led to a downwards shift in band size

indicating the presence of host-virus junction fragments in both integrated lines, although the effect was most visible in I_{31}.

3.3.2. The Status of HPV 16 E2 in the W12 Derivatives

During the integration of the HPV genome the normally episomal DNA must be linearised at some point in its sequence. This process often involves the disruption of the E2 ORF, with wide spread consequences for both the virus and host [414], and subsequently any model of HPV infection.

3.3.2.1. The Status and Transcription of the E2 ORF

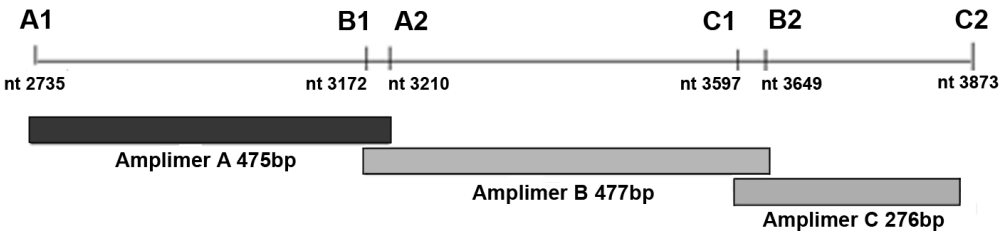

Figure 3.2: A schematic overview of the distribution of the E2 amplimers A, B and C across the E2 ORF. The initial nucleotide (nt) of each primer is shown along with its respective PCR product and size.

The E2 ORF was amplified in three overlapping fragments (amplimers A, B and C) as published by Graham and Herrington (2000) [414] from either genomic DNA (gDNA) or reverse transcribed cDNA (figure 3.2). When a cDNA template was used the housekeeping gene beta-2-microglobulin (B2M) was also included as a control for genomic DNA contamination. B2M is a constitutively expressed cellular protein utilised as a control during RT-PCR. As the B2M primers span an intron, any contaminating gDNA should be indicated by the presence of a 740bp band in addition to the 114bp cDNA product. Therefore, B2M PCR analysis of cDNA provides a dual control, confirming the presence of a suitable quality cDNA template and also detecting gDNA contamination.

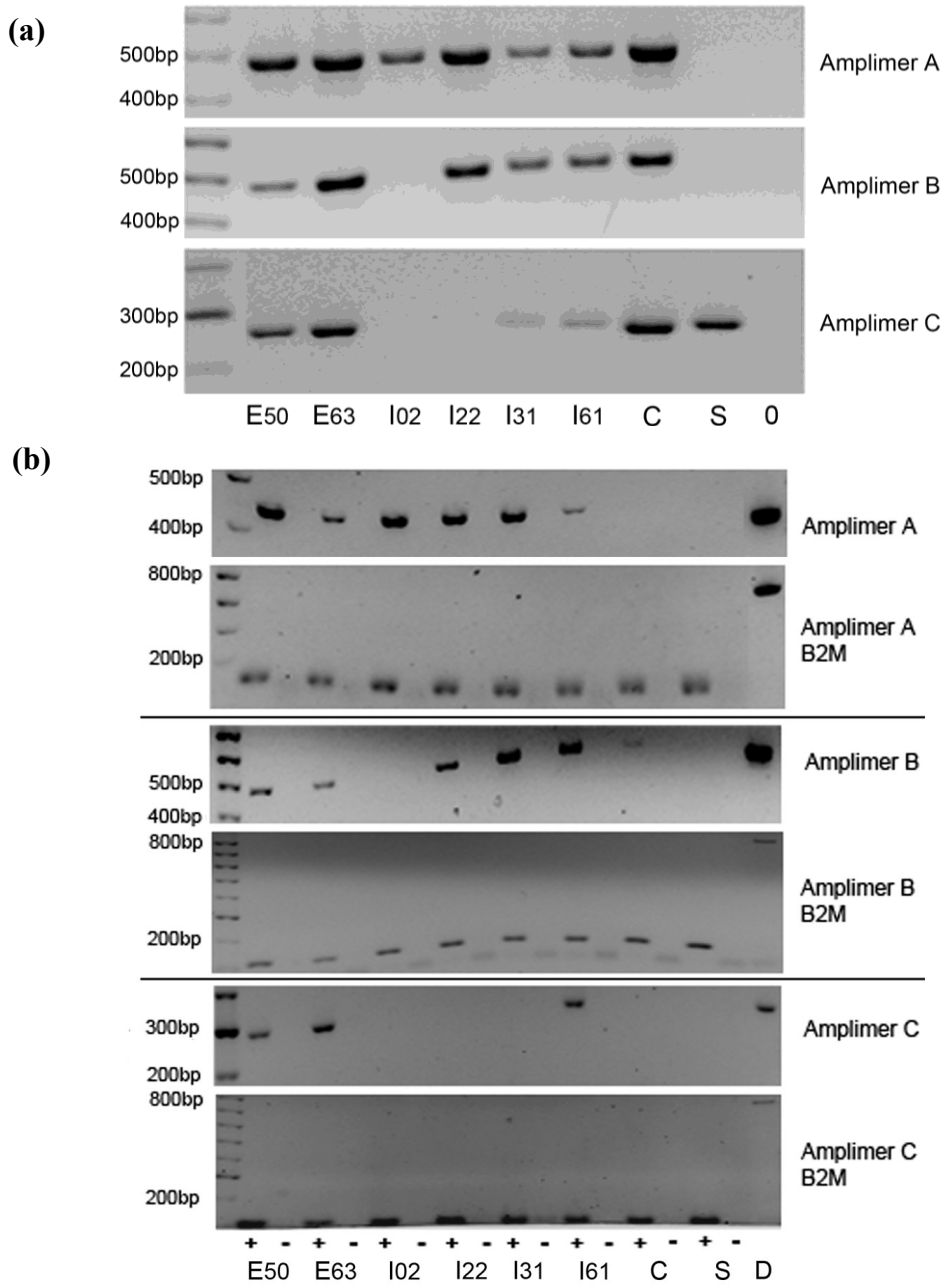

Figure 3.3: The status of E2 within the W12 derivatives and control lines CaSki and SiHa. (a) The amplification of the E2 ORF from genomic DNA. (b) The E2 ORF expression from mRNA in the presence (+) or absence (-) of reverse transcription. The lower panel of each set displays the results of B2M PCR, with the higher band present in lane D showing the result of B2M amplification from genomic DNA. Hyperladder II was used as a DNA ladder in the above gels.

As previously shown by Graham and Herrington (2000) [414], the CaSki cell line displayed the presence of the complete E2 ORF by DNA PCR, whist only the C-terminal amplimer was present within the SiHa cell line (figure 3.3a). The E_{50} and E_{63} W12 derivatives were found to encode and transcribe all three amplimer regions after PCR and RT-PCR analysis (figure 3.3a

and b), representing the complete E2 ORF. The status and transcription of the E2 ORF varied between the integrated derivatives, broadly defined by integration type. Both the type 1 integrated derivatives I_{02} and I_{22} showed an absence of amplimer region C in both genomic and cDNA templates, with the I_{02} cell line also found to be deficient in amplimer B. Cells containing type 2 integrated HPV (I_{31} and I_{61}) appeared to contain amplifiable sequences from all three of the PCR regions of E2 ORF, although both DNA and mRNA analysis indicated a notable reduction in the level of amplimer C. The detection of the C-terminal region in I_{31} and I_{61} appeared to be temperature dependent; at 58ºC strong signals were detected in the episomal derivatives and control lines, but signals were barely visible in I_{31} and I_{61}. By decreasing the annealing temp to 55ºC, band intensity was increased in the type 2 cells, but remained notably lower than the episomal and control lines. This annealing temperature sensitive response may indicate the presence of small alterations in sequence either within the actual primer binding site or in the immediate area, leading to a reduction in the efficiency of primer binding.

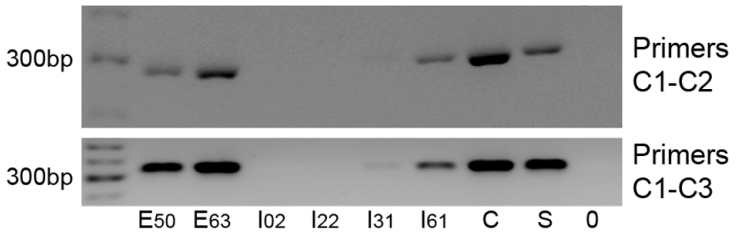

Figure 3.4: Variations in E2 amplimer C detection from viral genomic DNA using different primer combinations. The PCR using the original amplimer C primer combination (C1-C2 ^{414}) is shown in the upper panel, with the effects of replacing the reverse primer with C3 shown in the lower panel. Hyperladder II was used in to determine band size in both gels.

To investigate the possible source of the variation in amplimer C, a primer was designed 46bp downstream of C2 (primer C3, see 2.16.1) to determine if any possible mutations were located within the region of the C2 primer. As shown in figure 3.4, the alteration in primer location had little apparent effect on the expression of the I_{31} derivative, although I_{61} and SiHa both appeared to show slight increases in expression of the extended amplimer C.

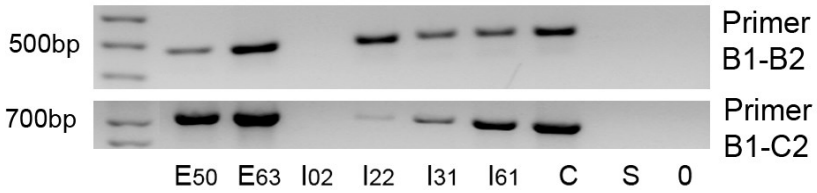

Figure 3.5: Variations in E2 amplimer B/C region detection from viral genomic DNA with different primer combinations. PCR results using the original amplimer B primer combination (B1-B2 [414]) are shown in the upper panel, in the lower panel the reverse primer B2 was replace with primer C2. Hyperladder II was used to determine band size.

The expression of the C1-C3 product suggested that sequence alterations away from the C2 primer location may also contribute to the lowered expression of amplimer C. When the upstream B1 primer was combined with C2 some rescue of the I_{61} expression in comparison to C1-C2 levels was again seen; however, little change in I_{31} was apparent (figure 3.5). These experiments also showed that in the presence of the B1-C2 primer combination little or no expression could be detected in I_{22} and SiHa representing a loss of the normally expressed amplimers B and C respectively.

3.3.2.2. E2 Protein Expression

E2 protein expression in cell lines such as the transfected U2OS clones can be easily detected using the TGV261 E2 antibody. These cell lines are based on vectors containing promoters such CMV in U2OS E2, and are associated with high levels of protein expression with greater ease of detection. However, as the W12 cells are derived from a naturally infected lesion and express relatively low *in vivo* levels of HPV 16 E2, detection from whole cell lysates has proven difficult. Attempts during these studies to detect E2 using the standard western blotting technique proved unsuccessful; although E2 expression was detected in the positive control transfected U2OS cells. In addition to the problems associated with low E2 expression, the W12 derivatives also displayed a non-specific band in the region of 47kDa, making identification of low level E2 expression problematic. In order to successfully detect E2 several alterations the standard protocol were required as described in section 2.12.7.3. To

provide maximum E2 expression W12 cells were harvested when highly subconfluent; this ensured that these cells were rapidly growing. Reduced growth associated with greater confluence may lead to a decrease in E2 expression due to reduced requirement for E2-mediated regulation of E6/E7. The levels of available E2 were further raised by the use of increased amounts of W12 lysate (increased from 20 to 70µg), the utilisation of a higher sensitivity chemiluminescent detection system, and a highly reflective surface during signal detection. In addition, protein separation was undertaken on an 8% midi SDS-PAGE gel allowing greater resolution within the 32-47kDa range, providing maximum distance between E2 and the non-specific band. The above alterations to the standard protocol allowed the detection of E2 protein from whole cell lysates of the W12 derivatives, as shown in figure 3.6.

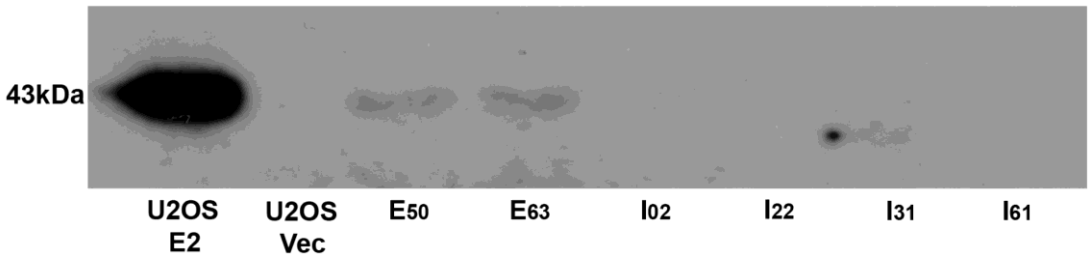

Figure 3.6: The expression of the E2 protein in the W12 derivatives and U2OS cells transfected with HPV 16 E2 or pCMV4 (U2OS Vec).

As predicted, E2 protein expression was confined to those W12 derivatives containing episomal HPV genomes, with no detectable protein expression in those with type 1 or type 2 integration (figure 3.6). However, even within the episomal lines expressing the E2 protein, the levels detected were particularly low.

3.3.3. Analysis of the HPV 16 E7 and E6/E7 Status of the Transduced Primary Human Keratinocytes

Primary human keratinocytes were transduced with HPV 16 E7 or E6/E7 and utilised to optimise the detection of the E6/E7 PCR and confirm the status of these cells. cDNA from the cultured cells was subjected to RT-PCR was undertaken using E7 and E6/E7 specific primers. The E6 and E7 genes are transcribed as a single mRNA transcript with differential splicing leading to three main products, the unspliced full length E6/E7 (525bp), and two major splice products E6*I (343bp) and E6*II (226bp).

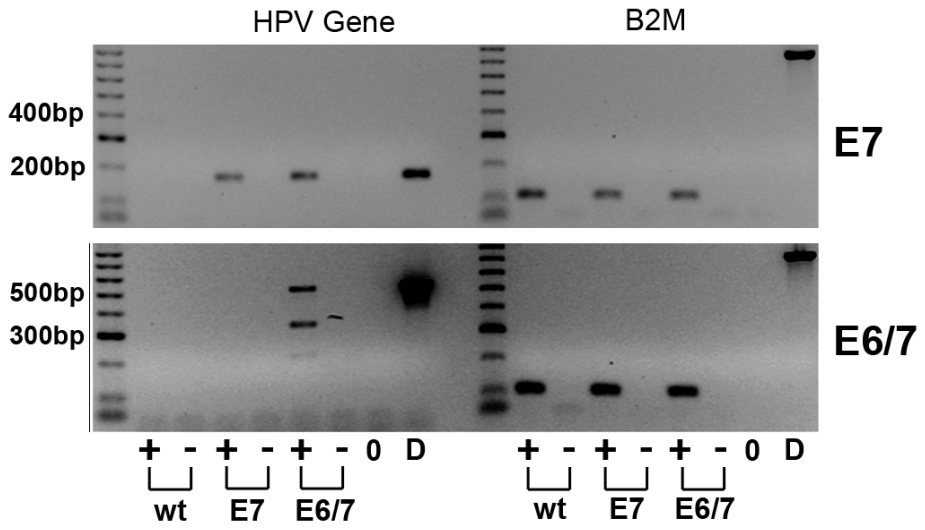

Figure 3.7: RT-PCR for E7 (upper panel) and E6/E7 (lower panel) using cDNA from E7 or E6/E7 transduced cell or wild type (wt) PHKs. Reverse transcription was undertaken in the presence (+) and absence (-) of reverse transcriptase, in the absence of template (0) and using CaSki gDNA (D) as a positive control. Amplification of the house keeping control B2M was undertaken concurrently on all samples.

In both E7 and E6/E7 RT-PCR no expression of the HPV oncogenes was detected in the wild type PHK, whilst both were present in some form in the CaSki DNA control (figure 3.7). HPV E7 alone was found to be present in cDNA derived from the both the E7 and E6/E7 transduced PHKs. E6/E7 transcripts were detected only within the appropriately transduced E6/E7 PHKs. In the E6/E7 transduced cells all three mRNA splice products were detected, with only the unspliced full length 525bp band present within the genomic CaSki DNA. The

full length E6/E7 and the E6*I splice products appeared to be equally represented within the mRNA, with the lower E6*II splice transcript notably less abundant.

3.3.4. Transcription of HPV 16 E6/E7 in the W12 Derivatives

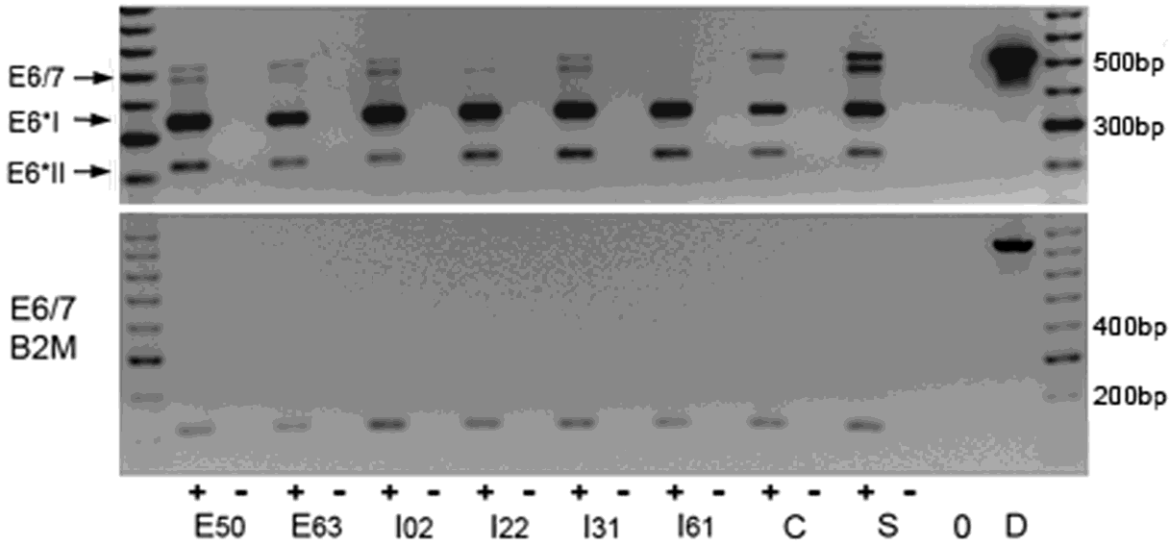

Figure 3.8: The expression of E6/E7 in the W12 derivatives which displayed the three splice variants E6/E7, E6*I and E6*II. The RT-PCR was undertaken in the presence (+) or absence (-) of reverse transcription in the W12 derivatives, CaSki (C) and SiHa (S), with CaSki gDNA control (D). B2M amplification from all samples is shown in the lower panel, with Hyperladder II used throughout.

All three E6/E7 splice products were identified in the cDNA derived from W12 derivatives and the cancer cell lines CaSki and SiHa, but as expected only full length E6/E7 detected in CaSki gDNA (figure 3.8). Interestingly the full length E6/E7 appears to be expressed in the form a doublet which can also be seen in E6/E7 RT-PCR undertaken by Tang *et al* (2006) [106]. As the upper band appear consistent with that amplified from the CaSki DNA control, the smaller PCR product may represent an alternative splice variant of the full length E6/E7 whose function remains unclear. Differences in the expression of the three transcripts were apparent within and between cell lines studied. In both the W12 derivatives and cancer cell lines E6*I was the dominant form, with the full length E6/E7 transcripts showing both the lowest overall levels and the majority of the intercellular variation. Lower full length E6/E7

transcript expression was detected in E_{63}, I_{22} and I_{61}, with particularly low levels in I_{61} derivative confirming previous observations by Doorbar *et al* (1990) [419].

3.4. Discussion

To provide a suitable model for the study of early HPV 16 associated neoplasia and the changes associated with integration, it is important to confirm the integration status of the W12 derivatives as proposed by Jeon *et al* (1995) [119] and functionality of the E2, E6 and E7 genes. Integration of the normally episomal HPV genome requires the linearisation which predominantly occurs within the E2 ORF [414]. This leads to a loss of E2 function with consequences for regulation of the oncogenic E6 and E7 genes and increased propensity for malignant progression. The aim of these studies was to confirm the status of the HPV 16 genome and the viral E2, E6 and E7 genes in the W12 derivatives and transduced primary cells (PHKs).

The episomal or integrated status of the W12 derivatives was confirmed directly via Southern blot analysis and indirectly by the status of the E2 ORF and its protein expression. Within the E_{50} and E_{63} derivatives the presence of the indicative open-circular, supercoiled and linear forms of the HPV 16 genome after Southern analysis, in combination with the presence of the translated E2 ORF, confirmed the presence of predominately episomal genomes. The reportedly integrated W12 derivatives lacked open-circular viral genomes indicative of episomal HPV and no E2 protein expression could be identified, consistent with their integrated status. Those cells containing type 1 integrated HPV 16 failed to display linearised HPV after to *Bam*HI digestion and also exhibited greater disruption to the E2 ORF, consistent with single copy integration. As previously reported by Jeon *et al* (1995) [119] the genome status of the type 2 integrated W12 derivatives I_{31} and I_{61} was complicated by the presence of

tandem repeats of the HPV 16 genome. However, *Bam*HI and H*ind*III digestion produced band shifts suggestive of the presence of full-length genomes in addition to host-virus junctions. This complex integrated status was further confirmed by the presence and apparent transcription of all three fragments of E2 ORF in both I_{31} and I_{61}.

Variation in the disruption of the E2 ORF was found within the integrated W12 derivatives suggesting that even within integration types there remain considerable differences in the site of integration and the amount of disruption caused. There appears to be a preference in the type 1 integrated cells for integration within the central or C-terminal regions of the E2 ORF, with the C-terminal region disrupted in both lines. The I_{22} derivative showed an absence of the C fragment only (nt 3597-3873), consistent with the published integration site of nt 3732 [119]. However, the I_{02} derivative displayed more prominent disruption, with integration appearing to have affected both the central and C-terminal regions (nt 3172-3873) as illustrated by the absence of amplimers B and C. The majority of the W12 derivatives were cloned from parental cells at passage 14/15, but I_{02} was derived from a later passage 17 of the parental line which may contribute to the greater level of damage detected within these cells. Jeon *et al* (1995) [119] have suggested that this I_{02} derivative may contain sequences from an additional integration event. This may explain the disruption detected in both the central and C–terminal regions of the sequence, and provide a mechanism for the reported dominance of this integration pattern in high passage cultures of the parental cell line [119].

Previous attempts by Jeon *et al* (1995) [119] failed to map the integration site within the type 2 integrated W12 derivatives due to the presence of concatemers of HPV 16, although S1 nuclease analysis did suggest integration within the E2 ORF. In the current study all three E2 DNA PCR products were amplifiable from the type 2 W12 derivatives I_{31} and I_{61}, but no protein was detectable; this suggests that the integration-associated linearisation is unlikely to

have occurred at a common site within the tandemly repeated viral genomes as all three regions were detected. This suggests that integration is likely to have occurred in different regions within the constituent concatemers. However, the notably reduced band intensity present with amplimer C may represent a possible predominance for disruption of E2 within the C-terminal region in the tandem repeats contained within both I_{31} and I_{61}, although in some cases this region must remain intact. Cleavage is therefore also likely to have occurred in alternative locations either within the E2 ORF or at different points within the HPV genome. The inability to rescue amplimer C expression in the I_{31} derivative by altering the primer location may indicate the presence of more severe C-terminal disruption within this cell line. It is possible the detection of all three E2 amplimers within the type 2 integrated cells could represent amplification from intact ORFs. However, the absence of E2 protein expression in these type 2 cells suggests the transcription of an intact E2 ORF is unlikely. The templates could also be derived from a pool of integrated genomes disrupted at different points within the E2 ORF. This may account for the E2 expression patterns shown in I_{31} and I_{61}. It is therefore possible that E2 DNA and mRNA templates in the type 2 integrated W12 cells could originate from more than one viral concatemer. However, Van Tine *et al* (2004) [30] have suggested that only those viral genomes located at the host junction are transcriptionally active with the majority of the remaining viral DNA being silenced. Therefore, the mRNA templates should be derived only from these viral-host junction sequences; however, the source of the mRNA templates could no be confirmed during studies. If only host junction sequences are utilised then the host junction genomes of the different concatemers must be derived from episomes cleaved in different regions of the E2 ORF in order to allow transcription from all three amplimer regions.

The successful detection of E7 and E6/E7 transcripts in the appropriately transduced primary cells confirmed the presence of these HPV oncogenes, allowing the function of these genes alone to be examined. Both of the E6 and E7 genes have been shown to be transcribed from a single promoter and subsequently subjected to post-transcriptional splicing producing three distinctive products E6/E7, E6*I and E6*II as discussed in section 1.1.7. The RT-PCR analysis performed during these studies confirmed that all three splice variants were expressed in the W12 derivatives. An unequal distribution of the splice transcripts was identified in the W12s, although as previously reported the E6*I variant formed the dominant PCR product [106,109]. The function of this dominant product is unclear. It has been proposed to encode the E7 protein, to decrease E6 protein levels, or to inhibit the interaction of E6 and E6-AP [103]. When the E6/E7 RT-PCR data are compared to the published E7 protein levels of the W12 derivatives it appears that lower levels of the full length E6/E7 transcript may be associated with higher levels of E7 expression in the I_{22} (1.1AU), I_{61} (1.3AU) and CaSki (1AU) [119], suggesting that splicing of the full length E6/E7 transcript may be required for the translation of the E7 protein [103]. Although no evidence for increased E6*I expression between the cell lines could be established during this study, possible raised E7 protein expression may still be obtained via translation of this spliced transcript [420].

The E6/E7 transduced PHKs expressed all three splice variants, although the proportions of each differed from those seen in the naturally infected W12 and cancer cell lines, with the proportion of full length E6/E7 much higher in the transduced cells. This suggests that the splicing of the E6/E7 transcript is innate to the mRNA sequence, with the cellular machinery utilised to cleave the transcript at encoded splice sites. However, the difference in the splicing pattern between the naturally infected and transduced cells suggests that other viral components, absent from the transduced PHKs, may play a role in the fine tuning of the splicing process. Splicing is undertaken within the spliceosome, this complex is composed of

a number of small nuclear ribonucleoprotein particles (snRNPs), with recruitment of these splicing factors controlled by the serine/arginine (SR) protein family [421] including SF2/ASF (Splicing Factor 2/Alternative Splicing Factor) [422]. Differential phosphorylation of these SR proteins has been shown to facilitate the alternative splicing of mRNA transcripts (reviewed by [423]). McPhillips *et al* (2004) [421] have suggested that the alternative splicing of the late viral transcripts is achieved by regulation of the splicing factor SF2/ASF, and that this is at least in part due to the action of HPV E2 [421]. However, as the integrated cell lines lack HPV E2 protein expression, the variable splicing of the E6/E7 transcript displayed by these lines must be regulated by alternative viral proteins expressed by both episomal and integrated HPV.

These studies suggest that the W12 derivatives provide a good model for cells containing both episomal and integrated HPV 16. The presence of E2 within the episomal derivatives should allow these cells to maintain tight transcriptional regulation of E6 and E7, minimising viral interference with cellular factors such as p53 and pRb. The loss of E2 in the integrated lines is likely to be associated with an increase in E6 and E7 expression within the cells as suggested in the previously published proteins levels [119,403]. The greater influence of E6 and E7 in the integrated cells is likely to increase their exposure to the potentially harmful activities of these oncoproteins, particularly via their interactions with cellular p53 and pRb. The apoptotic response in these integrated cells is reduced by two separate integration related effects; firstly a rise in E6/E7 leads to increased anti-apoptotic and decreased pro-apoptotic signalling, preventing cell-directed apoptosis. In addition, an anti-apoptotic effect may also be achieved directly via the loss of E2-mediated induction of apoptosis, which is known to occur in the upper suprabasal layers of the epithelium (section 1.6.5.2). The effects of differential E2, E6 and E7 expression in the W12 derivatives in the context of the whole viral

genome may alter the manner in which these cells respond to treatment with pro-apoptotic agents such as LMB.

Chapter 4: Alterations in Morphology and Colony Survival in Response to Leptomycin B

4.1. Introduction

Leptomycin B has previously been shown in our laboratory to induce apoptosis in primary human keratinocytes transduced with HPV 16 E6, E7 and E6/E7, but not normal wild type PHK cells [374]. The most pronounced apoptotic affect was seen in the presence of the E7 gene alone, with the inclusion of E6 appearing to attenuate the LMB response. The aim of the studies presented here were to test the hypothesis that the presence of the entire HPV 16 genome affects the sensitivity of a cell to LMB and that any integration of the normally episomal HPV genome will further influence this response. The treatment of episomal, type 1 (single copy) and type 2 (tandem repeat) integrated cells allowed the effect of genome status on LMB sensitivity to be assessed in cells that reflect the early pre-malignant changes that are thought to occur during the development of cervical neoplasia. In order to test this hypothesis the W12 derivatives were monitored for changes in morphology and colony forming behaviour in response to LMB, allowing the immediate and the post-treatment effects to be assessed in the context of HPV-associated cell lines. As HPV gene expression is known to alter during the progression of cells through the epithelium (section 1.1.2), organotypic raft culture was used to assess the effects of differential viral gene expression and cell differentiation on LMB sensitivity.

4.2. Methods

Cultured cells were treated with LMB as summarised in section 2.3. The morphological effects of LMB were investigated in both monolayer (section 2.5) and rafted (section 2.6) cells. The effect of treatment on colony forming ability was also investigated as described in section 2.11.

4.3. Results

4.3.1. Morphological Effects of LMB on W12 Derivatives in Monolayer

When cultured in monolayer the W12 derivatives demonstrated the typical keratinocyte morphology and tightly packed cell clusters (upper panel figure 4.1).

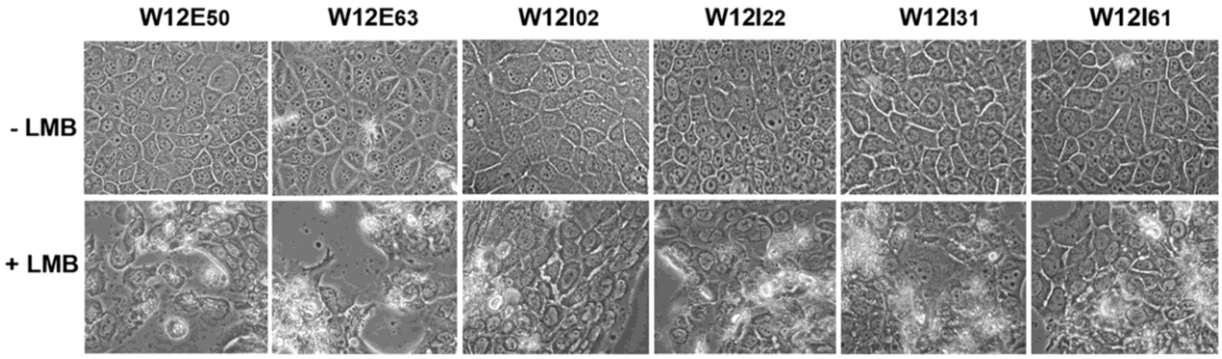

Figure 4.1: Phase contrast images (x200 magnification) of the W12 derivatives treated with 2nM LMB (40h) (lower panel) and time matched controls (upper panel) displaying the morphological changes associated with LMB treatment.

After incubation with 2nM LMB (40h), treated cultures and time matched controls were examined by phase contrast microscopy (x200 magnification). Analysis indicated that a notable loss of cells had been induced by LMB in all the cell lines, most likely due to the induction of apoptosis (lower panel figure 4.1). After treatment all cultures appeared to display typical apoptotic morphology in combination with a large increase in the numbers of detached cells and cellular debris.

4.3.2. Morphological Effects of LMB on W12 Organotypic Raft Culture

Organotypic raft culture provides an *in vitro* model that closely resembles the structure of human skin, allowing an assessment of the effect of LMB treatment on HPV 16 infected cells within a differentiating epithelium-like structure. This technique has previously been undertaken using PHKs transduced with HPV 16 E7, E6, and E6/E7 treated with 50nM LMB over 72h [374]. This treatment regime was sufficient to induce apoptosis in raft cultures

expressing E7 and E6/E7 [374]. In the current study the W12 derivatives E_{63} and I_{22} were treated with 50nM LMB (72h) to assess the effects on rafted cells containing the complete episomal or integrated HPV 16 genome.

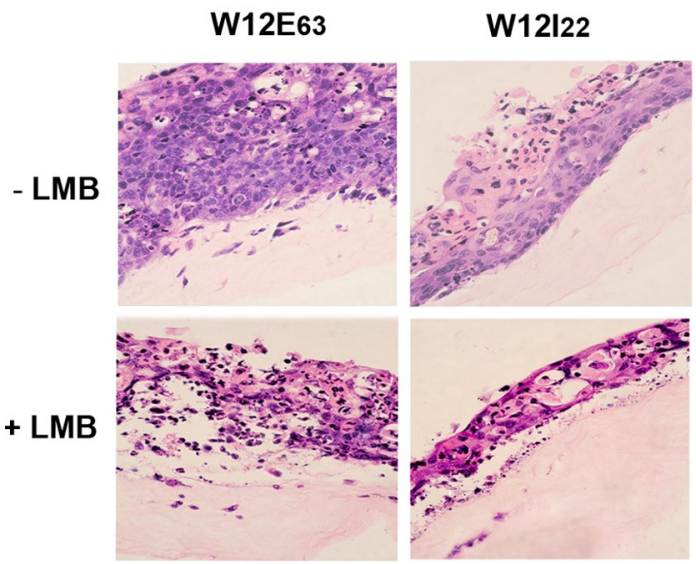

Figure 4.2: E_{63} and I_{22} organotypic raft cultures treated with 50nM LMB for 72h (lower panel) and time matched controls (upper panel), stained with haematoxylin and eosin (x200 magnification).

In the absence of LMB the W12 derivatives displayed distinct differences in their raft structure, as can be seen in figure 4.2 (upper panel). The episomal line produced a thick raft with a disorganised structure containing a low number of vacuoles throughout the suprabasal layers. The E_{63} raft also showed signs of differentiation indicated by the presence of keratinised cells within the upper layers of the raft. The type 1 integrated I_{22} derivative produced a raft that was notably thinner and displayed an overall more organised stratified structure with an ordered basal layer, a notably reduced number of vacuoles, and the presence of keratinised cells.

The addition of 50nM LMB (72h) to the media beneath the rafts led to structural and cellular changes in both the E_{63} and I_{22} epithelia, as shown in figure 4.2 (lower panel). The E_{63} rafts treated with LMB showed a decrease in overall thickness and in places an almost total

absence of an epithelial structure, with only apparently keratinised cells remaining in some regions. Treatment led to an almost total loss of cells in the lowest layers of the raft, representing the basal and immediately suprabasal regions. LMB-associated disruption was also present in the mid and upper regions of the E_{63} epithelium, with the vacuolated areas noted in the untreated raft increasing in size and number after treatment. In response to LMB the I_{22} derivatives also showed a notable loss of cells, although they did not show the same magnitude of cell loss, particularly in the middle and upper regions of the epithelium. Nevertheless, the integrated derivative did display the formation of vacuoles and an increased loss of the lowest cell layers leading to a thinning of the raft structure. The extent of these changes in the I_{22} raft was considerably lower when compared with the LMB treated E_{63} derivative.

4.3.3. LMB Affects the Colony Formation of Cells Containing HPV 16

The ability of cells to form colonies after increasing doses of LMB was assessed using a colony survival assay. In order to gain a broader view of the effectiveness of LMB in a range of HPV related lines, survival was assessed in both the E_{63} and I_{22} cell lines, PHK transduced with HPV 16 E7 and the integrated HPV 16 containing cancer cells lines CaSki and SiHa.

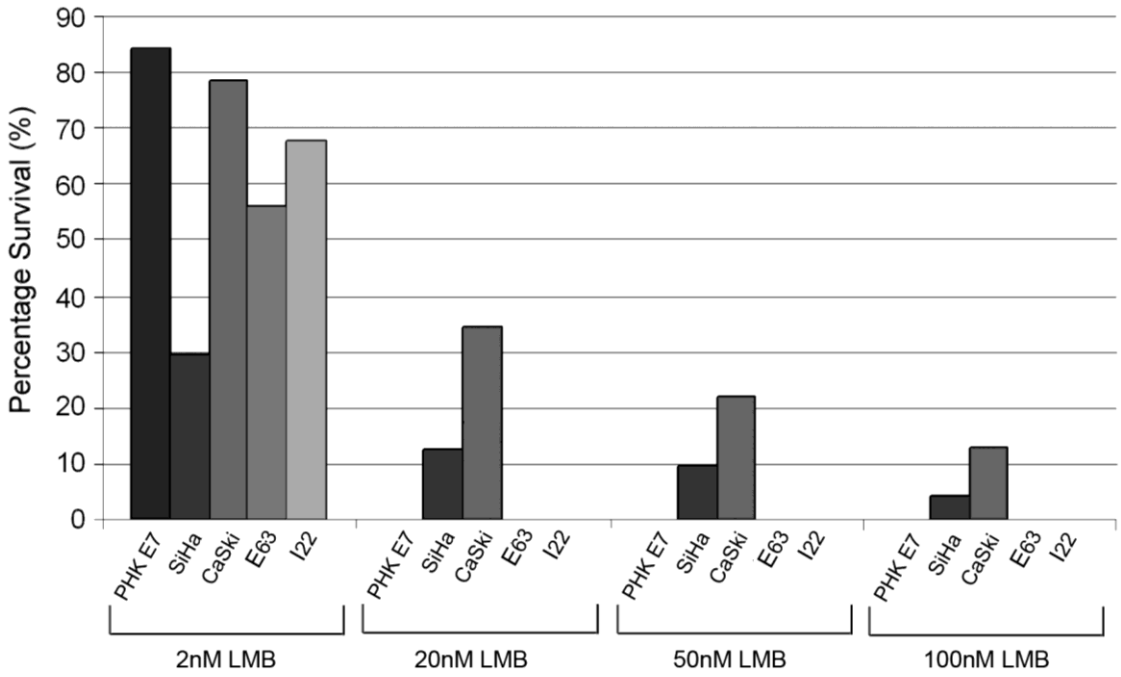

Figure 4.3: The colony forming ability of E_{63}, I_{22}, PHKs transduced with HPV 16 E7 (PHK E7), CaSki and SiHa cell lines after treatment with 2nM, 20nM, 50nM or 100nM LMB (40h). Results are displayed as the percentage of colonies formed after treatment with LMB, normalised against colonies formed from untreated cells (0h).

In all the cell lines, the levels of post-treatment survival decreased in response to increasing doses of LMB (40h), as shown in figure 4.3. However, the extent of this response varied considerably between the cell lines. The E7-transduced PHKs showed the highest survival of any cell line after 2nM treatment, but no colony formation was apparent at greater LMB concentrations. Both episomal and integrated W12 derivatives displayed reduced colony-forming ability in response to LMB treatment, with greater recovery seen with I_{22} cells than with E_{63} at a concentration of 2nM, suggesting a greater sensitivity of the episomal line to LMB. At concentrations of LMB greater than 2nM neither W12 derivative was found to form colonies. These patterns confirmed initial colony survival experiments with the E_{63} and I_{22} derivatives.

The HPV 16 infected cancer cell lines displayed differences in their colony formation at 2nM, with the level of survival in the type 2 integrated CaSki line only exceeded by the E7

transduced primary cells (figure 4.3). The type 1 integrated SiHa line displayed the lowest overall colony formation of any of the experimental cell lines at 2nM LMB. Only the cancer cell lines successfully formed colonies at LMB concentrations greater than 2nM, displaying a gradual decrease in colony formation with increasing doses of LMB. As shown in figure 4.3, the decrease in colony formation of the CaSki cell line in response to increasing LMB was more dramatic than that displayed by SiHa, although colony formation by CaSki cells remained higher than that with SiHa cells.

4.3.3.1. The Effect of LMB on Colony Size

Treatment of the cells with increasing doses of LMB caused a decrease in colony number. However, high levels of colony formation by the E7 transduced lines and the integrated derivative were unexpected due to the elevated LMB induced apoptosis previously seen in the E7 expressing cells [374] and the predicted sensitivity of the integrated W12 derivative. Therefore the colony size of the post-treatment colonies was also investigated to assess for any alternative long-term effects of LMB treatment.

The size of colonies in the untreated cell lines varied considerably. The smallest colonies were found with the episomal W12 derivative which formed colonies approximately 50% smaller than the type 1 integrated I_{22} and SiHa cells. The type 2 integrated CaSki cancer cell line and the E7 transduced PHKs formed notably larger colonies than the other cell lines (figure 4.4).

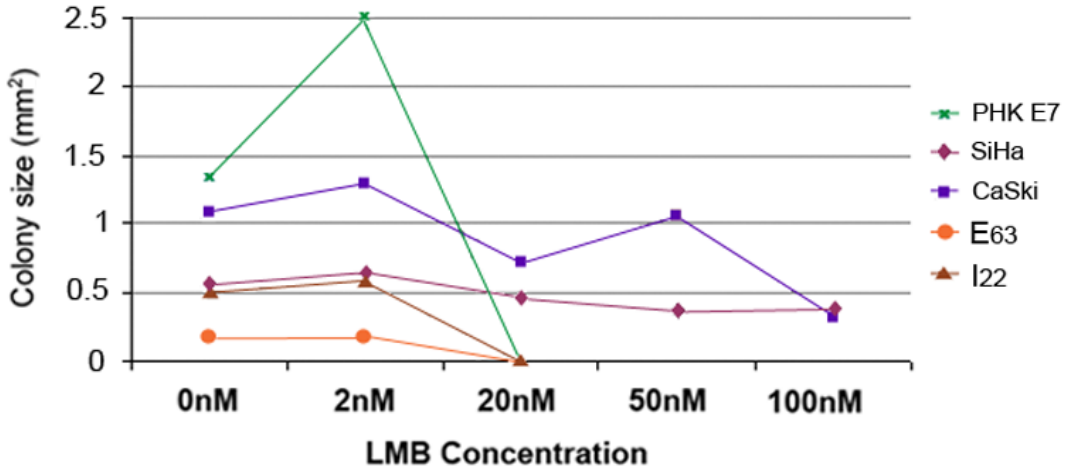

Figure 4.4: The variations in the size of colonies formed by E_{63}, I_{22}, PHKs transduced with HPV E7 (PHK E7), CaSki and SiHa cell lines after treatment with 2nM, 20nM, 50nM or 100nM LMB (40h). Results are displayed as the mean colony size in mm^2.

Treatment with 2nM LMB had little effect on colony size in most of the experimental cell lines, with the exception of E7-expressing PHKs where treatment led to a substantial increase in colony size (figure 4.4). In the cancer cell lines the colonies formed by SiHa were smaller than those of CaSki cultures, with SiHa colonies displaying little change in size with increased LMB dose. The CaSki colonies did show a gradual decrease in size with increasing dose although, with the exception of 100nM LMB, the CaSki colonies remained larger than those produced by the SiHa (figure 4.4).

4.4. Discussion

Previous data have shown that LMB induces apoptosis in primary human keratinocytes expressing HPV 16 E7 or E6/E7 genes, but not in normal keratinocytes [374]. However, the presence of the complete episomal or integrated viral genome may have a significant impact on the cells response. Treatment with LMB led to distinct morphological changes in both monolayer and rafted W12 cultures, in addition to alternations in their colony forming behaviour. This suggests that cells containing the whole HPV genome in either episomal or integrated form are sensitive to LMB treatment. The LMB-induced loss of cells witnessed in

both monolayer and rafted cultures is likely to have occurred via the activation of apoptotic pathways, as has previously been reported in the HPV transduced PHKs [374].

When rafted, the epithelium formed by the episomal and integrated W12 derivatives showed distinct variations in structure. Those formed by E_{63} appeared to show a more substantial yet disorganised structure, whilst I_{22} displayed a thinner yet more normal epithelium. A similar presence of a more organised basal layer and stratification within the integrated W12 raft has previously been observed in I_{61} derivatives grown in raft culture by Aasen *et al* (2003) [51]. As I_{61} contains type 2 instead of the type 1 integration found in I_{22}, these features may reflect general effects of HPV integration, rather than an influence of specific type 1 or 2 integration.

Within the episomal rafts the LMB-associated damage displayed a greater propensity to migrate up the epithelium than was present with the integrated derivative. These differences in the pattern of LMB response may reflect the changes in behaviour associated with HPV integration or the clonal nature of the W12 derivatives. Those cells containing the HPV genome in its normal episomal form should maintain typical differentiation-dependent expression of the viral genes (section 1.1.2). As keratinocytes move up the epithelium and begin to differentiate an increasing amount of viral interference is required to maintain a replication competent environment for the virus. Integration of HPV is associated with loss of this tight relationship through alterations in viral behaviour and loss of viral genes, particularly E1/E2. It is therefore likely that the effects exerted by the virus as the cells move up the epithelium will vary between the E_{63} and I_{22} rafts; potentially altering the response of these cells to LMB. In particular the episomal raft should maintain the virally derived pro-apoptotic mechanisms controlled partly by E2 and E4 (section 1.5.5.2) [332,342]. These systems function as part of the normal viral life cycle, but the viral pro-apoptotic pathways may also

assist the induction of apoptosis within the episomal rafts in response to LMB, particularly in the upper layers of the epithelium where virally induced apoptosis is thought to normally aid virion release.

The most notable loss of cells from the rafted cultures occurred within the lower regions of the structure, which represent the basal layer of the epithelium. As these cells form the most actively dividing layer of the epithelium, the interruption of nuclear export may lead to a greater amount of cellular disruption in this particular location than in other regions of the epithelium. Previous research on rafted PHKs containing the empty LXSN vector showed that LMB had little effect on this basal layer in normal cells [374], with the addition of E7 and E6/E7 to the PHKs leading to the initiation of apoptosis. These results combined with the current data from rafted W12 derivatives suggest that this preferential loss of cells from the basal epithelium is not solely due to an innate property of this region, but additional factors such as the presence of HPV are required to initiate cell loss. Also as this basal layer effect was present with both episomal and integrated genomes, it appears that this aspect of the response may be independent of genome status.

The formation of colonies after LMB treatment was found to decrease in all the cell lines studied, illustrating that LMB has long term effects on the survival of HPV-associated cells. The effect of treatment appeared to be more dramatic in the episomal E_{63} derivative which displayed lower colony formation than the type 1 integrated I_{22} suggesting a possible role for integration in colony survival. The levels of E6 and E7 may influence the colony survival response to LMB. The reportedly greater E6 protein expression in the I_{22} derivative compared with E_{63} [403] may act to sufficiently attenuate the p53 response allowing cells to escape LMB-induced apoptosis. The expression of E7 has been associated with greater LMB-induced

apoptosis in previous studies [374], but despite the elevated E7 protein expression within the transduced cells and the majority of the integrated derivatives [119] the levels of LMB-associated colony survival remained greater in I_{22} than E_{63}. The decrease in survival in the W12 derivatives compared with the E7 transduced PHKs may be due to the presence of the remaining components of the HPV genome particularly the E6 protein. This may support the view that in the presence of LMB the influence of E7 is attenuated by the apparently dominant E6 leading to increased survival.

Although CaSki and SiHa cells both contain integrated HPV 16 their malignant backgrounds are likely to have contributed to their greater survival at the higher concentrations of LMB. Those cells surviving at high doses may originate from a pre-existing sub-population of cells whose formation may have been assisted by the presence of integrated HPV and/or other additional cellular mutations. The differences in the level of colony formation and colony size between CaSki and SiHa may relate to the different type of HPV integration present in each (SiHa type 1 and CaSki type 2) or may be a function of the additional mutations they contain. The less dramatic changes in both number and size of SiHa colonies in response to LMB suggest that these cells contain notably different modifications to those contained in the CaSki cell line causing enhanced post-treatment survival. When compared with behaviour of the integrated W12 derivative (I_{22}) it appears that the presence of type 1 integrated HPV alone is insufficient to overcome the effects of LMB, and the additional cellular changes present in the cancer cell lines facilitate an increase in the resistance to LMB treatment.

During malignant conversion of HPV infected cells it has been proposed that E6 and E7 exert their strongest effects during different phases of the process. E7 primarily functions during the initial stages causing the formation of benign lesions, whilst E6 acts more prominently

during the conversion to malignancy [28] (section 1.1.8). A similar pattern of differential E6 and E7 behaviour may play a role in the response of HPV infected cells to treatment with LMB. Previous data have suggested that E7 transduction sensitises cells to LMB induced apoptosis, with the effect attenuated by the presence of E6 possibly via its interaction with p53 and absent from wild type cells [374]. The colony survival data presented here appears to suggest that the presence of E7 within the transduced cells may aid the cell's recovery post LMB treatment. Both E6 and E7 are present within the W12s at lower levels than in the transduced PHKs, therefore the decreased colony survival in these cells could be attributed to either a decrease in any recovery effect due to lower E7 levels or alternatively an attenuation of the E7 effect by the presence of E6. It is possible that E6 may act to protect cells from LMB induced apoptosis, while E7 may assist the recovery of cells after treatment.

These data suggest that W12 derivatives, which provide a model for early HPV associated neoplasia, are sensitive to the effects of the nuclear export inhibitor LMB. This response appears to be influenced not only by the presence of the complete HPV genome and its integration, but also by the differentiation state of the host cells. The normal lifecycle of the virus and any changes due to integration are likely to play an important role in the response of these cells to LMB.

Chapter 5: Leptomycin B Induces Apoptosis in Cells Containing the Whole HPV 16 Genome

5.1 Introduction

The LMB-induced effects previously reported in PHKs transduced with HPV 16 E7, E6 and E6/E7 have been shown to be due to the induction of apoptosis [374]. The data presented in this chapter aims to confirm that the morphological changes and reduction in colony formation in response to LMB in both monolayer and rafted W12 derivatives (chapter 4) can also be attributed to the induction of apoptosis.

Apoptotic cell death is associated with the activation or inhibition of numerous cellular pathways as discussed in section 1.4. The induction of this form of cell death can therefore be assessed in a number of ways, including the detection of apoptotic enzyme activation (e.g. activated caspase-3) and cytoskeletal breakdown (e.g. M30). As described in section 1.4, act-casp-3 acts as an executioner caspase, functioning late in the apoptotic initiation cascade to actively break down the cellular infrastructure. As act-casp-3 is one of a group of executioner caspases acting at this point in the pathway and because it is likely to be transiently expressed due to its enzymatic function, a second marker of apoptosis was also used to provide a more accurate measure of LMB-induced apoptotic cell death. The M30 antibody binds a neoepitope of CK18 formed by cleavage of the cytoskeletal protein at amino acids 387-396 [424]. This breakdown is achieved by a range of activated executioner caspases, including caspase-3, 6 and 7 [425] during the early stages of apoptosis [426]. Initial CK18 cleavage generates a 40kDa fragment with further processing later in apoptosis producing an additional smaller 24kDa protein [426]. The assessment of both act-casp-3 and M30 expression permitted the induction of apoptosis by LMB to be verified, while also allowing any differences in the response due to alterations in genome status to be assessed in both monolayer and raft culture.

5.2. Methods

Cells were cultured and treated with LMB as summarised in sections 2.2 and 2.3. The induction of apoptosis was assessed by immunocytochemistry (section 2.10) and western blotting (section 2.12.1-6 and 2.12.7.2.) by the detection of M30 and activated caspase-3 antibodies.

5.3. Results

5.3.1. Confirmation of Cytokeratin 18 Expression in the W12 Derivatives

The M30 antibody provides a useful method for the detection of early apoptosis in epithelial cells. However, in order to utilise this method the expression of CK18 within the W12 derivatives required confirmation utilising the antibody LE65 which stains for CK18 present within epithelial cells as described by Lane *et al* (1992) [427].

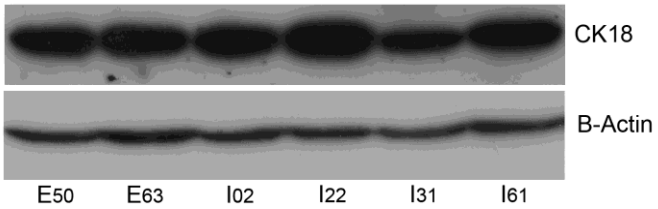

Figure 5.1: The expression of cytokeratin 18 (CK18) in the W12 derivatives and the β-Actin loading control.

Western analysis established the presence of CK18 expression in all the W12 derivatives, with no notable differences in the level of protein present (figure 5.1).

5.3.2. The Induction of Apoptosis by LMB in Monolayer Cultures Assessed by Immunocytochemistry

Initially LMB-induced apoptosis was assessed in adherent cells grown on chamber slides and subjected to immunocytochemistry for act-casp-3 and M30. The expression of the apoptotic markers was assessed at 500x magnification with the number of cells counted determined by the running mean method. This is achieved by calculating the total accumulated positivity as a percentage of the total accumulated cell count (positive and negative). When graphed the formation of a plateau indicates a reliable count (for example see appendix C1). This method ensures that statistically valid numbers of cells are counted from each slide and required cell counts ranging from 2,732 (E_{50} +LMB M30) to 49,087 (I_{22} –LMB M30).

The W12 derivatives showed low level baseline expression of act-casp-3 in the absence of LMB treatment, with levels varying between the derivatives (figure 5.2a). Treatment with 2nM LMB (38h) initiated a marked increase in caspase-3 activation in all the W12 cell lines (figure 5.2a), with considerably elevated act-casp-3 expression occurring in the episomal E_{50} cells. The induction of act-casp-3 was similar between E_{63}, I_{31} and I_{61}, but the type 1 integrated cells I_{02} and I_{22} displayed reduced levels, with I_{02} showing the lowest overall expression.

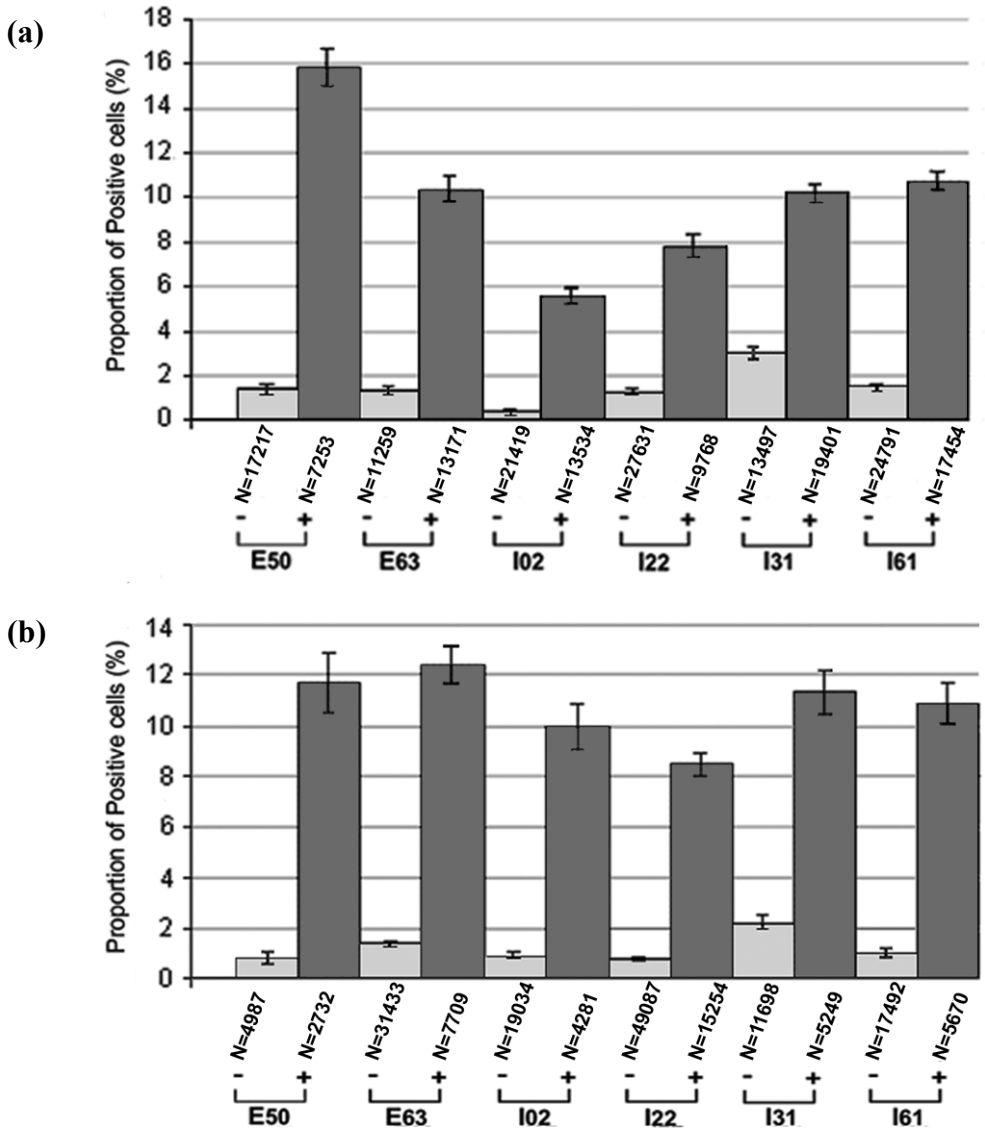

Figure 5.2: The expression of act-casp-3 (a) and M30 (b) detected by immunocytochemistry after treatment with 2nM LMB (38h). Both treated (+) and untreated controls (-) for each W12 derivative are shown, with *N* representing the number of counted cells and the error bars representing ±2x standard error of the proportion (SEP).

Immunocytochemistry for the M30 neoepitope also revealed a low baseline level of expression; although much less variability was apparent between the derivatives (figures 5.2). In response to 2nM LMB (38h) a considerable induction of CK18 cleavage occurred in all the cell lines, indicated by the rise in M30 positivity (figure 5.2b).

The expression of M30 and act-casp-3 indicated that although not strong there may be an association between the episomal, integrated type 1 (single copy) or integrated type 2

(concatemers) status of the viral genome and the sensitivity of these cells to LMB (figure 5.2b).

5.3.3. LMB Induces Apoptosis in W12 Derivatives Grown in Raft Culture

As previously discussed, the LMB induced changes in H&E stained organotypic rafts were suggestive of apoptosis (section 4.3.2). This apoptotic response was verified by examining the expression of act-casp-3 and M30 in raft sections by immunocytochemistry.

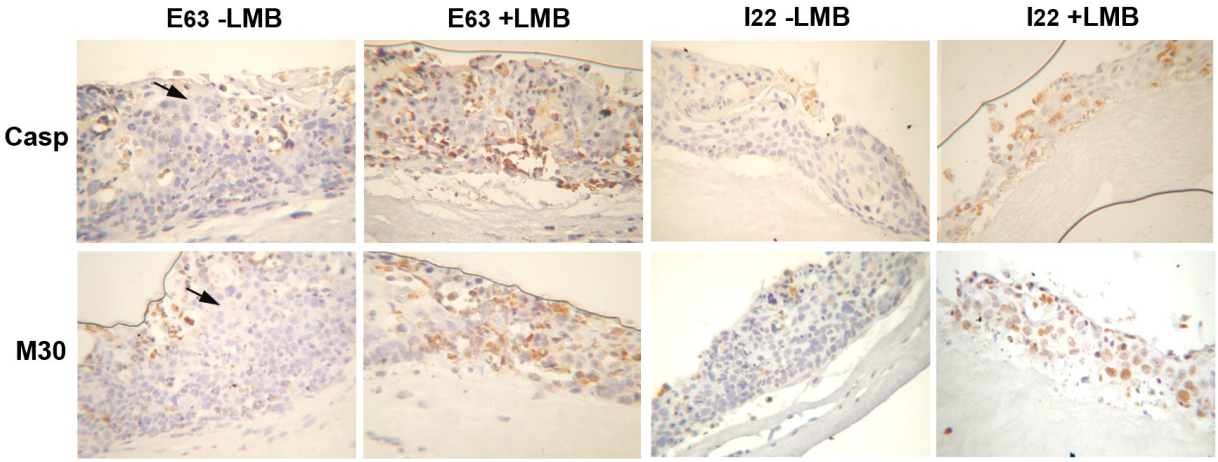

Figure 5.3: The induction of apoptosis in E_{63} and I_{22} rafted derivatives in the presence (+) and absence (-) of 50nM LMB (72h). Staining for both act-casp-3 (upper panel) and M30 (lower panel) are shown. Arrows indicate exemplar keratinised cells.

In the absence of LMB rafted E_{63} and I_{22} cells exhibited low amounts of act-casp-3 and M30 expression throughout the epithelium; although staining was particularly located in the mid-upper layers of both rafts (figure 5.3). The integrated derivative I_{22} demonstrated staining for both act-casp-3 and M30 that was somewhat lower in quantity than the episomal line and restricted to a region higher in the epithelium. Particularly within the episomal rafts, the staining for M30 was largely restricted to locations closer to the surface of the epithelium; a more widespread pattern of positivity was found with act-casp-3 where staining extended further into the mid-level of the raft. In both cell lines the largest concentrations of positivity in the absence of LMB were located in areas of vacuolation and abnormal structure, with

expression notably absent from the keratinised cells in both the episomal and integrated rafts. Treatment with 50nM LMB (72h) led to an increase in the amount and intensity of act-casp-3 and M30 staining throughout the E_{63} and I_{22} rafts (figure 5.3), with a continued association of positivity with areas of vacuolation. The rise in expression was particularly apparent within and immediately above the lost basal layers of the raft especially with act-casp-3, confirming the absence of this region.

Immunocytochemistry of monolayer and rafted cells appeared to show variations in the appearance of the M30 staining similar to that previously described by Duan *et al* (2003) [428] and Grassi *et al* (2004) [429]. These differences are likely to represent the M30 protein in distinct morphological settings, reflecting different stages of the apoptotic process. Early apoptosis is represented by weak/intermediate staining of relatively normal cells, while later stages of apoptosis are indicated by darker staining of cells often with either a highly compacted or granular appearance (figure 5.4). The variations in M30 staining provide a more detailed picture of apoptotic behaviour allowing a more accurate assessment of any pro- or anti-apoptotic effects.

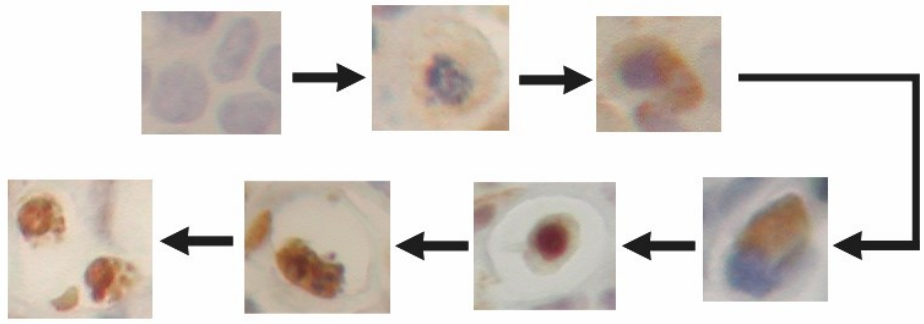

Figure 5.4: The changes in cell morphology and M30 expression in rafted W12 cells representing the progression of apoptosis from normal (upper left) to late apoptosis (lower left).

These changes in the appearance of M30 staining were apparent both episomal and integrated rafts as illustrated in figure 5.4. The untreated E_{63} rafts displayed a greater proportion of darker staining forms of M30, especially within the lower regions of the epithelium; while the

untreated I_{22} raft showed predominantly paler M30 staining. LMB treatment was associated with an increase in the intensity of M30 staining in both the episomal and integrated rafts. In particular the LMB treated episomal raft showed a rise in both the pale and dark forms of M30, although the increase in the darker form was greater, especially in cells displaying a notably granular appearance.

5.3.4. Induction of Apoptosis Assessed by Analysis of Protein Expression

The immunocytochemistry data for both act-casp-3 and M30 suggest that LMB induces apoptosis in all of the W12 derivatives. However, from the immunocytochemical data it remained unclear whether any variations in the response were present between these cell lines. In addition, immunocytochemistry can only assess antigen expression in residual cells that remain adherent to the slide. In order to consider the maximum population response and the time-dependence of the LMB effect, a 48h time course, assessed by western blotting, was undertaken in the W12 derivatives and PHKs transduced with E7 or E6/E7.

5.3.4.1. The Temporal Expression of Activated Caspase-3

Over the 48h time course very little or no act-casp-3 expression was detected in the absence of LMB in the E_{63}, I_{02}, and I_{22} derivatives or the transduced PHKs. E_{50}, I_{31} and I_{61} showed some low background expression which tended to increase slightly over time, indicating the presence of some innate apoptosis (figure 5.5).

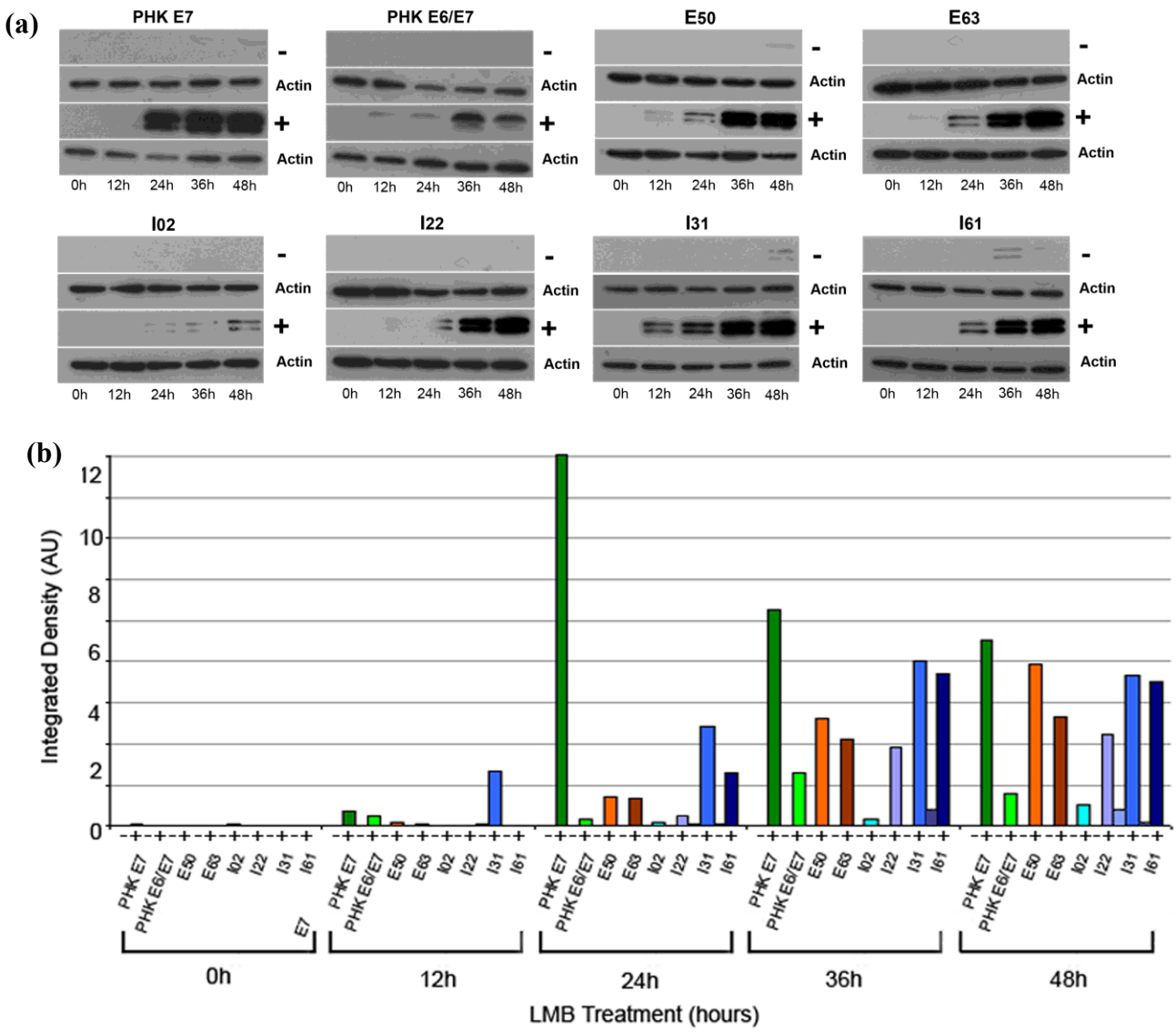

Figure 5.5: The expression of act-casp-3 detected by western blot after 2nM LMB (0-48h). Both untreated control (-) and LMB treated samples (+) are shown at each time point for the E7 or E6/E7 transduced PHKs and the W12 derivatives. (a) The upper panel shows act-casp-3 expression with the β-actin loading control. (b) The data were analysed and integrated density quantification undertaken using Image J with measurements expressed in arbitrary units. All values were normalised against β-actin.

In response to 2nM LMB, act-cap-3 production increased considerably in the W12 derivatives and transduced PHKs, with the response varying as illustrated in figure 5.5. The pattern of act-casp-3 expression was notably different between the two transduced PHK cell lines, with the maximum act-casp-3 expression achieved in the E6/E7 cells considerably lower than that of the E7 expressing cells. The E7 transduced PHKs attained maximal caspase-3 activation by 24h followed by a gradual decrease in expression, whereas activation in the cells

expressing E6/E7 did not peak until 12h later at the 36h time point. A different expression pattern was present within the episomal cells which showed a gradual rise in act-casp-3 up to and perhaps exceeding 48h of treatment (figure 5.5). A more rapid activation of caspase-3 was apparent in the cells containing integrated HPV than in those containing episomal viral genomes. Expression was markedly lower in the type 1 integrated cells, in particular I_{02}. The type 1 integrated HPV cell lines also demonstrated differences in their pattern of act-casp-3 expression. The I_{02} derivative exhibited a gradual rise in act-casp-3 over the entire time period, whereas a sharp increase in activation was present in the I_{22} line at 36h followed by a further gradual increase at 48h. The type 2 integrated derivatives attained levels of act-casp-3 expression similar to those seen in their episomal counterparts. However, I_{31} displayed considerably greater activation at 12h of treatment than any other W12 or transduced cell line, with this initial rapid induction followed by a further gradual increase in levels up to maximum production at 36h. The I_{61} derivative displayed a delayed rise in expression until 24h after the start of treatment, at which point levels rose rapidly and maintained this expression at subsequent time points.

5.3.4.2. Temporal Expression of the M30 Neoepitope

Analysis of M30 expression over the 48h time course allowed the identification of both the early (40kDa) and late (24kDa) CK18 cleavage products by western blot (figure 5.6a). In the absence of LMB the early 40kDa neoepitope, but not the later 24kDa product, could be identified in the W12 derivatives and transduced PHKs, although expression levels were very low, at less than 1 AU (figure 5.6).

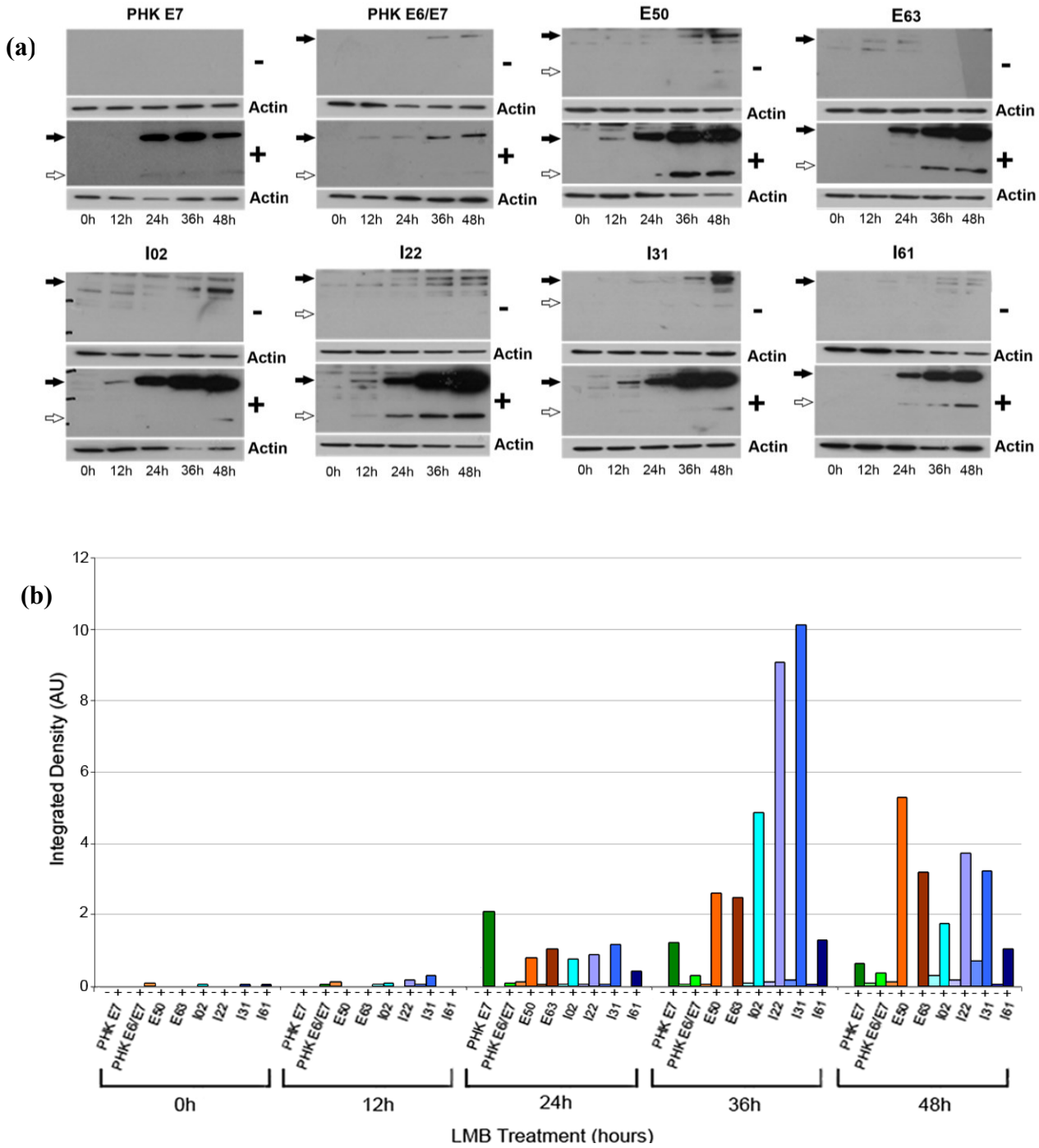

Figure 5.6: The expression of the total M30 expression by western blot after 2nM LMB (0-48h). Both untreated (-) and treated (+) samples of the transduced PHK and W12 cell lines are shown. (a) The upper panel shows M30 expression, where filled arrows indicate the position of the early 40kDa form of M30 and empty arrows denote the later 24kDa product. The β-actin loading control is shown in the lower panel. (b) The data was analysed and integrated density quantification undertaken using Image J with measurements expressed in arbitrary units. All values are shown as total M30 (both early and late forms) and normalised against β-actin.

In response to 2nM LMB, the cells displayed increased M30 production (figure 5.6) as previously reported by immunocytochemistry (figure 5.2). The E7 and E6/E7 transduced PHKs reacted differently to LMB treatment as reflected in the levels and patterns of M30 positivity. Throughout the time course, M30 expression in the E7 expressing cells exceeded that of the E6/E7 transduced cells, although notable decreases in E7 expression were present as the treatment progressed. The peak production of M30 in the E7 transduced cells occurred at 24h with subsequent expression gradually decreasing, whereas cells transduced with E6/E7 displayed a slower increase in M30 expression over the entire time course, with levels throughout notably lower than the other cell lines. The W12 derivatives also responded to LMB treatment with a rise in CK18 cleavage leading to increased levels of total M30. However, in these derivatives the peak levels of M30 were not reached until at least 12h after the E7 transduced cells at 36-48h (figure 5.6). The episomal cell lines displayed a pattern of M30 similar to that seen in the E6/E7 transduced PHKs, but with notably more M30 present. From 12-36hs of treatment the pattern of M30 expression remained similar between the two episomal cell lines; however, in the final 12h the E_{63} derivative maintained a slow increase in M30 levels, whilst a more rapid rise occurred in E_{50} consequently reaching a higher peak level of M30 than E_{63}. The integrated derivatives, with the exception of I_{61}, displayed levels of M30 similar to the episomal derivatives at the 24h and 48h time points. However, a rapid pulse of CK18 cleavage was apparent at 36h where M30 levels were notably greater than in either the transduced PHKs or episomal W12s. The I_{61} derivative exhibited lower expression of M30 with levels between that of the E7 and E6/E7 expressing PHKs.

Both the early and late forms of M30 were expressed in response to LMB treatment in the W12 derivatives and transduced lines (figure 5.6a). Throughout the time course the 40kDa early protein was found to be the dominant form, with the later 24kDa neoepitope occurring at

considerably lower levels. The expression of the later 24kDa form was particularly low in the E6/E7 expressing PHKs, even after 48h of treatment (figure 5.6a). Some overlap in the expression of the early and late neoepitopes was present over the 48h time course, although in most cases a lag period was present between the initiation of early and late protein production. However, in the E7 transduced PHKs and the type 2 integrated I_{22} there appeared to be concurrent expression of both forms of the M30 protein.

5.3.4.3. LMB Induces the Expression of Both Activated Caspase-3 and M30

The 48h time course data described above (sections 5.3.4.1/2) was also analysed to assess the cumulative expression of both act-casp-3 and M30 over the entire treatment period as illustrated in figure 5.7.

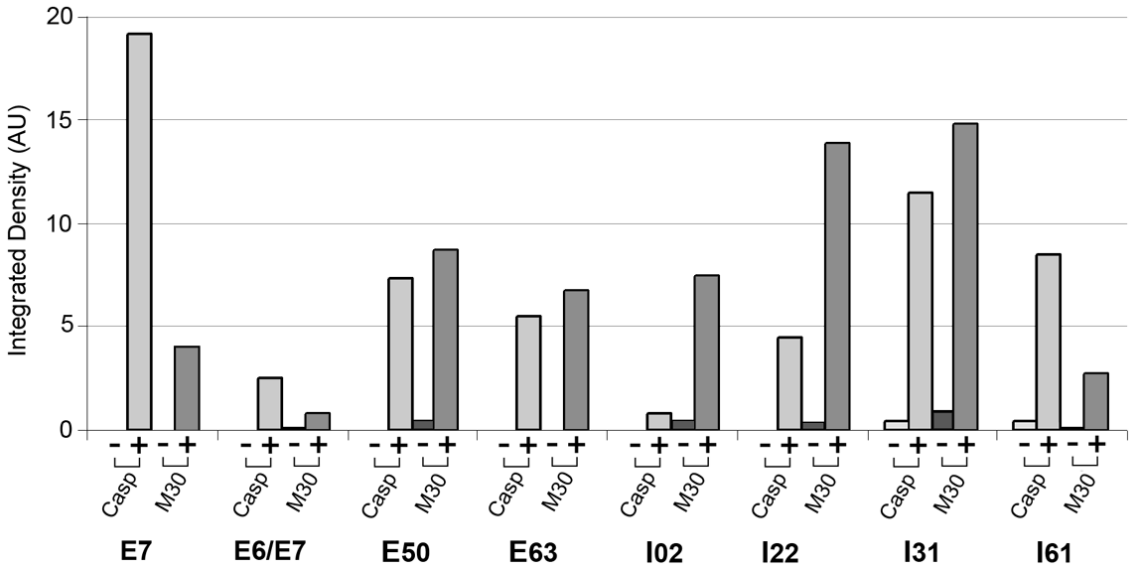

Figure 5.7: The cumulative expression of act-casp-3 (Casp) and M30 in response to 2nM LMB over the 48h time course. The expression of both markers of apoptosis within the E7 or E6/E7 transduced PHK lines and the W12 derivatives are shown in the absence (-) or presence (+) of 2nM LMB.

The majority of the W12 derivatives showed greater expression of M30 than act-casp-3. However, the level of expression and the discrepancy between the markers did appear to correlate with HPV genome status in the episomal and type 1 integrated derivatives. The episomal lines E_{50} and E_{63} displayed similar expression patterns of both apoptotic markers

with the expression of M30 only slightly higher than act-casp-3, although levels of both markers were slightly higher in E_{50}. The cells containing type 1 integrated genomes displayed a lower level of act-casp-3 than M30, with the least overall expression of act-casp-3 found within the I_{02} derivative. The discrepancy in the expression of the two markers was notably greater in I_{02} and I_{22} than in the episomal lines (figure 5.7). The type 2 integrants I_{31} and I_{61} exhibited different expression patterns, with the I_{31} derivative displaying high levels of both apoptotic markers with a divergence in expression similar to the episomal lines. The I_{61} derivative and the E7 and E6/E7 transduced PHKs displayed higher expression of act-casp-3 than M30, unlike the other cell lines, which displayed higher expression of M30 than act-casp-3. In cells containing E7 alone the level of act-casp-3 was markedly greater than the level of M30, in the presence of both E6 and E7 the expression levels of both markers dramatically decreased as did the difference between their expressions. The expression of act-casp-3 and M30 by the I_{61} derivative, were slightly higher than the E6/E7 transduced line as shown in figure 5.7.

5.3.4.4. Contribution of the W12 Feeder Layer to the Apoptotic Response

As the W12 derivatives were cultured on a feeder layer of mitomycin C treated J2 3T3 fibroblasts, the effect of LMB on these cells, including any possible contribution to the apoptosis reported above (sections 5.3.4.1-3), was assessed in these cells. Treatment was undertaken on a comparable numbers of J2 3T3 feeder cells in W12 culture conditions over a 48h time course, with E7-transduced PHKs used as a positive control for the effects of LMB.

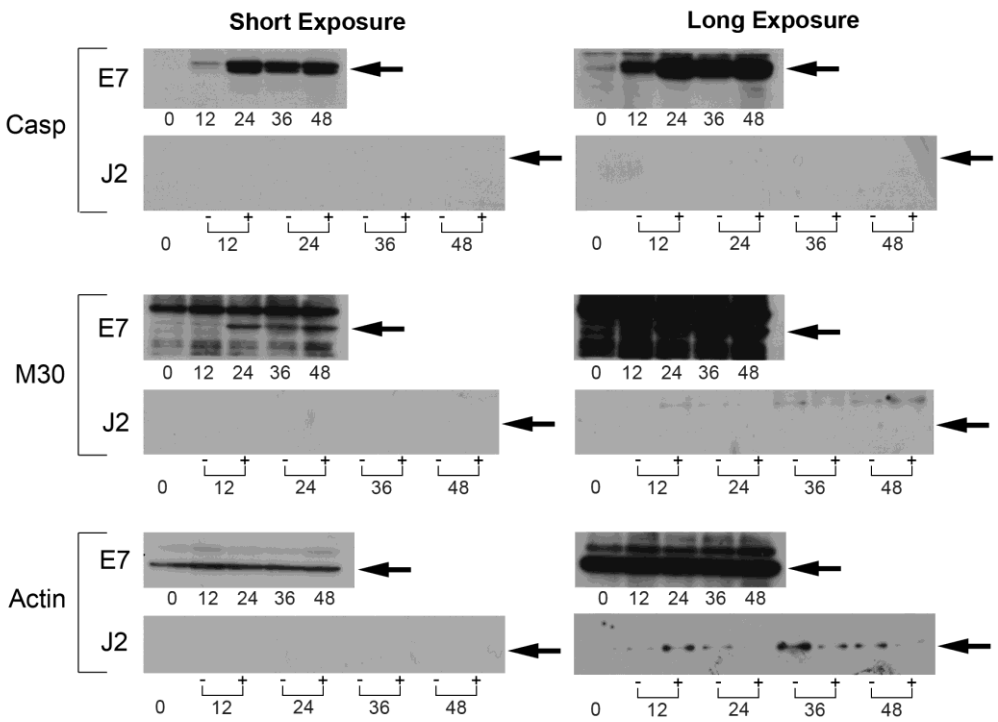

Figure 5.8: The effect of 2nM LMB on J2 3T3 grown under W12 culture conditions. The expression of act-casp-3 (a) and M30 (b) was assessed in J2 cells with (+) and without (-) LMB (upper panels) and E7 expressing cells treated with LMB (lower panels), with the loading assessed by detection of β-actin (c).

As shown in figure 5.8, when seeded at the same density used in the W12 experiments, no expression of either M30 or act-casp-3 could be detected in mitomycin C treated J2 3T3 cells in response to 2nM LMB over the 48h time course. However, the despite levels of both markers in the E7 transduced PHKs being comparable to the previous data (sections 5.3.4.1-3). This suggests that these cells are unlikely to contribute appreciably to the apoptosis reported in the time course data shown in figures 5.5-7, due to the low numbers of J2 fibroblasts and/or to a lack of LMB sensitivity.

5.4. Discussion

An induction of morphological changes and loss of cells was apparent in both the monolayer and rafted W12 cells after treatment with LMB. Previously in the E7 and E6/E7 transduced PHKs [374] these LMB-induced effects have been verified as apoptosis by examination of the

apoptotic markers activated caspase-3 (act-casp-3) [217] and the M30 neoepitope of CK18 [425,426]. This chapter provides evidence that LMB also induces a potent increase of the apoptotic markers act-casp-3 and M30 in derivatives of the W12 cell line containing predominantly episomal or integrated HPV 16 genomes, in both monolayer and rafted environments.

Raft cultures of both episomal and integrated cell lines E_{63} and I_{22} displayed notable differences in both their structure (section 4.3.2) and apoptotic marker expression (section 5.3.3) in the presence and absence of LMB. Although the untreated rafts displayed apoptotic marker expression throughout the epithelium, the concentrations of staining associated with vacuolation and abnormal structure suggested that these areas within the rafts are produced as either a consequence of apoptosis or represent regions more susceptible to apoptosis. The production of M30 is known to be catalyzed by a number of executioner caspases including act-casp-3. Therefore, the spatial differences in location of act-casp-3 and M30 within the raft may represent the earlier activation of caspase-3 lower in the epithelium. The more prominent activation of act-casp-3 at a lower level in the episomal derivatives may be due to a number of factors, including the cleavage of CK18 by alternative executioner caspases or a lower baseline level of apoptosis in the integrated derivative. As discussed in section 4.4, the both the untreated and treated E_{63} raft displayed higher levels apoptosis including cell loss within the mid to upper suprabasal layers. This could derive from virally induced apoptosis, which has been suggested to have a number of possible functions, including limiting the viral impact on the host via control of progeny levels and/or facilitating the release of virions by disrupting the cytoskeleton [111,332,342] (see section 1.5.5.2). However, as these functions are thought to be highly dependent on the presence of the viral proteins E2 [342,343] and E1^E4 [332], the loss of E2 during HPV integration is likely to contribute to the lower levels of apoptosis present within the upper regions of the integrated raft.

Treatment with LMB was associated with the upregulation of act-casp-3 and M30 in both E_{63} and I_{22} rafts. As noted in the morphological studies (chapter 4.3.2), the effects of LMB were most pronounced in the basal layers of both rafts, confirming the particular sensitivity of these rapidly dividing cells to the apoptotic effects of LMB in the presence of both episomal and integrated HPV. As this LMB-induced effect on the basal epithelium appears absent in rafted wild type human keratinocytes [374], this loss of cells within this region is likely to be due to the presence of integrated or episomal virus and its interaction with the cell.

Analysis of protein expression in monolayer W12 derivatives in the absence of LMB indicated variation in the expression of the apoptotic markers, representing differences in the level of innate apoptosis. These variations may be due to the clonal nature of the cells and/or differences in their viral genome status. The I_{31} cell line in particular appeared to consistently display a high level of background apoptosis indicating that the specific clonal or virally induce changes within this particular derivative. This increased propensity for apoptosis may be influenced by increased the cellular pro-apoptotic response via mechanisms such as increased p53 signalling and/or a decrease in viral anti-apoptotic signalling, which would lead to increased innate apoptosis.

Considerable inter-derivative variation in the levels of LMB-induced apoptosis was apparent by both immunocytochemistry and western blot, with the status of the viral genome and the clonal nature of the derivatives probably contributing to the variation in LMB sensitivity. The episomal cell lines did not share a common level of LMB-induced apoptosis, with E_{50} proving to be the more sensitive of the two, suggesting the presence of variation between these cell lines, the differences in E7 expression of the two lines reported by Jeon *et al* (1995) [119] may contribute to the differences in behaviour. In additional, Southern analysis of the E_{63}

derivative (section 3.3.1) indicated the possible presence of integrated sequences; however, Pett *et al* (2007) [5] have proposed that the presence of E2 derived from episomal HPV inhibits gene expression from co-existing integrated sequences. Indeed data suggests that expansion of cells containing integrated HPV does not occur until the episomal viral genomes are lost [133]. Therefore, it remains unclear what, if any influence the presence of any integrated sequences within the E_{63} derivative would have on their LMB response.

Although the type 2 integrated I_{31} and I_{61} line showed similar medium levels of act-casp-3 induction in response to LMB, the levels were slightly lower in I_{61}. In addition the expression of M30 was found to be notably lower in the I_{61} derivative after western blot analysis, suggesting the presence of prominent differences with this line. The cumulative time course data indicated that I_{61} appears to behave as an intermediate between PHK E7 and PHK E6/E7 in terms of both the expression levels of act-casp-3 and M30, and in the discrepancy between the two markers. These data, combined with high levels of both E6 and E7 reported in the literature [119,430], suggest that the oncogene expression in this derivative are influencing the response of these cells to LMB. The similarity in act-casp-3 and M30 expression between I_{22} and I_{31} may be a response to clonal differences or an effect of general rather than type specific integration. The I_{02} derivative showed lower levels of both markers and a larger discrepancy in expression between the two apoptotic proteins, with very low levels of act-casp-3 but higher levels of M30. This expression pattern may be a consequence of the clonal selection of I_{02} from a later passage 17 (instead of 14/15) of the parental W12 cell line which has been shown to accumulate cellular changes over time increasing the likelihood that further alterations in both viral and cellular mechanisms have occurred [117,119,311].

Both the early and late forms of the M30 protein were detected in the W12 derivatives and transduced PHKs representing cells at difference stages of apoptosis. Universally the major product was the early 40kDa form with variable amounts of further cleavage apparent between the different cell lines. Variations in both the amount and timing of the 24kDa M30 production were noted, with the delayed expression of the late form in the E6/E7 transduced PHKs and the W12 derivatives, suggestive of a more gradual progression of apoptosis. However, the concurrent expression of the two forms of M30 in both the E7 transduced PHKs and the I_{22} derivative; suggest that these lines undergo a more rapid onset of secondary M30 cleavage. The virus is known to manipulate the host apoptotic mechanisms by interacting with the pathways at various points. This can be achieved by either down regulating pro-apoptotic proteins such as pro-caspase 8 (E6) [110] or upregulating anti-apoptotic proteins such as c-IAP (E6 and E7) [329] (section 1.5.5.1). In the presence of LMB these pre-existing alterations to the apoptotic pathways may influence the progression of apoptosis, particularly where the proteins involved undergo CRM1-mediated nuclear export (e.g. IAP1/2 [391] and Survivin [394]).

The time course data suggest that the presence of selected genes or the whole genome from HPV 16 in specific configurations, correlates with temporal expression of the apoptotic markers act-casp-3 and M30 (figure 5.8). The most rapid expression of both apoptotic markers was present in the E7 transduced cells after 24h of LMB treatment. A dramatic change in sensitivity, similar to that shown previously in rafted and monolayer cells by Gray *et al* (2007) [374], was provoked by the introduction of the E6 gene, delaying peak apoptosis by at least 12h. Interestingly the presence of E6 also appears to be associated with a temporal dissociation of apoptotic markers with act-casp-3 levels peaking 12hs prior to M30. These differences in the induction of apoptosis by LMB in the E7 and E6/E7 transduced PHKs,

suggest that the E6 protein may play a role in protecting cells from LMB induced apoptosis, possibly in a p53-dependent manner as suggested by Lain *et al* (1999) [182]. This E6-mediated attenuation of LMB-induced apoptosis is thought to be achieved by the continued utilisation of nuclear proteasomes during LMB treatment. The degradation of p53 by E6 utilises cellular components such as proteasomes and E6-AP, which although primarily cytoplasmic are also located within the nucleus [179,263,431]. It has been illustrated in HPV 18 E6 transfected cells that treatment with LMB does not lead to a total loss of p53 degradation, indicating that E6 can mediate p53 degradation via both nuclear and cytoplasmic proteasomes [179].

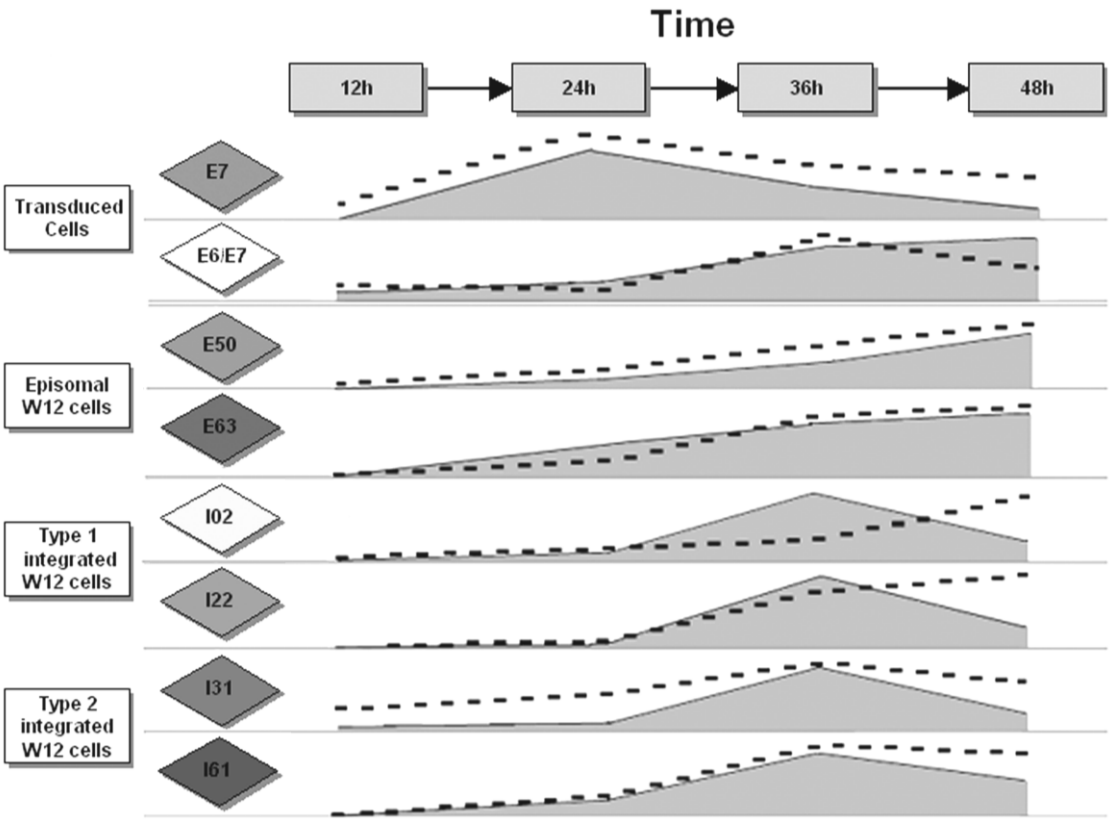

Figure 5.9: LMB-induced expression of the apoptotic markers act-casp-3 and M30 varies amongst the transduced PHKs and the W12 derivatives and correlates with the genome status of the cells. The dotted lines represent the act-casp-3 levels with the shaded areas indicating M30 expression after treatment with 2nM LMB over a 48h time course.

As illustrated in figure 5.9, the integration status of the viral genome in the W12 cell lines correlated with the temporal expression pattern of act-casp-3 and M30. The delay in apoptosis exhibited by the W12 derivatives in comparison to the E7 cells is reminiscent of the

change seen in response to the presence of E6 in the E6/E7 transduced PHKs. The episomal lines E_{50} and E_{63} demonstrated the most prolonged delay in reaching peak act-casp-3 and M30, with levels rising up to and possibly beyond the 48h time point, at least 24h after the E7 expressing cells. HPV integration in the W12 derivatives is associated with more rapid induction of maximum apoptotic marker expression than present in the episomal lines. This implies that integration has an important role in increasing the rate of the apoptotic response of these cells to LMB; this may be a consequence of the presence of greater E6/E7 expression, a lack of E2, or some other integration-related mechanism. The type 1 integrated derivatives displayed a dissociation in the expression of the two markers, with M30 peaking at 36h and act-casp-3 delayed by at least 12h. However, the type 2 integrated W12s displayed peak levels of both apoptotic markers at 36h; this coincident expression of M30 and act-casp-3 was also exhibited by the E7 expressing PHKs. These differences in expression in the integrated cells suggest that, although integration in general appears have some bearing on the response to treatment, the type of HPV integration event also has an influence on the response of these cells to LMB.

The mechanisms by which LMB-induced apoptosis occurs in the W12 derivatives and transduced cells appears to be, at least partially, act-casp-3 dependent [374,399]. Evidence from Jang *et al* (2004) [399] proposes that caspase-9 and caspase-3 play a specific role in the initiation of CK18 cleavage, with expression shown to increase in response to LMB treatment of U937 leukaemic cells. However, in the time course experiment, the W12 derivatives and in particular the type 2 integrated cells showed a lack of correlation between act-casp-3 and M30 production. LMB-induced act-casp-3 expression in most of the remaining cell lines was either concurrent with or subsequent to M30. This suggests that executioner caspases other than act-casp-3 may play an important role in the induction of apoptosis by LMB in HPV 16

infected cells. Caspase activation, and other factors influencing the apoptotic response to LMB are likely to be affected by the context of the HPV genome within these cells, with subsequent effects on the level and pattern of LMB induced apoptosis.

LMB has previously been shown to induce apoptosis in cells expressing HPV oncogenes, but not in wild type PHKs [374], suggesting that the presence or absence of viral genes influences the manner in which keratinocytes respond to LMB. The data presented above demonstrate that LMB also induces apoptosis in keratinocytes containing the whole viral genome in both episomal and integrated states, and thus provides a mechanism for the changes in morphology and colony survival described in chapter 4. Furthermore, the viral genome status of the three W12 types appears to influence the pattern of LMB-induced apoptosis in both monolayer and raft culture.

Chapter 6: The Expression of p53 and p21 in Response to LMB Treatment

6.1. Introduction

LMB is able to induce apoptosis in W12 derivatives containing either episomal or integrated genomes (chapter 5). In addition to this induction of apoptosis, LMB treatment has previously been associated with increased expression of the cell cycle regulator p53 in a range of cell types including HPV infected cancer cell lines [182,203], HPV transduced primary cells [374], primary human fibroblasts [203] and prostate epithelial cells [375]. Therefore, increased expression of p53 may also play a role in the LMB-induced response of the W12 derivatives shown in chapters 4 and 5, particularly in those cells expressing integrated HPV.

The cell cycle regulator p21 may also play a role in mediating LMB-induced effects. p21 is known to be expressed in both a p53-dependent and independent manner and may therefore play a role in any LMB-induced p53 response. In addition, LMB is known to induce a rise in p21 in a number of cell types [385,432], while also inducing a possibly p21-dependent temporary cell cycle arrest in wild type primary human keratinocytes [374]. In this study, the LMB-dependent and independent expression of p53 and p21 was assessed by immunocytochemistry of W12 raft cultures and western blot of the time course samples.

6.2. Methods

Rafted W12 cells were cultured as described in section 2.6 prior to treatment with 50nM LMB. Treated rafts were then stained for p53 and p21 by immunocytochemistry (section 2.10.2). The effects of LMB on the expression of p53 and p21 in monolayer was assessed by western analysis, this allowed the time dependence of any response to be assessed and in addition, prevented any variations in results due to the loss of cell adherence noted in section

5.3.4. The 48h time course was undertaken as described in section 2.12 and 2.12.7.2 with the expression of both markers assessed by western analysis. Further investigation of the p21 doublet was performed by phosphatase treatment (section 2.12.7.5) and the use of an alternative p21 antibody (2.12.7.2).

6.3. Results

6.3.1. The Expression of p53 and p21 in W12 Rafts

In the absence of LMB the rafted E_{63} and I_{22} cells displayed focal staining for p53 throughout the suprabasal region of the epithelium, with expression slightly greater within the I_{22} cells (figure 6.1, upper panel). Rafted E_{63} cells displayed the strongest and most prolific staining within the lower suprabasal region, while the rafts containing integrated HPV demonstrated expression that appeared more evenly distributed throughout the epithelium. In both cases staining was low or absent in abnormal or vacuolated areas of the raft. In the presence of 50nM LMB (72h) the E_{63} raft displayed a small increase in the amount and intensity of p53 staining throughout the epithelium, particularly within the mid to upper regions (figure 6.1, upper panel). The integrated I_{22} rafts appeared to show little change in the amount or distribution of p53 in response to LMB (figure 6.1, upper panel) and in some cases expression actually appeared to decrease, although this may be due to the cells of the basal region having already been lost via apoptosis as described in chapters 4 and 5. Both LMB treated rafts exhibited little evidence of staining within the lost basal layers positive for the apoptotic markers act-casp-3 and M30 (section 5.3.3).

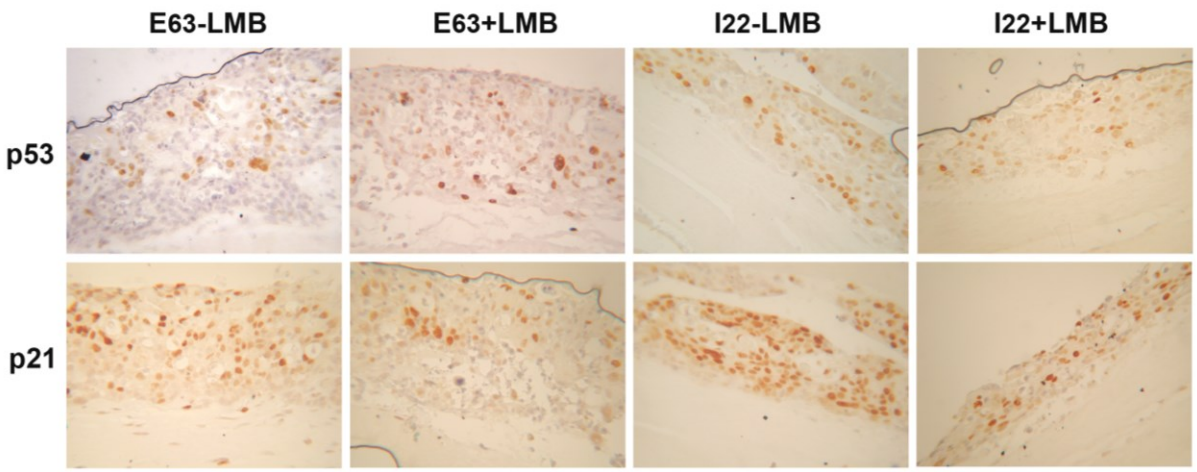

Figure 6.1: The expression of p53 and p21 in rafted W12 derivatives E_{63} and I_{22} grown in the presence (+) or absence (-) of 50nM LMB (72h).

High background levels of p21 were present in the majority of the epithelium of both the E_{63} and I_{22} rafts (figure 6.1, lower panel). However, expression was notably reduced within the basal and immediately suprabasal regions of the rafts, particularly in the E_{63} derivative. 50nM LMB (72h) led to a decrease in p21 in both raft types, although the effect was more pronounced in E_{63}. A large proportion of this decrease in staining is probably due to the loss of cells in the basal and lower suprabasal layers of the rafts (figure 6.1, lower panel).

6.3.2. LMB Induces Changes in p53 Expression in the W12 Derivatives Over a 48h Time Course

Background levels of p53 expression were present in the majority of the cell lines in monolayer time course (figure 6.2), as was previously seen in the raft model (figure 6.1). This background expression tended to increase over the time course, as shown in figure 6.2. The highest basal levels were displayed by the E7 transduced PHKs where levels continued to rise up to the 36h time point. Conversely, the E6/E7 transduced PHKs displayed very little background expression until late in the time course (36h) with levels remaining low. The p53 expression of the untreated W12 cells varied between the individual derivatives, with the initial increase in baseline expression followed by a plateau or a gradual decrease in most of

the cells. The exception was I_{61} where background expression continued to rise throughout the time course reaching a high level by 48h.

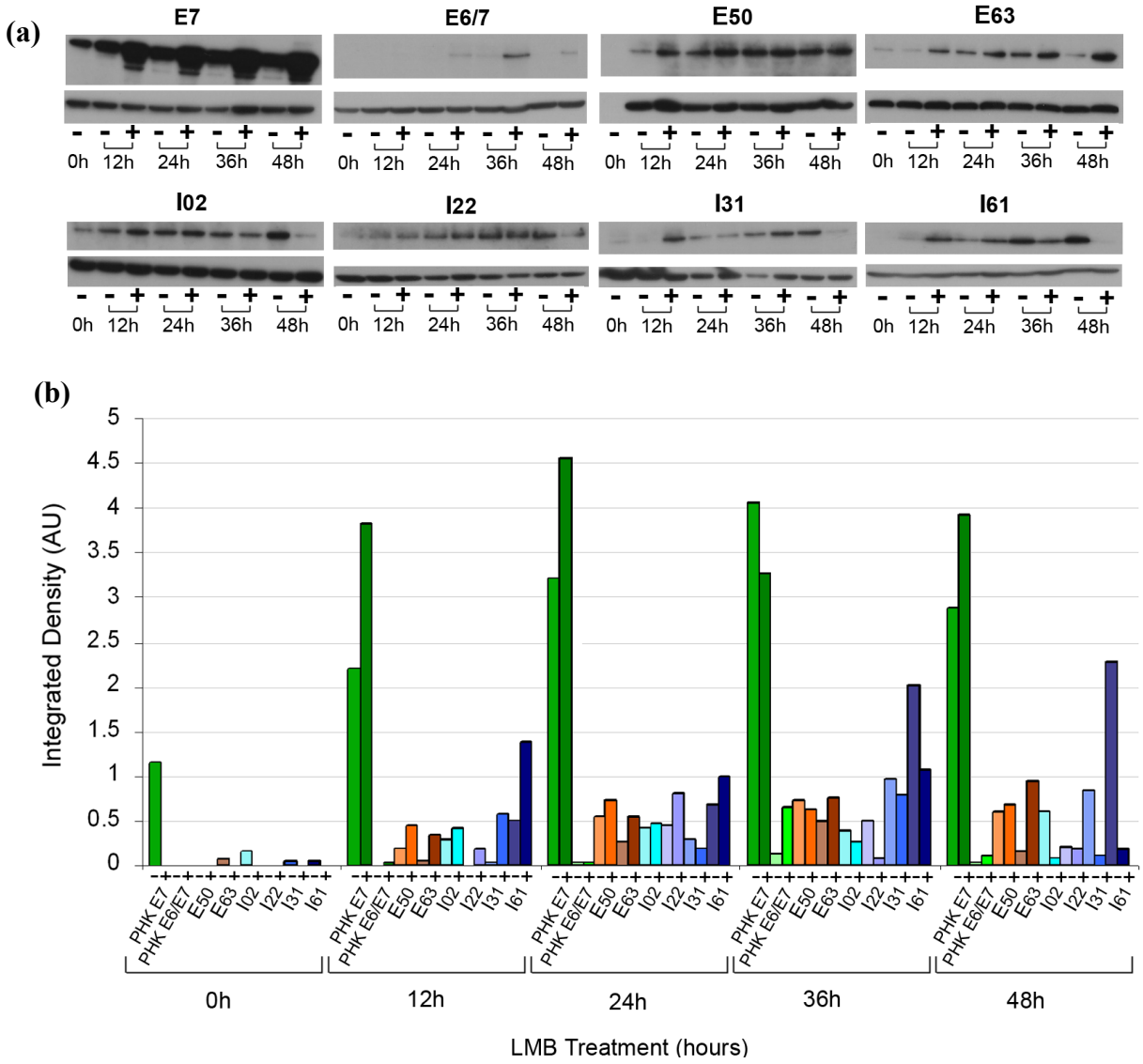

Figure 6.2: The expression of p53 protein detected by western blot after 2nM LMB (0-48h). Both untreated (-) and LMB treated samples (+) are shown for E7 or E6/E7 transduced PHKs and W12 derivatives at each time point. (a) The upper panel shows p53 expression with the β-actin loading control in the lower panel, (b) the data was analysed and integrated density quantification undertaken using Image J with measurements expressed in arbitrary units. All values were normalised against β-actin.

In response to 2nM LMB the expression of p53 increased in both the transduced and W12 cell lines (figure 6.2). The E7 transduced PHKs had the greatest levels of p53 in response to LMB, reaching a maximum expression considerably greater than the remaining lines 12-24h after treatment commenced. The E6/E7 expressing cells displayed very little induction of p53

in response to LMB, with notable increased expression only present at 36h. The W12 derivatives, with the exception of E_{63} and I_{22}, demonstrated a rapid induction of peak p53 expression 12h after LMB treatment. The remaining two derivatives had a delay in attaining maximum p53 response with I_{22} reaching peak expression by 24h and the E_{63} derivative displaying levels that continued to rise up to at least 48h (figure 6.2).

6.3.3. LMB Induces Increased Expression of p21 in the W12 Derivatives

p21 expression in the absence of LMB was present in the W12 derivatives and the E7 transduced PHKs, with levels varying considerably between the cell lines over time (figure 6.3). The increased p21 expression over time seen in many of the cell lines in the absence of LMB is likely to be great influenced by the confluence of the cell cultures. The untreated p21 response was especially high in the type 2 integrated derivatives I_{31} and I_{61} particularly at the 48h time point (figure 6.3). However, background expression of p21 was absent from the E6/E7 transduced PHKs over the entire time course. In the case of the E_{63} derivative which expressed p21 as a doublet, the sum of the upper and lower bands was used for analysis of the p21 response. By the 48h time point, cultures grown in the absence of LMB would have reached an increase level of confluence with a likely decrease in nutrient availability, this may have subsequently contributed to the high levels of p21 displayed by the majority of the cell lines.

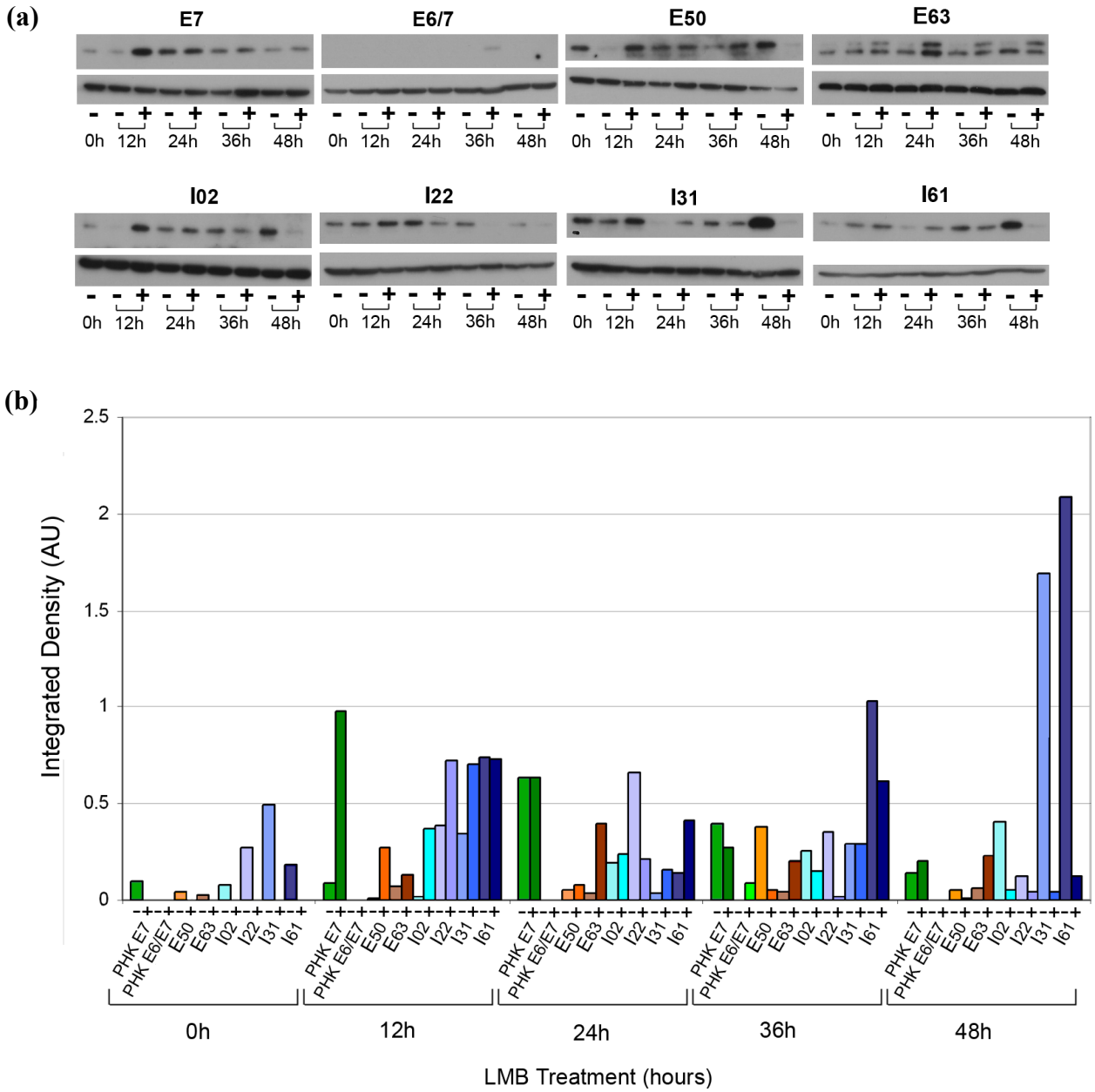

Figure 6.3: The expression of p21 protein detected by western blot after 2nM LMB (0-48h). Both untreated (-) and LMB treated samples (+) are shown for E7 or E6/E7 transduced PHKs and W12 derivatives at each time point. (a) The upper panel shows p21 expression with the β-actin loading control in the lower panel, (b) the data was analysed and integrated density quantification undertaken using Image J with measurements expressed in arbitrary units. All values were normalised against β-actin.

After 2nM LMB a p21 response was elicited in the W12 derivatives and transduced PHKs (figure 6.3). The p21 response varied between the derivatives, although the differences were less dramatic than those between the two transduced lines. The E7 transduced PHKs contained the highest induced levels of p21 while the expression in E6/E7 transduced PHKs

remained markedly lower than the other cells. The majority of cell lines studied showed a rapid response to LMB with p21 expression peaking after only 12h of treatment (figure 6.3). However, a more prolonged rise in p21 expression was apparent in certain cell lines; E6/E7 transduced PHK cells not expressing p21 until 36h after treatment, and the W12 derivatives E_{63} and I_{61} both peaking after 24h. With the exception of E_{63}, maximum p21 induction was followed by a rapid decrease in expression over the following hours. E_{63} showed a less dramatic decrease in p21 levels, with its peak expression at 24h followed by a gradual decrease, then plateau as shown in figure 6.3.

6.3.4. The Expression of p21 as a Doublet in the E_{63} Derivative

During western analysis, the W12 derivative E_{63} was consistently found to express p21 in the form of a doublet, where the lower band represented both a novel and a dominant signal 1.2-2.5kDa smaller than the native form. The time course data (figure 6.4) indicated the majority of the p21 induction appears to originate in the upper band of this doublet, particularly during the cellular response to LMB treatment. The lower band of the doublet was found to be strongly expressed throughout the time course, with very little variation associated with changes in the time point or treatment status. Only where peak expression of the upper band was apparent at 24h was there a notable increase in the intensity of the lower band (figure 6.4).

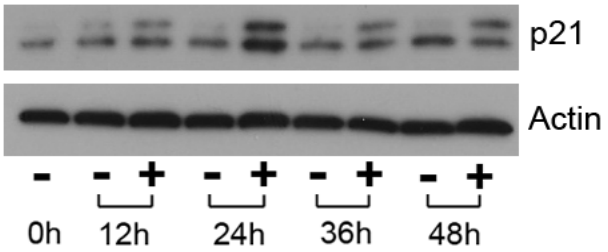

Figure 6.4: The expression of the doublet form of p21 in the E_{63} derivative in the presence (+) or absence (-) of LMB treatment over a 48h time course.

The mechanism for the formation of the doublet within this single W12 derivative alone was unclear. Evidence from the literature [433] suggested that similarly sized p21 doublets have reportedly been formed by changes in the phosphorylation status of the p21 protein. Phosphatase digestion of protein derived from W12 cells was therefore undertaken to ascertain if dephosphorylation of the E_{63} p21 protein had led to the formation of the lower novel band.

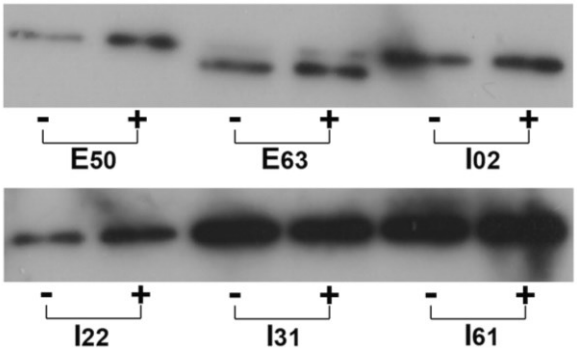

Figure 6.5: The effect of phosphatase digestion on the expression of p21 in the W12 derivatives. Western analysis was undertaken for p21 on undigested (-) or phosphatase digested (+) protein lysates.

Phosphatase treatment (figure 6.5) appeared to have no effect on the doublet formation in the E_{63} line, suggesting that dephosphorylation of p21 is unlikely to have led to the formation of the novel doublet signal. Alternatively the p21 doublet may have been formed by cleavage of the native p21 leading to the formation of the smaller band. This was investigated by the use of antibodies with two distinct epitope locations (figure 6.6a); the previously used C-terminal antibody (SX118) and an alternative internally located antibody (EA10).

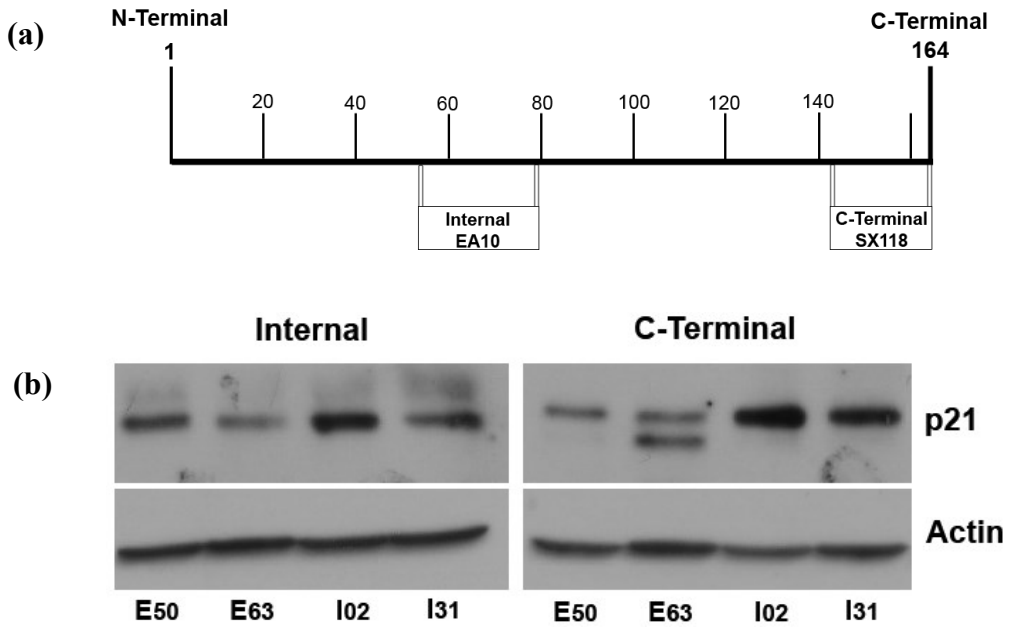

Figure 6.6: Differences in the pattern of p21 expression using antibodies against C-terminal and internally located epitopes. (a) A schematic showing the positions of the internal (a-a 58-77) and C-terminal (a-a 146-164) p21 antibody epitopes. The a-a positions of the E2 protein are shown above the line with the antibody positions below. (b) Western blot analysis of p21 expression by C-terminal (SX118) and internal (EA10) antibodies in the E_{50}, E_{63}, I_{02} and I_{31}. Equal loading is shown in the lower panel by β-Actin (Actin).

As found during the time course experiment, a doublet p21 was detected by the C-terminal antibody in the E_{63} derivative, but was absent in the other W12 representatives (E_{50}, I_{02} and I_{31}). The presence of a doublet with the C-terminal antibody suggests that this portion of the p21 protein is present in both the native and novel bands of the doublet. Western analysis using the internal p21 antibody did not detect a doublet in the E_{63} sample, suggesting that this region of p21 protein may be partially or totally absent from the novel p21 protein.

6.4. Discussion

LMB has been shown to cause changes in morphology, colony survival and the induction of apoptosis not only in the W12 derivatives (chapters 4 and 5) but also in other HPV associated cells during previous studies [182,374]. The mechanisms by which LMB induces apoptosis remain unclear. HPV infection appears to sensitise the cells to LMB-induced cell death;

however, other factors such as the BCR-ABL mutation [400] or the changes associated with leukaemic [399] or prostate cancers [375] have also been shown to effect the susceptibility of cells to LMB as discussed in section 1.6.2. A number of studies have shown an association between LMB treatment and increased p53 expression [182,203,374,375], providing a possible mechanism for the apoptotic effects of LMB. In addition, wild type PHKs are reported to undergo quiescence in response to LMB [374]; this may be caused by the cell cycle regulator p21 therefore the possible role of p21 was also investigated.

The data presented in this chapter show that increased levels of p53 and p21 protein in response to treatment with LMB were present in monolayer W12 derivatives and PHKs transduced with E7 and E6/E7 over a 48h time course. The rafted W12 derivatives displayed some increase in expression of p53 in response to LMB, but no such p21 response could be detected.

6.4.1. The Expression of p53 and p21 within Rafted W12 Cells

When untreated, both the level and pattern of p53 and p21 expressed in the rafted W12 cells varied between the episomal E_{63} and integrated I_{22} derivatives. Low expression of p53 and p21 was present within the basal region of the epithelium in both rafts, as was previously observed in episomal rafts by Flores *et al* (2000) [27]. This epithelial region contains rapidly dividing cells, and should require less viral interference than other regions as the replication machinery required by the virus is already present. Therefore, this lower level of viral interference the requirement for expression of the cellular regulators p53 and p21 is likely to have contributed to their decreased expression.

In the absence of LMB, both p53 staining and the greatest levels of apoptosis (section 5.3.3) were located within the mid-upper epithelium in both the episomal and integrated W12s; in addition, this correlation between p53 and innate apoptosis has previously been observed in rafted E_{63} cells by Flores *et al* (2000) [27]. The notably greater expression of p53 in the suprabasal region of the untreated episomal raft is likely to reflect the consequences of HPV 16 infection, particularly differences in oncogene expression. Cells containing episomal genomes maintain transcriptional control of E6/E7 activity throughout the epithelium and subsequently cells are more likely to retain a greater ability to respond to viral interference allowing the expression of larger amounts of p53. It is possible that the p53 detected during these studies may represent non-active E7-bound protein. HPV 16 E7 is known to cause the stabilisation and subsequent inactivation of p53 without altering the wild type conformation or directly inhibiting the proteasome [27,138,266,434] providing a mechanism for the accumulation of non-active p53. The stabilisation of p53 by E7 is likely to be particularly prevalent in cells containing integrated sequences, where higher levels of E6 and E7 are likely to increase cellular disturbance and consequently raise p53 expression, whilst also providing additional E6 for p53 degradation and E7 for p53 stabilisation.

Treatment with 2nM LMB (72h) led to a small increase in p53 expression within the episomal E_{63} raft, but little change in the I_{22} raft. The interaction of p53 with HPV 16 E6 is likely to play an important role in p53 regulation in the presence of LMB. The E6-mediated degradation of p53 by nuclear proteasomes [179,263,431] leaves p53 vulnerable to E6-mediated degradation in the presence of LMB (section 5.4). However, free p53 accumulating in the nucleus in response to LMB may be in the inactive monomeric or active tetrameric form (section 1.3.1). Although the inactive form may be degraded by the nuclear proteasomes, activated p53 has been shown to display reduced binding to Mdm2 due to post-activation

modifications [171], leading to a reduction in Mdm2-associated proteasomal degradation (section 1.3.1). If this activated p53 also remains non-degraded by E6-mediated pathways, then it potentially provides a pool of transcriptionally active p53 to facilitate the induction of apoptosis. As predicted by their viral genome status, the I_{22} derivative has been shown to express increased levels of E6 compared with the E_{63} cells [403]. Therefore, the lower levels of p53 detected in the integrated raft after LMB treatment are likely influenced by the greater nuclear E6-mediated degradation of p53.

In the absence of LMB both rafts exhibited large amounts of p21 staining suggesting the presence of a substantial innate p21 response in the W12 derivatives, confirming the pattern previously reported in the same cells by Shai *et al* (2007) [403]. The presence of viral infection with its abnormal DNA synthesis within the suprabasal region is likely to activate the cellular p21 response. Both HPV E6 and E7 are known to inhibit p21 function, with E7 linked with increased expression p21 in previous raft models [27]. Some of the p21 detected may represent stabilised, non-active forms through short or long term interaction with the viral proteins as occurs with E7-stabilised p53 [203,239]. Although the virus must counteract the cell cycle regulatory role of p21, it has been suggested that during the productive phase of the viral life-cycle E7 may actually utilises the p21 protein to act as a scaffold to facilitating the assembly of cyclin–cyclin-dependent kinase complexes. This causes the cells of the mid to upper layers to remain replication competent aiding the viral life-cycle [27]. Therefore, it is possible that some of the staining located in the upper regions of the raft may also represent virally sanctioned presence of p21. A proportion of the p21 staining detected within the E_{63} raft may represent the novel p21 form highlighted during the western analysis (section 6.3.4 and 6.4.3) and therefore its functionality is uncertain.

Treatment with 50nM LMB led to a decrease in levels of p21 in both the rafts, suggesting an LMB induced effect. Although treatment with LMB was associated with a decrease in p21 expression, the induction of apoptosis within these rafts (section 5.3.3) and the early p21 response during the time course, suggest that this p21 staining may reflect the progression of these cells to a post-p21 stage of the pro-apoptotic pathway.

6.4.2. Time Course Expression of p53 and p21 in the W12 Derivatives in Response to LMB

Over the 48h time course both p53 and p21 were found to be expressed in the untreated W12 derivatives and E7 transduced cells; however, p21 could not be detected in the untreated E6/E7 transduced PHKs.

As discussed above (section 6.4.1) background expression of p53 is likely to be highly influenced by the presence of HPV 16, in particular by the levels of oncogenic E6 and E7 which are known to interact with p53 (section 1.5.1). The high expression of p53 by the E7 transduced PHKs indicates that greater levels of E7 may be associated with increased p53; however, most of this protein is likely to be bound by E7 therefore stabilised and transcriptionally inactive [138,266]. The presence of particularly high background p53 in the I_{61} derivative over time suggests that these cells may contain particularly high levels of the E7 protein, leading to the accumulation of bound p53. PHKs transduced with E6 and E7 displayed much lower baseline p53 expression reflecting efficient E6-mediated degradation.

The untreated type 2 integrated W12 derivatives I_{31} and I_{61}, by 48hs, displayed substantially greater levels of p21 than the remaining cell lines. This expression appears to be related to the viral genome status and is likely to reflect differences in E6 and E7 expression. In the presence of LMB this high expression of p21 was lost, although the increased levels of

apoptosis presented in section 5.3.4 suggest this decrease probably reflects a loss of cells rather than a decrease in expression.

The W12 derivatives and transduced PHKs showed increased expression of p53 after treatment with 2nM LMB, although in most cases the response was low level and short lived. As in the untreated samples, the response to LMB is likely to have been substantially influenced by variable expression of E6 and E7 between the different cell lines. The high levels of E7 in the transduced PHKs would lead to the accumulation of substantially greater levels of p53 when nuclear export was inhibited. As E7-bound p53 is reportedly capable of nuclear export [138], the trapped p53 is likely to represent a mixed population of both free and E7-bound protein. Although degradation of p53 is not effected by E7 binding [138], it is unclear whether transcriptional activity is effected, with Eichen *et al* (2002) [138] showing a notable decrease in p53 transcriptional activity. Therefore, during LMB-induced nuclear accumulation E7-bound p53 has a reduced ability to activate p53-response genes including those required for the induction of apoptosis. In high E7 expressing cells, although reduced, the cumulative transcriptional potential of the free and E7-associated p53 may provide sufficient transcriptional activity to overcome the weaker apoptotic resistance. Within the E7 transduced PHKs, this mechanism may have facilitated the re-activation of the act-casp-3 response as seen in chapter 5, although further investigation is required.

The efficiency of the E6 anti-p53 response has previously been illustrated by the extremely low levels of p53 detected in E6-transduced PHKs in the presence or absence of LMB [374]. This effect is further demonstrated in both the current and previous studies [374] by the substantial decrease in the level and duration of p53 response in both the treated and untreated E6/E7 transduced PHKs compared with E7 alone. In the presence of LMB the E6 protein

appears to maintain its ability to mediate the degradation of p53 by utilising nuclear proteasomes, as indicated by the maintenance of low levels of p53 in the treated E6/E7 cells. The minimal p53 response by the E6/E7 transduced cells, particularly at the 48h time point may represent a saturation of either the E6, E7 or proteosome components allowing the persistence of a small pool of either free or E7-bound p53. In addition, the lack of a p53 response of E6/E7 cells also suggests that E6 is able to bypass the stabilisation of p53 apparent in the E7 transduced cells leading to degradation of the protein. This is possibly achieved via the E6-mediated ubiquitination of p53 even in the presence of the E7 protein, leading to degradation of the p53 protein as suggested by Eichten *et al* (2002) [138]. Any interplay between E6 and E7 in controlling cellular p53 expression is likely to aid viral survival. During a natural infection E7 may bind p53 preventing possible stress related activity until the E6-mediated degradation occurs, thus helping to inhibit the initiation of cell cycle arrest or apoptosis.

The cell cycle is controlled by numerous cellular proteins including p53, p21 and pRb, which act together to block the unwanted progression of cells through cycle checkpoints. Manipulation of the cell cycle by HPV is primarily controlled by the E7 protein, with the presence of E6 increasing this cell cycle control particularly at the G_2/M checkpoint [171,267]. Although both p21 and pRb are targeted by the virus, the main effect appears to be aimed at the pRb stage of the pathway downstream of p21, as shown in figure 1.9. Any viral regulation of the cell cycle involving p21 appears to be supplementary to the main viral mechanisms involving the manipulation of proteins such as pRb. In addition to any cell cycle effects, the interaction of E7 with p21 is also likely to have other pro-viral functions such as blocking the interaction of p21 with proteins such as PCNA which decreases DNA replication [27,209] (section 1.5.2), thus helping to maintain the replication competent environment. The potency of E6 in the E6/E7 transduced PHKs appears to be sufficient to produce upstream

interference that in the absence of LMB is able to totally block p21 expression. The lack of p21 expression could reflect E6 directly targeting p21 and/or the consequence of efficient upstream degradation of p53 leading to attenuated p53-dependent p21 transcription. Due to the absence of E6 in E7 only expressing cells such as the transduced PHKs, a greater checkpoint function is reported to be retained which may contribute to the limited life span of E7 transduced cells in culture [268].

The initial rise in p21 expression by the cells in response to LMB is possibly due to the prevention of p21 degradation by nuclear accumulation or maintained p21 activation, causing an effect on nuclear exported of various proteins in a HPV dependent or independent manner. Although p21 acts as an early event in the p53 pathway it can also be activated in a p53-independent manner [213]. Therefore, some of the p21 response within these cells may represent p53-independent induction of p21. Indeed the p53-dependency of the response may differ in the presence or absence of LMB. However, the p53-dependence of the p21 response detected during theses studies cannot be determined from this data partly because of the interaction of HPV with both the p53 and p21 pathways. The pattern of p53 and p21 detected during these time studies is likely also to have been highly influenced by the level of apoptosis. From 24h onwards in the E7 transduced PHKs and 36h in the remaining cell lines, the expression of both proteins would naturally decrease as increasing numbers of cells become apoptotic.

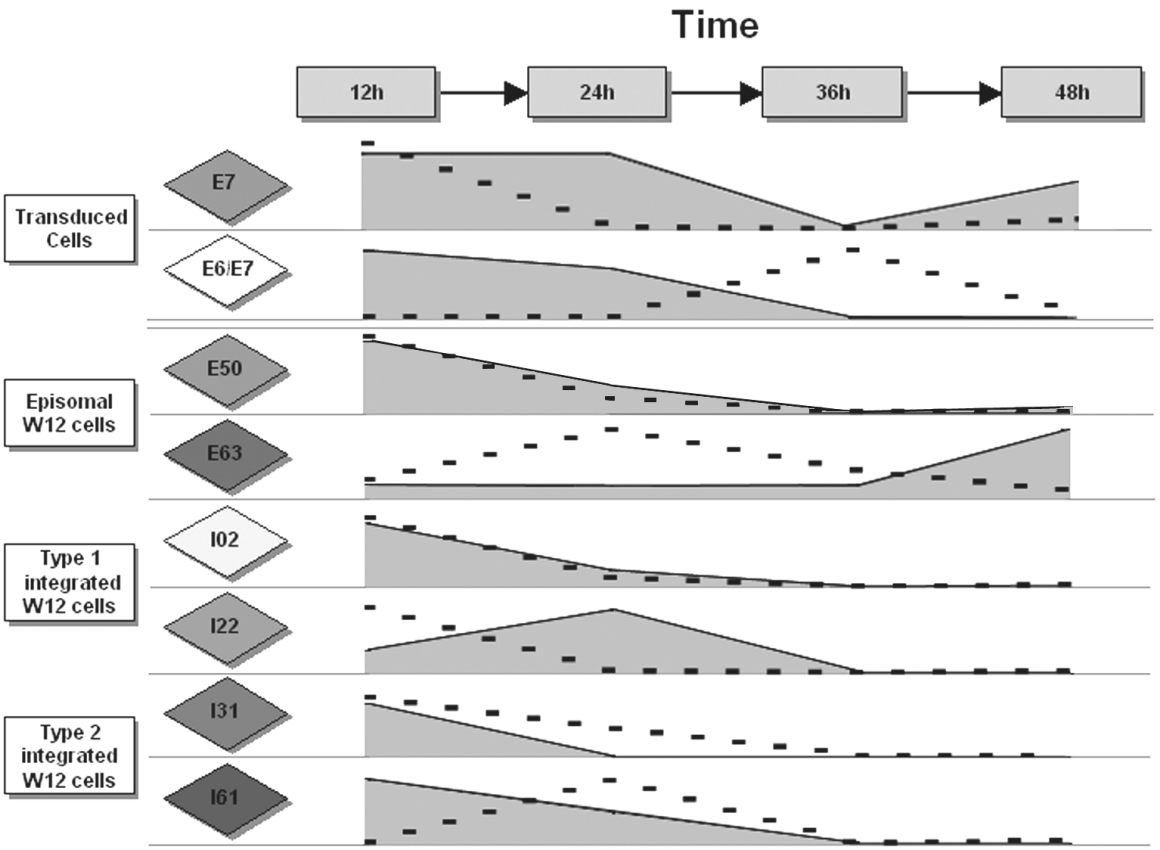

Figure 6.7: The LMB-induced expression of the cell regulators p53 and p21 varies amongst the transduced PHKs and the W12 derivatives. The dotted lines represent the p21 levels with the shaded areas indicating p53 expression after 2nM LMB over a 48h time course.

Unlike the apoptotic markers (figure 5.8, chapter 5), the expression patterns of p53 and p21 over the 48h time course do not appear to correlate with the genome status of the cells (figure 6.7). This suggests that the p53 and p21 expression patterns within the W12 derivatives and transduced lines appear to be influenced by differences other than integration type alone; this may include the clonal nature of the cells and direct or indirect consequences of viral infection.

Most of the cell lines appeared to show a pulse of both p53 and p21 after 12h of LMB treatment. However, as shown in figure 6.7 some deviation from this pattern was apparent with p53 expression delayed in I_{22} and E_{63}, and p21 expression delayed in E_{63}, I_{61}, and E6/E7. The presence of both the E6/E7 and the whole viral genome is likely to influence the p53 and

p21 responses to LMB. This is likely to be primarily achieved by direct interaction of E6 and E7 with these regulatory proteins. However, variations in the direct interaction of other viral proteins and the differences in the cellular responses may also influence the expression of p53 and p21 (see section 1.5). For example, higher E6 expression by a cell line may cause greater inhibition of the DNA repair protein XRCC1 [316], leading to the increased cellular stress signalling including p53 and p21.

The extreme delay in p53 expression by the E_{63} derivative may be a consequence of the late induction of apoptosis reported in these cells in chapter 5, allowing the accumulation of greater amounts of p53 in these cells than in those where cells are destroyed more rapidly (integrated and transduced cell lines) or where levels of apoptosis appear greater (E_{50}). However, other factors such as possible integrated sequences and the presence of the p21 doublet may also heavily influence this response.

Although the E7 and E6/E7 transduced PHKs provide a useful model for the influence of the E6 and E7 oncogenes on the pattern of p53 and p21, the expression within the W12 derivatives is influenced by a more complex viral environment, where E6 and E7 are expressed in the presence of the whole HPV 16 genome in a regulated (episomal) and unregulated (integrated) manner; however, some contributions of E6 and E7 can be clearly identified. The E7 transduced PHKs expressed high levels of p53 as did the untreated W12 derivative I_{61}, which has previously been reported to express high levels of E7 [119]. In I_{61} derivative, the presence of a maintained rise in untreated p53 levels appears to mirror the expression in the E6/E7 transduced PHKs, supporting the previously reported presence of high levels of both oncoproteins within this W12 derivative [119,403]. A possible role for E7 in the p53 response is also suggested by the early and largely maintained expression of p53 in

both the E7 and E6/E7 transduced lines, a similar pattern to that present in some of the W12 derivatives particularly I_{61}. Also a delay was apparent in the p21 response of the E6/E7 transduced PHKs which was absent in the E7 transduced line, suggesting that high E6 expression may delay the p21 response. A similar pattern of p21 expression is also apparent in the E_{63} and I_{61} derivatives; however, the doublet p21 in the E_{63} line may be responsible for the effect present in this episomal line. The results for the type 2 integrated derivative I_{61} clearly suggest that both E6 and E7 play important roles in both untreated and LMB treated cells, probably due to increased expression as a consequence of integration.

6.4.3. p21 Doublet Formation in W12E_{63}

Both p21 and p53 expression in the E_{63} derivative proved different from the remaining cell lines. The most striking difference was the expression of a doublet form of p21 apparent during western blotting. The use of both C-terminal and internal p21 antibodies suggests that the novel band may be formed by the alteration or more likely splicing of the p21 sequence in the N-terminal portion of the protein with alteration in the epitope of the internally located antibody preventing association. This event has produced a novel band estimated to be between 1.2-2.5kDa smaller than the native form. The size of the band shift between the native and novel forms suggests that it is unlikely that all 77 amino acids located from the internal antibody epitope to the N-terminus have been lost, as a larger band shift of approximately 8.7kDa would be present if the whole of this region was absent (see appendix C2 for N-terminal sequence details). The expression of the smaller novel protein was accompanied by the wild type 21kDa protein suggesting there may be variations in the RNA sequence/splicing or possible post-translational protein modifications. It remains unclear if the lower band retains function; the majority of the LMB-dependent or independent induction of p21 in E_{63} appears to have occurred in the upper p21 band, suggesting that some functional

differences may be present between the two forms. The amino terminal domain of p21 is known to be required for inhibition of the cell cycle control cyclin/cdk complex [204]. It is therefore possible that the loss of relatively few amino acids from this region of the protein may be sufficient to prevent or attenuate this function leading to abnormal cell cycle progression. The presence of the doublet form of p21 within E_{63} may influence the behaviour of these cells in the presence or absence of LMB, including the expression of p53 and the apoptotic markers act-casp-3 and M30 (chapter 5).

The data presented indicates that there is no clear association between delayed apoptosis and increased expression of p21, suggesting that prolonged induction of p21 is unlikely to be the cause of the delay in apoptosis displayed in chapter 5. It also remains unclear if the short induction of p53 presented in these studies would be sufficient to cause the induction of apoptosis presented in chapters 4 and 5, with the data indicating no direct correlation between the cell lines displaying higher or more rapid p53 expression and those shown to undergo a more rapid or greater apoptotic response. It is possible that the early induction of p53 may still contribute to the apoptotic effect, with the response delayed by alterations in the downstream transmission of the proapoptotic signal.

Chapter 7: The Contribution of p53 to LMB-Induced Apoptosis

7.1. Introduction

LMB-induced apoptosis of the W12 derivatives has been shown to be associated with increased levels of both p53 and p21 (chapters 5 and 6). However, the role of p53 in LMB-induced apoptosis of the W12 derivatives remains unclear. The large range of possible cargoes utilising the REV type nuclear export pore, means that p53 is just one of a huge range of proteins affected by the LMB-induced inhibition of CRM1 mediated export (section 1.7.1). Therefore, the induction of apoptosis could be induced by disrupting of one or more of these proteins, which may or may not include p53. In the presence of a HPV infection the activities of the virus itself may also influence the mechanisms by which LMB induces apoptosis. The actions of both HPV 16 E6 and E7 mean that the functionality of nuclear accumulated p53 and its potential role in the induction of apoptosis is difficult to discern. These studies aimed to clarify the role of p53 in LMB-induced apoptosis by assessing the effect of a dominant negative p53 on LMB-induced apoptosis.

7.2. Methods

Retroviral packaging cells were transfected with the dominant negative (Dnp53) expression construct (53R248W) or empty pBabe-puro (section 2.7.3). This puromycin resistant construct was utilised due the existing neomycin resistance of the pLXSN vector within the E7 and E6/E7 transduced PHKs. The retroviral supernatants from the Dnp53 transfected packaging cells were used to transduce E7 and E6/E7 expressing PHK lines, W12 derivatives E_{50}, I_{22} and I_{31}, and the osteosarcoma cell line U2OS, as described in section 2.8. The successful transfer of the Dnp53 construct to all the relevant transduced cell lines was confirmed by PCR analysis, as described in section 2.16.4. The ability of the dominant

negative construct to reduce p53 DNA binding was assessed by luciferase reporter assay of U2OS cells (section 2.19), with the LMB sensitivity also assessed by western analysis (section 2.12.7.6). The sensitivity of the Dnp53 transduced W12 and PHK cells lines to LMB treatment was assessed by western blotting, as described in section 2.12.7.7.

7.3. Results

The dominant negative p53 R248W (Dnp53R248W, Dnp53) [412] contains a point mutation at codon 248, where the arginine is replaced by tryptophan [435]. In the wild type p53 protein this region is associated with DNA binding, and is required for the interaction of the positively charged side chain of arginine 248 with the negatively charged components of the DNA backbone [435]. Therefore, although the overall structure of the protein remains unaffected [435], the dominant negative protein is unable to bind DNA and subsequently cannot undertake p53-dependent transcriptional activity [412]. Some p53 transcriptional activity may be retained due to the continued presence of normal p53 protein which may form wild type tetramers (section 1.3.1). However, the R248W mutant p53 and any tetramers containing it, will be unable to bind DNA and therefore transcription of p53 responsive genes is restricted [435].

7.3.1. Confirmation of the Presence of the Dnp53R248W Construct

The Dnp53R248W dominant negative construct was transduced into the E7 and E6/E7 transduced PHKs, W12 derivatives E_{50}, I_{22} and I_{31}, and the wild type p53 osteosarcoma cell line U2OS [409,410]. Although puromycin selection was applied to select for successfully transduced cells, the presence of the Dnp53 construct in the selected cells was also confirmed by PCR analysis using a forward primer located in the vector backbone (pLXSN2S) and the reverse primer located in the p53 sequence (p53A).

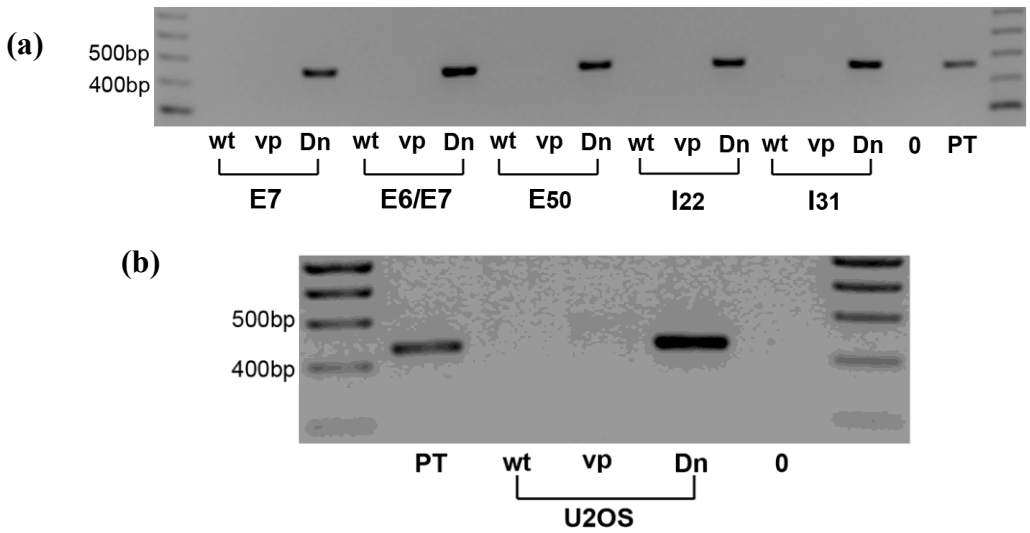

Figure 7.1: The presence of the Dnp53R248W plasmid within the transduced cells was confirmed by PCR. Amplification was undertaken on (a) PHK lines containing E7 and E6/7, W12 derivatives E_{50}, I_{22} and I_{31} and (b) the U2OS cell line. For each cell line DNA from non-Dnp53 transduced (wt), vector only (vp) and dominant negative (Dn) cell were analysed in combination with DNA from Dnp53 transfected PT67 packaging cell (PT) and a no template control (0).

The PCR analysis confirmed amplification of an appropriate 467bp band from all the Dnp53 transduced cell lines, which was absent in the wild type/pLXSN and vector only cell lines, as shown in figure 7.1. This represents the expression of similar amounts of integrated construct.

7.3.2. Decrease in p53 Dependent Transcriptional Activity in Cells Transduced with Dominant Negative p53

The ability of Dnp53R248W to reduce p53 transcriptional activity was assessed using a p53 reporter assay utilising the pSynp53 luciferase reporter construct. Initial optimisation of the assay using W12 derivatives and the E7 and E6/E7 transduced PHKs failed to detect any p53 transcriptional activity. Therefore, the osteosarcoma cell line U2OS was used as these cells are known to express wild type p53 [409,410] and grow robustly in culture. They therefore provide a good model to test the effectiveness of the p53 luciferase reporter assay. Optimisation was also undertaken on E7 expressing PHK cells to test the effectiveness of

HPV E7 anti-p53 activities as a possible mechanism for the lack of signal previously encountered in the W12 derivatives and HPV transduced PHKs. As described in section 1.3.1, p53 is normally maintained in the cell at low levels due to proteasomal degradation. However, increased expression and stabilisation of p53 occurs in response to a number of stress stimuli such as nucleotide depletion and DNA damage. Therefore, the p53 dependent transcriptional activity of these cells was assessed in the presence of minimal cellular stress (no LMB) and after the induction of a cellular stress response via the addition of 2nM LMB (12h).

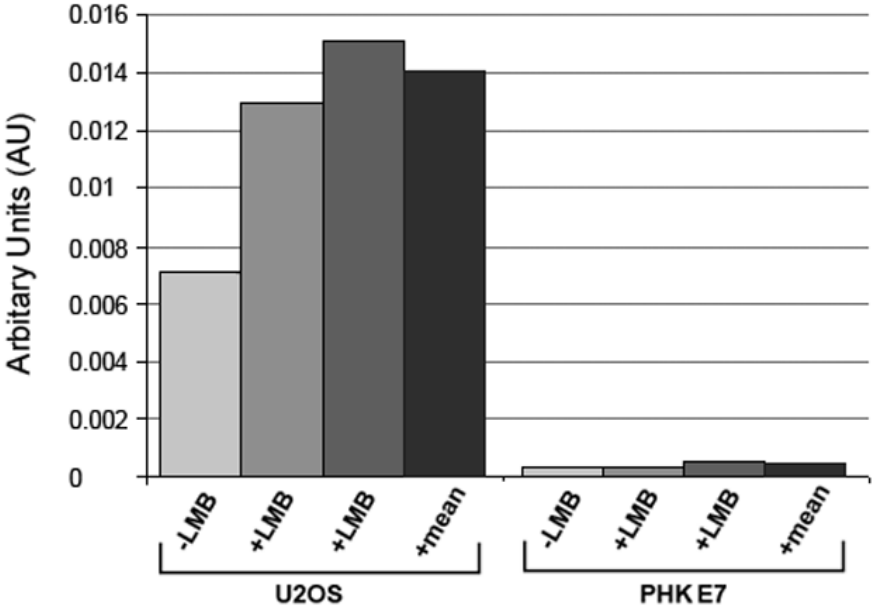

Figure 7.2: The detection of p53 dependent transcriptional activity in U2OS and E7 transduced PHKs (PHKE7). The luciferase expression of U2OS and E7 transduced cells transfected with pSynp53 and luciferase control pRL-CMV was assessed with (+) and without (-) 2nM LMB (12h).

In the absence of cellular stress the U2OS cells were shown to exhibit notable levels of p53 dependent transcriptional activity (figure 7.2), with LMB treatment (2nM, 12h) causing a notable upregulation of p53 activity with transcription increasing approximately 2-fold. However, the p53 expressed by the E7 transduced PHKs failed to show any notable p53 dependent transcriptional activity even in the presence of increased cellular stress (figure 7.2).

Previous experiments with E2 expressing U2OS and vector only controls are shown below in figure 7.3. They indicate that no induction of apoptosis could be detected in the E2 expressing or pCMV vector only U2OS cell lines following LMB treatment (figure 7.3), despite a substantial apoptotic response in the W12 derivatives similar to that previously noted in chapter 5.

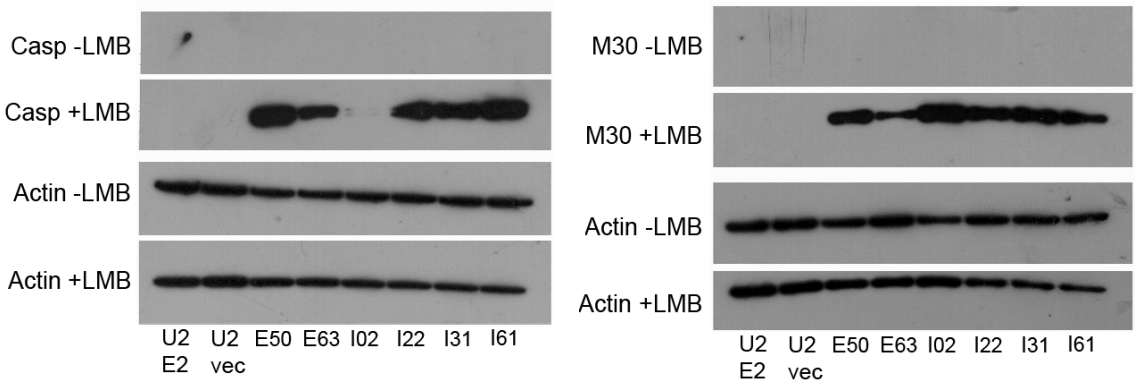

Figure 7.3: U2OS cells (U2) in the presence (U2 E2) or absence (U2 vec) of HPV 16 E2 in combination with the W12 derivatives were treated with 2nM LMB (38h). In the presence (+) or absence (-) of 2nM LMB (38h) alterations in act-casp-3 (Casp) or M30 were assessed by western blotting with β-actin utilised as a loading control.

The experiments shown above suggested that the U2OS cells would provide a suitable model in which to confirm the effectiveness of the dominant negative p53 in decreasing p53–dependent transcriptional activity. Therefore, the luciferase reporter assay was undertaken with wild type (wt), pBabe vector only (vp) and Dnp53 (Dn) transduced U2OS cell lines.

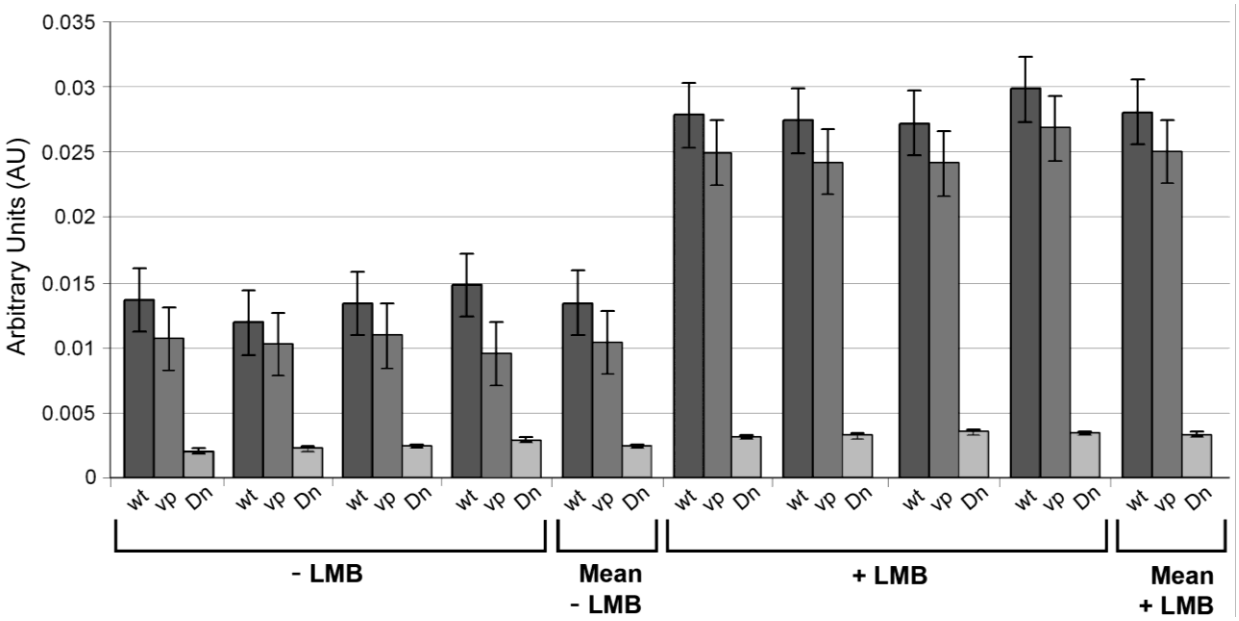

Figure 7.4: The assessment of p53 dependent transcriptional activity in Dnp53 transduced cells. Wild type (wt), vector only (vp) or Dnp53 transduced U2OS cells were transiently transfected with the p53 luciferase reporter pSynp53 and control pRL-CMV. The luciferase activity was then assessed with (+) and without (-) 2nM LMB (38h).

In the absence of LMB both the wild type and vector only U2OS cells expressed notable levels of p53 dependent transcriptional activity (figure 7.4). The presence of dominant negative p53 led to a sizeable decrease in p53 dependent transcriptional activity, reducing activity by an average at least 6 fold. Under LMB-induced stress conditions the p53 dependent transcriptional activity of the wild type and vector only U2OS cells increased substantially, representing an almost 3 fold increase in activity. However, even in the presence of LMB-induced cellular stress the cells containing the dominant negative p53 displayed only minimal increases in their p53 dependent transcriptional activity 10 fold lower than in the wild type and vector only cells (figure 7.4).

7.3.3. Effect of Dominant Negative p53 on LMB-Induced Apoptosis in HPV 16 Infected Cells

The role of p53 in LMB-induced apoptosis was assessed in the wild type, vector only and dominant negative transduced lines in the presence or absence of 2nM LMB (38h), by

examining changes in the apoptotic markers act-casp-3 and M30, as previously described in chapter 5.

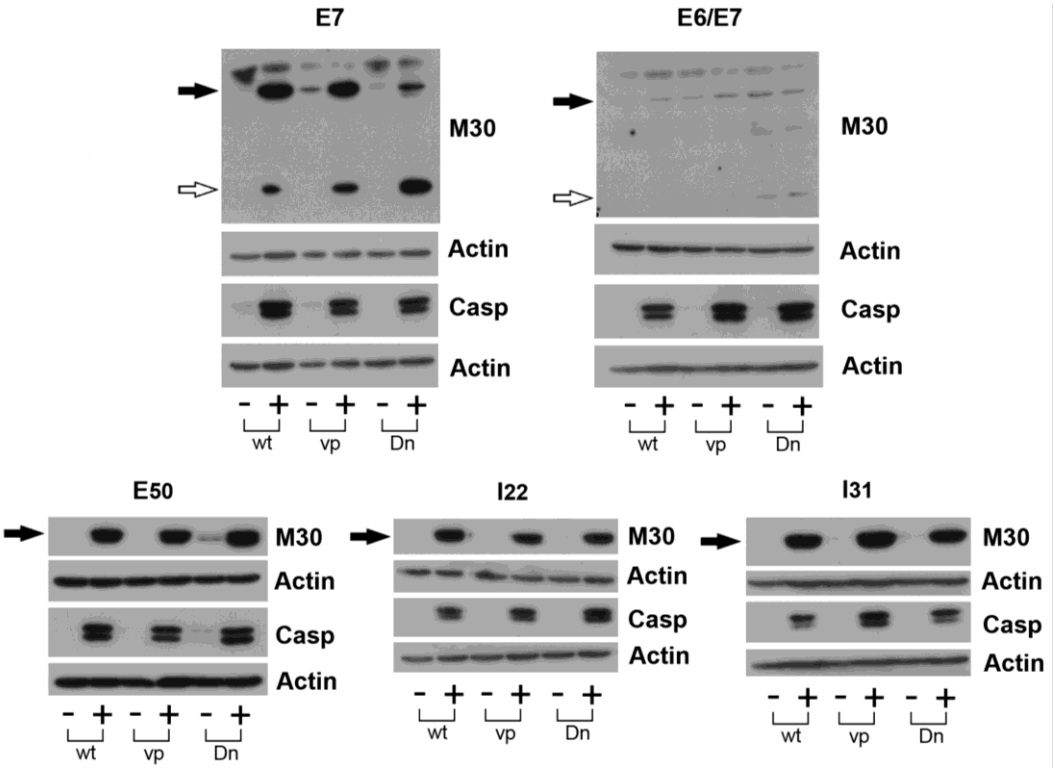

Figure 7.5: The effect of dominant negative p53 expression on LMB-induced apoptosis. The expression of act-casp-3 (Casp) and M30 in the non-Dnp53 (wt), vector only transduced (vp) and Dnp53 transduced cell lines (Dn), was assessed in the presence (+) or absence (-) of 2nM LMB (38h). The 40kDa M40 band is indicated by the filled arrow and where present the 24kDa form indicated by an empty arrow.

In the absence of LMB no notable induction of apoptosis was detected in any of the wild type, vector only or Dnp53 cells with the exception of E_{50}, where small increases in the basal activity of both act-casp-3 and M30 were detected (figure 7.5). As previously shown (chapter 5), the treatment of both W12 derivatives and transduced PHKS in the absence of Dnp53 caused a notable upregulation of both act-casp-3 and M30 (figure 7.5), with the presence of the pBabe-puro vector alone having little effect on this response. The presence of the dominant negative p53 also had little effect on the expression of either act-casp-3 or M30 in the presence of 2nM LMB (38h), indicating that no notable change in the induction of apoptosis occurred despite abrogation of the p53 response. Both the early 40kDa and late

24kDa forms of M30 were apparent in E7 and E6/E7 transduced PHKs; however, the later 24kDa form was absent in the W12 derivatives. Although LMB treatment of the Dnp53 transduced cells did not induce changes in the total M30 expression, some alteration in the pattern of early and late M30 was apparent within the E7 and E6/E7 transduced PHKs. The E7 expressing PHKs transduced with Dnp53 showed an increase in the later 24kDa form with a corresponding decrease in the 40kDa early protein in the presence of LMB (figure 7.5). The E6/E7 transduced PHKs containing Dnp53 displayed an increase in the late 24kDa form of M30 in both the presence and absence of LMB; although expression levels were particularly low as previously described (chapter 5) no detectable corresponding decrease in the 40kDa form could be detected.

7.4. Discussion

The data presented in chapters 5 and 6, combined with previous research from our own laboratory [374] and others [182,203,375], suggest that LMB-induced effects may be facilitated by the cellular regulator p53, with LMB treatment previously shown to induce increased levels in p53. In wild type PHKs [374] and normal human fibroblasts [398], LMB treatment is associated with the induction of cellular quiescence, whilst in HPV-associated cell lines LMB causes the induction of apoptosis (chapter 6) [182,203,374]. However, whether this accumulated p53 plays a role in the induction of apoptosis by LMB remains unclear. Previous results from this laboratory [374] and the data reported in chapters 5 and 6 show that, although an increase in p53 is present in response to LMB, this rise is temporally distinct from the induction of apoptosis. Therefore, the proposed induction of apoptosis by the direct perturbation of p53 nuclear export is brought into question. In addition, the general nature of CRM1-mediated nuclear export provides many possible alternative mechanisms by which LMB-induced apoptosis could be initiated within these cells.

The normal p53 dependent transcriptional activity of the U2OS cell lines was confirmed by luciferase reporter assay, suggesting a wild type p53 conformation was present as proposed by both Soni *et al* (2001)[410] and Li *et al* (2002)[409]. The p53 dependent transcriptional activity suggests that the p53 transcriptional response is likely to have remained intact despite the malignant status of these cells.

The unstressed U2OS cells showed clear evidence of p53 transcriptional activity in the absence of LMB. This activation may be slightly greater than would normally be present in an unstressed state due to the malignant nature of the cell lines and/or the possible induction of low levels of cellular stress during transfection of the p53 luciferase reporter. Treatment of the U2OS cells with 2nM LMB indicated the presence of a LMB-induced p53-dependent transcriptional response, but a failure to induce apoptosis. This suggests that the U2OS cells do not innately contain factors that would sensitise them to LMB-induced apoptosis. In addition, the presence of HPV 16 E2 alone appears insufficient to induce apoptosis in response to LMB under conditions previously shown to induce apoptosis in PHKs transduced with E7 and E6/E7 [374]. However, the failure of the E7 transduced PHKs to exhibit a significant p53 dependent transcriptional activity during the luciferase assay implies that this response in these cells is severely impaired. This is probably due to the interaction of HPV E7 with the p53 protein, causing the formation of a transcriptionally inactive complex. Therefore, any contribution of p53 to LMB-induced apoptosis is likely to be independent of its transcriptional activity in this setting.

As previously reported by Shamanin and Androphy (2004) [412], even in the presence of a dominant negative p53 mutant the protein does retain some p53 dependent transcriptional

activity, although at greatly reduced level. This diminished response is likely to be a consequence of the native p53 whose expression remains unaffected by the dominant negative protein. In the presence of this mixed population of native and mutant p53, some native tetramers are likely to form facilitating limited p53-dependent transcriptional activity. LMB treatment of the Dnp53 U2OS cells was associated with a slight increase in p53 dependent transcriptional activity likely to represent an increase in native p53 tetramer formation. This may be due to either an increase in p53 expression or an increase propensity for tetramer formation in response to LMB.

LMB-induced upregulation of p53 dependent transcriptional activity in the wild type and vector only transduced U2OS cells is likely to represent the cumulative effects of a number of p53 activation pathways (section 1.3.1). When exposed to cellular stress the cells not only raise the levels of *de novo* protein by upregulation of p53 transcription [176], but also alter the status of existing protein leading to the stabilisation and nuclear accumulation of p53. Upon activation existing p53 is actively imported into the nucleus [179,195], and forms into tetramers further aiding nuclear accumulation by masking the p53 nuclear export signal. In addition, p53 degradation is reduced by relocation of the p53 agonist Mdm2 to an alternative nuclear region [171] (section 1.3.1) and the inhibition of Mdm2 mediated degradation by N-terminal phosphorylation of the accumulated p53 [138,171].

The presence of Dnp53 had no effect on LMB-induced expression of either act-casp-3 or M30 in the W12 derivatives; this suggests that the apoptotic response of these cells is not mediated by p53-dependent transcription. Interestingly, the presence of the dominant negative p53 in the LMB treated E7 transduced PHKs and the treated and untreated E6/E7 expressing cells led to an altered pattern of M30 expression. In both cases an increase in the later 24kDa

CK18 cleavage product was seen, representing a more rapid progression of apoptosis. This suggests that in the absence of the complete HPV 16 viral genome in either episomal or integrated form, the interaction of E6 and E7 with the native p53 slows the progression of apoptosis. However, any effect on the rate of apoptosis in the transduced lines does not appear to alter the overall induction of apoptosis, as shown by the unchanged expression of act-casp-3 and total M30.

Even in the absence of p53-dependent transcription, the p53 protein may still play a role in the initiation of apoptosis by LMB. Indeed in normal cells it is likely that the transcription-dependent and independent p53 pathways work together to respond to cellular stress [222]. The transcription independent mechanisms of p53 include the release of pro-apoptotic mitochondrial products [170] by the inhibition of mitochondrial anti-apoptotic proteins Bcl-XL and Bcl-2, and activation of the pro-apoptotic protein BAK by a truncated form of the activated p53 protein [251].

These data suggest that the induction of apoptosis may be occurring via p53-independent mechanisms. A possible candidate for this role is the p53 family member p73 [387] which like p53, plays a role in the regulation of both the cell cycle and apoptosis [436]. p73 has been shown to be over expressed in human tumours including cervical neoplasia [437], but is rarely found to be mutated unlike its family member p53 [438-440] (reviewed in ref [169]). The p53 family, including the additional member p63, share a highly conserved amino acid sequence and are all able to activate p53 response elements [387,441,442] leading to the transcription of genes normally associated with p53 [443,444]. Indeed studies have suggested that both p63 and p73 may be required for p53-dependent apoptosis [445]. Although evidence suggests that degradation of p73 can be mediated by ubiquitin-dependent or independent mechanisms, in an LMB-dependent manner (table 1.2), the pathways employed appear distinct from those used

by p53 [169,446,447]. However, the apoptotic stimuli to which p73 responds appears to be distinct from those of p53 [169,448].

In human neuroblastoma cells and normal human fibroblasts treatment with LMB has been associated with a p53-dependent cytotoxicity, which displays a minimal p73 response [398]. However, the data presented in this chapter suggests that in the W12 derivatives and PHKs containing HPV E7 or E6/E7, LMB-induced apoptosis is not dependent on p53 and, therefore, in this context p73 may provide an alternative mechanism for the mediation of apoptosis. In HPV 16 infected cells, significant upregulation of BAX and p73 in the absence of notable p53 expression has been shown to induce apoptosis in response to hydrogen peroxide [436]. The subsequent induction of apoptosis mediated by the mitochondrial pathway was shown to be associated with increased expression of the initiator caspase-9 and the executioner caspase-3 [436], this act-casp-3 association is reminiscent of that present in response to LMB during the current studies (chapter 5). The occurrence of a p73 response in the absence of p53 induction suggests that p73 is able to evade the virally derived mechanisms used to control the expression of p53, although it remains unclear if direct viral regulation of p73 occurs in HPV infected cells. Studies on squamous cell carcinomas of the oesophagus have suggested that a complex interaction is present between the virus, p53 and p73 indicating that anti-p73 virus mechanisms may exist. This alternative mechanism for the mediation of apoptosis provides a possible explanation for the interaction of the virus at several different of stages of the relevant regulatory and apoptotic pathways, and could be interpreted as an attempt by the virus to close loopholes by which the cell may induce cell cycle arrest or apoptosis.

It remains unclear if the initiation of apoptosis could be achieved by the disruption of p73 alone. Although p73 is known to utilise the REV type nuclear pore (section 1.6.1-2 and table

1.2), treatment with LMB also affects numerous other proteins which are directly or indirectly dependent on CRM1-mediated export. The data presented in these studies (chapter 5) combined with previous studies from this laboratory [374] suggests that the presence of HPV 16 E7 alone is sufficient to induce the pro-apoptotic effects of LMB. Sensitisation to LMB is therefore likely to be a response to the disruption of an E7 susceptible process, with the effect decreased in the presence of both E6 and E7 by either E6-mediated attenuation or a reduction in the levels of E7 protein. p73 appears resistant to the effects of E7 [449] and although unable to degrade the protein it is uncertain whether E6 can inhibit the transcriptional activity of p73 [450]. Therefore, it seems unlikely that direct disruption of p73 trafficking is initiating LMB-induced apoptosis. The apoptotic trigger is likely to originate from the disruption of one or more of the alternative E7-sensitive CRM1-exportable proteins, subsequently leading to the activation of the p73 regulated apoptotic pathway.

The data presented in this chapter suggest that the LMB-induced apoptosis in W12 derivatives, and E7 or E6/E7 transduced PHKs is unlikely to be a p53-dependent process. The rise in p53 levels in LMB treated cells does not appear to contribute to the induction of apoptosis via p53-dependent transcriptional mechanisms, although p53 may contribute to the effect in a transcription-independent manner. However, it appears likely that LMB-induced apoptosis in these cells is mediated primarily by an alternative cell regulator such as the p73 in response to an E7-sensitive trigger.

Chapter 8: Conclusions and Further Studies

8.1. Conclusions

The nuclear export inhibitor leptomycin B (LMB) has previously been shown to induce apoptosis in HPV-infected cancer cell lines [182,203] and HPV 16 E6, E7 and E6/E7 transduced primary human keratinocytes [374]. This LMB-induced effect has been associated with an increase in the detectable levels of p53, providing a possible mechanism for the induction of cell death. However, increased levels of apoptosis in response to LMB have also been demonstrated in other cells such as human leukaemia cell line U937 [399], prostate epithelial cell line LNCaP, [375] and cells expressing the abnormal BCR-ABL fusion protein [400]. In these cases, the primary cause of the sensitivity to LMB is not viral infection, but carcinogenic transformation or the presence of abnormal gene translocations. The common link between these cases of increased LMB sensitivity is the existence of considerable alterations in vital cell regulatory systems, which appear to be sufficient to alter the behaviour of the cells in response to LMB-induced inhibition of nuclear export.

The overall aim of this project was to assess the effects of LMB on cells containing the whole HPV 16 genome in either episomal or integrated forms, with particular interest in the induction of apoptosis by LMB and the impact of HPV 16 infection on this process. The episomal and integrated derivatives of the W12 cell line provided a useful model for the further study of HPV-associated disease, allowing investigation of the effects of HPV integration on the LMB response.

Chapter 3: The Status of HPV 16 in W12 Cells Containing Episomal and Integrated Viral Genomes

1) The genome status of the episomal W12 episomal derivatives was confirmed, in combination with viral genomic differences associated with type 1 and 2 integrated genomes.
2) As predicted by their integrated status, W12 cells containing both types of HPV integration failed to produce a detectable E2 protein, despite the apparent amplification and transcription of the complete E2 ORF from the type 2 integrants.
3) The transcription and subsequent splicing of the HPV 16 E6/E7 transcript was detected in all the W12 derivatives, with E6*I dominant throughout. The pattern of splicing present in PHKs transduced with E6/E7 suggests that, although the ability to splice the full length mRNA may be innate to the transcript, but the presence of the whole viral genome appears to regulate the pattern of splicing activity.
4) The viral genome status of the W12 derivatives described in these studies is likely to have consequences for the interaction of the virus with the host cell systems and the sensitivity of the cells to LMB.

Chapter 4: Alterations in Morphology and Colony Survival in Response to Leptomycin B

1) When grown in raft culture the W12 derivatives showed variation in epithelial structure between those containing episomal and integrated HPV. Episomal rafts appeared thicker, with greater amounts of abnormal structure and vacuolation, while rafts formed by cells containing integrated HPV formed a more organised structure.
2) Treatment with LMB induced morphological changes in the W12 derivatives grown in both monolayer and raft culture. In both models, the LMB response was characterised by

a loss of cells in combination with apparently apoptotic morphology. Although levels of LMB-induced damage appeared greater in the episomal raft, no definitive differences between episomal and integrated lines could be established in monolayer culture.

3) W12 derivatives and E7 transduced PHKs displayed no colony forming ability at concentrations greater than 2nM LMB (40h). However, the HPV-associated cancer cell lines successfully formed colonies after treatment with up to 100nM LMB (40h). The W12 derivatives containing integrated HPV displayed greater colony survival than their episomal counterparts, although the greatest colony formation was present in the primary keratinocytes expressing only HPV E7. This suggests that, although the presence of E7 has previously been shown to sensitise cells to LMB-induced apoptosis in the current and previous studies [374], its presence may in fact be beneficial to the post-treatment survival of HPV infected cells.

Chapter 5: Leptomycin B Induces Apoptosis in Cells Containing the Whole HPV 16 Genome

1) In the absence of LMB, both monolayer and rafted W12 derivatives displayed greater levels of innate apoptosis than previously reported for E7 or E6/E7 transduced PHKs [374]. These high levels of innate apoptosis are likely to be at least in part due to the induction of virally mediated pro-apoptotic mechanisms which may sensitise cells to undergo apoptosis in response to LMB. In the raft model this pro-apoptotic response appeared particularly strong in those cells containing episomal HPV; this may be a response to the expression of E2 which is known to have pro-apoptotic function.
2) LMB treatment was associated with upregulation of the apoptotic markers activated caspase-3 and M30 in both monolayer and rafted cells. Variations in expression between

the different HPV-associated cell lines were apparent and are likely to reflect the impact of the viral genome and the clonal nature of the derivatives.

3) The viral genome status of the cells appears to influence both the temporal and the cumulative pattern of act-casp-3 and M30 expression, but not necessarily the levels of these markers. E7 alone is associated with a more rapid induction of peak apoptosis and a greater discrepancy between the two markers. However, the presence of E6 causes a delay in reaching peak apoptosis and a temporal separation between the two markers. Episomal HPV was associated with a slow induction of apoptosis with little difference between the markers; viral integration induced more rapid apoptosis with integration type affecting the expression pattern of markers. Cells containing type 2 integrants displayed concurrent expression both markers, whilst cells containing type 1 integrants showed a delay in reaching peak levels of act-casp-3.
4) High levels of E7 protein in the transduced PHKs and I_{61} derivative appeared to be associated with greater expression of act-casp-3 as apposed to M30 in the remainder of the cell lines. This is suggestive of a possible relationship between E7, act-casp-3 and LMB in the induction of apoptosis.

Chapter 6: The Expression of p53 and p21 in Response to LMB Treatment

1) High innate expression of both p53 and p21 was present in the raft cultures of the cells containing episomal and integrated HPV. The pattern of expression of these regulatory proteins varied over the raft suggesting alterations in behaviour throughout the raft structure. In response to LMB the levels of p53 showed little alteration, whilst p21 appeared to decrease.
2) In monolayer W12 cultures both p53 and p21 were expressed in the absence of LMB and displayed particularly high levels of innate p53. This innate response is likely to be

greatly influence by the interplay between E6 and E7, with stabilisation of p53 by E7 balanced by E6-mediated degradation, as illustrated in the differences between E7 and E6/E7 transduced PHKs.

3) A novel p21 band forming a doublet with the native form was detected in the E_{63} derivative. This smaller protein is likely to be produced by splicing within the central/ N-terminal region of the protein. It remains unclear if the novel protein retains any functional properties, although the reduced responsiveness to LMB treatment and the probable disruption of the cyclin/cdk inhibitory function may indicate some loss of function is likely to have occurred.
4) An increase in p53 and p21 expression in response to LMB treatment was induced in both the transduced PHKs and W12 derivatives. In the majority of cells, both p21 and p53 were expressed rapidly after only 12h of treatment.
5) It remains unclear if the rise in p53 levels at the 12h time point would be sufficient to elicit the apoptotic response shown in chapters 4 and 5. The similarity of the p53 response suggests that if the p53 is in any way associated with induction of apoptosis, then other clonal or virally related factors must also influence the response, leading to the variations in apoptosis shown during these studies.

Chapter 7: The Contribution of p53 to LMB-Induced Apoptosis

1) Notable levels of transcriptionally active p53 could not be detected in E7 transduced PHKs, even in the presence of LMB-induced stress. This suggests that in these cells the majority of the p53 is bound to E7 in a transcriptionally inactive state.
2) Despite its malignant nature, the U2OS cell line expressed protein capable of p53 dependent transcriptional activity, whose potential transcriptional activity is increased in response to LMB. The presence of the dominant negative p53 caused a substantial

decrease in luciferase production confirming the ability of the Dnp53 construct to inhibit p53 dependent transcription from a synthetic reporter.

3) The induction of apoptosis by LMB did not decrease in response to the dominant negative p53 in the W12 derivatives and E7 or E6/E7 transduced PHKs. However, the transduced cells did display an alteration in the rate of apoptosis in the presence of the dominant negative protein with increasing levels of the later form of the M30 neoepitope.
4) The induction of apoptosis by LMB does not appear to be dependent on the presence of transcriptionally active p53. It is therefore likely that the effects of LMB are mediated and/or induced via alternative pathways.
5) The p53 family member p73 is a possible candidate for the mediation of LMB-induced apoptosis. However, due to the promiscuous nature of CRM1-mediated export, the actual induction of apoptotic signalling may be a reaction to the direct or indirect disruption of numerous different proteins. The apoptotic response of the E7 transduced PHKs suggests that the effects of LMB are likely to be induced by disruption of an E7 sensitive protein.

Clinical Relevance

LMB has been proposed as a potential therapeutic for the treatment of HPV-associated cervical neoplasia. The W12 model of episomal and integrated cells, in combination with the oncogene-transduced PHKs, provides a model of the effects of LMB and should therefore contribute to the future therapeutic use of LMB. These studies show that the status of the viral genome, with its subsequent impact on oncogene expression, will influence the way in which HPV infected lesions respond to LMB. Therefore in order to attain a successful clinical outcome, variations in treatment schedule will be required.

Cells containing episomal HPV 16 appeared to undergo less rapid induction of LMB-induced apoptosis compared with their integrated counterparts. Therefore, early pre-integration lesions will likely require more prolonged or higher dosage treatment with LMB to attain the same clinical outcome. It appears that lesions expressing high levels of E6 may be associated with decreased effectiveness of LMB. Conversely increased levels of E7 apparently sensitised cells to LMB; therefore, the expression of E6 and E7 are likely to prove important in influencing the LMB response of infected lesions. Interestingly, a greater resilience to higher LMB doses was seen in the HPV cancer cell lines, suggesting that malignant lesions are likely to prove more resistant to treatment.

These and previous studies have suggested that LMB is a potential therapeutic for both early and late stage lesions containing episomal or integrated HPV 16 infections. By understanding the variations in LMB-induced response during malignant progression and the mechanisms driving these effects, LMB could be utilised as an additional treatment for patients with HPV-associated anogenital lesions particularly in the presence of integrated HPV.

8.2. Further studies

Chapter 3: The Status of HPV 16 in Cells Expressing Episomal and Integrated Viral Genomes

1) The use of 2-dimensional electrophoresis would allow further investigation of the possible integrated sequences detected in the E_{63} derivative during the Southern analysis.
2) The effect of integration-associated loss of E2 and its effect on LMB sensitivity could be examined further by undertaking E2 siRNA in the episomal derivatives.

3) Examination of E6/E7 protein expression was not undertaken during these studies due to the low quality of available antibodies. In future studies the investigation of possible new antibodies and the optimisation of staining would prove very useful.

Chapter 4: Alterations in Morphology and Colony Survival in Response to Leptomycin B

1) The rafting of the remaining W12 derivatives with subsequent immunocytochemistry would allow the role of clonal differences and integration type in the presence or absence of LMB to be investigated.
2) The LMB treatment of the W12 rafts could also be undertaken over a time course. This would allow a greater understanding of the pattern of morphological and apoptotic changes throughout a differentiated epithelium, and the role of the cell regulatory response in these effects.
3) Repeating the colony survival assay on all the W12 derivatives would allow the role of integration on post-treatment survival to be assessed. The addition of wild type, E6 and E6/E7 transduced PHKs in combination with other HPV negative and positive cell lines would allow further assessment of the role of HPV in post-LMB survival.

Chapter 5: Leptomycin B Induces Apoptosis in Cells Containing the Whole HPV 16 Genome

1) An extension of the time course experiment past 48h would allow greater resolution of the response to LMB, particularly for the episomal derivatives where both apoptotic markers continued to rise up to the 48h time point.

2) The examination of alternative members of the executioner caspase family would allow the possible role of other caspases in the induction of apoptosis in the W12 derivatives and transduced PHK cells to be assessed in the presence or absence of LMB.
3) The analysis of the current apoptosis data could be combined with that from other alternative methods such as the TUNEL assay or FACS analysis to provide a more accurate measure of the induction of cell death in response to LMB. In addition, the use of a number of different methods would allow examination of any variation in the LMB-induced response during different phases of the apoptotic pathway.

Chapter 6: The Expression of p53 and p21 in Response to LMB Treatment

1) A more detailed time course experiment focusing on the response to LMB at 0-24h with subsequent analysis of p53, p21 and other potential regulatory proteins would allow a more detailed examination of the role of these proteins in both untreated and LMB treated cells.
2) The nature of the p21 doublet in the E_{63} derivative requires further examination. This could be undertaken by PCR mapping and/or protein sequencing to establish the origin and size of the novel band. The functionality of this form of p21 could be assessed using a p21-luciferase reporter construct similar to that undertaken for the dominant negative p53.

Chapter 7: The Contribution of p53 to LMB-Induced Apoptosis

1) The use of alternative dominant negative p53 constructs, containing a range of mutations and/or truncations, would confirm the absence of p53-dependence in the induction of LMB-induced apoptosis.

2) To assess if p53 may play a transcription-independent role in the LMB response, siRNA against p53 could be used in the W12 derivatives and transduced lines.
3) Western analysis for p73 within the W12 derivatives and transduced PHKs will allow an assessment of the normal expression in the presence or absence of HPV and the effect of LMB. If increased p73 was present a dominant negative p73 could be used to assess its role in the induction of apoptosis.
4) As p53 does not appear to be initiating LMB-induced apoptosis and alterations in p73 appear an unlikely stimulatory signal, a proteomic screen of E7 and LMB sensitive proteins could be undertaken.
5) The mechanisms by which HPV derived proteins are exported from the nucleus is unclear. Western analysis of LMB treated nuclear and cytoplasmic fractions using HPV specific antibodies, would allow CRM1 exported viral proteins to be identified.

References

1. Gray, L., Jolly, C. & Herrington, C.S. Human papillomaviruses and their effects on cell cycle control and apoptosis. in *Molecular Pathogenesis of Virus Infections*, Vol. 64 235 - 252 (SGM symposium, Cambridge University Press, 2005).
2. Munger, K. et al. Biological activities and molecular targets of the human papillomavirus E7 oncoprotein. *Oncogene* **20**, 7888-98 (2001).
3. Kirwan, J.M. & Herrington, C.S. Human papillomavirus and cervical cancer: where are we now? *Bjog* **108**, 1204-13 (2001).
4. zur Hausen, H. Viruses in human cancers. *Science* **254**, 1167-73 (1991).
5. Pett, M. & Coleman, N. Integration of high-risk human papillomavirus: a key event in cervical carcinogenesis? *J Pathol* **212**, 356-67 (2007).
6. Doorbar, J. Molecular biology of human papillomavirus infection and cervical cancer. *Clin Sci (Lond)* **110**, 525-41 (2006).
7. Tachezy, R. et al. Avian papillomaviruses: the parrot Psittacus erithacus papillomavirus (PePV) genome has a unique organization of the early protein region and is phylogenetically related to the chaffinch papillomavirus. *BMC Microbiol* **2**, 19 (2002).
8. Heino, P., Zhou, J. & Lambert, P.F. Interaction of the papillomavirus transcription/replication factor, E2, and the viral capsid protein, L2. *Virology* **276**, 304-14 (2000).
9. Munger, K. et al. Mechanisms of human papillomavirus-induced oncogenesis. *J Virol* **78**, 11451-60 (2004).
10. Bernard, H.U. et al. Identification and assessment of known and novel human papillomaviruses by polymerase chain reaction amplification, restriction fragment length polymorphisms, nucleotide sequence, and phylogenetic algorithms. *J Infect Dis* **170**, 1077-85 (1994).
11. Chan, S.Y. et al. Phylogenetic analysis of 48 papillomavirus types and 28 subtypes and variants: a showcase for the molecular evolution of DNA viruses. *J Virol* **66**, 5714-25 (1992).
12. Chan, S.Y., Delius, H., Halpern, A.L. & Bernard, H.U. Analysis of genomic sequences of 95 papillomavirus types: uniting typing, phylogeny, and taxonomy. *J Virol* **69**, 3074-83 (1995).
13. Heinzel, P.A. et al. Variation of human papillomavirus type 6 (HPV-6) and HPV-11 genomes sampled throughout the world. *J Clin Microbiol* **33**, 1746-54 (1995).
14. de Villiers, E.M., Fauquet, C., Broker, T.R., Bernard, H.U. & zur Hausen, H. Classification of papillomaviruses. *Virology* **324**, 17-27 (2004).
15. Trus, B.L. et al. Localization of the HPV-16 Minor Capsid Protein L2 by Difference Imaging. *Microsc Microanal* **11 (Suppl 2)**, 642-643 (2005).
16. Christensen, N.D., Kreider, J.W., Kan, N.C. & DiAngelo, S.L. The open reading frame L2 of cottontail rabbit papillomavirus contains antibody-inducing neutralizing epitopes. *Virology* **181**, 572-9 (1991).
17. Roden, R.B., Lowy, D.R. & Schiller, J.T. Papillomavirus is resistant to desiccation. *J Infect Dis* **176**, 1076-9 (1997).
18. Stanley, M.A., Browne, H.M., Appleby, M. & Minson, A.C. Properties of a non-tumorigenic human cervical keratinocyte cell line. *Int J Cancer* **43**, 672-6 (1989).
19. Flores, E.R., Allen-Hoffmann, B.L., Lee, D., Sattler, C.A. & Lambert, P.F. Establishment of the human papillomavirus type 16 (HPV-16) life cycle in an immortalized human foreskin keratinocyte cell line. *Virology* **262**, 344-54 (1999).
20. Shafti-Keramat, S. et al. Different heparan sulfate proteoglycans serve as cellular receptors for human papillomaviruses. *J Virol* **77**, 13125-35 (2003).

21. Evander, M. et al. Identification of the alpha6 integrin as a candidate receptor for papillomaviruses. *J Virol* **71**, 2449-56 (1997).
22. Day, P.M., Lowy, D.R. & Schiller, J.T. Papillomaviruses infect cells via a clathrin-dependent pathway. *Virology* **307**, 1-11 (2003).
23. Anderson, R.G. The caveolae membrane system. *Annu Rev Biochem* **67**, 199-225 (1998).
24. Shin, J.S. & Abraham, S.N. Cell biology. Caveolae--not just craters in the cellular landscape. *Science* **293**, 1447-8 (2001).
25. Bousarghin, L., Touze, A., Sizaret, P.Y. & Coursaget, P. Human papillomavirus types 16, 31, and 58 use different endocytosis pathways to enter cells. *J Virol* **77**, 3846-50 (2003).
26. Strauss, J.H. & Strauss, E.G. Viral RNA replication. With a little help from the host. *Science* **283**, 802-4 (1999).
27. Flores, E.R., Allen-Hoffmann, B.L., Lee, D. & Lambert, P.F. The human papillomavirus type 16 E7 oncogene is required for the productive stage of the viral life cycle. *J Virol* **74**, 6622-31 (2000).
28. Song, S., Liem, A., Miller, J.A. & Lambert, P.F. Human papillomavirus types 16 E6 and E7 contribute differently to carcinogenesis. *Virology* **267**, 141-50 (2000).
29. Flores, E.R. & Lambert, P.F. Evidence for a switch in the mode of human papillomavirus type 16 DNA replication during the viral life cycle. *J Virol* **71**, 7167-79 (1997).
30. Van Tine, B.A. et al. Clonal selection for transcriptionally active viral oncogenes during progression to cancer. *J Virol* **78**, 11172-86 (2004).
31. Bodily, J.M. & Meyers, C. Genetic analysis of the human papillomavirus type 31 differentiation-dependent late promoter. *J Virol* **79**, 3309-21 (2005).
32. Florin, L., Sapp, C., Streeck, R.E. & Sapp, M. Assembly and translocation of papillomavirus capsid proteins. *J Virol* **76**, 10009-14 (2002).
33. GenBank.
34. Cripe, T.P. et al. Transcriptional regulation of the human papillomavirus-16 E6-E7 promoter by a keratinocyte-dependent enhancer, and by viral E2 trans-activator and repressor gene products: implications for cervical carcinogenesis. *Embo J* **6**, 3745-53 (1987).
35. Sedman, J. & Stenlund, A. Co-operative interaction between the initiator E1 and the transcriptional activator E2 is required for replicator specific DNA replication of bovine papillomavirus in vivo and in vitro. *Embo J* **14**, 6218-28 (1995).
36. Swindle, C.S. & Engler, J.A. Association of the human papillomavirus type 11 E1 protein with histone H1. *J Virol* **72**, 1994-2001 (1998).
37. Hou, S.Y., Wu, S.Y. & Chiang, C.M. Transcriptional activity among high and low risk human papillomavirus E2 proteins correlates with E2 DNA binding. *J Biol Chem* **277**, 45619-29 (2002).
38. Wells, S.I. et al. Papillomavirus E2 induces senescence in HPV-positive cells via pRB- and p21(CIP)-dependent pathways. *Embo J* **19**, 5762-71 (2000).
39. Goodwin, E.C. & DiMaio, D. Repression of human papillomavirus oncogenes in HeLa cervical carcinoma cells causes the orderly reactivation of dormant tumor suppressor pathways. *Proc Natl Acad Sci U S A* **97**, 12513-8 (2000).
40. Doorbar, J., Evans, H.S., Coneron, I., Crawford, L.V. & Gallimore, P.H. Analysis of HPV-1 E4 gene expression using epitope-defined antibodies. *Embo J* **7**, 825-33 (1988).
41. Doorbar, J. et al. Characterization of events during the late stages of HPV16 infection in vivo using high-affinity synthetic Fabs to E4. *Virology* **238**, 40-52 (1997).

42. Doorbar, J., Ely, S., Sterling, J., McLean, C. & Crawford, L. Specific interaction between HPV-16 E1-E4 and cytokeratins results in collapse of the epithelial cell intermediate filament network. *Nature* **352**, 824-7 (1991).
43. Storey, A. et al. Comparison of the in vitro transforming activities of human papillomavirus types. *Embo J* **7**, 1815-20 (1988).
44. DiMaio, D. & Mattoon, D. Mechanisms of cell transformation by papillomavirus E5 proteins. *Oncogene* **20**, 7866-73 (2001).
45. Kabsch, K. & Alonso, A. The human papillomavirus type 16 (HPV-16) E5 protein sensitizes human keratinocytes to apoptosis induced by osmotic stress. *Oncogene* **21**, 947-53 (2002).
46. zur Hausen, H. Papillomaviruses and cancer: from basic studies to clinical application. *Nat Rev Cancer* **2**, 342-50 (2002).
47. Ashrafi, G.H., Haghshenas, M.R., Marchetti, B., O'Brien, P.M. & Campo, M.S. E5 protein of human papillomavirus type 16 selectively downregulates surface HLA class I. *Int J Cancer* **113**, 276-83 (2005).
48. Stoppler, M.C., Straight, S.W., Tsao, G., Schlegel, R. & McCance, D.J. The E5 gene of HPV-16 enhances keratinocyte immortalization by full-length DNA. *Virology* **223**, 251-4 (1996).
49. Chen, S.L., Huang, C.H., Tsai, T.C., Lu, K.Y. & Tsao, Y.P. The regulation mechanism of c-jun and junB by human papillomavirus type 16 E5 oncoprotein. *Arch Virol* **141**, 791-800 (1996).
50. Thomsen, P., van Deurs, B., Norrild, B. & Kayser, L. The HPV16 E5 oncogene inhibits endocytic trafficking. *Oncogene* **19**, 6023-32 (2000).
51. Aasen, T., Hodgins, M.B., Edward, M. & Graham, S.V. The relationship between connexins, gap junctions, tissue architecture and tumour invasion, as studied in a novel in vitro model of HPV-16-associated cervical cancer progression. *Oncogene* **22**, 7969-80 (2003).
52. Oelze, I., Kartenbeck, J., Crusius, K. & Alonso, A. Human papillomavirus type 16 E5 protein affects cell-cell communication in an epithelial cell line. *J Virol* **69**, 4489-94 (1995).
53. Southern, S.A. & Herrington, C.S. Disruption of cell cycle control by human papillomaviruses with special reference to cervical carcinoma. *Int J Gynecol Cancer* **10**, 263-274 (2000).
54. Southern, S.A. & Herrington, C.S. Molecular events in uterine cervical cancer. *Sex Transm Infect* **74**, 101-9 (1998).
55. Zhou, J. & Frazer, I.H. Papilliomaviridiae: Capsid structure and capsid protein function. *Papillomavirus reviews:current Research on Papillomaviruses*, 93-100 (1996).
56. Zhou, J., Sun, X.Y., Stenzel, D.J. & Frazer, I.H. Expression of vaccinia recombinant HPV 16 L1 and L2 ORF proteins in epithelial cells is sufficient for assembly of HPV virion-like particles. *Virology* **185**, 251-7 (1991).
57. Schiller, J.T. & Hidesheim, A. Developing HPV virus-like particle vaccines to prevent cervical cancer: a progress report. *J Clin Virol* **19**, 67-74 (2000).
58. Stauffer, Y., Raj, K., Masternak, K. & Beard, P. Infectious human papillomavirus type 18 pseudovirions. *J Mol Biol* **283**, 529-36 (1998).
59. Roden, R.B. et al. Positively charged termini of the L2 minor capsid protein are necessary for papillomavirus infection. *J Virol* **75**, 10493-7 (2001).
60. Modis, Y., Trus, B.L. & Harrison, S.C. Atomic model of the papillomavirus capsid. *Embo J* **21**, 4754-62 (2002).

61. Finnen, R.L., Erickson, K.D., Chen, X.S. & Garcea, R.L. Interactions between papillomavirus L1 and L2 capsid proteins. *J Virol* **77**, 4818-26 (2003).
62. Day, P.M., Baker, C.C., Lowy, D.R. & Schiller, J.T. Establishment of papillomavirus infection is enhanced by promyelocytic leukemia protein (PML) expression. *Proc Natl Acad Sci U S A* **101**, 14252-7 (2004).
63. Zhou, J., Sun, X.Y., Louis, K. & Frazer, I.H. Interaction of human papillomavirus (HPV) type 16 capsid proteins with HPV DNA requires an intact L2 N-terminal sequence. *J Virol* **68**, 619-25 (1994).
64. Stoler, M.H., Wolinsky, S.M., Whitbeck, A., Broker, T.R. & Chow, L.T. Differentiation-linked human papillomavirus types 6 and 11 transcription in genital condylomata revealed by in situ hybridization with message-specific RNA probes. *Virology* **172**, 331-40 (1989).
65. Milligan, S.G., Veerapraditsin, T., Ahamet, B., Mole, S. & Graham, S.V. Analysis of novel human papillomavirus type 16 late mRNAs in differentiated W12 cervical epithelial cells. *Virology* **360**, 172-81 (2007).
66. Stünkel, W. & Bernard, H. The Chromatin Structure of the Long Control Region of Human Papillomavirus Type 16 Represses Viral Oncoprotein Expression. *Journal of Virology* **73**, 1918 -1930 (1999).
67. Moodley, M., Moodley, J., Chetty, R. & Herrington, C.S. The role of steroid contraceptive hormones in the pathogenesis of invasive cervical cancer: a review. *Int J Gynecol Cancer* **13**, 103-10 (2003).
68. Sailaja, G., Watts, R.M. & Bernard, H.U. Many different papillomaviruses have low transcriptional activity in spite of strong epithelial specific enhancers. *J Gen Virol* **80 (Pt 7)**, 1715-24 (1999).
69. Apt, D., Chong, T., Liu, Y. & Bernard, H.U. Nuclear factor I and epithelial cell-specific transcription of human papillomavirus type 16. *J Virol* **67**, 4455-63 (1993).
70. Romanczuk, H., Thierry, F. & Howley, P.M. Mutational analysis of cis elements involved in E2 modulation of human papillomavirus type 16 P97 and type 18 P105 promoters. *J Virol* **64**, 2849-59 (1990).
71. Thierry, F. & Yaniv, M. The BPV1-E2 trans-acting protein can be either an activator or a repressor of the HPV18 regulatory region. *Embo J* **6**, 3391-7 (1987).
72. Bernard, B.A. et al. The human papillomavirus type 18 (HPV18) E2 gene product is a repressor of the HPV18 regulatory region in human keratinocytes. *J Virol* **63**, 4317-24 (1989).
73. Sanders, C.M., Stern, P.L. & Maitland, N.J. Characterization of human papillomavirus type 16 E2 protein and subdomains expressed in insect cells. *Virology* **211**, 418-33 (1995).
74. Cooper, C.S., Upmeyer, S.N. & Winokur, P.L. Identification of single amino acids in the human papillomavirus 11 E2 protein critical for the transactivation or replication functions. *Virology* **241**, 312-22 (1998).
75. Tan, S.H., Leong, L.E., Walker, P.A. & Bernard, H.U. The human papillomavirus type 16 E2 transcription factor binds with low cooperativity to two flanking sites and represses the E6 promoter through displacement of Sp1 and TFIID. *J Virol* **68**, 6411-20 (1994).
76. Dowhanick, J.J., McBride, A.A. & Howley, P.M. Suppression of cellular proliferation by the papillomavirus E2 protein. *J Virol* **69**, 7791-9 (1995).
77. Thain, A., Jenkins, O., Clarke, A.R. & Gaston, K. CpG methylation directly inhibits binding of the human papillomavirus type 16 E2 protein to specific DNA sequences. *J Virol* **70**, 7233-5 (1996).

78. Wilson, V.G., West, M., Woytek, K. & Rangasamy, D. Papillomavirus E1 proteins: form, function, and features. *Virus Genes* **24**, 275-90 (2002).
79. Park, P. et al. The cellular DNA polymerase alpha-primase is required for papillomavirus DNA replication and associates with the viral E1 helicase. *Proc Natl Acad Sci U S A* **91**, 8700-4 (1994).
80. Smale, S.T. & Tjian, R. T-antigen-DNA polymerase alpha complex implicated in simian virus 40 DNA replication. *Mol Cell Biol* **6**, 4077-87 (1986).
81. Voitenleitner, C. et al. Cell cycle-dependent regulation of human DNA polymerase alpha-primase activity by phosphorylation. *Mol Cell Biol* **19**, 646-56 (1999).
82. Donaldson, M.M., Boner, W. & Morgan, I.M. TopBP1 regulates human papillomavirus type 16 E2 interaction with chromatin. *J Virol* **81**, 4338-42 (2007).
83. Honda, Y. et al. Cooperation of HECT-domain ubiquitin ligase hHYD and DNA topoisomerase II-binding protein for DNA damage response. *J Biol Chem* **277**, 3599-605 (2002).
84. Makiniemi, M. et al. BRCT domain-containing protein TopBP1 functions in DNA replication and damage response. *J Biol Chem* **276**, 30399-406 (2001).
85. Yamane, K. & Tsuruo, T. Conserved BRCT regions of TopBP1 and of the tumor suppressor BRCA1 bind strand breaks and termini of DNA. *Oncogene* **18**, 5194-203 (1999).
86. Hines, C.S. et al. DNA structure and flexibility in the sequence-specific binding of papillomavirus E2 proteins. *J Mol Biol* **276**, 809-18 (1998).
87. Chong, T., Apt, D., Gloss, B., Isa, M. & Bernard, H.U. The enhancer of human papillomavirus type 16: binding sites for the ubiquitous transcription factors oct-1, NFA, TEF-2, NF1, and AP-1 participate in epithelial cell-specific transcription. *J Virol* **65**, 5933-43 (1991).
88. Dong, G., Broker, T.R. & Chow, L.T. Human papillomavirus type 11 E2 proteins repress the homologous E6 promoter by interfering with the binding of host transcription factors to adjacent elements. *J Virol* **68**, 1115-27 (1994).
89. Ushikai, M. et al. trans activation by the full-length E2 proteins of human papillomavirus type 16 and bovine papillomavirus type 1 in vitro and in vivo: cooperation with activation domains of cellular transcription factors. *J Virol* **68**, 6655-66 (1994).
90. Kruppel, U., Muller-Schiffmann, A., Baldus, S.E., Smola-Hess, S. & Steger, G. E2 and the co-activator p300 can cooperate in activation of the human papillomavirus type 16 early promoter. *Virology* **377**, 151-9 (2008).
91. Skiadopoulos, M.H. & McBride, A.A. Bovine papillomavirus type 1 genomes and the E2 transactivator protein are closely associated with mitotic chromatin. *J Virol* **72**, 2079-88 (1998).
92. Lehman, C.W. & Botchan, M.R. Segregation of viral plasmids depends on tethering to chromosomes and is regulated by phosphorylation. *Proc Natl Acad Sci U S A* **95**, 4338-43 (1998).
93. Ilves, I., Kivi, S. & Ustav, M. Long-term episomal maintenance of bovine papillomavirus type 1 plasmids is determined by attachment to host chromosomes, which Is mediated by the viral E2 protein and its binding sites. *J Virol* **73**, 4404-12 (1999).
94. McPhillips, M.G., Ozato, K. & McBride, A.A. Interaction of bovine papillomavirus E2 protein with Brd4 stabilizes its association with chromatin. *J Virol* **79**, 8920-32 (2005).

95. Huang, S.M. & McCance, D.J. Down regulation of the interleukin-8 promoter by human papillomavirus type 16 E6 and E7 through effects on CREB binding protein/p300 and P/CAF. *J Virol* **76**, 8710-21 (2002).
96. Parish, J.L., Bean, A.M., Park, R.B. & Androphy, E.J. ChlR1 is required for loading papillomavirus E2 onto mitotic chromosomes and viral genome maintenance. *Mol Cell* **24**, 867-76 (2006).
97. Garcia-Alai, M.M., Dantur, K.I., Smal, C., Pietrasanta, L. & de Prat-Gay, G. High-risk HPV E6 oncoproteins assemble into large oligomers that allow localization of endogenous species in prototypic HPV-transformed cell lines. *Biochemistry* **46**, 341-9 (2007).
98. Barbosa, M.S., Lowy, D.R. & Schiller, J.T. Papillomavirus polypeptides E6 and E7 are zinc-binding proteins. *J Virol* **63**, 1404-7 (1989).
99. Cole, S.T. & Danos, O. Nucleotide sequence and comparative analysis of the human papillomavirus type 18 genome. Phylogeny of papillomaviruses and repeated structure of the E6 and E7 gene products. *J Mol Biol* **193**, 599-608 (1987).
100. Smotkin, D. & Wettstein, F.O. The major human papillomavirus protein in cervical cancers is a cytoplasmic phosphoprotein. *J Virol* **61**, 1686-9 (1987).
101. McIntyre, M.C., Frattini, M.G., Grossman, S.R. & Laimins, L.A. Human papillomavirus type 18 E7 protein requires intact Cys-X-X-Cys motifs for zinc binding, dimerization, and transformation but not for Rb binding. *J Virol* **67**, 3142-50 (1993).
102. Greenfield, I., Nickerson, J., Penman, S. & Stanley, M. Human papillomavirus 16 E7 protein is associated with the nuclear matrix. *Proc Natl Acad Sci U S A* **88**, 11217-21 (1991).
103. Stacey, S.N. et al. Leaky scanning is the predominant mechanism for translation of human papillomavirus type 16 E7 oncoprotein from E6/E7 bicistronic mRNA. *J Virol* **74**, 7284-97 (2000).
104. Baker, C.C. Post-Transcriptional Regulation of Papillomavirus Gene Expression. (1997).
105. Smotkin, D., Prokoph, H. & Wettstein, F.O. Oncogenic and nononcogenic human genital papillomaviruses generate the E7 mRNA by different mechanisms. *J Virol* **63**, 1441-7 (1989).
106. Tang, S., Tao, M., McCoy, J.P., Jr. & Zheng, Z.M. The E7 oncoprotein is translated from spliced E6*I transcripts in high-risk human papillomavirus type 16- or type 18-positive cervical cancer cell lines via translation reinitiation. *J Virol* **80**, 4249-63 (2006).
107. Stacey, S.N. et al. Translation of the human papillomavirus type 16 E7 oncoprotein from bicistronic mRNA is independent of splicing events within the E6 open reading frame. *J Virol* **69**, 7023-31 (1995).
108. Glahder, J.A., Hansen, C.N., Vinther, J., Madsen, B.S. & Norrild, B. A promoter within the E6 ORF of human papillomavirus type 16 contributes to the expression of the E7 oncoprotein from a monocistronic mRNA. *J Gen Virol* **84**, 3429-41 (2003).
109. Selinka, H.C. et al. Detection of human papillomavirus 16 transcriptional activity in cervical intraepithelial neoplasia grade III lesions and cervical carcinomas by nested reverse transcription-polymerase chain reaction and in situ hybridization. *Lab Invest* **78**, 9-18 (1998).
110. Filippova, M., Parkhurst, L. & Duerksen-Hughes, P.J. The human papillomavirus 16 E6 protein binds to Fas-associated death domain and protects cells from Fas-triggered apoptosis. *J Biol Chem* **279**, 25729-44 (2004).

111. Finzer, P., Aguilar-Lemarroy, A. & Rosl, F. The role of human papillomavirus oncoproteins E6 and E7 in apoptosis. *Cancer Lett* **188**, 15-24 (2002).
112. Scheffner, M., Huibregtse, J.M. & Howley, P.M. Identification of a human ubiquitin-conjugating enzyme that mediates the E6-AP-dependent ubiquitination of p53. *Proc Natl Acad Sci U S A* **91**, 8797-801 (1994).
113. Scheffner, M., Werness, B.A., J.M, H., Levine, A.J. & Howley, P.M. The E6 Oncoprotein Encoded by Human Papillomavirus Types 16 and 18 Promotes the Degradation of p53. *Cell* **63**, 1129-36 (1990).
114. Thomas, M. & Banks, L. Inhibition of Bak-induced apoptosis by HPV-18 E6. *Oncogene* **17**, 2943-54 (1998).
115. Gross-Mesilaty, S. et al. Basal and human papillomavirus E6 oncoprotein-induced degradation of Myc proteins by the ubiquitin pathway. *Proc Natl Acad Sci U S A* **95**, 8058-63 (1998).
116. Kalantari, M., Blennow, E., Hagmar, B. & Johansson, B. Physical state of HPV16 and chromosomal mapping of the integrated form in cervical carcinomas. *Diagn Mol Pathol* **10**, 46-54 (2001).
117. Alazawi, W. et al. Changes in cervical keratinocyte gene expression associated with integration of human papillomavirus 16. *Cancer Res* **62**, 6959-65 (2002).
118. Peitsaro, P., Johansson, B. & Syrjanen, S. Integrated human papillomavirus type 16 is frequently found in cervical cancer precursors as demonstrated by a novel quantitative real-time PCR technique. *J Clin Microbiol* **40**, 886-91 (2002).
119. Jeon, S., Allen-Hoffmann, B.L. & Lambert, P.F. Integration of human papillomavirus type 16 into the human genome correlates with a selective growth advantage of cells. *J Virol* **69**, 2989-97 (1995).
120. Wagatsuma, M., Hashimoto, K. & Matsukura, T. Analysis of integrated human papillomavirus type 16 DNA in cervical cancers: amplification of viral sequences together with cellular flanking sequences. *J Virol* **64**, 813-21 (1990).
121. Murakami, Y. et al. Large scaled analysis of hepatitis B virus (HBV) DNA integration in HBV related hepatocellular carcinomas. *Gut* **54**, 1162-8 (2005).
122. Klimov, E. et al. Human papilloma viruses and cervical tumours: mapping of integration sites and analysis of adjacent cellular sequences. *BMC Cancer* **2**, 24 (2002).
123. Yu, T. et al. The role of viral integration in the development of cervical cancer. *Cancer Genet Cytogenet* **158**, 27-34 (2005).
124. Wentzensen, N., Vinokurova, S. & von Knebel Doeberitz, M. Systematic review of genomic integration sites of human papillomavirus genomes in epithelial dysplasia and invasive cancer of the female lower genital tract. *Cancer Res* **64**, 3878-84 (2004).
125. Sutherland, G.R. & Richards, R.I. The molecular basis of fragile sites in human chromosomes. *Curr Opin Genet Dev* **5**, 323-7 (1995).
126. Lazo, P.A. The molecular genetics of cervical carcinoma. *Br J Cancer* **80**, 2008-18 (1999).
127. Lambert, P.F. & Howley, P.M. Bovine papillomavirus type 1 E1 replication-defective mutants are altered in their transcriptional regulation. *J Virol* **62**, 4009-15 (1988).
128. Munger, K., Phelps, W.C., Bubb, V., Howley, P.M. & Schlegel, R. The E6 and E7 genes of the human papillomavirus type 16 together are necessary and sufficient for transformation of primary human keratinocytes. *J Virol* **63**, 4417-21 (1989).
129. Jeon, S. & Lambert, P.F. Integration of human papillomavirus type 16 DNA into the human genome leads to increased stability of E6 and E7 mRNAs: implications for cervical carcinogenesis. *Proc Natl Acad Sci U S A* **92**, 1654-8 (1995).

130. De Marco, D. et al. Development and validation of a molecular method for the diagnosis of medically important fungal infections. *New Microbiol* **30**, 308-12 (2007).
131. Bechtold, V., Beard, P. & Raj, K. Human papillomavirus type 16 E2 protein has no effect on transcription from episomal viral DNA. *J Virol* **77**, 2021-8 (2003).
132. Parish, J.L. et al. E2 proteins from high- and low-risk human papillomavirus types differ in their ability to bind p53 and induce apoptotic cell death. *J Virol* **80**, 4580-90 (2006).
133. Pett, M.R. et al. Selection of cervical keratinocytes containing integrated HPV16 associates with episome loss and an endogenous antiviral response. *Proc Natl Acad Sci U S A* **103**, 3822-7 (2006).
134. Schiffman, M. et al. The carcinogenicity of human papillomavirus types reflects viral evolution. *Virology* **337**, 76-84 (2005).
135. Hong, K., Greer, C.E., Ketter, N., Van Nest, G. & Paliard, X. Isolation and characterization of human papillomavirus type 6-specific T cells infiltrating genital warts. *J Virol* **71**, 6427-32 (1997).
136. Durst, M., Gissmann, L., Ikenberg, H. & zur Hausen, H. A papillomavirus DNA from a cervical carcinoma and its prevalence in cancer biopsy samples from different geographic regions. *Proc Natl Acad Sci U S A* **80**, 3812-5 (1983).
137. Milde-Langosch, K., Riethdorf, S. & Loning, T. Association of human papillomavirus infection with carcinoma of the cervix uteri and its precursor lesions: theoretical and practical implications. *Virchows Arch* **437**, 227-33 (2000).
138. Eichten, A., Westfall, M., Pietenpol, J.A. & Munger, K. Stabilization and functional impairment of the tumor suppressor p53 by the human papillomavirus type 16 E7 oncoprotein. *Virology* **295**, 74-85 (2002).
139. Bercovich, J.A., Centeno, C.R., Aguilar, O.G., Grinstein, S. & Kahn, T. Presence and integration of human papillomavirus type 6 in a tonsillar carcinoma. *J Gen Virol* **72 (Pt 10)**, 2569-72 (1991).
140. Boshart, M. & zur Hausen, H. Human papillomaviruses in Buschke-Lowenstein tumors: physical state of the DNA and identification of a tandem duplication in the noncoding region of a human papillomavirus 6 subtype. *J Virol* **58**, 963-6 (1986).
141. DiLorenzo, T.P., Tamsen, A., Abramson, A.L. & Steinberg, B.M. Human papillomavirus type 6a DNA in the lung carcinoma of a patient with recurrent laryngeal papillomatosis is characterized by a partial duplication. *J Gen Virol* **73 (Pt 2)**, 423-8 (1992).
142. Farr, A., Wang, H., Kasher, M.S. & Roman, A. Relative enhancer activity and transforming potential of authentic human papillomavirus type 6 genomes from benign and malignant lesions. *J Gen Virol* **72 (Pt 3)**, 519-26 (1991).
143. Kitasato, H. et al. Sequence rearrangements in the upstream regulatory region of human papillomavirus type 6: are these involved in malignant transition? *J Gen Virol* **75 (Pt 5)**, 1157-62 (1994).
144. Oft, M., Bohm, S., Wilczynski, S.P. & Iftner, T. Expression of the different viral mRNAs of human papilloma virus 6 in a squamous-cell carcinoma of the bladder and the cervix. *Int J Cancer* **53**, 924-31 (1993).
145. Rando, R.F., Lancaster, W.D., Han, P. & Lopez, C. The noncoding region of HPV-6vc contains two distinct transcriptional enhancing elements. *Virology* **155**, 545-56 (1986).
146. Barbosa, M.S. et al. The region of the HPV E7 oncoprotein homologous to adenovirus E1a and Sv40 large T antigen contains separate domains for Rb binding and casein kinase II phosphorylation. *Embo J* **9**, 153-60 (1990).

147. Munger, K. et al. Biochemical and biological differences between E7 oncoproteins of the high- and low-risk human papillomavirus types are determined by amino-terminal sequences. *J Virol* **65**, 3943-8 (1991).
148. Guccione, E., Massimi, P., Bernat, A. & Banks, L. Comparative analysis of the intracellular location of the high- and low-risk human papillomavirus oncoproteins. *Virology* **293**, 20-5 (2002).
149. Swindle, C.S. et al. Human papillomavirus DNA replication compartments in a transient DNA replication system. *J Virol* **73**, 1001-9 (1999).
150. Everett, R.D. & Murray, J. ND10 components relocate to sites associated with herpes simplex virus type 1 nucleoprotein complexes during virus infection. *J Virol* **79**, 5078-89 (2005).
151. Everett, R.D. & Maul, G.G. HSV-1 IE protein Vmw110 causes redistribution of PML. *Embo J* **13**, 5062-9 (1994).
152. Muller, S. & Dejean, A. Viral immediate-early proteins abrogate the modification by SUMO-1 of PML and Sp100 proteins, correlating with nuclear body disruption. *J Virol* **73**, 5137-43 (1999).
153. Cuschieri, K.S. et al. Multiple high risk HPV infections are common in cervical neoplasia and young women in a cervical screening population. *J Clin Pathol* **57**, 68-72 (2004).
154. Parkin, D.M., Bray, F., Ferlay, J. & Pisani, P. Global cancer statistics, 2002. *CA Cancer J Clin* **55**, 74-108 (2005).
155. Xi, L.F. et al. Analysis of human papillomavirus type 16 variants indicates establishment of persistent infection. *J Infect Dis* **172**, 747-55 (1995).
156. UK, C.R. UK Cervical Cancer Incidence Statistics. (Cancer Research UK).
157. Walboomers, J.M. et al. Human papillomavirus is a necessary cause of invasive cervical cancer worldwide. *J Pathol* **189**, 12-9 (1999).
158. Park, J.S. et al. Physical status and expression of HPV genes in cervical cancers. *Gynecol Oncol* **65**, 121-9 (1997).
159. Woodman, C.B. et al. Natural history of cervical human papillomavirus infection in young women: a longitudinal cohort study. *Lancet* **357**, 1831-6 (2001).
160. Middleton, K. et al. Organization of human papillomavirus productive cycle during neoplastic progression provides a basis for selection of diagnostic markers. *J Virol* **77**, 10186-201 (2003).
161. Cuschieri, K.S. et al. Persistent high risk HPV infection associated with development of cervical neoplasia in a prospective population study. *J Clin Pathol* **58**, 946-50 (2005).
162. Peto, J., Gilham, C., Fletcher, O. & Matthews, F.E. The cervical cancer epidemic that screening has prevented in the UK. *Lancet* **364**, 249-56 (2004).
163. Kitchener, H.C., Castle, P.E. & Cox, J.T. Chapter 7: Achievements and limitations of cervical cytology screening. *Vaccine* **24 Suppl 3**, S63-70 (2006).
164. Trimble, C.L. et al. Spontaneous regression of high-grade cervical dysplasia: effects of human papillomavirus type and HLA phenotype. *Clin Cancer Res* **11**, 4717-23 (2005).
165. Daling, J.R. et al. Cigarette smoking and the risk of anogenital cancer. *Am J Epidemiol* **135**, 180-9 (1992).
166. Prokopczyk, B., Cox, J.E., Hoffmann, D. & Waggoner, S.E. Identification of tobacco-specific carcinogen in the cervical mucus of smokers and nonsmokers. *J. Natl. Cancer Inst.*
89, 868-873 (1997).
167. Prokopczyk, B., Trushin, N., Leszczynska, J., Waggoner, S.E. & El-Bayoumy, K. Human cervical tissue metabolizes the tobacco-specific nitrosamine, 4-

(methylnitrosamino)-1-(3-pyridyl)-1-butanone, via alpha-hydroxylation and carbonyl reduction pathways. *Carcinogenesis* **22**, 107-14 (2001).
168. Lane, D.P. Cancer. p53, guardian of the genome. *Nature* **358**, 15-6 (1992).
169. Ozaki, T. & Nakagawara, A. p73, a sophisticated p53 family member in the cancer world. *Cancer Sci* **96**, 729-37 (2005).
170. Hofseth, L.J., Hussain, S.P. & Harris, C.C. p53: 25 years after its discovery. *Trends Pharmacol Sci* **25**, 177-81 (2004).
171. Vogelstein, B., Lane, D. & Levine, A.J. Surfing the p53 network. *Nature* **408**, 307-10 (2000).
172. Hollstein, M., Sidransky, D., Vogelstein, B. & Harris, C.C. p53 mutations in human cancers. *Science* **253**, 49-53 (1991).
173. Levine, A.J., Momand, J. & Finlay, C.A. The p53 tumour suppressor gene. *Nature* **351**, 453-6 (1991).
174. Milner, J. Flexibility: the key to p53 function? *Trends Biochem Sci* **20**, 49-51 (1995).
175. Shieh, S.Y., Taya, Y. & Prives, C. DNA damage-inducible phosphorylation of p53 at N-terminal sites including a novel site, Ser20, requires tetramerization. *Embo J* **18**, 1815-23 (1999).
176. O'Brate, A. & Giannakakou, P. The importance of p53 location: nuclear or cytoplasmic zip code? *Drug Resist Updat* **6**, 313-22 (2003).
177. Jones, D.L. & Munger, K. Analysis of the p53-mediated G1 growth arrest pathway in cells expressing the human papillomavirus type 16 E7 oncoprotein. *J Virol* **71**, 2905-12 (1997).
178. Miconnet, I., Servis, C., Cerottini, J.C., Romero, P. & Levy, F. Amino acid identity and/or position determines the proteasomal cleavage of the HLA-A*0201-restricted peptide tumor antigen MAGE-3271-279. *J Biol Chem* **275**, 26892-7 (2000).
179. Stewart, D., Ghosh, A. & Matlashewski, G. Involvement of nuclear export in human papillomavirus type 18 E6-mediated ubiquitination and degradation of p53. *J Virol* **79**, 8773-83 (2005).
180. Honda, R., Tanaka, H. & Yasuda, H. Oncoprotein MDM2 is a ubiquitin ligase E3 for tumor suppressor p53. *FEBS Lett* **420**, 25-7 (1997).
181. Dey, A., Verma, C.S. & Lane, D.P. Updates on p53: modulation of p53 degradation as a therapeutic approach. *Br J Cancer* **98**, 4-8 (2008).
182. Lain, S., Xirodimas, D. & Lane, D.P. Accumulating active p53 in the nucleus by inhibition of nuclear export: a novel strategy to promote the p53 tumor suppressor function. *Exp Cell Res* **253**, 315-24 (1999).
183. Grossman, S.R. et al. Polyubiquitination of p53 by a ubiquitin ligase activity of p300. *Science* **300**, 342-4 (2003).
184. Coux, O., Tanaka, K. & Goldberg, A.L. Structure and functions of the 20S and 26S proteasomes. *Annu Rev Biochem* **65**, 801-47 (1996).
185. Voges, D., Zwickl, P. & Baumeister, W. The 26S proteasome: a molecular machine designed for controlled proteolysis. *Annu Rev Biochem* **68**, 1015-68 (1999).
186. Kudo, N. et al. Leptomycin B inactivates CRM1/exportin 1 by covalent modification at a cysteine residue in the central conserved region. *Proc Natl Acad Sci U S A* **96**, 9112-7 (1999).
187. Roth, J., Dobbelstein, M., Freedman, D.A., Shenk, T. & Levine, A.J. Nucleo-cytoplasmic shuttling of the hdm2 oncoprotein regulates the levels of the p53 protein via a pathway used by the human immunodeficiency virus rev protein. *Embo J* **17**, 554-64 (1998).
188. Mattaj, I.W. & Englmeier, L. Nucleocytoplasmic transport: the soluble phase. *Annu Rev Biochem* **67**, 265-306 (1998).

189. Pemberton, L.F., Blobel, G. & Rosenblum, J.S. Transport routes through the nuclear pore complex. *Curr Opin Cell Biol* **10**, 392-9 (1998).
190. Stommel, J.M. et al. A leucine-rich nuclear export signal in the p53 tetramerization domain: regulation of subcellular localization and p53 activity by NES masking. *Embo J* **18**, 1660-72 (1999).
191. Carr, A.M. Cell cycle. Piecing together the p53 puzzle. *Science* **287**, 1765-6 (2000).
192. Meek, D.W. Mechanisms of switching on p53: a role for covalent modification? *Oncogene* **18**, 7666-75 (1999).
193. Sherr, C.J. & Weber, J.D. The ARF/p53 pathway. *Curr Opin Genet Dev* **10**, 94-9 (2000).
194. Lowe, S.W. & Lin, A.W. Apoptosis in cancer. *Carcinogenesis* **21**, 485-95 (2000).
195. Liang, S.H. & Clarke, M.F. Regulation of p53 localization. *Eur J Biochem* **268**, 2779-83 (2001).
196. el-Deiry, W.S., Kern, S.E., Pietenpol, J.A., Kinzler, K.W. & Vogelstein, B. Definition of a consensus binding site for p53. *Nat Genet* **1**, 45-9 (1992).
197. Jimenez, G.S., Khan, S.H., Stommel, J.M. & Wahl, G.M. p53 regulation by post-translational modification and nuclear retention in response to diverse stresses. *Oncogene* **18**, 7656-65 (1999).
198. Shieh, S.Y., Ikeda, M., Taya, Y. & Prives, C. DNA damage-induced phosphorylation of p53 alleviates inhibition by MDM2. *Cell* **91**, 325-34 (1997).
199. Unger, T. et al. Critical role for Ser20 of human p53 in the negative regulation of p53 by Mdm2. *Embo J* **18**, 1805-14 (1999).
200. Zhao, R. et al. Analysis of p53-regulated gene expression patterns using oligonucleotide arrays. *Genes Dev* **14**, 981-93 (2000).
201. Riley, T., Sontag, E., Chen, P. & Levine, A. Transcriptional control of human p53-regulated genes. *Nat Rev Mol Cell Biol* **9**, 402-12 (2008).
202. Seoane, J., Le, H.V. & Massague, J. Myc suppression of the p21(Cip1) Cdk inhibitor influences the outcome of the p53 response to DNA damage. *Nature* **419**, 729-34 (2002).
203. Lain, S., Midgley, C., Sparks, A., Lane, E.B. & Lane, D.P. An inhibitor of nuclear export activates the p53 response and induces the localization of HDM2 and p53 to U1A-positive nuclear bodies associated with the PODs. *Exp Cell Res* **248**, 457-72 (1999).
204. Blundell, R.A. The Biology of P21 $^{Waf1/Cip1}$ - Review Paper. *American Journal fo Biochemistry and Biotechnology* **2**, 33 - 40 (2006).
205. el-Deiry, W.S. et al. WAF1, a potential mediator of p53 tumor suppression. *Cell* **75**, 817-25 (1993).
206. Chen, J., Saha, P., Kornbluth, S., Dynlacht, B.D. & Dutta, A. Cyclin-binding motifs are essential for the function of p21CIP1. *Mol Cell Biol* **16**, 4673-82 (1996).
207. Bates, S., Ryan, K.M., Phillips, A.C. & Vousden, K.H. Cell cycle arrest and DNA endoreduplication following p21Waf1/Cip1 expression. *Oncogene* **17**, 1691-703 (1998).
208. Fredersdorf, S., Milne, A.W., Hall, P.A. & Lu, X. Characterization of a panel of novel anti-p21Waf1/Cip1 monoclonal antibodies and immunochemical analysis of p21Waf1/Cip1 expression in normal human tissues. *Am J Pathol* **148**, 825-35 (1996).
209. Sherr, C.J. & Roberts, J.M. Inhibitors of mammalian G1 cyclin-dependent kinases. *Genes Dev* **9**, 1149-63 (1995).
210. Costanzi-Strauss, E., Strauss, B.E., Naviaux, R.K. & Haas, M. Restoration of growth arrest by p16INK4, p21WAF1, pRB, and p53 is dependent on the integrity of the

endogenous cell-cycle control pathways in human glioblastoma cell lines. *Exp Cell Res* **238**, 51-62 (1998).
211. Snowden, A.W., Anderson, L.A., Webster, G.A. & Perkins, N.D. A novel transcriptional repression domain mediates p21(WAF1/CIP1) induction of p300 transactivation. *Mol Cell Biol* **20**, 2676-86 (2000).
212. Carrier, F. et al. Gadd45, a p53-responsive stress protein, modifies DNA accessibility on damaged chromatin. *Mol Cell Biol* **19**, 1673-85 (1999).
213. Murakami, H. & Nurse, P. DNA replication and damage checkpoints and meiotic cell cycle controls in the fission and budding yeasts. *Biochem J* **349**, 1-12 (2000).
214. Wang, W. et al. HuR regulates p21 mRNA stabilization by UV light. *Mol Cell Biol* **20**, 760-9 (2000).
215. Kim, G.Y. et al. The stress-activated protein kinases p38 alpha and JNK1 stabilize p21(Cip1) by phosphorylation. *J Biol Chem* **277**, 29792-802 (2002).
216. Hagen, G., Muller, S., Beato, M. & Suske, G. Sp1-mediated transcriptional activation is repressed by Sp3. *Embo J* **13**, 3843-51 (1994).
217. Igney, F.H. & Krammer, P.H. Death and anti-death: tumour resistance to apoptosis. *Nat Rev Cancer* **2**, 277-288 (2002).
218. Borner, C. & Monney, L. Apoptosis without caspases: an inefficient molecular guillotine? *Cell Death Differ* **6**, 497-507 (1999).
219. Xiang, J., Chao, D.T. & Korsmeyer, S.J. BAX-induced cell death may not require interleukin 1 beta-converting enzyme-like proteases. *Proc Natl Acad Sci U S A* **93**, 14559-63 (1996).
220. Sperandio, S., de Belle, I. & Bredesen, D.E. An alternative, nonapoptotic form of programmed cell death. *Proc Natl Acad Sci U S A* **97**, 14376-81 (2000).
221. Daniel, P.T., Wieder, T., Sturm, I. & Schulze-Osthoff, K. The kiss of death: promises and failures of death receptors and ligands in cancer therapy. *Leukemia* **15**, 1022-32 (2001).
222. Haupt, S., Berger, M., Goldberg, Z. & Haupt, Y. Apoptosis - the p53 network. *J Cell Sci* **116**, 4077-85 (2003).
223. Muzio, M. Signalling by proteolysis: death receptors induce apoptosis. *Int J Clin Lab Res* **28**, 141-7 (1998).
224. Krueger, A., Baumann, S., Krammer, P.H. & Kirchhoff, S. FLICE-inhibitory proteins: regulators of death receptor-mediated apoptosis. *Mol Cell Biol* **21**, 8247-54 (2001).
225. Sprick, M.R. et al. FADD/MORT1 and caspase-8 are recruited to TRAIL receptors 1 and 2 and are essential for apoptosis mediated by TRAIL receptor 2. *Immunity* **12**, 599-609 (2000).
226. Kischkel, F.C. et al. Cytotoxicity-dependent APO-1 (Fas/CD95)-associated proteins form a death-inducing signaling complex (DISC) with the receptor. *Embo J* **14**, 5579-88 (1995).
227. Kischkel, F.C. et al. Death receptor recruitment of endogenous caspase-10 and apoptosis initiation in the absence of caspase-8. *J Biol Chem* **276**, 46639-46 (2001).
228. Scaffidi, C. et al. Two CD95 (APO-1/Fas) signaling pathways. *Embo J* **17**, 1675-87 (1998).
229. Kelekar, A. & Thompson, C.B. Bcl-2-family proteins: the role of the BH3 domain in apoptosis. *Trends Cell Biol* **8**, 324-30 (1998).
230. Yu, J., Zhang, L., Hwang, P.M., Kinzler, K.W. & Vogelstein, B. PUMA induces the rapid apoptosis of colorectal cancer cells. *Mol Cell* **7**, 673-82 (2001).
231. Zamzami, N. & Kroemer, G. The mitochondrion in apoptosis: how Pandora's box opens. *Nat Rev Mol Cell Biol* **2**, 67-71 (2001).

232. Martinou, J.C. & Green, D.R. Breaking the mitochondrial barrier. *Nat Rev Mol Cell Biol* **2**, 63-7 (2001).
233. Marchenko, N.D., Zaika, A. & Moll, U.M. Death signal-induced localization of p53 protein to mitochondria. A potential role in apoptotic signaling. *J Biol Chem* **275**, 16202-12 (2000).
234. Verhagen, A.M. et al. Identification of DIABLO, a mammalian protein that promotes apoptosis by binding to and antagonizing IAP proteins. *Cell* **102**, 43-53 (2000).
235. Du, C., Fang, M., Li, Y., Li, L. & Wang, X. Smac, a mitochondrial protein that promotes cytochrome c-dependent caspase activation by eliminating IAP inhibition. *Cell* **102**, 33-42 (2000).
236. Pawlowski, J. & Kraft, A.S. Bax-induced apoptotic cell death. *Proc Natl Acad Sci U S A* **97**, 529-31 (2000).
237. Rathmell, J.C. & Thompson, C.B. The central effectors of cell death in the immune system. *Annu Rev Immunol* **17**, 781-828 (1999).
238. Dash, P. Reproductive and Cardiovascular Disease Research Group. Vol. 2008 (2008).
239. Savill, J. & Fadok, V. Corpse clearance defines the meaning of cell death. *Nature* **407**, 784-8 (2000).
240. Azuma, Y., Inami, Y. & Matsumoto, K. Alterations in cell surface phosphatidylserine and sugar chains during apoptosis and their time-dependent role in phagocytosis by macrophages. *Biol Pharm Bull* **25**, 1277-81 (2002).
241. Nagata, S. & Golstein, P. The Fas death factor. *Science* **267**, 1449-56 (1995).
242. Fuchs, E.J., McKenna, K.A. & Bedi, A. p53-dependent DNA damage-induced apoptosis requires Fas/APO-1-independent activation of CPP32beta. *Cancer Res* **57**, 2550-4 (1997).
243. O'Connor, L., Harris, A.W. & Strasser, A. CD95 (Fas/APO-1) and p53 signal apoptosis independently in diverse cell types. *Cancer Res* **60**, 1217-20 (2000).
244. Bennett, M. et al. Cell surface trafficking of Fas: a rapid mechanism of p53-mediated apoptosis. *Science* **282**, 290-3 (1998).
245. Wu, G.S. et al. KILLER/DR5 is a DNA damage-inducible p53-regulated death receptor gene. *Nat Genet* **17**, 141-3 (1997).
246. Ashkenazi, A. & Dixit, V.M. Death receptors: signaling and modulation. *Science* **281**, 1305-8 (1998).
247. Burns, T.F., Bernhard, E.J. & El-Deiry, W.S. Tissue specific expression of p53 target genes suggests a key role for KILLER/DR5 in p53-dependent apoptosis in vivo. *Oncogene* **20**, 4601-12 (2001).
248. Gupta, S., Radha, V., Furukawa, Y. & Swarup, G. Direct transcriptional activation of human caspase-1 by tumor suppressor p53. *J Biol Chem* **276**, 10585-8 (2001).
249. Schuler, M., Bossy-Wetzel, E., Goldstein, J.C., Fitzgerald, P. & Green, D.R. p53 induces apoptosis by caspase activation through mitochondrial cytochrome c release. *J Biol Chem* **275**, 7337-42 (2000).
250. Yin, Y., Liu, Y.X., Jin, Y.J., Hall, E.J. & Barrett, J.C. PAC1 phosphatase is a transcription target of p53 in signalling apoptosis and growth suppression. *Nature* **422**, 527-31 (2003).
251. Mihara, M. et al. p53 has a direct apoptogenic role at the mitochondria. *Mol Cell* **11**, 577-90 (2003).
252. Dotto, G.P. p21(WAF1/Cip1): more than a break to the cell cycle? *Biochim Biophys Acta* **1471**, M43-56 (2000).
253. Fotedar, R. et al. Effect of p21waf1/cip1 transgene on radiation induced apoptosis in T cells. *Oncogene* **18**, 3652-8 (1999).

254. Bulavin, D.V., Tararova, N.D., Aksenov, N.D., Pospelov, V.A. & Pospelova, T.V. Deregulation of p53/p21Cip1/Waf1 pathway contributes to polyploidy and apoptosis of E1A+cHa-ras transformed cells after gamma-irradiation. *Oncogene* **18**, 5611-9 (1999).
255. Graves, J.D. et al. Caspase-mediated activation and induction of apoptosis by the mammalian Ste20-like kinase Mst1. *Embo J* **17**, 2224-34 (1998).
256. Zhang, Y., Fujita, N. & Tsuruo, T. Caspase-mediated cleavage of p21Waf1/Cip1 converts cancer cells from growth arrest to undergoing apoptosis. *Oncogene* **18**, 1131-8 (1999).
257. McKay, B.C., Ljungman, M. & Rainbow, A.J. Persistent DNA damage induced by ultraviolet light inhibits p21waf1 and bax expression: implications for DNA repair, UV sensitivity and the induction of apoptosis. *Oncogene* **17**, 545-55 (1998).
258. Gervais, J.L., Seth, P. & Zhang, H. Cleavage of CDK inhibitor p21(Cip1/Waf1) by caspases is an early event during DNA damage-induced apoptosis. *J Biol Chem* **273**, 19207-12 (1998).
259. Daniels, P.R., Sanders, C.M. & Maitland, N.J. Characterization of the interactions of human papillomavirus type 16 E6 with p53 and E6-associated protein in insect and human cells. *J Gen Virol* **79 (Pt 3)**, 489-99 (1998).
260. Scheffner, M., Huibregtse, J.M., Vierstra, R.D. & Howley, P.M. The HPV-16 E6 and E6-AP complex functions as a ubiquitin-protein ligase in the ubiquitination of p53. *Cell* **75**, 495-505 (1993).
261. Oda, H., Kumar, S. & Howley, P.M. Regulation of the Src family tyrosine kinase Blk through E6AP-mediated ubiquitination. *Proc Natl Acad Sci U S A* **96**, 9557-62 (1999).
262. Nuber, U., Schwarz, S.E. & Scheffner, M. The ubiquitin-protein ligase E6-associated protein (E6-AP) serves as its own substrate. *Eur J Biochem* **254**, 643-9 (1998).
263. Huibregtse, J.M., Scheffner, M. & Howley, P.M. Cloning and expression of the cDNA for E6-AP, a protein that mediates the interaction of the human papillomavirus E6 oncoprotein with p53. *Mol Cell Biol* **13**, 775-84 (1993).
264. Reznikoff, C.A. et al. Long-term genome stability and minimal genotypic and phenotypic alterations in HPV16 E7-, but not E6-, immortalized human uroepithelial cells. *Genes Dev* **8**, 2227-40 (1994).
265. Jones, D.L., Thompson, D.A., Suh-Burgmann, E., Grace, M. & Munger, K. Expression of the HPV E7 oncoprotein mimics but does not evoke a p53-dependent cellular DNA damage response pathway. *Virology* **258**, 406-14 (1999).
266. Massimi, P. & Banks, L. Repression of p53 transcriptional activity by the HPV E7 proteins. *Virology* **227**, 255-9 (1997).
267. Mantovani, F. & Banks, L. The human papillomavirus E6 protein and its contribution to malignant progression. *Oncogene* **20**, 7874-87 (2001).
268. Thomas, J.T. & Laimins, L.A. Human papillomavirus oncoproteins E6 and E7 independently abrogate the mitotic spindle checkpoint. *J Virol* **72**, 1131-7 (1998).
269. Wells, J., Boyd, K.E., Fry, C.J., Bartley, S.M. & Farnham, P.J. Target gene specificity of E2F and pocket protein family members in living cells. *Mol Cell Biol* **20**, 5797-807 (2000).
270. Knudsen, E.S. & Wang, J.Y. Dual mechanisms for the inhibition of E2F binding to RB by cyclin-dependent kinase-mediated RB phosphorylation. *Mol Cell Biol* **17**, 5771-83 (1997).
271. Chellappan, S. et al. Adenovirus E1A, simian virus 40 tumor antigen, and human papillomavirus E7 protein share the capacity to disrupt the interaction between transcription factor E2F and the retinoblastoma gene product. *Proc Natl Acad Sci U S A* **89**, 4549-53 (1992).

272. Wu, E.W., Clemens, K.E., Heck, D.V. & Munger, K. The human papillomavirus E7 oncoprotein and the cellular transcription factor E2F bind to separate sites on the retinoblastoma tumor suppressor protein. *J Virol* **67**, 2402-7 (1993).
273. Dick, F.A. & Dyson, N.J. Three regions of the pRB pocket domain affect its inactivation by human papillomavirus E7 proteins. *J Virol* **76**, 6224-34 (2002).
274. Ferreira, R., Magnaghi-Jaulin, L., Robin, P., Harel-Bellan, A. & Trouche, D. The three members of the pocket proteins family share the ability to repress E2F activity through recruitment of a histone deacetylase. *Proc Natl Acad Sci U S A* **95**, 10493-8 (1998).
275. Watanabe, S., Kanda, T., Sato, H., Furuno, A. & Yoshiike, K. Mutational analysis of human papillomavirus type 16 E7 functions. *J Virol* **64**, 207-14 (1990).
276. Zerfass, K. et al. Sequential activation of cyclin E and cyclin A gene expression by human papillomavirus type 16 E7 through sequences necessary for transformation. *J Virol* **69**, 6389-99 (1995).
277. Tommasino, M. et al. HPV16 E7 protein associates with the protein kinase p33CDK2 and cyclin A. *Oncogene* **8**, 195-202 (1993).
278. Nguyen, C.L. & Munger, K. Direct association of the HPV16 E7 oncoprotein with cyclin A/CDK2 and cyclin E/CDK2 complexes. *Virology* **380**, 21-5 (2008).
279. He, W., Staples, D., Smith, C. & Fisher, C. Direct activation of cyclin-dependent kinase 2 by human papillomavirus E7. *J Virol* **77**, 10566-74 (2003).
280. Dyson, N., Guida, P., Munger, K. & Harlow, E. Homologous sequences in adenovirus E1A and human papillomavirus E7 proteins mediate interaction with the same set of cellular proteins. *J Virol* **66**, 6893-902 (1992).
281. Zhang, B., Chen, W. & Roman, A. The E7 proteins of low- and high-risk human papillomaviruses share the ability to target the pRB family member p130 for degradation. *Proc Natl Acad Sci U S A* **103**, 437-42 (2006).
282. Zerfass-Thome, K. et al. Inactivation of the cdk inhibitor p27KIP1 by the human papillomavirus type 16 E7 oncoprotein. *Oncogene* **13**, 2323-30 (1996).
283. Helt, A.M., Funk, J.O. & Galloway, D.A. Inactivation of both the retinoblastoma tumor suppressor and p21 by the human papillomavirus type 16 E7 oncoprotein is necessary to inhibit cell cycle arrest in human epithelial cells. *J Virol* **76**, 10559-68 (2002).
284. Vousden, K.H. & Lu, X. Live or let die: the cell's response to p53. *Nat Rev Cancer* **2**, 594-604 (2002).
285. Funk, J.O. et al. Inhibition of CDK activity and PCNA-dependent DNA replication by p21 is blocked by interaction with the HPV-16 E7 oncoprotein. *Genes Dev* **11**, 2090-100 (1997).
286. Jones, D.L., Alani, R.M. & Munger, K. The human papillomavirus E7 oncoprotein can uncouple cellular differentiation and proliferation in human keratinocytes by abrogating p21Cip1-mediated inhibition of cdk2. *Genes Dev* **11**, 2101-11 (1997).
287. Duensing, S. et al. The human papillomavirus type 16 E6 and E7 oncoproteins cooperate to induce mitotic defects and genomic instability by uncoupling centrosome duplication from the cell division cycle. *Proc Natl Acad Sci U S A* **97**, 10002-7 (2000).
288. Plug-Demaggio, A.W. & McDougall, J.K. The human papillomavirus type 16 E6 oncogene induces premature mitotic chromosome segregation. *Oncogene* **21**, 7507-13 (2002).
289. Noya, F., Chien, W.M., Broker, T.R. & Chow, L.T. p21cip1 Degradation in differentiated keratinocytes is abrogated by costabilization with cyclin E induced by human papillomavirus E7. *J Virol* **75**, 6121-34 (2001).

290. Tsao, Y.P., Li, L.Y., Tsai, T.C. & Chen, S.L. Human papillomavirus type 11 and 16 E5 represses p21(WafI/SdiI/CipI) gene expression in fibroblasts and keratinocytes. *J Virol* **70**, 7535-9 (1996).
291. Gonzalez, S.L., Stremlau, M., He, X., Basile, J.R. & Munger, K. Degradation of the retinoblastoma tumor suppressor by the human papillomavirus type 16 E7 oncoprotein is important for functional inactivation and is separable from proteasomal degradation of E7. *J Virol* **75**, 7583-91 (2001).
292. Davy, C.E. et al. Identification of a G(2) arrest domain in the E1 wedge E4 protein of human papillomavirus type 16. *J Virol* **76**, 9806-18 (2002).
293. Nakahara, T. et al. Modulation of the cell division cycle by human papillomavirus type 18 E4. *J Virol* **76**, 10914-20 (2002).
294. Wells, S.I. et al. Transcriptome signature of irreversible senescence in human papillomavirus-positive cervical cancer cells. *Proc Natl Acad Sci U S A* **100**, 7093-8 (2003).
295. Sorathia, R., Davey, C., Sterlinko, H. & al, e. The E4 protein of HPV16 Interacts with E2 and Regulates the trans-activation and Replication Functions of E2. in *21st International Papillomavirus Conference* p318 (Mexico City, Mexico, 2004).
296. Duensing, S. & Munger, K. Mechanisms of genomic instability in human cancer: insights from studies with human papillomavirus oncoproteins. *Int J Cancer* **109**, 157-62 (2004).
297. Brehm, A. et al. The E7 oncoprotein associates with Mi2 and histone deacetylase activity to promote cell growth. *Embo J* **18**, 2449-58 (1999).
298. Antinore, M.J., Birrer, M.J., Patel, D., Nader, L. & McCance, D.J. The human papillomavirus type 16 E7 gene product interacts with and trans-activates the AP1 family of transcription factors. *Embo J* **15**, 1950-60 (1996).
299. Massimi, P., Shai, A., Lambert, P. & Banks, L. HPV E6 degradation of p53 and PDZ containing substrates in an E6AP null background. *Oncogene* (2007).
300. Nguyen, M.L., Nguyen, M.M., Lee, D., Griep, A.E. & Lambert, P.F. The PDZ ligand domain of the human papillomavirus type 16 E6 protein is required for E6's induction of epithelial hyperplasia in vivo. *J Virol* **77**, 6957-64 (2003).
301. Kiyono, T. et al. Binding of high-risk human papillomavirus E6 oncoproteins to the human homologue of the Drosophila discs large tumor suppressor protein. *Proc Natl Acad Sci U S A* **94**, 11612-6 (1997).
302. Thomas, M. et al. Oncogenic human papillomavirus E6 proteins target the MAGI-2 and MAGI-3 proteins for degradation. *Oncogene* **21**, 5088-96 (2002).
303. Laimins, L.A. The biology of human papillomaviruses: from warts to cancer. *Infect Agents Dis* **2**, 74-86 (1993).
304. Zhang, Y. et al. Structures of a human papillomavirus (HPV) E6 polypeptide bound to MAGUK proteins: mechanisms of targeting tumor suppressors by a high-risk HPV oncoprotein. *J Virol* **81**, 3618-26 (2007).
305. Thomas, M., Glaunsinger, B., Pim, D., Javier, R. & Banks, L. HPV E6 and MAGUK protein interactions: determination of the molecular basis for specific protein recognition and degradation. *Oncogene* **20**, 5431-9 (2001).
306. Brazil, D.P., Yang, Z.Z. & Hemmings, B.A. Advances in protein kinase B signalling: AKTion on multiple fronts. *Trends Biochem Sci* **29**, 233-42 (2004).
307. Cantley, L.C. The phosphoinositide 3-kinase pathway. *Science* **296**, 1655-7 (2002).
308. Habermann, J.K. et al. A recurrent gain of chromosome arm 3q in primary squamous carcinoma of the vagina. *Cancer Genet Cytogenet* **148**, 7-13 (2004).

309. Heselmeyer, K. et al. Gain of chromosome 3q defines the transition from severe dysplasia to invasive carcinoma of the uterine cervix. *Proc Natl Acad Sci U S A* **93**, 479-84 (1996).
310. Duensing, S. et al. Centrosome abnormalities and genomic instability by episomal expression of human papillomavirus type 16 in raft cultures of human keratinocytes. *J Virol* **75**, 7712-6 (2001).
311. Pett, M.R. et al. Acquisition of high-level chromosomal instability is associated with integration of human papillomavirus type 16 in cervical keratinocytes. *Cancer Res* **64**, 1359-68 (2004).
312. Duensing, S., Duensing, A., Crum, C.P. & Munger, K. Human papillomavirus type 16 E7 oncoprotein-induced abnormal centrosome synthesis is an early event in the evolving malignant phenotype. *Cancer Res* **61**, 2356-60 (2001).
313. Lee, D. et al. Human papillomavirus E2 down-regulates the human telomerase reverse transcriptase promoter. *J Biol Chem* **277**, 27748-56 (2002).
314. Oh, S.T., Kyo, S. & Laimins, L.A. Telomerase activation by human papillomavirus type 16 E6 protein: induction of human telomerase reverse transcriptase expression through Myc and GC-rich Sp1 binding sites. *J Virol* **75**, 5559-66 (2001).
315. Du, M., Fan, X., Hong, E. & Chen, J.J. interaction of Oncogenic Papillomavirus E6 Proteins with Fibulin-1. *Biochemical and Biophysical Research Communications* **296**, 962-969 (2002).
316. Iftner, T. et al. Interference of papillomavirus E6 protein with single-strand break repair by interaction with XRCC1. *Embo J* **21**, 4741-8 (2002).
317. Sherman, L. et al. Inhibition of serum- and calcium-induced differentiation of human keratinocytes by HPV16 E6 oncoprotein: role of p53 inactivation. *Virology* **237**, 296-306 (1997).
318. Chen, J.J., Reid, C.E., Band, V. & Androphy, E.J. Interaction of papillomavirus E6 oncoproteins with a putative calcium-binding protein. *Science* **269**, 529-31 (1995).
319. Tong, X. & Howley, P.M. The bovine papillomavirus E6 oncoprotein interacts with paxillin and disrupts the actin cytoskeleton. *Proc Natl Acad Sci U S A* **94**, 4412-7 (1997).
320. Gao, Q., Srinivasan, S., Boyer, S.N., Wazer, D.E. & Band, V. The E6 oncoproteins of high-risk papillomaviruses bind to a novel putative GAP protein, E6TP1, and target it for degradation. *Mol Cell Biol* **19**, 733-44 (1999).
321. Jones, D.L., Thompson, D.A. & Munger, K. Destabilization of the RB tumor suppressor protein and stabilization of p53 contribute to HPV type 16 E7-induced apoptosis. *Virology* **239**, 97-107 (1997).
322. Butz, K. et al. siRNA targeting of the viral E6 oncogene efficiently kills human papillomavirus-positive cancer cells. *Oncogene* **22**, 5938-45 (2003).
323. Thompson, D.A. et al. The HPV E7 oncoprotein inhibits tumor necrosis factor alpha-mediated apoptosis in normal human fibroblasts. *Oncogene* **20**, 3629-40 (2001).
324. Corden, S.A., Sant-Cassia, L.J., Easton, A.J. & Morris, A.G. The integration of HPV-18 DNA in cervical carcinoma. *Mol Pathol* **52**, 275-82 (1999).
325. Kabsch, K. et al. The HPV-16 E5 protein inhibits TRAIL- and FasL-mediated apoptosis in human keratinocyte raft cultures. *Intervirology* **47**, 48-56 (2004).
326. Filippova, M., Song, H., Connolly, J.L., Dermody, T.S. & Duerksen-Hughes, P.J. The human papillomavirus 16 E6 protein binds to tumor necrosis factor (TNF) R1 and protects cells from TNF-induced apoptosis. *J Biol Chem* **277**, 21730-9 (2002).
327. Klingelhutz, A.J., Foster, S.A. & McDougall, J.K. Telomerase Activation by the E6 Gene Product of Human Papillomavirus Type 16. **380**, 79-82 (1996).

328. Kiyono, T. et al. Both Rb/p16INK4a inactivation and telomerase activity are required to immortalize human epithelial cells. *Nature* **396**, 84-8 (1998).
329. Yuan, H. et al. Human papillomavirus type 16 E6 and E7 oncoproteins upregulate c-IAP2 gene expression and confer resistance to apoptosis. *Oncogene* **24**, 5069-78 (2005).
330. Finzer, P., Kuntzen, C., Soto, U., zur Hausen, H. & Rosl, F. Inhibitors of histone deacetylase arrest cell cycle and induce apoptosis in cervical carcinoma cells circumventing human papillomavirus oncogene expression. *Oncogene* **20**, 4768-76 (2001).
331. Garnett, T.O. & Duerksen-Hughes, P.J. Modulation of apoptosis by human papillomavirus (HPV) oncoproteins. *Arch Virol* **151**, 2321-35 (2006).
332. Raj, K., Berguerand, S., Southern, S., Doorbar, J. & Beard, P. E1 empty set E4 protein of human papillomavirus type 16 associates with mitochondria. *J Virol* **78**, 7199-207 (2004).
333. Vikhanskaya, F., Falugi, C., Valente, P. & Russo, P. Human papillomavirus type 16 E6-enhanced susceptibility to apoptosis induced by TNF in A2780 human ovarian cancer cell line. *Int J Cancer* **97**, 732-9 (2002).
334. Fan, X., Liu, Y. & Chen, J.J. Down-regulation of p21 contributes to apoptosis induced by HPV E6 in human mammary epithelial cells. *Apoptosis* **10**, 63-73 (2005).
335. Pim, D. & Banks, L. HPV-18 E6*I protein modulates the E6-directed degradation of p53 by binding to full-length HPV-18 E6. *Oncogene* **18**, 7403-8 (1999).
336. Stoppler, H. et al. The E7 protein of human papillomavirus type 16 sensitizes primary human keratinocytes to apoptosis. *Oncogene* **17**, 1207-14 (1998).
337. Howes, K.A. et al. Apoptosis or retinoblastoma: alternative fates of photoreceptors expressing the HPV-16 E7 gene in the presence or absence of p53. *Genes Dev* **8**, 1300-10 (1994).
338. Webster, K. et al. The human papillomavirus (HPV) 16 E2 protein induces apoptosis in the absence of other HPV proteins and via a p53-dependent pathway. *J Biol Chem* **275**, 87-94 (2000).
339. Basile, J.R., Zacny, V. & Munger, K. The cytokines tumor necrosis factor-alpha (TNF-alpha) and TNF-related apoptosis-inducing ligand differentially modulate proliferation and apoptotic pathways in human keratinocytes expressing the human papillomavirus-16 E7 oncoprotein. *J Biol Chem* **276**, 22522-8 (2001).
340. Aguilar-Lemarroy, A. et al. Restoration of p53 expression sensitizes human papillomavirus type 16 immortalized human keratinocytes to CD95-mediated apoptosis. *Oncogene* **21**, 165-75 (2002).
341. Blachon, S. & Demeret, C. The regulatory E2 proteins of human genital papillomaviruses are pro-apoptotic. *Biochimie* **85**, 813-9 (2003).
342. Demeret, C., Garcia-Carranca, A. & Thierry, F. Transcription-independent triggering of the extrinsic pathway of apoptosis by human papillomavirus 18 E2 protein. *Oncogene* **22**, 168-75 (2003).
343. Desaintes, C., Goyat, S., Garbay, S., Yaniv, M. & Thierry, F. Papillomavirus E2 induces p53-independent apoptosis in HeLa cells. *Oncogene* **18**, 4538-45 (1999).
344. Sanchez-Perez, A.M., Soriano, S., Clarke, A.R. & Gaston, K. Disruption of the human papillomavirus type 16 E2 gene protects cervical carcinoma cells from E2F-induced apoptosis. *J Gen Virol* **78 (Pt 11)**, 3009-18 (1997).
345. Green, K.L., Brown, C., Roeder, G.E., Southgate, T.D. & Gaston, K. A cancer cell-specific inducer of apoptosis. *Hum Gene Ther* **18**, 547-61 (2007).
346. Desaintes, C., Demeret, C., Goyat, S., Yaniv, M. & Thierry, F. Expression of the papillomavirus E2 protein in HeLa cells leads to apoptosis. *Embo J* **16**, 504-14 (1997).

347. Maitland, N.J. et al. Expression patterns of the human papillomavirus type 16 transcription factor E2 in low- and high-grade cervical intraepithelial neoplasia. *J Pathol* **186**, 275-80 (1998).
348. Govan, V.A. A novel vaccine for cervical cancer: quadrivalent human papillomavirus (types 6, 11, 16 and 18) recombinant vaccine (Gardasil). *Ther Clin Risk Manag* **4**, 65-70 (2008).
349. UK, C.R. Cervical Cancer Questions. Vol. 2008.
350. Stanley, M. Immunobiology of HPV and HPV vaccines. *Gynecol Oncol* **109**, S15-21 (2008).
351. Harper, D.M. et al. Sustained efficacy up to 4.5 years of a bivalent L1 virus-like particle vaccine against human papillomavirus types 16 and 18: follow-up from a randomised control trial. *Lancet* **367**, 1247-55 (2006).
352. Smith, J.F. et al. Antibodies from women immunized with Gardasil cross-neutralize HPV 45 pseudovirions. *Hum Vaccin* **3**, 109-15 (2007).
353. Hildesheim, A. et al. Effect of human papillomavirus 16/18 L1 viruslike particle vaccine among young women with preexisting infection: a randomized trial. *Jama* **298**, 743-53 (2007).
354. Kubbutat, M.H., Jones, S.N. & Vousden, K.H. Regulation of p53 stability by Mdm2. *Nature* **387**, 299-303 (1997).
355. Bottger, A. et al. Molecular characterization of the hdm2-p53 interaction. *J Mol Biol* **269**, 744-56 (1997).
356. Bottger, A. et al. Design of a synthetic Mdm2-binding mini protein that activates the p53 response in vivo. *Curr Biol* **7**, 860-9 (1997).
357. Tovar, C. et al. Small-molecule MDM2 antagonists reveal aberrant p53 signaling in cancer: implications for therapy. *Proc Natl Acad Sci U S A* **103**, 1888-93 (2006).
358. Cullen, B.R. Nuclear RNA export. *J Cell Sci* **116**, 587-97 (2003).
359. Chook, Y.M. & Blobel, G. Karyopherins and nuclear import. *Curr Opin Struct Biol* **11**, 703-15 (2001).
360. Kutay, U. & Guttinger, S. Leucine-rich nuclear-export signals: born to be weak. *Trends Cell Biol* **15**, 121-4 (2005).
361. Ullman, K.S., Powers, M.A. & Forbes, D.J. Nuclear export receptors: from importin to exportin. *Cell* **90**, 967-70 (1997).
362. Ossareh-Nazari, B., Bachelerie, F. & Dargemont, C. Evidence for a role of CRM1 in signal-mediated nuclear protein export. *Science* **278**, 141-4 (1997).
363. Gorlich, D. et al. A novel class of RanGTP binding proteins. *J Cell Biol* **138**, 65-80 (1997).
364. Fried, H. & Kutay, U. Nucleocytoplasmic transport: taking an inventory. *Cell Mol Life Sci* **60**, 1659-88 (2003).
365. Mosammaparast, N. & Pemberton, L.F. Karyopherins: from nuclear-transport mediators to nuclear-function regulators. *Trends Cell Biol* **14**, 547-56 (2004).
366. Stade, K., Ford, C.S., Guthrie, C. & Weis, K. Exportin 1 (Crm1p) is an essential nuclear export factor. *Cell* **90**, 1041-50 (1997).
367. Asscher, Y. et al. Leptomycin B: An Important Tool for the Study of Nuclear Export. *LifeScience Quarterly* **2**(2001).
368. Meissner, T., Krause, E. & Vinkemeier, U. Ratjadone and leptomycin B block CRM1-dependent nuclear export by identical mechanisms. *FEBS Lett* **576**, 27-30 (2004).
369. Adachi, Y. & Yanagida, M. Higher order chromosome structure is affected by cold-sensitive mutations in a Schizosaccharomyces pombe gene crm1+ which encodes a 115-kD protein preferentially localized in the nucleus and its periphery. *J Cell Biol* **108**, 1195-207 (1989).

370. Kudo, N. et al. Molecular cloning and cell cycle-dependent expression of mammalian CRM1, a protein involved in nuclear export of proteins. *J Biol Chem* **272**, 29742-51 (1997).
371. Kudo, N. et al. Leptomycin B inhibition of signal-mediated nuclear export by direct binding to CRM1. *Exp Cell Res* **242**, 540-7 (1998).
372. Fischer, U., Huber, J., Boelens, W.C., Mattaj, I.W. & Luhrmann, R. The HIV-1 Rev activation domain is a nuclear export signal that accesses an export pathway used by specific cellular RNAs. *Cell* **82**, 475-83 (1995).
373. Engelsma, D., Bernad, R., Calafat, J. & Fornerod, M. Supraphysiological nuclear export signals bind CRM1 independently of RanGTP and arrest at Nup358. *Embo J* **23**, 3643-52 (2004).
374. Gray, L.J. et al. Selective induction of apoptosis by leptomycin B in keratinocytes expressing HPV oncogenes. *Int J Cancer* **120**, 2317-24 (2007).
375. Lecane, P.S., Kiviharju, T.M., Sellers, R.G. & Peehl, D.M. Leptomycin B stabilizes and activates p53 in primary prostatic epithelial cells and induces apoptosis in the LNCaP cell line. *Prostate* **54**, 258-67 (2003).
376. Sciences, S.L. Leptomycin. http://www.leptomycin.com (2005).
377. Fornerod, M., Ohno, M., Yoshida, M. & Mattaj, I.W. CRM1 is an export receptor for leucine-rich nuclear export signals. *Cell* **90**, 1051-60 (1997).
378. Wolff, B., Sanglier, J.J. & Wang, Y. Leptomycin B is an inhibitor of nuclear export: inhibition of nucleo-cytoplasmic translocation of the human immunodeficiency virus type 1 (HIV-1) Rev protein and Rev-dependent mRNA. *Chem Biol* **4**, 139-47 (1997).
379. Wada, A., Fukuda, M., Mishima, M. & Nishida, E. Nuclear export of actin: a novel mechanism regulating the subcellular localization of a major cytoskeletal protein. *Embo J* **17**, 1635-41 (1998).
380. Tomoda, K., Kubota, Y. & Kato, J. Degradation of the cyclin-dependent-kinase inhibitor p27Kip1 is instigated by Jab1. *Nature* **398**, 160-5 (1999).
381. Taagepera, S. et al. Nuclear-cytoplasmic shuttling of C-ABL tyrosine kinase. *Proc Natl Acad Sci U S A* **95**, 7457-62 (1998).
382. Kumagai, A. & Dunphy, W.G. Binding of 14-3-3 proteins and nuclear export control the intracellular localization of the mitotic inducer Cdc25. *Genes Dev* **13**, 1067-72 (1999).
383. Yang, J. et al. Control of cyclin B1 localization through regulated binding of the nuclear export factor CRM1. *Genes Dev* **12**, 2131-43 (1998).
384. Jang, B.C. et al. Leptomycin B, an inhibitor of the nuclear export receptor CRM1, inhibits COX-2 expression. *J Biol Chem* **278**, 2773-6 (2003).
385. Freedman, D.A. & Levine, A.J. Nuclear export is required for degradation of endogenous p53 by MDM2 and human papillomavirus E6. *Mol Cell Biol* **18**, 7288-93 (1998).
386. Glover-Collins, K. & Thompson, M.E. Nuclear export of BRCA1 occurs during early S phase and is calcium-dependent. *Cell Signal* **20**, 958-68 (2008).
387. Inoue, T., Stuart, J., Leno, R. & Maki, C.G. Nuclear import and export signals in control of the p53-related protein p73. *J Biol Chem* **277**, 15053-60 (2002).
388. Han, X., Saito, H., Miki, Y. & Nakanishi, A. A CRM1-mediated nuclear export signal governs cytoplasmic localization of BRCA2 and is essential for centrosomal localization of BRCA2. *Oncogene* **27**, 2969-77 (2008).
389. Seimiya, H. et al. Involvement of 14-3-3 proteins in nuclear localization of telomerase. *Embo J* **19**, 2652-61 (2000).
390. Hagting, A., Karlsson, C., Clute, P., Jackman, M. & Pines, J. MPF localization is controlled by nuclear export. *Embo J* **17**, 4127-38 (1998).

391. Vischioni, B., Giaccone, G., Span, S.W., Kruyt, F.A. & Rodriguez, J.A. Nuclear shuttling and TRAF2-mediated retention in the cytoplasm regulate the subcellular localization of cIAP1 and cIAP2. *Exp Cell Res* **298**, 535-48 (2004).
392. Sachdev, S. & Hannink, M. Loss of IkappaB alpha-mediated control over nuclear import and DNA binding enables oncogenic activation of c-Rel. *Mol Cell Biol* **18**, 5445-56 (1998).
393. Plenchette, S. et al. Translocation of the inhibitor of apoptosis protein c-IAP1 from the nucleus to the Golgi in hematopoietic cells undergoing differentiation: a nuclear export signal-mediated event. *Blood* **104**, 2035-43 (2004).
394. Stauber, R.H., Mann, W. & Knauer, S.K. Nuclear and cytoplasmic survivin: molecular mechanism, prognostic, and therapeutic potential. *Cancer Res* **67**, 5999-6002 (2007).
395. Adachi, M., Fukuda, M. & Nishida, E. Nuclear export of MAP kinase (ERK) involves a MAP kinase kinase (MEK)-dependent active transport mechanism. *J Cell Biol* **148**, 849-56 (2000).
396. Blachon, S., Bellanger, S., Demeret, C. & Thierry, F. Nucleo-cytoplasmic shuttling of high risk human Papillomavirus E2 proteins induces apoptosis. *J Biol Chem* **280**, 36088-98 (2005).
397. Monte, M. et al. hGTSE-1 expression stimulates cytoplasmic localization of p53. *J Biol Chem* **279**, 11744-52 (2004).
398. Smart, P. et al. Effects on normal fibroblasts and neuroblastoma cells of the activation of the p53 response by the nuclear export inhibitor leptomycin B. *Oncogene* **18**, 7378-86 (1999).
399. Jang, B.C. et al. Leptomycin B-induced apoptosis is mediated through caspase activation and down-regulation of Mcl-1 and XIAP expression, but not through the generation of ROS in U937 leukemia cells. *Biochem Pharmacol* **68**, 263-74 (2004).
400. Vigneri, P. & Wang, J.Y. Induction of apoptosis in chronic myelogenous leukemia cells through nuclear entrapment of BCR-ABL tyrosine kinase. *Nat Med* **7**, 228-34 (2001).
401. Newlands, E.S., Rustin, G.J. & Brampton, M.H. Phase I trial of elactocin. *Br J Cancer* **74**, 648-9 (1996).
402. Sterling, J., Stanley, M., Gatward, G. & Minson, T. Production of human papillomavirus type 16 virions in a keratinocyte cell line. *J Virol* **64**, 6305-7 (1990).
403. Shai, A., Brake, T., Somoza, C. & Lambert, P.F. The human papillomavirus E6 oncogene dysregulates the cell cycle and contributes to cervical carcinogenesis through two independent activities. *Cancer Res* **67**, 1626-35 (2007).
404. Jeon, S. University of Wisconsin, Madison (1995).
405. Pattillo, R.A. et al. Tumor antigen and human chorionic gonadotropin in CaSki cells: a new epidermoid cervical cancer cell line. *Science* **196**, 1456-8 (1977).
406. Yee, C., Krishnan-Hewlett, I., Baker, C.C., Schlegel, R. & Howley, P.M. Presence and expression of human papillomavirus sequences in human cervical carcinoma cell lines. *Am J Pathol* **119**, 361-6 (1985).
407. Friedl, F., Kimura, I., Osato, T. & Ito, Y. Studies on a new human cell line (SiHa) derived from carcinoma of uterus. I. Its establishment and morphology. *Proc Soc Exp Biol Med* **135**, 543-5 (1970).
408. Halbert, C.L., Demers, G.W. & Galloway, D.A. The E7 gene of human papillomavirus type 16 is sufficient for immortalization of human epithelial cells. *J Virol* **65**, 473-8 (1991).
409. Li, C., Chen, L. & Chen, J. DNA damage induces MDMX nuclear translocation by p53-dependent and -independent mechanisms. *Mol Cell Biol* **22**, 7562-71 (2002).

410. Soni, R. et al. Selective in vivo and in vitro effects of a small molecule inhibitor of cyclin-dependent kinase 4. *J Natl Cancer Inst* **93**, 436-46 (2001).
411. Taylor, E.R., Boner, W., Dornan, E.S., Corr, E.M. & Morgan, I.M. UVB irradiation reduces the half-life and transactivation potential of the human papillomavirus 16 E2 protein. *Oncogene* **22**, 4469-77 (2003).
412. Shamanin, V.A. & Androphy, E.J. Immortalization of human mammary epithelial cells is associated with inactivation of the p14ARF-p53 pathway. *Mol Cell Biol* **24**, 2144-52 (2004).
413. Hirt, B. Selective extraction of polyoma DNA from infected mouse cell cultures. *J Mol Biol* **26**, 365-9 (1967).
414. Graham, D.A. & Herrington, C.S. HPV-16 E2 gene disruption and sequence variation in CIN 3 lesions and invasive squamous cell carcinomas of the cervix: relation to numerical chromosome abnormalities. *Mol Pathol* **53**, 201-6 (2000).
415. Zhang, X., Ding, L. & Sandford, A.J. Selection of reference genes for gene expression studies in human neutrophils by real-time PCR. *BMC Mol Biol* **6**, 4 (2005).
416. Nees, M. et al. Human papillomavirus type 16 E6 and E7 proteins inhibit differentiation-dependent expression of transforming growth factor-beta2 in cervical keratinocytes. *Cancer Res* **60**, 4289-98 (2000).
417. Kern, S.E. et al. Oncogenic forms of p53 inhibit p53-regulated gene expression. *Science* **256**, 827-30 (1992).
418. Wettstein, F.O. & Stevens, J.G. Variable-sized free episomes of Shope papilloma virus DNA are present in all non-virus-producing neoplasms and integrated episomes are detected in some. *Proc Natl Acad Sci U S A* **79**, 790-4 (1982).
419. Doorbar, J. et al. Detection of novel splicing patterns in a HPV16-containing keratinocyte cell line. *Virology* **178**, 254-62 (1990).
420. Cornelissen, M.T. et al. Uniformity of the splicing pattern of the E6/E7 transcripts in human papillomavirus type 16-transformed human fibroblasts, human cervical premalignant lesions and carcinomas. *J Gen Virol* **71 (Pt 5)**, 1243-6 (1990).
421. McPhillips, M.G. et al. SF2/ASF binds the human papillomavirus type 16 late RNA control element and is regulated during differentiation of virus-infected epithelial cells. *J Virol* **78**, 10598-605 (2004).
422. Krainer, A.R., Mayeda, A., Kozak, D. & Binns, G. Functional expression of cloned human splicing factor SF2: homology to RNA-binding proteins, U1 70K, and Drosophila splicing regulators. *Cell* **66**, 383-94 (1991).
423. Graveley, B.R. Sorting out the complexity of SR protein functions. *Rna* **6**, 1197-211 (2000).
424. Ueno, T. et al. Measurement of an apoptotic product in the sera of breast cancer patients. *Eur J Cancer* **39**, 769-74 (2003).
425. Caulin, C., Salvesen, G.S. & Oshima, R.G. Caspase cleavage of keratin 18 and reorganization of intermediate filaments during epithelial cell apoptosis. *J Cell Biol* **138**, 1379-94 (1997).
426. Leers, M.P. et al. Immunocytochemical detection and mapping of a cytokeratin 18 neo-epitope exposed during early apoptosis. *J Pathol* **187**, 567-72 (1999).
427. Lane, E.B. Monoclonal antibodies provide specific intramolecular markers for the study of epithelial tonofilament organization. *J Cell Biol* **92**, 665-73 (1982).
428. Duan, W.R. et al. Comparison of immunohistochemistry for activated caspase-3 and cleaved cytokeratin 18 with the TUNEL method for quantification of apoptosis in histological sections of PC-3 subcutaneous xenografts. *J Pathol* **199**, 221-8 (2003).

429. Grassi, A. et al. Detection of the M30 neoepitope as a new tool to quantify liver apoptosis: timing and patterns of positivity on frozen and paraffin-embedded sections. *Am J Clin Pathol* **121**, 211-9 (2004).
430. Shai, A., Nguyen, M.L., Wagstaff, J., Jiang, Y.H. & Lambert, P.F. HPV16 E6 confers p53-dependent and p53-independent phenotypes in the epidermis of mice deficient for E6AP. *Oncogene* **26**, 3321-8 (2007).
431. Joseph, T.W., Zaika, A. & Moll, U.M. Nuclear and cytoplasmic degradation of endogenous p53 and HDM2 occurs during down-regulation of the p53 response after multiple types of DNA damage. *Faseb J* **17**, 1622-30 (2003).
432. Alimirah, F. et al. Expression of androgen receptor is negatively regulated by p53. *Neoplasia* **9**, 1152-9 (2007).
433. Jarviluoma, A. et al. Phosphorylation of the cyclin-dependent kinase inhibitor p21Cip1 on serine 130 is essential for viral cyclin-mediated bypass of a p21Cip1-imposed G1 arrest. *Mol Cell Biol* **26**, 2430-40 (2006).
434. Seavey, S.E., Holubar, M., Saucedo, L.J. & Perry, M.E. The E7 oncoprotein of human papillomavirus type 16 stabilizes p53 through a mechanism independent of p19(ARF). *J Virol* **73**, 7590-8 (1999).
435. Loging, W.T. & Reisman, D. Elevated expression of ribosomal protein genes L37, RPP-1, and S2 in the presence of mutant p53. *Cancer Epidemiol Biomarkers Prev* **8**, 1011-6 (1999).
436. Singh, M. & Singh, N. Induction of apoptosis by hydrogen peroxide in HPV 16 positive human cervical cancer cells: involvement of mitochondrial pathway. *Mol Cell Biochem* **310**, 57-65 (2008).
437. Moll, U.M. & Slade, N. p63 and p73: roles in development and tumor formation. *Mol Cancer Res* **2**, 371-86 (2004).
438. Yokomizo, A. et al. Overexpression of the wild type p73 gene in human bladder cancer. *Oncogene* **18**, 1629-33 (1999).
439. Casciano, I., Ponzoni, M., Lo Cunsolo, C., Tonini, G.P. & Romani, M. Different p73 splicing variants are expressed in distinct tumour areas of a multifocal neuroblastoma. *Cell Death Differ* **6**, 391-3 (1999).
440. Tokuchi, Y. et al. The expression of p73 is increased in lung cancer, independent of p53 gene alteration. *Br J Cancer* **80**, 1623-9 (1999).
441. Kaghad, M. et al. Monoallelically expressed gene related to p53 at 1p36, a region frequently deleted in neuroblastoma and other human cancers. *Cell* **90**, 809-19 (1997).
442. Jost, C.A., Marin, M.C. & Kaelin, W.G., Jr. p73 is a simian [correction of human] p53-related protein that can induce apoptosis. *Nature* **389**, 191-4 (1997).
443. Di Como, C.J., Gaiddon, C. & Prives, C. p73 function is inhibited by tumor-derived p53 mutants in mammalian cells. *Mol Cell Biol* **19**, 1438-49 (1999).
444. Gaiddon, C., Lokshin, M., Ahn, J., Zhang, T. & Prives, C. A subset of tumor-derived mutant forms of p53 down-regulate p63 and p73 through a direct interaction with the p53 core domain. *Mol Cell Biol* **21**, 1874-87 (2001).
445. Flores, E.R. et al. p63 and p73 are required for p53-dependent apoptosis in response to DNA damage. *Nature* **416**, 560-4 (2002).
446. Zeng, X. et al. MDM2 suppresses p73 function without promoting p73 degradation. *Mol Cell Biol* **19**, 3257-66 (1999).
447. Ohtsuka, T., Ryu, H., Minamishima, Y.A., Ryo, A. & Lee, S.W. Modulation of p53 and p73 levels by cyclin G: implication of a negative feedback regulation. *Oncogene* **22**, 1678-87 (2003).

448. Marabese, M., Vikhanskaya, F., Rainelli, C., Sakai, T. & Broggini, M. DNA damage induces transcriptional activation of p73 by removing C-EBPalpha repression on E2F1. *Nucleic Acids Res* **31**, 6624-32 (2003).
449. Marin, M.C. et al. Viral oncoproteins discriminate between p53 and the p53 homolog p73. *Mol Cell Biol* **18**, 6316-24 (1998).
450. Park, J.S. et al. Functional inactivation of p73, a homolog of p53 tumor suppressor protein, by human papillomavirus E6 proteins. *Int J Cancer* **91**, 822-7 (2001).
451. Sambrook, J. & Russell, D.W. *Molecular Cloning A Laboratory Manual*, (Cold Spring Harbour Laboratory Press, New York, 2001).

Appendices

Appendix A: Suppliers

- ADDgene: Cambridge, UK.
- Ambion: Texas, USA.
- Amresco: Ohio, USA.
- ATCC/ LGC Promochem: London, UK.
- BDH/VWR: Pennsylvania, USA.
- Beckman Coulter: California, USA.
- Becton and Dickinson: New Jersey, USA.
- Bioline: London, UK.
- Biometra: Goettingen, Germany.
- BMG LABTECH: Offenburg, Germany.
- Calbiochem/Merck Biosciences: Darmstadt, Germany.
- Cell Signaling: Massachusetts, USA.
- Clontech: California, USA.
- DakoCytomation: Glostrup, Denmark.
- Fisher Scientific/ Thermo Fisher Scientific: New York, USA.
- GE Healthcare: New Jersey, USA.
- Globepharm: Surrey, UK.
- Hoefer: California, USA.
- Hybaid/ Thermo Fisher Scientific: Massachusetts, USA.
- Invitrogen (Gibco/Invitrogen): California, USA.
- Johnson Screens: Minnesota, USA.
- Launch Diagnostics: Kent, UK.
- List Biological Laboratories: California, USA.
- Melford: Suffolk, UK.
- Millipore: Massachusetts, USA.
- Nalgene/ Thermo Fisher Scientific: New York, USA.
- New England Biolabs: Massachusetts, USA.
- Novartis: Basel, Switzerland.
- NUNC/Thermo Fisher Scientific: Massachusetts, USA.
- Oxiod/ Thermo Fisher Scientific: Massachusetts, USA.
- Packard Instruments: Illinois, USA.
- PerkinElmer: Massachusetts, USA.
- Pharmacia Biotech: Uppsala, Sweden.
- Pierce: Illinois, USA.
- Promega: Wisconsin, USA.
- PromoCell: Heidelberg, Germany.
- Roche Applied Science: Basel, Switzerland.
- SCIE-PLAS: Warwickshire, UK
- Sigma-Aldrich: Missouri, USA.
- Stratagene: California, USA.
- Syngene: Maryland, USA.
- Thermo Electron/ Thermo Fisher Scientific: Massachusetts, USA.
- Thistle Scientific: Glasgow, UK.
- ULTRA TEC: California, USA.
- Upstate/Millipore: Massachusetts, USA.
- Vector labs: California, USA.
- VWR: Pennsylvania, USA.

Appendix B – Protocol Details

B1. Solutions and Buffers

B1.1. Complete DMEM

ITEM	Volume	Proportion	Source
DMEM	500ml		Gibco/Invitrogen
Fetal calf serum (FCS)	50ml	10% (v/v)	Globepharm
Penicillin-streptomycin-glutamine	5ml	1% (v/v)	Gibco/Invitrogen

B1.2. Incomplete F-Medium (400ml)

ITEM	Volume	Stock solution	Final concentration	Source
Hams F12 nutrient mix	300ml		3/4	Gibco/Invitrogen
Complete DMEM	100ml		1/4	As above
Hydrocortisone	3.2ml	50µg/ml	400ng/ml	Sigma-Aldrich
Insulin (bovine pancreas)	400µl	5mg/ml	5µg/ml	Sigma-Aldrich
Cholera toxin	4µl	10µM	0.1nM	List Biological Laboratories
Adenine	5ml	2.42mg/ml	30.25µg/ml	Sigma-Aldrich

B1.3. 1x TBS

Tris	8.8g (10mM)
NaCl	1.2g(150mM)
Water	1L
pH	7.5

B1.4. Laemmli Reducing Sample Buffer

ITEM	Volume	Stock solution	Source
Sodium dodecyl sulphate (SDS)	1ml	10%	BDH
Glycerol	1ml	20%	BDH
Tris (hydroxymethyl) methylamine (Tris)	600µl	0.5M (pH6.8)	BDH
Dithiothreitol (DTT)	500µl	1M	Melford
Water	1.9ml		

B2. Protein Assay Gels and Buffers

B2.1. Resolving Gel – Mini (10ml)

Item	Stock	Source	Volume		
			8% gel	10% gel	12% gel
dH_2O			4.65ml	3.95ml	3.3ml
Tris	1.5M pH 8.8	BDH	2.5ml	2.5ml	2.5ml
Bis acrylamide	30% acrylamide	Thistle	2.65ml	3.35ml	4ml
SDS	10%	BDH	100µl	100µl	100µl
Ammonium Persulphate (APS)	10%	Amresco	100µl	100µl	100µl
Tetramethylethylenediamine (TEMED)		Gibco	6µl	4µl	4µl

B2.2. Resolving Gel – Midi (30ml)

Item	Stock	Source	Volume 8% gel
dH_2O			14ml
Tris	1.5M, pH 8.8	BDH	7.5ml
Bis acrylamide	30% acrylamide	Thistle	7.95ml
SDS	10%	BDH	300µl
APS	10%	Amresco	300µl
TEMED		Gibco	18µl

B2.3. Stacking Gel – Mini (3 ml)

Item	Stock	Volume
dH_2O		2.05ml
Tris	0.5M, pH6.8	375µl
Acrylamide-bis*	30% acrylamide	500µl
SDS	10%	30µl
APS	10%	30µl
TEMED		3µl

B2.4. Stacking Gel – Midi (10 ml)

Item	Stock	Volume
dH_2O		6.15ml
Tris	0.5M, pH6.8	1.1ml
Acrylamide-bis*	30% acrylamide	1.5ml
SDS	10%	90µl
APS	10%	90µl
TEMED		9µl

B2.5. SDS-PAGE Running and Transfer Buffers

	10x Running Buffer	10x Transfer Buffer
Tris	30g	30g
Glycine	144g	144g
SDS	10g	
Water	1L	1L

B3. Solutions for Southern Blotting

B3.1. 5x Random Priming Buffer

	Final concentration	Stock Solution	Ratio	Per 5ml
Tris (pH 8)	250mmM	500mM	1:2	2.5ml
$MgCl_2$	25mM	1M	1:40	125µl
NaCl	100mM	5M	1:50	100µl
HEPES	1M	3M	1:3	1.6ml
DTT*	10mM	1M	1:100	50ul
Water				515µl

*add immediately prior to use from frozen 1M stock
Taken from Sambrook and Russell (2001) [451]

B3.2. Random Priming Stop/Storage Buffer

	Final concentration	Stock Solution	Ratio	Per 5ml
Tris-HCl (pH 7.5)	50mM	500mM	1:10	500µl
NaCl	50mM	5M	1:100	50µl
EDTA (pH 8)	5mM	0.5M	1:100	50µl
SDS	0.5% (w/v)	10% (w/v)	1:20	250µl
Water				4.50ml

Taken from Sambrook and Russell (2001) [451]

B3.3. Denhardt's Solution (50x)

	Amount	Source
Ficoll	1g	Pharmacia biotech
Polyvinylpyrrolidone	1g	Sigma-Aldrich
Bovine Serum Albumen	1g	Sigma-Aldrich
dH_2O	100ml	

Store at 4ºC

B3.4 Hybridisation Solution

	Stock	Volume (ml)
Denhardts Solution	50x	3
SSC	20x	7.5
SDS	10%	3
dH_2O		16.5

B4. Antibody Details

B4.1. Primary Antibody Details

Antibody	Source	Clone	Raised in	Mono/poly	M.W (kDa)
β-Actin	Sigma-Aldrich	AC-15	Mouse	Monoclonal	42
Caspase-3	Cell Signaling	Asp175	Rabbit	Polyclonal	17/19
Cytokeratin-18 (CK-18)	E. B. Lane (Dundee) [427]	LE65	Mouse	Monoclonal	47
E2-monoclonal	I. Morgan (Glasgow)	TGV261	Mouse	Monoclonal	42
M30	Roche	M30	Mouse	Monoclonal	40 (early) 24 (late)
P21 (C-terminal)	Dako	SX118	Mouse	Monoclonal	21
P21 (internal)	Calbiochem	mAbl	Mouse	Monoclonal	21
P53	S. Lain (Dundee)	DO-1	Mouse	Monoclonal	53

B4.2. Secondary Antibody Details

Antibody	Conjugate	Source	Use
Rabbit anti-mouse $F(ab')_2$ fragment	Biotin	Dako	Immuno
Swine anti-rabbit $F(ab')_2$ fragment	Biotin	Dako	Immuno
Goat anti-mouse IgG (H+L)	Horseradish Peroxidase	Pierce	Western
Goat anti-rabbit IgG (H+L)	Horseradish Peroxidase	Pierce	Western

B4.3. Antibody use in Immunocytochemistry

Antibody	ICC Dilution		Secondary Dilution
	Monolayer	Rafts	
Caspase-3	1:100	1:100	1:300
CK-18	Neat/1:5		1:200
M30	1:100	1:20	1:200
P21	1:25	1:50	1:200*
P53	1:50	1:50	1:200*

* component of ABC elite Vectorstain mouse or universal staining kits

B4.4. Antibody use in the Analysis of Protein and Western Blot

Antibody	Gel percentage	Dilution	Primary time	Secondary Diluted in	Detect
β-Actin	all	1:5000	1hr	PBST*	10-15s
Caspase-3	12%	1:800	Overnight	PBST	1/3/10min
CK-18	12%	1:500	Overnight	mPBST**	3/5/8min
E2-mono (mini)	10%	1:1000	Overnight	mPBST	1h
E2-mono (midi)	8%	1:1000	Overnight	3% mPBST	10min/1h
M30	12%	1:500	Overnight	PBST	3/5/15min
p21	12%/15%	1:250	Overnight	PBST	45min
Internal p21	15%	1:100	Overnight	PBST	45min /1h
p53	12%	1:1000	1h	3% mPBST	45min

PBST = PBS+0.1% Tween-20 (Sigma) **mPBST = PBST+ semi skimmed milk powder

Appendix C: Additional Information

C1. Example of Running Mean Calculation for Immunocytochemistry

C1.1. Example of raw data from immunocytochemistry

W12E50 (13) + LMB 17/5/06 M30 M					
Blue (negative)	Red (positive)	Running Red	Total	Running Total	Running % positivity
20	3	3	23	23	13.04348
22	1	4	23	46	8.695652
24	2	6	26	72	8.333333
22	1	7	23	95	7.368421
18	1	8	19	114	7.017544
25	1	9	26	140	6.428571
17	3	12	20	160	7.5
9	1	13	10	170	7.647059
39	4	17	43	213	7.981221
1	0	17	1	214	7.943925
2	0	17	2	216	7.87037
33	8	25	41	257	9.727626
49	6	31	55	312	9.935897
4	0	31	4	316	9.810127
20	5	36	25	341	10.55718
60	12	48	72	413	11.62228
16	6	54	22	435	12.41379
11	0	54	11	446	12.10762
1	0	54	1	447	12.08054
23	5	59	28	475	12.42105
16	1	60	17	492	12.19512
15	2	62	17	509	12.18075
23	2	64	25	534	11.98502
7	0	64	7	541	11.82994
12	2	66	14	555	11.89189
5	0	66	5	560	11.78571
11	0	66	11	571	11.55867
1	0	66	1	572	11.53846
46	4	70	50	622	11.25402
10	0	70	10	632	11.07595
5	0	70	5	637	10.98901
25	2	72	27	664	10.84337
8	0	72	8	672	10.71429
22	4	76	26	698	10.88825
37	8	84	45	743	11.30552
29	6	90	35	778	11.56812
29	1	91	30	808	11.26238
30	2	93	32	840	11.07143
6	0	93	6	846	10.99291
1	0	93	1	847	10.97993
6	0	93	6	853	10.9027

14	1	94	15	868	10.82949
11	0	94	11	879	10.69397
8	1	95	9	888	10.6982
2	0	95	2	890	10.67416
25	2	97	27	917	10.57797
11	2	99	13	930	10.64516
82	9	108	91	1021	10.57786
31	3	111	34	1055	10.52133
36	10	121	46	1101	10.99001
5	0	121	5	1106	10.94033
27	4	125	31	1137	10.99384
30	10	135	40	1177	11.46984
18	1	136	19	1196	11.37124
1	0	136	1	1197	11.36174
35	5	141	40	1237	11.39854
49	9	150	58	1295	11.58301
15	1	151	16	1311	11.51793
1	1	152	2	1313	11.57654
12	1	153	13	1326	11.53846
56	10	163	66	1392	11.70977
13	2	165	15	1407	11.72708
10	0	165	10	1417	11.64432
31	7	172	38	1455	11.82131
52	9	181	61	1516	11.93931
17	0	181	17	1533	11.80691
63	18	199	81	1614	12.32962
9	1	200	10	1624	12.31527
24	1	201	25	1649	12.18921
8	0	201	8	1657	12.13036
63	5	206	68	1725	11.94203
25	1	207	26	1751	11.82182
28	3	210	31	1782	11.78451
7	0	210	7	1789	11.7384
19	1	211	20	1809	11.6639
20	1	212	21	1830	11.5847
1	0	212	1	1831	11.57837
21	2	214	23	1854	11.54261
1		214	1	1855	11.53639
20	4	218	24	1879	11.60192
7	3	221	10	1889	11.69931
2	0	221	2	1891	11.68694
34	6	227	40	1931	11.75557
7	1	228	8	1939	11.75864
8	2	230	10	1949	11.80092
9	5	235	14	1963	11.97147
15	10	245	25	1988	12.32394
9	3	248	12	2000	12.4
33	2	250	35	2035	12.28501
26	3	253	29	2064	12.25775
32	7	260	39	2103	12.36329
41	4	264	45	2148	12.2905
4	0	264	4	2152	12.26766

12	5	269	17	2169	12.40203
26	3	272	29	2198	12.37489
33	1	273	34	2232	12.23118
32	3	276	35	2267	12.17468
32	9	285	41	2308	12.34835
4	0	285	4	2312	12.32699
2	0	285	2	2314	12.31634
5	5	290	10	2324	12.47849
21	3	293	24	2348	12.47871
13	2	295	15	2363	12.48413
16	2	297	18	2381	12.47375
8	1	298	9	2390	12.46862
55	5	303	60	2450	12.36735
21	5	308	26	2476	12.43942
6	3	311	9	2485	12.51509
23	6	317	29	2514	12.60939
2	0	317	2	2516	12.59936
26	1	318	27	2543	12.50492
17	3	321	20	2563	12.52439
3	0	321	3	2566	12.50974
29	2	323	31	2597	12.43743
20	2	325	22	2619	12.40932
42	8	333	50	2669	12.47658
42	3	336	45	2714	12.38025

C1.2. Example of Rnning Mean Plot from Immunocytochemistry Data

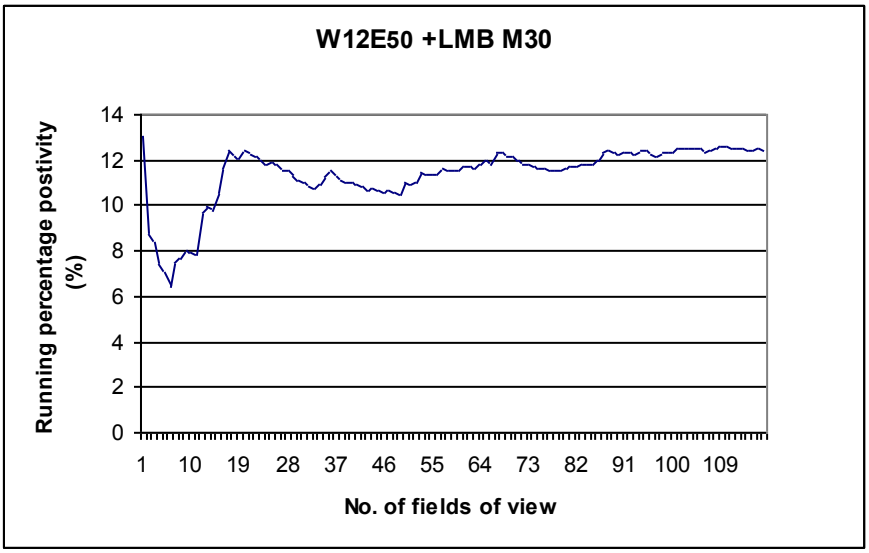

Res No.	Amino Acid		MW (Da)	Res No.	Amino Acid		MW (Da)
1	M	Methionine	131.2	40	G	Glycine	57.05
2	S	Serine	87.08	41	C	Cystine	103.14
3	E	Glutamic Acid	129.12	42	I	Isoleucine	113.16
4	P	Proline	97.12	43	Q	Glutamine	128.13
5	A	Alanine	71.08	44	E	Glutamic Acid	129.12
6	G	Glycine	57.05	45	A	Alanine	71.08
7	D	Aspartic acid	115.09	46	R	Arginine	156.19
8	V	Valine	99.13	47	E	Glutamic Acid	129.12
9	R	Arginine	156.19	48	R	Arginine	156.19
10	Q	Glutamine	128.13	49	W	Tryptophan	186.21
11	N	Asparagine	114.1	50	N	Asparagine	114.1
12	P	Proline	97.12	51	F	Phenylalanine	147.18
13	C	Cystine	103.14	52	D	Aspartic acid	115.09
14	G	Glycine	57.05	53	F	Phenylalanine	147.18
15	S	Serine	87.08	54	V	Valine	99.13
16	K	Lysine	128.17	55	T	Threonine	101.11
17	A	Alanine	71.08	56	E	Glutamic Acid	129.12
18	C	Cystine	103.14	57	T	Threonine	101.11
19	R	Arginine	156.19	58	P	Proline	97.12
20	R	Arginine	156.19	59	L	Leucine	113.16
21	L	Leucine	113.16	60	E	Glutamic Acid	129.12
22	F	Phenylalanine	147.18	61	G	Glycine	57.05
23	G	Glycine	57.05	62	D	Aspartic acid	115.09
24	P	Proline	97.12	63	F	Phenylalanine	147.18
25	V	Valine	99.13	64	A	Alanine	71.08
26	D	Aspartic acid	115.09	65	W	Tryptophan	186.21
27	S	Serine	87.08	66	E	Glutamic Acid	129.12
28	E	Glutamic Acid	129.12	67	R	Arginine	156.19
29	Q	Glutamine	128.13	68	V	Valine	99.13
30	L	Leucine	113.16	69	R	Arginine	156.19
31	S	Serine	87.08	70	G	Glycine	57.05
32	R	Arginine	156.19	71	L	leucine	113.16
33	D	Aspartic acid	115.09	72	G	Glycine	57.05
34	C	Cystine	103.14	73	L	Leucine	113.16
35	D	Aspartic acid	115.09	74	P	Proline	97.12
36	A	Alanine	71.08	75	K	Lysine	128.17
37	L	Leucine	113.16	76	L	Leucine	113.16
38	M	Methionine	131.2	77	Y	Tyrosine	163.18
39	A	Alanine	71.08				

The N-terminal amino acids of the p21 proteins, residues 1-77 (MW 8.7kDa, accession no. NCBI AAB29246). The location of the internal antibody AB-1 (calbiochem) epitope is shown in grey (a-a 58-77) with a molecular weight of 2.3kDa.

Appendix D – Publications

D.1. Published Meeting Abstracts

C. Jolly, S. Talukdar, L. Gray, and C.S. Herrington (2005). Leptomycin B induces apoptosis in keratinocytes containing the whole HPV 16 genome. 3rd Joint Meeting of the British Division of the IAP and the Pathological Society of Great Britain and Ireland, Newcastle, UK.

C. Jolly, S. Talukdar, L. Gray, and C.S. Herrington (2006). Leptomycin B induces apoptosis in keratinocytes containing the whole HPV 16 genome. 23rd International Papillomavirus Conference, Prague, Czech Republic.

D.2. Review and Research Publications

Gray, L., Jolly, C. & Herrington, C.S. Human papillomaviruses and their effects on cell cycle control and apoptosis. in *Molecular Pathogenesis of Virus Infections*, Vol. 64 235 - 252 (SGM symposium, Cambridge University Press, 2005).

Gray, L.J, Bjelogrlic, P., Appleyard, V.C.L., Thompson, A.M., Jolly, C.E., Lain, S., and Herrington, C.S. Selective induction of apoptosis by leptomycin B in keratinocytes expressing HPV oncogenes. *Int J Cancer* **120**, 2317-24 (2007).